Three-dimensional Abelian and non-Abelian gauge Higgs theories

Claudio Bonati

Dipartimento di Fisica dell'Università di Pisa and INFN Sezione di Pisa, Largo Pontecorvo 3, I-56127 Pisa, Italy

Andrea Pelissetto

Dipartimento di Fisica dell'Università di Roma Sapienza and INFN Sezione di Roma I, I-00185 Roma, Italy

Ettore Vicari

Dipartimento di Fisica dell'Università di Pisa, Largo Pontecorvo 3, I-56127 Pisa, Italy

Abstract

Gauge symmetries and Higgs mechanisms are key features of theories describing high-energy particle physics and collective phenomena in statistical and condensed-matter physics. In this review we address the collective behavior of systems of multicomponent scalar fields interacting with gauge fields, which can be already present in the underlying microscopic system or emerge only at criticality. The interplay between local gauge and global symmetries determines the phase diagram, the nature of the Higgs phases, and the nature of phase transitions between the high-temperature disordered and the low-temperature Higgs phases. However, additional crucial features determine the universal properties of the critical behavior at continuous transitions. Specifically, their nature also depends on the role played by the gauge modes at criticality. Effective (Abelian or non-Abelian) gauge Higgs field theories emerge when gauge modes develop critical correlations. On the other hand, a more standard critical behavior, which admits an effective description in terms of Landau-Ginzburg-Wilson Φ^4 theories, occurs when gauge-field modes are short ranged at the transition. In the latter case, gauge fields only prevent non-gauge invariant correlation functions from becoming critical. This review covers the recent progress made in the study of Higgs systems with Abelian and non-Abelian gauge fields. We discuss the equilibrium thermodynamic properties of systems with a classical partition function, focusing mainly on three-dimensional systems, and only briefly discussing two-dimensional models. However, by using the quantum-to-classical mapping, the results on the critical behavior for classical systems in D = d + 1 dimensions can be extended to quantum transitions in d dimensions.

Keywords: Abelian and non-Abelian gauge theories with scalar fields, Higgs mechanism, Phase transitions, Critical behavior in the presence of gauge symmetries, Landau-Ginzburg-Wilson paradigm, Charged transitions with critical gauge fields, Topological transitions.

Contents

1	Plan of the review	4
	1.1 Introduction	4
	1.2 Plan	5
2	Phase transitions, critical phenomena, and the Landau-Ginzburg-Wilson framework	8
	2.1 Phase transitions and critical phenomena	8

Email addresses: claudio.bonati@unipi.it (Claudio Bonati), andrea.pelissetto@roma1.infn.it (Andrea Pelissetto), ettore.vicari@unipi.it (Ettore Vicari)

	2.2	The field-theoretical Landau-Ginzburg-Wilson approach to continuous phase transitions	
		2.2.1 $O(N)$ -symmetric Φ^4 theory	10
		2.2.2 $U(N)$ -symmetric Φ^4 theory	
		2.2.3 Generic Landau-Ginzburg-Wilson Φ^4 theory with a single quadratic invariant	
		2.2.4 Multicritical $O(N_1) \oplus O(N_2) \Phi^4$ theories	12
3	Pha	ase transitions and critical phenomena in the presence of gauge symmetries	13
	3.1		14
	3.2		15
		3.2.1 Three-dimensional \mathbb{CP}^{N-1} models	15
		3.2.2 Three-dimensional $\mathbb{R}P^{N-1}$ models	17
		3.2.3 Finite-temperature transition of hadronic matter in the chiral limit	17
	3.3	LGW^{\times} transitions with a gauge-dependent order parameter	19
	3.4	GFT transitions described by effective field theories with gauge fields	20
	3.5	Topological transitions in lattice gauge models	21
		3.5.1 The three-dimensional inverted XY model	21
		3.5.2 Three-dimensional lattice \mathbb{Z}_Q gauge theories	22
		3.5.3 Topological transitions in low-temperature Higgs phases	23
1	۸h	olion Himma mauma field theories	24
4		elian Higgs gauge field theories $SU(N)$ -symmetric Abelian Higgs field theory	24
	4.1	4.1.1 The model	
		4.1.1 The model	
		*	
		4.1.4 Three-dimensional Abelian Higgs field theory in the large-N limit	
	4.2	Abelian Higgs field theories with multiparameter scalar potentials	
	4.2	4.2.1 SO(N)-symmetric Abelian Higgs field theories: Definition of the model	
		4.2.1 SO(N)-symmetric Abelian Higgs field theories: Renormalization-group flow	
		4.2.3 Further extensions of the Abelian Higgs field theories	
	4.3	Summary	
5		1 0 0	29
	5.1	1 ()	29
			29
	- 0		31
	5.2	•	33
			33
	۲.0	9 99	
	5.3		35
		5.3.1 The Coulomb, Molecular, and Higgs phases	35
		5.3.2 The Coulomb-Molecular transition line	36
		5.3.3 The Coulomb-Higgs transition line	37
	5.4	5.3.4 The Molecular-Higgs transition line	38 39
	5.4	N-component $SO(N)$ -invariant lattice Abelian Higgs model	39
6	Lat	1 (/8 8	40
	6.1	The compact formulation of lattice Abelian Higgs models	40
	6.2	The compact lattice Abelian Higgs model with one-component scalar fields	41
	6.3	The multicomponent compact lattice Abelian Higgs model	42
		6.3.1 Phase diagram for $Q = 1$	43
		6.3.2 Phase diagram for $Q \ge 2$	43
		6.3.3 Relation between the compact and the noncompact lattice Abelian Higgs models	44

		6.3.4	Relevance of monopole configurations	45
7	7.1	The \mathbb{Z}	in systems with discrete gauge symmetries $_2$ -gauge N -vector models	46 47
	7.2	Phase 7.2.1	diagram and critical behavior of \mathbb{Z}_2 -gauge N -vector models with $N \geq 2$	47 48
		7.2.2	RP^{N-1} -like transitions along the DD-O transition line	48
	7 0	7.2.3	$O(N)^{\times}$ transitions along the DO-O transition line	48
	7.3 7.4		cochastic gauge fixing	50 52
	1.4	7.4.1	The phase diagram of the three-dimensional \mathbb{Z}_2 -gauge Higgs model	53
		7.4.2	Order parameters driving the $\operatorname{Ising}^{\times}$ transitions	53
		7.4.3	Multicritical behavior at the intersection point of the transition lines	55
	7.5		models with discrete symmetries	56
		7.5.1 $7.5.2$	Compact models with $\mathbb{Z}_{\mathcal{N}}$ local symmetry	56 58
				90
8			ian Higgs field theories	60
	8.1	$SU(N_c 8.1.1)$	e) gauge Higgs theory with scalar fields in the fundamental representation	60 60
		8.1.2	Higgs phases and breaking patterns of the global symmetry	61
		8.1.3	Renormalization-group flow	62
	8.2	,	gauge Higgs theory with scalar fields in the fundamental representation	63
	8.3	$SU(N_c)$	e) gauge Higgs theory with scalar fields in the adjoint representation	64
9	Latt	ice no	n-Abelian Higgs models	64
	9.1		e $\mathrm{SU}(N_c)$ gauge Higgs models with multiflavor scalar fields	65
	9.2		diagram and critical behaviors of lattice $SU(N_c)$ gauge Higgs models	66 66
		9.2.1 $9.2.2$	General considerations related to the low-temperature Higgs phases Lattice SU(2) gauge Higgs models	67
		9.2.3	O(5) multicritical behavior of the two-flavor SU(2) gauge Higgs model	68
		9.2.4	Lattice $SU(N_c)$ gauge Higgs models with $N_c \geq 3$	69
	9.3		al behaviors associated with the charged fixed point of the $\mathrm{SU}(N_c)$ gauge Higgs field	00
	9.4	theory Lattice	e $\mathrm{SU}(N_c)$ gauge Higgs models with scalar fields in the adjoint representation	69 70
	0.1	9.4.1	Lattice Hamiltonian	71
		9.4.2	Higgs phases and phase transitions	72
	0.5	9.4.3	The adjoint SU(2) gauge Higgs model with four flavors	73
	9.5	Lattic	e $\mathrm{SO}(N_c)$ gauge models with multiflavor scalar fields	75
10			nsional lattice Abelian and non-Abelian gauge Higgs models	76
			al conjecture for the zero-temperature continuum limit	76
	10.2		nuum limits of multiflavor lattice gauge theories	76 77
			Lattice $\mathrm{SU}(N_c)$ gauge models	77
			Lattice $SO(N_c)$ gauge models	78
11	Effo	cts of	perturbations breaking the local gauge symmetry	79
11			-symmetry breaking in lattice Abelian Higgs models with noncompact gauge fields	79
		_	-symmetry breaking in lattice Abelian Higgs models with compact gauge fields	82
12	Con	clusio	ns and outlook	83

Appendix A	Renormalization-group theory of critical phenomena	84
Appendix A.1	Universal power laws at the critical point	85
Appendix A.2	Scaling laws in the thermodynamic limit	85
Appendix A.3	Finite-size scaling	86
Appendix	A.3.1 Free-energy density	87
Appendix	A.3.2 Energy cumulants	88
Appendix	A.3.3 The order-parameter correlation function	88
Appendix	A.3.4 Renormalization-group invariant quantities	89
Appendix A.4	Scaling behavior at a multicritical point	90
Appendix A.5	Two-dimensional spin models with continuous symmetry	90
Appendix A.6	Finite-size scaling at first-order transitions	91
Appendix B	Critical exponents of some $O(N)$ -vector universality classes	92
Appendix C	Mean-field analysis of the low-temperature Higgs phases	94

1. Plan of the review

1.1. Introduction

Gauge symmetries and Higgs mechanisms are key features of theories describing high-energy particle physics [1–4] and collective phenomena in statistical and condensed-matter physics [2, 5–16]. The large-scale properties of three-dimensional (3D) gauge models and the nature of their phase transitions are of interest in several physical contexts. For instance, they are relevant for superconductivity [17–19], for topological order and unconventional quantum transitions [16, 20, 21], and also in high-energy physics, to address some aspects of the finite-temperature electroweak and strong-interaction transitions (or, most likely, sharp crossovers) occurring in the early universe [22, 23], and the quark-gluon and chiral transitions in hadronic matter [24, 25], presently studied in heavy-ion collisions [26]. In both high-energy and condensed-matter contexts, it is crucial to have a solid understanding of the interplay between global and gauge symmetries, and, in particular, of the role that local gauge symmetries play in determining the phase structure of a model, the nature of its different phases and of its thermal and quantum transitions.

Many collective phenomena in condensed-matter physics are modelled by using effective Abelian Higgs (AH) theories, which describe a d-dimensional system of degenerate N-component scalar fields minimally coupled with an Abelian U(1) gauge field. We mention transitions in superconductors, see, e.g., Refs. [18, 19], and in quantum SU(N) antiferromagnets, see, e.g., Refs. [20, 27–32], and some unconventional quantum transitions characterized by the so-called deconfined quantum criticality, see, e.g., Refs. [33–40]. The phase structure and universal features of AH models have been extensively studied, see, e.g., Refs. [18–21, 30–32, 35, 41–93], paying particular attention to the role of the gauge fields and of the related topological features, like monopoles and Berry phases, which cannot be captured by effective Landau-Ginzburg-Wilson (LGW) theories [2, 5, 6, 94, 95] with gauge-invariant scalar order parameters, see, e.g., Refs. [20, 21, 33].

Various lattice AH models have been considered, using both compact and noncompact gauge fields, with the purpose of identifying the possible universality classes of the continuous transitions occurring in the presence of gauge invariance. These models provide examples of topological transitions, which are driven by extended charged excitations with no local order parameter, and of transitions characterized by a nontrivial interplay between long-range scalar fluctuations and nonlocal topological gauge modes. Most of the literature focused so far on Abelian gauge models, but, recently, these studies have been extended to non-Abelian Higgs (NAH) theories, in which multicomponent scalar fields are coupled with non-Abelian gauge fields, see, e.g., Refs. [20, 96–99], formally similar to those used in the Standard Model of electroweak interactions [1, 2], in which the interplay between gauge and global symmetries becomes even more complex.

From the theoretical point of view, the existence of continuous phase transitions that cannot be described by the standard gauge-invariant LGW paradigm is related to the nonperturbative infrared behavior

of strongly coupled gauge theories, and, in particular, to the existence of infrared stable charged fixed points (FPs) of their renormalization-group (RG) flow, entailing also critical gauge-field correlations. At a fundamental level, the existence of these nontrivial transitions also provides a way to define gauge field theories in a nonperturbative framework.

Over the past decade, researchers with different backgrounds, working in high-energy, statistical, and condensed-matter physics, have made important steps forward in the theoretical understanding of the non-perturbative physics of Higgs models in less than four dimensions. In light of this steady progress, a survey of the field seems to be useful for two different reasons: First, one can present the state of the art in the field; second, there is the possibility to collect and discuss in a unified fashion results that appeared in different contexts. This will also promote a more efficient communication and interdisciplinary interactions among researchers working in different areas.

To the best of our knowledge, a review on lower-dimensional, i.e., three-dimensional (3D) and two-dimensional (2D), AH and NAH theories is still missing, and we would like to fill such gap. Of course, some of the aspects we plan to cover have already been reviewed—emerging gauge fields and deconfined criticality are obvious examples, see, e.g., Refs. [20, 21]. However, the existing reviews focus on specific issues and do not report a general discussion of lower-dimensional lattice AH and NAH theories. In this review we thoroughly examine the phenomenology of gauge systems, in particular their phase diagram and the nature of the critical transitions observed when varying the gauge and global symmetries.

1.2. Plan

This review focuses on lower-dimensional AH and NAH theories, in which multicomponent scalar fields are coupled with Abelian and non-Abelian gauge fields. We discuss these models in a statistical framework [2–4, 10, 100], in which the partition function is defined as a sum over classical lattice configurations, thus providing a regularization of the functional path integral and, possibly, paving the way for a nonperturbative definition of the corresponding statistical field theory. The quantum-to-classical mapping allows us to apply the classical results for the critical behavior (equivalently, continuum limit) in (d+1) dimensions to quantum transitions of many-body systems in d dimensions, see, e.g., Refs. [14, 101]. In particular, since we consider isotropic (d+1)-dimensional statistical models, the results can be applied to the large class of continuous quantum transitions characterized by a dynamic exponent z=1, i.e., to transitions in which the critical gap decays as the inverse of the spatial size [14, 101]. We mainly consider 3D classical systems, but we also briefly discuss 2D systems.

The review covers the recent developments in the studies of lattice AH and NAH systems (LAH and LNAH, respectively), addressing their phase diagram, the main features of their Higgs ordered phases [102–105], where gauge correlations are gapped and nonlocal charged operators may condense, and the nature of their phase transitions, paying particular attention to transitions characterized by a nontrivial interplay of gauge and scalar modes. We will show that the standard effective LGW Φ^4 field theory approach [2, 94, 95], which is commonly applied to critical phenomena in statistical systems without gauge symmetries, is not always able to describe transitions in gauge models. In some cases different effective approaches are needed to correctly capture the nature of the critical behavior. We pay particular attention to the comparison with the predictions of the corresponding AH and NAH field theories (AHFTs and NAHFTs, respectively), to understand when, and how, the critical behavior of lattice systems is effectively described by the field-theory model. If this is the case, the lattice model provides a way, the so-called continuum limit, to define nonperturbatively the field theory.

In Secs. 2 and 3 we begin by discussing the possible types of critical behavior that emerge at continuous transitions in the presence of gauge symmetries. This requires an extension of the standard LGW paradigm, in particular when gauge modes play an active role at criticality. Secs. 4-6 focus on systems characterized by an Abelian U(1) gauge invariance, i.e., the AHFTs and the corresponding LAH models. We consider models with both noncompact and compact gauge fields, which turn out to present significantly different features. Lattice models with discrete Abelian gauge symmetries are addressed in Sec. 7. Secs. 8 and 9 focus instead on field theories and lattice systems with non-Abelian gauge symmetries. Two-dimensional models, with Abelian and non-Abelian gauge symmetries are discussed in Sec. 10. Finally, in Sec. 11 we discuss the effects of perturbations explicitly breaking the gauge symmetry, an issue which is particularly

relevant for systems in which the gauge symmetry effectively emerges at the transitions but which are not gauge invariant at the microscopic level. A more detailed description of the content of the review follows.

- In Sec. 2 we introduce the main ideas at the basis of the modern understanding of phase transitions and critical phenomena in statistical systems. In particular, we discuss the LGW approach in which transitions have an effective description in terms of Φ^4 field theories. Their RG flows, and in particular the corresponding stable FPs, characterize the universal features of the critical behavior of systems without gauge symmetries. We also discuss some notable examples, in which the LGW field-theoretical approach is applied.
- In Sec. 3, we discuss the key features of the critical behavior of statistical systems with local gauge symmetries. We argue that different types of critical behaviors may be realized. There are transitions driven by scalar fields whose nature depends on the role played by the gauge modes, in particular whether they develop or not critical correlations, and transitions driven by topological gauge modes without local order parameters. The effective description of these different critical behaviors requires different effective approaches, such as the standard gauge-invariant LGW approach when gauge fields are not critical, or the more complex gauge field theory (GFT) approach with explicit gauge fields in the presence of critical gauge correlations. This distinction is crucial to understand which statistical field theory (SFT) is actually realized by the various continuous phase transitions occurring in the presence of gauge symmetries.
- In Sec. 4 we focus on AHFTs, or scalar quantum electrodynamics (QED), which describe d-dimensional systems of degenerate N-component scalar fields minimally coupled with Abelian U(1) gauge fields. In particular, we consider systems with global SU(N) and SO(N) symmetry. We review the main features of their RG flow, whose stable charged FP is expected to describe the critical behavior at charged continuous transitions, when both scalar and gauge fields are critical.
- In Sec. 5 we analyze lattice models corresponding to the AHFTs discussed in Sec. 4, which are characterized by the same global and local symmetries. We consider 3D LAH models in which a noncompact Abelian gauge field is coupled with an N-component scalar field, providing a straightforward lattice discretization of the AHFT. We review results for their phase diagrams, which present various phases, including a Higgs phase, and for their critical behavior along the various transition lines. Different critical behaviors occur, which can be described by using the different approaches outlined in Sec. 3. In particular, the transitions separating the Coulomb and Higgs phases realize the critical continuum limit associated with the RG flow of the AHFTs for a sufficiently large number of scalar components.
- In Sec. 6 we consider an alternative lattice discretization of the AHFT, based on a compact formulation of the gauge variables. Its phase diagram and transitions show notable differences with respect to those of the noncompact formulation considered in Sec. 5. In particular, the phase diagram also depends on the charge of the scalar field. These LAH systems present transition lines in which the gauge modes play different roles and require different effective descriptions. The relation with the AHFT turns out to be less straightforward. The differences with the noncompact LAH models, discussed in Sec. 5, may be related to the existence of topological objects. We close this section by discussing the nontrivial relation between the LAH models with noncompact gauge fields and the compact LAH models with higher-charge scalar fields.
- In Sec. 7 we discuss lattice Higgs systems characterized by discrete Abelian gauge symmetries. We mainly discuss the 3D lattice \mathbb{Z}_2 -gauge N-vector models, obtained by minimally coupling N-component real variables with \mathbb{Z}_2 -gauge variables. They are paradigmatic models with different phases characterized by the spontaneous breaking of the global O(N) symmetry and by the different topological properties of the \mathbb{Z}_2 -gauge correlations. In particular, the N=1 model corresponds to the \mathbb{Z}_2 -gauge Higgs model, which is an interesting model showing (self-)duality and a nontrivial multicritical behavior. Other models with discrete gauge symmetries are also briefly discussed.

- In Sec. 8 we review NAHFTs, in which multiflavor scalar fields are coupled with non-Abelian gauge fields. We discuss models with $SU(N_c)$ and $SO(N_c)$ gauge symmetries, with scalar fields transforming in different representations of the gauge group, such as the fundamental and adjoint representations. We outline the known features of their RG flow, whose stable infrared FPs are expected to describe the critical behavior at some continuous phase transitions in statistical models.
- In Sec. 9 we consider LNAH models, which are lattice non-Abelian gauge theories with multicomponent degenerate scalar fields. We present results for their phase diagram, paying particular attention to their low-temperature Higgs phases. We discuss the interplay between non-Abelian gauge symmetries and global symmetries, which crucially determines the properties of the various Higgs phases, and therefore the nature of the phase transitions between the disordered and the Higgs phases. In particular we consider $SU(N_c)$ gauge theories with multicomponent scalar fields in the fundamental and adjoint representations of the gauge group, two choices which lead to different Higgs phases. Some of the transitions between the disordered and the Higgs phases are continuous and can be associated with the charged FP of the corresponding NAHFT. We close this section by briefly discussing $SO(N_c)$ gauge theories with multiflavor scalar matter.
- In Sec. 10 we review results for the critical continuum limit of 2D LAH and LNAH models with continuous global symmetries. They show that also the critical continuum limit of 2D LAH and LNAH models in the zero-temperature limit arises from a nontrivial interplay between gauge and global symmetries. The emerging results lead us to conjecture that the zero-temperature critical behavior, and therefore the continuum limit, of 2D lattice gauge models with scalar fields belongs to the zero-temperature universality classes associated with 2D field theories (σ models) defined on symmetric spaces.
- In Sec. 11 we discuss the effects of perturbations that give rise to an explicit gauge-symmetry breaking (GSB) in lattice gauge theories. This issue is discussed in LAH models with noncompact and compact gauge fields in the presence of photon-mass terms. We argue that their effect is irrelevant at the continuous transitions where gauge correlations are not critical, and the critical behavior can be described by effective LGW theories with gauge-invariant order-parameter fields. On the other hand, photon-mass terms are expected to be relevant at charged transitions where the gauge modes develop critical correlations.

Finally, in Sec. 12 we report some concluding remarks and outlook. To make this review self-contained some appendices have been added, with the aim of summarizing a few related topics required to fully appreciate some details of the methodology adopted in the main text.

- In Appendix A we report an overview of the homogeneous scaling laws expected at generic continuous phase transitions, as inferred from the RG theory of critical phenomena. We report the RG scaling relations valid in the thermodynamic limit and in the finite-size scaling (FSS) limit, at critical and multicritical points. We also briefly discuss FSS at first-order transitions.
- For reference, in Appendix B we report the presently most accurate estimates of the critical exponents of the 3D Ising, XY, and O(3) vector (Heisenberg) universality classes, which are often referred to in this review.
- In Appendix C we present some details on the mean-field analyses of the Higgs phases of LNAH models with $SU(N_c)$ gauge symmetry and N_f flavors in the fundamental representation.

We limit our review to low-dimensional Abelian and non-Abelian gauge Higgs models, in particular to three-dimensional models. We do not discuss four-dimensional (4D) Abelian and non-Abelian gauge Higgs models, which are particularly relevant for high-energy physics and are generally investigated by using perturbative approaches. Beside the extensive studies of the Standard Model of the electroweak interactions [1], based on a $SU(2) \otimes U(1)$ gauge model with a doublet of scalar fields, gauge theories with

scalar fields have been investigated as possible extensions beyond the Standard Model, for example in the context of the so-called technicolor or composite Higgs models, see, e.g., Refs. [106–110]. Note also that 4D gauge theories with scalar fields are believed to be generally affected by the so-called triviality problem, like the simpler 4D Φ^4 field theories [2, 64, 95, 111], i.e., the impossibility of constructing a corresponding 4D field theory beyond perturbation theory that is consistent (in the sense of satisfying all usual physical requirements) on all energy scales for nonzero coupling (the renormalized coupling goes to zero logarithmically when the ultraviolet cutoff is removed, so the 4D field theory turns out to eventually describe free fields). Note, however, that in the framework of effective field theories [1] triviality is not a relevant issue.

Another important issue that is not addressed in this review concerns the new features that may arise when fermionic fields are added. This topic is quite interesting, since field-theoretical models with emerging gauge symmetries in condensed-matter physics often involve fermionic excitations beside scalar modes, see, e.g., Refs. [20, 96]. We believe that this issue may provide further interesting developments, that would extend our present understanding of the phenomenology of the transitions in the presence of gauge symmetries. However, 3D gauge Higgs models including fermionic fields have been much less studied so far, so we prefer to restrict our review to gauge models with scalar matter only, for which there is already a large amount of results.

In the following we report a list of the abbreviations and symbols used throughout this review (in alphabetic order):

2D	Two-dimensional	LGW	Landau-Ginzburg-Wilson
3D	Three-dimensional	LAH	Lattice Abelian Higgs
4D	Four-dimensional	LNAH	Lattice non-Abelian Higgs
AH	Abelian Higgs	MS	Minimal subtraction
AHFT	Abelian Higgs field theory	MC	Monte Carlo
BKT	Berezinskii-Kosterlitz-Thouless	MCP	Multicritical point
CFT	Conformal field theory	NAH	Non-Abelian Higgs
d	Space dimensionality	NAHFT	Non-Abelian Higgs field theory
FSS	Finite-size scaling	QCD	Quantum chromodynamics
FP	Fixed Point	QED	Quantum electrodynamics
GFT	Gauge fied theory	QFT	Quantum field theory
GSB	Gauge symmetry breaking	RG	Renormalization-group
IXY	Inverted XY	SFT	Statistical field theory
L	Lattice size	V	Volume

2. Phase transitions, critical phenomena, and the Landau-Ginzburg-Wilson framework

2.1. Phase transitions and critical phenomena

Classical and quantum phase transitions are phenomena of great interest in modern physics, both theoretically and experimentally. Classical phase transitions are generally driven by thermal fluctuations [2, 5, 6, 94, 95, 112–117], while their quantum counterparts arise from quantum fluctuations in the zero-temperature limit [14, 101, 117, 118]. Phase transitions separate different phases characterized by distinctive properties. In many cases they are associated with the spontaneous breaking of a global symmetry, due to the condensation of an order parameter and the emergence of a corresponding ordering. Notable exceptions occur in the presence of gauge symmetries. In this case the transition may be driven by topological excitations [12, 20, 119, 120], without a local order parameter and without breaking any global symmetry.

Phase transitions occur when the free-energy density, or the ground-state properties at quantum transitions, are singular in the thermodynamic limit [2, 6, 14, 94, 95, 101, 112–118, 121–127]. Depending on the nature of the singularity, phase transitions are generally distinguished as first-order or continuous phase transitions. They are continuous when the bulk properties change continuously at the transition point and

the correlation functions are characterized by a length scale that diverges at criticality. They are of first order when the thermodynamic or ground-state properties in the infinite-volume (thermodynamic) limit are discontinuous across the transition point.

The basic concepts underlying our understanding of phase transitions were developed in a classical setting, in several seminal works by Kadanoff, Fisher, Wilson, among others (see, e.g., Refs. [6, 94, 113, 114, 124, 125, [128-130]). Prototypical d-dimensional continuous transitions are characterized by one relevant parameter r, which is associated with a perturbation of the critical theory that does not break the global symmetry. It is defined so that the critical point corresponds to r=0, the disordered phase to r>0, and the ordered phase to r < 0. At thermal transitions r corresponds to the reduced temperature, i.e., $r \sim T/T_c - 1$, where T_c is the critical temperature. When approaching the critical point from the disordered phase, the length scale ξ of the critical modes diverges as $\xi \sim r^{-\nu}$, where ν is a universal length-scale critical exponent that is related to the RG dimension $y_r = 1/\nu$ of the parameter r. The description of the critical behavior at a phase transition is generally supplemented with a second relevant parameter h—e.g., an external homogeneous magnetic field in magnetic systems—coupled with the order parameter whose condensation drives the spontaneous breaking of the symmetry. The parameter h corresponds to a RG perturbation that explicitly breaks the global symmetry. This perturbation is relevant and therefore the correlation length ξ does not diverge when $h \neq 0$ (in particular, for r = 0 the length scale diverges as $\xi \sim |h|^{-1/y_h}$ when decreasing |h|, where y_h is the RG dimension of the parameter h). Therefore, the critical behavior occurs only for r=0 and h=0. This critical behavior is crucial to define the continuum limit of statistical models, providing a nonperturbative realization of a corresponding continuum SFT [2-4, 100, 131].

Paradigmatic examples of models undergoing finite-temperature continuous transitions are the N-vector models, defined by the Hamiltonian

$$H = -J \sum_{x,\mu} s_x \cdot s_{x+\hat{\mu}} - \sum_x h \cdot s_x, \qquad s_x \cdot s_x = 1, \tag{1}$$

on a cubic lattice, with the partition function $Z = \sum_{\{s\}} e^{-H/T}$. The one-component (N = 1) case corresponds to the Ising model.

A summary of the most important scaling aspects of the RG theory of critical phenomena at classical finite-temperature transitions, see, e.g., Refs. [2, 6, 8, 9, 94, 95, 113, 114, 124, 125, 127, 129, 130, 132–137], is reported in Appendix A. The extension to quantum systems is based on the quantum-to-classical mapping, which allows us to map a quantum system defined in a spatial volume V_s onto a classical one defined in a box of volume $V_c = V_s \times L_T$, with $L_T = 1/T$ (in the appropriate units) [14, 101, 118, 138] and periodic or antiperiodic boundary conditions for bosonic and fermionic excitations, respectively. Under the quantum-to-classical mapping, the inverse temperature corresponds to the system size in the imaginary-time direction. Thus, the universal zero-temperature critical behavior observed at a quantum transition in d dimensions is analogous to the behavior of a corresponding D-dimensional classical system with D = d + 1.

In this review we discuss statistical systems undergoing classical transitions. However, many results on the general features of the transitions and the corresponding critical behavior can be extended to quantum transitions in a lower dimension by means of the quantum-to-classical mapping.

¹It is important to remark that the quantum-to-classical mapping does not generally lead to standard classical isotropic systems. In some instances one obtains complex-valued Boltzmann weights. Moreover, the corresponding classical systems are generally anisotropic. If the dynamic exponent z that controls the scaling behavior of the energy gap [14, 101] is equal to 1, as for Ising-like quantum transitions, the anisotropy is weak, as in the classical Ising model with direction-dependent couplings. In these cases, a straightforward rescaling of the imaginary time allows one to recover space-time rotationally invariant (relativistic) statistical field theories. Therefore, the critical behavior in isotropic (d+1)-dimensional classical statistical systems is directly related with that in d-dimensional quantum systems only if the dynamic exponent satisfies z = 1. However, there are also interesting quantum transitions with $z \neq 1$, such as the superfluid-to-vacuum and Mott transitions in lattice particle systems described by the Hubbard and Bose-Hubbard models [14, 139] (in this case, z = 2 when the transitions are driven by the chemical potential). For continuous quantum transitions with $z \neq 1$, the anisotropy is strong, i.e., correlations have different exponents in the spatial and thermal directions. Indeed, in the case of quantum systems of size L, under a RG rescaling by a factor b such that $\xi \to \xi/b$ and $L \to L/b$, the additional length L_T scales differently, as $L_T \to L_T/b^z$. However, RG theory also applies to classical strongly anisotropic systems [140]. An even stronger anisotropy arises in first-order quantum transitions, which may actually qualitatively depend on the spatial boundary conditions [117].

2.2. The field-theoretical Landau-Ginzburg-Wilson approach to continuous phase transitions

The Landau paradigm [141, 142] for continuous phase transitions is based on the idea that a phase transition is driven by the condensation of an order parameter, which characterizes the two phases separated by the transition: it vanishes in the disordered phase, up to the critical point, then it takes a nonzero value (in the limit $h \to 0$), giving rise to the spontaneous breaking of the symmetry.²

In the Landau description of continuous phase transitions, extended to incorporate the scaling and universality hypotheses [94, 113, 128, 129, 144, 145], the most important assumptions are the following:

- (i) The existence of an order parameter, which effectively describes the critical modes and signals the spontaneous breaking of the global symmetry.
- (ii) The scaling hypothesis, which assumes that the singular part of the thermodynamic observables and of the correlation functions of the order parameter are scale invariant at criticality. Close to the critical point, they satisfy scaling relations when expressed in terms of appropriately defined scaling fields.
- (iii) The universality of the critical behavior, which is only determined by a few global properties of the model, such as the space dimensionality, the nature and the symmetry of the order parameter, the symmetry-breaking pattern, and the range of the effective interactions.

The RG theory of critical phenomena [94, 113, 145, 146] provides a general framework, in which these properties naturally arise. It considers the RG flow in the Hamiltonian-parameter space. The critical behavior is associated with a stable FP of the RG flow, where only a few RG perturbations are relevant. The corresponding positive eigenvalues of the linearized theory around the FP are related to the critical exponents ν , η , etc. In Appendix A we briefly review the key points of the RG theory, such as the homogeneous scaling laws for the thermodynamic functions and for the correlation functions of the order-parameter field.

In the RG framework, a quantitative description of many continuous phase transitions can be obtained by considering effective LGW Φ^4 field theories. The fundamental field is a multicomponent field $\Phi(x)$, which can be thought as obtained by coarse-graining the order parameter. The dynamics of $\Phi(x)$ is specified by the LGW Lagrangian, which is the most general fourth-order polynomial in $\Phi(x)$, which is invariant under the global symmetry transformations of the system. Higher powers of $\Phi(x)$ are supposed to be irrelevant (this is an exact result sufficiently close to four dimensions, which is assumed to be valid in three dimensions, too). The LGW theory predicts the possible symmetry-breaking patterns at the transition. The corresponding critical behaviors are controlled by the FPs of the RG flow in the space of the parameters of the quartic scalar potential, which is determined by the corresponding β functions [2, 8, 95].

As already mentioned, the quantum-to-classical mapping allows us to extend the classical results to the corresponding quantum transitions, since d-dimensional quantum transitions are described by (d+1)-dimensional statistical (quantum) field theories.

We now present more details for some specific LGW theories that will be particularly relevant in the following.

2.2.1. O(N)-symmetric Φ^4 theory

The simplest LGW model is the O(N)-symmetric Φ^4 theory, defined by the Lagrangian density

$$\mathcal{L}_{\mathcal{O}(N)} = \partial_{\mu} \mathbf{\Phi} \cdot \partial_{\mu} \mathbf{\Phi} + r \mathbf{\Phi} \cdot \mathbf{\Phi} + u (\mathbf{\Phi} \cdot \mathbf{\Phi})^{2}, \tag{2}$$

²Note, however, that the symmetry of the long-range behavior of the correlation functions at criticality does not necessarily coincide with the actual global symmetry of the model. In some cases the critical modes show an effective enlargement of the symmetry. If G is the symmetry group of the model, the critical behavior is invariant under a larger symmetry group G', if the operators responsible for the breaking $G' \to G$ are irrelevant at the transition. For instance, this occurs in the 3D \mathbb{Z}_Q clock models [143], which are invariant under \mathbb{Z}_Q transformations. For Q > 4 the critical behavior belongs to the XY universality class with an enlarged U(1) global symmetry (see Sec. 3.5.2).

where $\Phi(x)$ is an N-component real field. It is associated with the so-called N-vector universality class, characterized by an N-component vector order parameter and by the symmetry-breaking pattern $O(N) \rightarrow O(N-1)$. Several continuous transitions belong to these universality classes, such as the finite-temperature transitions in the N-vector models with Hamiltonian (1). The Ising universality class corresponds to N=1. It is relevant for the liquid-vapor transition in simple fluids, for the Curie transition in uniaxial magnetic systems, etc. The XY universality class (N=2) describes the superfluid transition in ⁴He, the formation of Bose-Einstein condensates in interacting bosonic gases, transitions in magnets with easy-plane anisotropy and in superconductors. The Heisenberg universality class (N=3) describes the Curie transition in isotropic magnets. The O(4)-symmetric model is believed to be the effective critical theory for the hadronic finite-temperature transition with two light quarks in the chiral limit. Moreover, the N-vector model for $N \rightarrow 0$ describes the behavior of dilute homopolymers in a good solvent, in the limit of large polymerization. See, e.g., Refs. [2, 95] for reviews on the O(N)-symmetric Φ^4 field theories. In Appendix B we report accurate estimates of the critical exponents for the 3D Ising, XY, and Heisenberg universality classes.

2.2.2. U(N)-symmetric Φ^4 theory

We now discuss a straightforward generalization of the O(N) Φ^4 theory, appropriate to describe transitions in U(N)-symmetric models driven by a complex N-dimensional vector order parameter. The corresponding LGW theory is defined in terms of a complex N-component vector field $\Psi(x)$. The most general U(N)-symmetric LGW Lagrangian is

$$\mathcal{L}_{\mathrm{U}(N)} = \partial_{\mu}\bar{\mathbf{\Psi}}\cdot\partial_{\mu}\mathbf{\Psi} + r\bar{\mathbf{\Psi}}\cdot\mathbf{\Psi} + u(\bar{\mathbf{\Psi}}\cdot\mathbf{\Psi})^{2}.$$
 (3)

A remarkable property of this $\mathrm{U}(N)$ -invariant LGW Lagrangian is that it is symmetric under a larger $\mathrm{O}(2N)$ symmetry group. This can be easily seen by noting that the Lagrangian (3) is equivalent to that of the $\mathrm{O}(2N)$ -vector models, cf. Eq. (2), if the complex field component Ψ^a is rewritten as $\Psi^a = \Phi^a + i\Phi^{a+N}$, where Φ^a is a real (2N)-component vector. As one can easily check, $\mathrm{U}(N)$ -symmetric terms that break the $\mathrm{O}(2N)$ symmetry require higher powers of the field Ψ . Indeed, the lowest-dimensional scalar operator breaking the $\mathrm{O}(2N)$ symmetry is the dimension-six operator $\sum_{\mu} |\bar{\Psi} \cdot \partial_{\mu} \Psi|^2$.

Therefore, the LGW theory predicts that the critical behavior of U(N)-symmetric systems, at phase transitions driven by the condensation of a complex N-component order parameter, belong to the O(2N) vector universality class, which implies an effective enlargement of the symmetry of the critical modes, from U(N) to O(2N). The U(N)-symmetric RG perturbations breaking the O(2N) symmetry are irrelevant in the critical limit, giving only rise to suppressed scaling corrections.

Note however that, although the critical modes show an effective enlarged O(2N) symmetry, and therefore they are associated with a $O(2N) \rightarrow O(2N-1)$ symmetry-breaking pattern, there is no enlargement of the symmetry within the low-temperature phase, which is only invariant under $U(1) \otimes U(N-1)$ transformations. This is crucial to determine the properties of the gapless Goldstone modes characterizing the low-temperature phase. In particular, their number is significantly smaller than that associated with the spontaneous symmetry breaking $O(2N) \rightarrow O(2N-1)$, see, e.g., Ref. [2].

2.2.3. Generic Landau-Ginzburg-Wilson Φ^4 theory with a single quadratic invariant

Beside O(N) and U(N) invariant models, there are physically interesting transitions that are described by LGW Φ^4 field theories that are characterized by more complex symmetries and symmetry-breaking patterns, see, e.g., Refs. [2, 95, 130, 147–149]. The most general LGW Lagrangian for an N-component order-parameter field $\Phi_i(\boldsymbol{x})$ (with i=1,2,...N) can be written as

$$\mathcal{L}_{LGW} = \sum_{i} (\partial_{\mu} \Phi_{i})^{2} + \sum_{i} r_{i} \Phi_{i}^{2} + \sum_{ijkl} u_{ijkl} \Phi_{i} \Phi_{j} \Phi_{k} \Phi_{l}. \tag{4}$$

The number of independent quadratic r_i and quartic u_{ijkl} parameters crucially depends on the symmetry group of the theory. An interesting class of models are those in which $\sum_i \Phi_i^2$ is the unique quadratic term that is invariant under the symmetry group of the theory [2, 147]. In this case, all r_i are equal, $r_i = r$, and

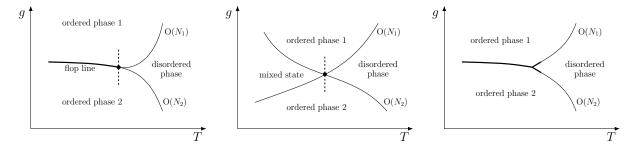


Figure 1: Possible phase diagrams in the T-g plane for the $O(N_1) \oplus O(N_2)$ LGW theory. The critical lines intersect at a bicritical point (left), a tetracritical point (center), and at a first-order transition point (right), located at $(T_{\rm mc}, g_{\rm mc})$. Here, T is the temperature and g is a second relevant parameter. The thick line ("flop line") represents first-order transitions. A bicritical behavior (left) is characterized by the presence of a first-order line that starts at the MCP and separates the two different ordered low-temperature phases. In the tetracritical case (center), there exists a mixed low-temperature phase in which both types of ordering coexist and which is bounded by two critical lines meeting at the tetracritical point. The dashed lines in the two leftmost figures show trajectories at fixed $T = T_{\rm mc}$, going from one ordered phase to the other one across a continuous transition at the MCP. It is also possible that the transition at the meeting point is of first order (right). In this case the two first-order lines, which start at the intersection point and separate the disordered phase from the ordered phases, end in tricritical points and then continue as critical lines. See Refs. [95, 172–176] for studies of the RG flow and scaling behavior at MCPs, and also Appendix A.4 for a brief overview.

 u_{ijkl} must satisfy the trace condition $[147] \sum_i u_{iikl} \propto \delta_{kl}$, to avoid the generation of other quadratic invariant terms under RG transformations. In these models, criticality is driven by tuning the single parameter r, which may correspond to the reduced temperature. Therefore, these cases correspond to the prototypical transitions outlined in Sec. 2.1. All field components become critical simultaneously and the two-point function in the disordered phase is diagonal, that is, $G_{ij}(x,y) \equiv \langle \Phi_i(x)\Phi_j(y)\rangle = \delta_{ij}G(x,y)$. LGW theories with multiparameter quartic terms provide effective descriptions of complex phase transitions in several physical contexts [95]. We mention anisotropic magnets (see, e.g., Refs. [130, 150]), disordered systems (see, e.g., Refs. [151–154]), frustrated systems (see, e.g., Refs. [155–160]), spin and density wave models (see, e.g., Refs. [161–166]), LAH models in the strong gauge-coupling limit (see, e.g., Refs. [84, 167, 168]), multiflavor scalar chromodynamics [97, 169], and also the finite-temperature chiral transition in hadronic matter with N_f light flavors [25, 170, 171].

The RG flow in Φ^4 theories, such as those with Lagrangian density (4), has generally several FPs. Among them, the stable FP controls the critical behavior of the corresponding continuous transitions, and therefore can be associated with their universality class. If there is no stable FP, the transitions in the corresponding class of models are generally expected to be first order, unless the considered field-theoretical model misses some relevant features of the transitions under investigation.

2.2.4. Multicritical $O(N_1) \oplus O(N_2) \Phi^4$ theories

LGW theories (4) in which the symmetry allows several quadratic terms are also relevant phenomenologically. In particular, they provide effective field-theoretical models describing the multicritical behaviors that occur in the presence of competing orderings [172–174]. The main features of the critical behavior at multicritical points (MCPs) are discussed in Appendix A.4.

As a paradigmatic example, one may consider multicritical LGW theories that describe the competition of order parameters associated with two different global $O(N_1)$ and $O(N_2)$ symmetries. They can be obtained by constructing the most general $O(N_1) \oplus O(N_2)$ -symmetric Φ^4 theory with two order-parameter real vector fields $\phi_1(\boldsymbol{x})$ and $\phi_2(\boldsymbol{x})$, with N_1 and N_2 components, respectively. Their Lagrangian density reads [95, 172–175]

$$\mathcal{L}_{\text{mc}} = \sum_{a=1}^{2} \left[\partial_{\mu} \phi_{a} \cdot \partial_{\mu} \phi_{a} + r_{a} \phi_{a} \cdot \phi_{a} + v_{a} (\phi_{a} \cdot \phi_{a})^{2} \right] + w \phi_{1} \cdot \phi_{1} \phi_{2} \cdot \phi_{2}.$$
 (5)

The multicritical theory is characterized by two relevant quadratic operators, those proportional to r_1 and r_2 in the Lagrangian (5). Therefore, in the microscopic model and in the absence of external fields breaking the global $O(N_1) \oplus O(N_2)$ symmetry, there are two relevant parameters which should be tuned to approach the MCP: beside the temperature T, there is a second relevant parameter that is referred to as g in Fig. 1. The parameters r_1 and r_2 will be in general linear combinations of $T - T_{\rm mc}$ and of $g - g_{\rm mc}$, where $T_{\rm mc}$ and $g_{\rm mc}$ are the values of T and g at the MCP.

The phase diagram of the model (5) shows different disordered and ordered phases, separated by transition lines meeting in one point. A standard mean-field analysis of the model shows that, by varying the quartic coupligs v_1 , v_2 , and w, one can obtain qualitatively different phase diagrams [172–174], as shown in Fig. 1. The multicritical behavior of models associated with a multicritical LGW theory is again determined by the RG flow in the space of the quartic parameters [95, 172–180]. Again, a multicritical universality class is generally associated with a stable FP of such RG flow.

This issue has been addressed by using perturbative field-theoretical methods [172, 174, 175, 179], for example by computing and analyzing high-order ε -expansion series [175], and numerical methods, see, e.g., Ref. [176, 178]. The predicted behavior crucially depends on the number N_1 and N_2 of components of the competing order parameters. The RG flow of the multicritical $O(N_1) \oplus O(N_2)$ LGW theories for $N_1 + N_2 \ge 4$, see, e.g., Refs. [95, 172–175, 178–180], shows that continuous MCPs are tetracritical (see the central panel of Fig. 1), because the only stable FP is associated with a decoupled $O(N_1)$ and $O(N_2)$ critical behavior. Therefore, when the phase diagram is characterized by three transition lines meeting in one point, the competition of the $O(N_1)$ and $O(N_2)$ order parameters gives generally rise to first-order transitions close to the meeting point, as shown in the right panel of Fig. 1 (unless an additional tuning of the model parameters is performed). On the other hand, the competition of two Ising order parameters— $N_1 = N_2 = 1$ in this case—(see also Sec. 7.4.3) can give rise to a phase diagram such as that shown in the left panel of Fig. 1. In this case the multicritical behavior is controlled by the XY FP, thus, the global symmetry of the multicritical modes at the MCP enlarges from $\mathbb{Z}_2 \oplus \mathbb{Z}_2$ to O(2). Finally, for $N_1 + N_2 = 3$ the stable FP of the 3D RG flow is the so-called biconical FP, which is believed to be associated with a tetracritical point [172–175, 179, 180]. No stable FP corresponding to a bicritical point (left panel of Fig. 1) exists, although the corresponding bicritical O(3)-symmetric FP turns out to be very weakly unstable [175, 179].

We finally remark that a continuous MCP separates different ordered phases, see Fig. 1. For example, assume that g is increased for fixed $T=T_{\rm mc}$ (see the dashed lines reported in the leftmost and central panel of Fig. 1). The system is at the beginning in the low-g ordered phase, then undergoes a continuous transition at the MCP, and finally is in the second ordered phase. Therefore, multicritical LGW theories can describe continuous transitions between phases characterized by different orderings. Note, however, that the multicritical behavior requires the tuning of an additional parameter. This observation clarifies when the Landau paradigm— there are no continuous transitions between phases with different symmetry—holds. Indeed, while it holds for generic transitions, it may be violated by an appropriate tuning of the parameters.

3. Phase transitions and critical phenomena in the presence of gauge symmetries

The description of the main features of phase transitions in the presence of gauge symmetries is more complex than that outlined in the previous Section. First of all, while conventional transitions are always related to the condensation of a local order parameter, in the presence of gauge fields, we may have transitions without local order parameter (topological transitions). When an order parameter is present, we also need to distinguish its behavior under gauge transformations: the order parameter may be gauge invariant as well as not gauge invariant. Moreover, the role of gauge fields may differ. In some transitions, gauge fields are only relevant to define the set of critical modes (the gauge-invariant ones), while in some other cases, the phase transition is due to a nontrivial interplay between matter and gauge fields, so that gauge fields determine the critical behavior and should be included in the corresponding effective field theory (these transitions will be named charged transitions).

It is worth noting that the study of the critical behavior of gauge-symmetric models is also relevant to understand the critical behavior of unconventional transitions in condensed-matter physics, in which a gauge symmetry is supposed to emerge at criticality, see, e.g., Refs. [7, 12, 13, 15, 20, 21, 181, 182].

Unconventional quantum transitions [20, 21, 183] are observed between topological phases [69, 184–186], in the context of the integer and fractional quantum Hall effect [187–190]. We also mention transitions between topologically-ordered and valence-bond-solid (VBS) phases [27], and direct transitions between differently ordered phases, such as the Néel-to-VBS transition of 2D quantum magnets [33, 191]. *Deconfined* quantum transitions that exhibit fractionalization of the low-energy excitations, topological order, and long-range entanglement also admit an effective description in terms of field theories with emergent gauge fields coupled with matter fields carrying fractional quantum numbers of the microscopic global symmetry, see, e.g., Refs. [20, 21] for reviews. Studies of deconfined transitions are reported in, e.g., Refs. [21, 31–34, 37–40, 72, 74, 80, 83, 191–203], and references therein.

3.1. Different types of critical scenarios in statistical models with gauge symmetries

As we have mentioned above, in the presence of gauge symmetries, the effective LGW approach discussed in Sec. 2 cannot be generically applied. Other approaches should also be used to obtain an effective description of the critical behavior. The choice of the appropriate approach depends on the main features of the mechanism driving the particular phase transition of the lattice gauge model under study.

In general, four classes of transitions may be distinguished in statistical systems with gauge symmetry, each one admitting a different description:

- LGW transitions, in which only gauge-invariant correlations of the matter field are critical. They admit a conventional effective LGW field-theoretical description in terms of a gauge-invariant order-parameter field, which orders at the transition, driving the spontaneous breaking of the global symmetry. Gauge fields do not display critical correlations. The gauge symmetry only prevents nongauge-invariant observables from becoming critical.
- LGW^{\times} transitions, in which only matter fields develop critical correlations, similarly to LGW transitions. They also admit a LGW description, but in this case the order-parameter field is not gauge invariant.³ Therefore, to distinguish them from standard LGW transitions, we add the superscript \times .⁴ In particular, systems with discrete gauge groups undergo LGW $^{\times}$ transitions for sufficiently weak gauge couplings.
- GFT transitions, in which the critical behavior is due to a nontrivial interplay of scalar and gauge critical excitations. Therefore, their description requires an effective gauge field theory (GFT), with dynamical gauge and matter fields. GFT transitions are observed in the presence of continuous Abelian and non-Abelian gauge symmetries. They also occur in models that are locally invariant under discrete groups when the gauge symmetry enlarges at criticality, so that the critical modes are invariant under a continuous group.
- Topological transitions, driven by topological modes, in which one cannot identify a local order-parameter field. A typical example is provided by the topological transition of the 3D lattice \mathbb{Z}_2 -gauge model [119].

We do not claim that the above classification is exhaustive, i.e., that all classical and quantum phase transitions in the presence of gauge symmetries belong to one of these four classes. However, the above classes of transitions cover all classical (thermal) phase transitions that we will discuss in this review, and the corresponding quantum transitions related by the quantum-to-classical mapping. In the following subsections we discuss the four possibilities in more detail, mentioning some examples. Other examples will be found in the following sections.

 $^{^3}$ It is important to note that the gauge symmetry can never be broken [8, 43, 204, 205], despite the common use of referring to the Higgs mechanism as a spontaneous gauge symmetry breaking. The statement that in some cases a nongauge invariant order parameter is needed does not refer to the description of the thermodynamic phases, but to the definition of the effective model which encodes the universal critical properties of the continuous phase transition. In LGW $^{\times}$ transitions the critical behavior of gauge-invariant quantities is the same as that of composite operators defined in terms of a nongauge invariant field, which is considered the fundamental field in the effective LGW description. As it is not gauge invariant, the order-parameter field can be identified in the gauge model only if an appropriate gauge fixing condition is added.

⁴Note that transitions with similar properties have been sometimes called LGW* transitions, see, e.g., Ref. [21].

3.2. LGW transitions with a gauge-invariant order parameter

The first class of transitions, the LGW transitions, is characterized by the fact that only gauge-invariant matter correlations are critical. Gauge fields have apparently only the role of hindering some scalar degrees of freedom, those that are not gauge invariant, from becoming critical. It seems thus natural to assume that the transition is driven by a gauge-invariant order parameter and that only gauge-invariant matter modes are relevant at criticality. Although this assumption seems natural, it is important to stress that it is not strictly necessary. There are indeed transitions (the LGW[×] transitions that we will discuss in Sec. 3.3) that are analogous to the LGW transitions as only matter fields are critical, but that require a scalar nongauge invariant order parameter. If the scalar order parameter is gauge invariant, the approach is the conventional one. Once an order parameter has been identified, one considers the corresponding order-parameter field and LGW Lagrangian. The critical behavior is then determined by studying the field-theoretical model as outlined in Sec. 2.2. Note that the gauge fields do not appear in the effective description: the gauge symmetry plays only a role in selecting the order-parameter field, which should be gauge invariant.

In the next subsections we present some examples of LGW transitions, which will be also useful for the rest of the review. Other examples will be presented later in the review.

3.2.1. Three-dimensional CP^{N-1} models

The transition in the 3D lattice CP^{N-1} model, and also the transitions in LAH models (they are discussed in Secs. 5 and 6) in the strong gauge-coupling (small- κ) regime, are examples of LGW transitions. In the \mathbb{CP}^{N-1} field theory the fundamental field is a complex N-component unit-length vector $\boldsymbol{z}(\boldsymbol{x})$, associated with an element of the complex projective manifold \mathbb{CP}^{N-1} [2]. The Lagrangian reads

$$\mathcal{L}_{CP} = \frac{1}{2g} \overline{D_{\mu} z} \cdot D_{\mu} z, \qquad D_{\mu} = \partial_{\mu} + i A_{\mu}, \qquad A_{\mu} = i \bar{z} \cdot \partial_{\mu} z, \tag{6}$$

where A_{μ} is a composite real gauge field. The model is characterized by a global U(N) symmetry $z(x) \rightarrow$ Uz(x) with $U \in U(N)$, and a local U(1) gauge symmetry $z(x) \to e^{i\Lambda(x)}z(x)$.

The corresponding simplest lattice formulation is

$$Z = \sum_{\{\boldsymbol{z}\}} e^{-H_{\text{CP}}/T}, \qquad H_{\text{CP}} = -J \sum_{\boldsymbol{x},\mu} |\bar{\boldsymbol{z}}_{\boldsymbol{x}} \cdot \boldsymbol{z}_{\boldsymbol{x}+\hat{\mu}}|^2, \qquad \bar{\boldsymbol{z}}_{\boldsymbol{x}} \cdot \boldsymbol{z}_{\boldsymbol{x}} = 1, \tag{7}$$

where the sum is over the sites x of a cubic lattice, μ runs from 1 to 3, and $\hat{\mu} = \hat{1}, \hat{2}, \dots$ are unit vectors along the lattice directions. An alternative formulation (gauge \mathbb{CP}^{N-1} model) is obtained by introducing link gauge variables $\lambda_{x,\mu}$ with $|\lambda_{x,\mu}| = 1$, and defining [82, 206–208]⁶

$$Z = \sum_{\{\boldsymbol{z},\lambda\}} e^{-H_{\lambda}/T}, \qquad H_{\lambda} = -2NJ \sum_{\boldsymbol{x},\mu} \operatorname{Re}\left(\lambda_{\boldsymbol{x},\mu} \, \bar{\boldsymbol{z}}_{\boldsymbol{x}} \cdot \boldsymbol{z}_{\boldsymbol{x}+\hat{\mu}}\right), \qquad \bar{\boldsymbol{z}}_{\boldsymbol{x}} \cdot \boldsymbol{z}_{\boldsymbol{x}} = 1.$$
(8)

The lattice \mathbb{CP}^{N-1} models have a finite-temperature transition in 3D that admits a LGW description. The order parameter is the gauge-invariant bilinear perator

$$Q_x^{ab} = \bar{z}_x^a z_x^b - \frac{1}{N} \delta^{ab}, \tag{9}$$

which is a Hermitian and traceless $N \times N$ matrix. Therefore, to study the nature of the transition, one may construct an effective LGW theory in terms of a traceless Hermitian field $\Phi^{ab}(x)$, which can be formally obtained from the average of Q_x^{ab} over a large but finite lattice domain. The LGW field theory is obtained

⁵The CP¹ field theory is equivalent to the O(3) non-linear σ model with the identification $s^a = \sum_{ij} \bar{z}^i \sigma^a_{ij} z^j$, where a = 1, 2, 3and σ^a are the Pauli matrices. An analogous equivalence applies to the corresponding N=2 lattice models (7) and (8). ⁶Since there is no kinetic term for the gauge fields, the link variables can be integrated out, obtaining Z

 $[\]sum_{\{\boldsymbol{z},\lambda\}} \exp(-H_{\lambda}) = \sum_{\{\boldsymbol{z}\}} \prod_{\boldsymbol{x},\mu} I_0(2NJ|\bar{\boldsymbol{z}}_{\boldsymbol{x}} \cdot \boldsymbol{z}_{\boldsymbol{x}+\hat{\mu}}|), \text{ where } I_0(x) \text{ is a modified Bessel function (here we set } T=1).$

by considering the most general fourth-order polynomial in Φ consistent with the global U(N) symmetry, i.e.,

$$\mathcal{L} = \text{Tr}(\partial_u \Phi)^2 + r \text{Tr} \Phi^2 + w \text{Tr} \Phi^3 + u (\text{Tr} \Phi^2)^2 + v \text{Tr} \Phi^4.$$
 (10)

The stable FP of the RG flow of the LGW theory (10) is expected to control the critical behavior of the continuous transitions in lattice CP^{N-1} models. In the absence of a stable FP, a first-order transition is

For N=2, the cubic term in Eq. (10) is absent, and the two quartic terms are equivalent. Therefore, one recovers the O(3)-symmetric LGW theory, consistently with the equivalence between the CP¹ and the Heisenberg model, see footnote 5. For N > 3, the cubic term is generically expected to be present. This is usually considered as the indication that the phase transitions occurring in this class of systems are of first order, as one can easily infer using mean-field arguments.⁸ Continuous transitions may still occur, but they require a fine tuning of the microscopic parameters leading to the effective cancellation of the cubic term.⁹

Numerical simulations of the lattice gauge \mathbb{CP}^{N-1} model (8) confirm the LGW predictions [82]. For $N \geq 3$ the transition is of first order, the first-order nature becoming stronger and stronger as N increases [210]. In the effective description the gauge group plays no role and thus one expects the same critical behavior in any SU(N) invariant model that has a bilinear Hermitian order parameter, irrespective of the nature of the gauge group. This conclusion is supported by the results of Ref. [214], which studied a discretized gauge model with Hamiltonian still given by Eq. (8) but with a reduced \mathbb{Z}_Q gauge symmetry, obtained by requiring the gauge fields to take only the values $\exp(2\pi i n/Q)$ with $n=0,\ldots Q-1$. For N=2the model undergoes an O(3) transition for any $Q \geq 3$, as the CP¹ model—this can be shown by explicitly performing the summation over the gauge degrees of freedom—indicating that the nature of the gauge group is not important.

The LGW prediction is apparently in contradiction with the results obtained by performing a standard 1/N expansion in the lattice model (8), as they predict a continuous transition [206–208]. It turns out that these calculations are based on the incorrect assumption that the relevant large-N saddle-point solutions are spatially homogeneous and that the gauge fields are ordered for all values of J [210]. While this assumption is correct in the large-J phase, it does not hold for small values of J, because of the presence of topologically nontrivial configurations, for instance those discussed in Ref. [215], which forbid the ordering of the gauge fields.

Finally, it is interesting to note that an analysis within the 1/N-expansion framework indicates that the \mathbb{CP}^{N-1} field theory with Lagrangian (6) is equivalent [2, 64] to the Abelian Higgs field theory (AHFT), or scalar electrodynamics, which will be presented in Sec. 3.4, whose RG flow has a stable charged FP for large values of N, see Sec. 4. This result however does not apply to the lattice \mathbb{CP}^{N-1} models. Indeed, gauge fields can be integrated out in the lattice gauge \mathbb{CP}^{N-1} models, obtaining a Hamiltonian that can be written as a sum of local gauge-invariant scalar terms. Thus, gauge modes cannot be relevant for the critical

⁷The same effective description applies to antiferromagnetic \mathbb{CP}^{N-1} models, i.e., to the model with Hamiltonian (7) and J < 0 (in the Hamiltonian (8) the sign of J is irrelevant, and therefore the model is always ferromagnetic). In this case, however, there is an additional Z₂ symmetry related to translations of one site [209], which implies that the corresponding effective LGW theory (the order-parameter field is related to a staggered gauge-invariant composite operator) must also be invariant under $\Phi \to -\Phi$. This implies the absence of the cubic term in the LGW theory (10), i.e., w=0. For N=3 this LGW Hamiltonian is equivalent to that of the O(8) vector model, thus predicting a critical behavior belonging to the O(8) vector universality class, with an effective enlargement of the symmetry group of the critical modes from SU(3) to O(8). This prediction has been confirmed numerically [209]. The critical behavior for larger values of N is discussed in Refs. [167, 209].

⁸ The mean-field argument that predicts a first-order transition in the presence of a cubic term in the LGW Lagrangian is strictly valid in four dimensions. The nature of the transition should not change sufficiently close to four dimensions, as long as statistical fluctuations are small. In particular, it is usually assumed that the four-dimensional mean-field prediction also applies in three dimensions.

If this occurs, the critical behavior is controlled by the effective theory relevant for antiferromagnetic models, see footnote

^{7.} For N=3 continuous transitions would belong to the O(8) vector universality class [209].

10 It should be noted that results for other models that are expected to behave as the CP^{N-1} model are less clear. In particular, there is no general agreement that all models undergo a first-order transition for N=3, see, e.g., Refs. [64, 82, 167, 209, 211–

behavior, as instead would be the case if the CP^{N-1} transition were effectively described by a gauge field theory with dynamical gauge fields, as the AHFT presented in Sec. 3.4 below. A more detailed discussion is presented in Secs. 5 and 6.

3.2.2. Three-dimensional RP^{N-1} models

 RP^{N-1} models are the real analogues of the CP^{N-1} models. The fundamental field is a real N-vector field s_x satisfying $s_x \cdot s_x = 1$. The standard RP^{N-1} Hamiltonian is

$$H_{\rm RP} = -J \sum_{\boldsymbol{x},\mu} (\boldsymbol{s}_{\boldsymbol{x}} \cdot \boldsymbol{s}_{\boldsymbol{x}+\hat{\mu}})^2. \tag{11}$$

Equivalently, one can introduce a \mathbb{Z}_2 gauge field $\sigma_{x,\mu}$ associated with the links of the lattice, and define

$$H_{\sigma} = -J \sum_{\boldsymbol{x},\mu} \sigma_{\boldsymbol{x},\mu} \, \boldsymbol{s}_{\boldsymbol{x}} \cdot \boldsymbol{s}_{\boldsymbol{x}+\hat{\mu}}, \qquad \sigma_{\boldsymbol{x},\mu} = \pm 1. \tag{12}$$

Both models are invariant under SO(N) global transformations and the \mathbb{Z}_2 gauge transformations

$$s_{x} \to w_{x} s_{x}, \qquad \sigma_{x,\mu} \to w_{x} \sigma_{x,\mu} w_{x+\hat{\mu}}, \qquad w_{x} = \pm 1.$$
 (13)

 $\mathbb{R}P^{N-1}$ models are expected to describe the universal features of the isotropic-nematic transition in liquid crystals [216]. They have been mostly investigated in two dimensions [217–223].

 $3D\ RP^{N-1}$ models undergo a finite-temperature transition. Since the gauge fields are not dynamical, the transition is a LGW transition in terms of a gauge-invariant order parameter, which is identified with the bilinear symmetric tensor

$$R_{\boldsymbol{x}}^{ab} = s_{\boldsymbol{x}}^a s_{\boldsymbol{x}}^b - \frac{1}{N} \delta^{ab}. \tag{14}$$

Therefore, the LGW field is a symmetric and traceless real tensor $\Phi^{ab}(\boldsymbol{x})$, obtained by coarse-graining $R_{\boldsymbol{x}}^{ab}$, and the LGW Lagrangian [167, 168] is¹²

$$\mathcal{L} = \text{Tr}(\partial_u \Phi)^2 + r \text{Tr} \Phi^2 + w \text{Tr} \Phi^3 + u (\text{Tr} \Phi^2)^2 + v \text{Tr} \Phi^4.$$
 (15)

For N=2 the field Φ^{ab} has only two independent components, the Φ^3 term is absent, and the Lagrangian (15) is equivalent to that of the standard XY vector model. Thus, continuous transitions should belong to the XY universality class. In this case the field Φ^{ab} is equivalent to an O(2) vector field. This implies that the RG dimension of R_x^{ab} coincides with the RG dimension of the vector field in the standard XY model.

For larger values of N, the LGW approach predicts [84] first-order transitions due to the presence of the Φ^3 term (see footnote 8 for a discussion of the relation between cubic terms in the LGW Lagrangian and first-order transitions).

3.2.3. Finite-temperature transition of hadronic matter in the chiral limit

As another example where the LGW approach is expected to hold, we consider the finite-temperature transition of hadronic matter in the chiral limit, which was analyzed by Pisarski and Wilczek [25] using the

¹¹Formally, the model corresponds to fields that are defined on the real projective space, which is obtained starting from the sphere S^{N-1} in N dimensions and identifying points that differ by a reflection, i.e., s_x is identified with $-s_x$. In the lattice model, this identification is obtained by requiring the Hamiltonian to be invariant under local reflections of the spins.

¹²The LGW Lagrangian (15) is also relevant for the critical behavior of antiferromagnetic RP^{N-1} models, such as the lattice models (11) with J < 0, at least for $N \le 3$. In this case, however, the effective theory is also invariant under Φ → −Φ, which implies w = 0. For N = 3 the corresponding LGW Hamiltonian is equivalent to that of the O(5) vector theory, implying an effective enlargement of the symmetry group, from O(3) to O(5), at the transition [224]. Numerical results confirm this prediction. For $N \ge 4$ there are discrepancies between the numerical results and the field-theoretical predictions obtained from high-order perturbative analyses of the RG flow of the LGW theory. The origin of these differences is still an open problem, see Ref. [168].

LGW approach. The strong hadronic interactions are described by quantum chromodynamics (QCD), which is a non-Abelian gauge theory with gauge group SU(3) and quark fields in the fundamental representation of the gauge group. The thermodynamics of the system is characterized by a finite-temperature transition at $T_c \simeq 200$ MeV, which separates a low-temperature confined hadronic phase, in which chiral symmetry is broken, from a high-temperature phase with deconfined quarks and gluons (quark-gluon plasma), in which chiral symmetry is restored [225–227]. Our present understanding of this finite-T transition is based on the symmetry properties of the system. In the presence of N_f light quarks, and, in particular, in their massless limit, the relevant symmetry is the chiral symmetry $SU(N_f)_L \otimes SU(N_f)_R$, where L,R stand for left and right quark components. Below T_c , this symmetry is spontaneously broken to $SU(N_f)_V$, the group of vector quark transformations, with a nonzero quark condensate $\langle \bar{\psi}\psi \rangle$. The finite-T transition is therefore characterized by the symmetry-breaking pattern $SU(N_f)_L \otimes SU(N_f)_R \to SU(N_f)_V$.

Let us report here the main assumptions of the approach used by Pisarski and Wilczek to predict the nature of the finite-T chiral transition [25, 149, 170, 171]:

- (i) One assumes that the phase transition is continuous for vanishing quark masses. In this case the length scale of the critical modes diverges approaching T_c , becoming eventually much larger than $1/T_c$, which is the size of the euclidean "temporal" dimension at T_c . Therefore, the asymptotic critical behavior must be associated with a 3D universality class with the same symmetry-breaking pattern.
- (ii) One assumes—this is the crucial unproved assumption in the approach—that gauge modes do not become critical at the transition and that only gauge-invariant quark correlations are relevant at criticality. In other words, one assumes that the finite-T transition is a LGW transition, according to the classification given in Sec. 3.1.
- (iii) To define the LGW theory, an order parameter should be specified. It is identified with the gauge-invariant bilinear quark matrix $\bar{\psi}_{Li}\psi_{Rj}$, $i,j=1,\ldots N_f$. In the LGW framework one introduces a complex-matrix field Ψ_{ij} , which is obtained by coarse-graining the order parameter.
- (iv) The LGW Lagrangian is obtained by considering the most general Lagrangian that is symmetric under the global symmetry group of the original model [170, 171]:

$$\mathcal{L}_{SU(N_f)} = \mathcal{L}_{U(N_f)} + \mathcal{L}_{det},$$

$$\mathcal{L}_{U(N_f)} = \text{Tr}(\partial_{\mu}\Psi^{\dagger})(\partial_{\mu}\Psi) + r\text{Tr}\Psi^{\dagger}\Psi + u\left(\text{Tr}\Psi^{\dagger}\Psi\right)^{2} + v\text{Tr}\left(\Psi^{\dagger}\Psi\right)^{2},$$

$$\mathcal{L}_{det} = w_{1}\left(\det\Psi^{\dagger} + \det\Psi\right) + w_{2}\left(\text{Tr}\Psi^{\dagger}\Psi\right)\left(\det\Psi^{\dagger} + \det\Psi\right) + w_{3}\left[\left(\det\Psi^{\dagger}\right)^{2} + \left(\det\Psi\right)^{2}\right],$$
(16)

where $\mathcal{L}_{\mathrm{U}(N_f)}$ is invariant under $\mathrm{U}(N_f)_L \otimes \mathrm{U}(N_f)_R$ transformations. The Lagrangian $\mathcal{L}_{\mathrm{det}}$ contains terms involving the determinant of Ψ_{ij} , which effectively takes into account the explicit breaking of the $\mathrm{U}(1)_A$ axial symmetry due to the anomaly (Eq. (16) reports all terms that are relevant for $N_f = 2$). Nonvanishing quark masses can be accounted for by adding an external-field term $\mathrm{Tr}(H\Psi + \mathrm{h.c.})$.

The analysis of the RG flow of the model depends on the value of N_f . For $N_f \geq 4$, a continuous finite-T transition is only possible if there is a stable FP of the RG flow that lies in the parameter region in which the symmetry-breaking pattern $SU(N_f)_L \otimes SU(N_f)_R \to SU(N_f)_V$ occurs. Since there is no FP associated with this symmetry-breaking pattern, continuous transitions cannot occur (thus, contradicting the first assumption leading to the LGW approach), and therefore first-order transitions are generally predicted. For $N_f = 3$, the Lagrangian contains a cubic term (the term proportional to w_1), and therefore the transition

 $^{^{13}}$ If the axial U(1)_A symmetry is effectively restored at T_c , the symmetry-breaking pattern becomes U(N_f)_L \otimes U(N_f)_R \rightarrow U(N_f)_V. The restoration of this symmetry is not expected in QCD. However, semiclassical calculations in the high-temperature phase [24] show that instanton effects are exponentially small for $T \gg T_c$, implying that the effect of the breaking the axial U(1)_A symmetry becomes small in this limit. This scenario has been also confirmed by numerical studies, see, e.g., Refs. [228–230]. RG studies of the LGW theory appropriate to describe the finite-T transition with symmetry-breaking pattern U(N_f)_L \otimes U(N_f)_R \rightarrow U(N_f)_V are reported in Refs. [171, 231].

is expected to be of first order, too. For $N_f = 1$ the Lagrangian (16) with $w_i = 0$ reduces to the O(2) symmetric Φ^4 theory, corresponding to the 3D XY universality class, and the term proportional to w_1 plays the role of an external field. Thus, no transitions are expected, but only a crossover.

Given the actual values of the quark masses [232], this approach is mainly of interest for systems with two flavors, i.e., for $N_f = 2$, in which there are only the lightest quarks u and d, that are the building blocks of ordinary hadronic matter, e.g., of the nucleons. The effective LGW theory contains two quadratic terms (those proportional to r and w_1), making the analysis more complex, see Refs. [149, 170, 171]. A detailed analysis suggests that, if the transition is continuous in the chiral limit, it must belong to the 3D O(4) vector universality class, as originally predicted in Ref. [25]. This result can also be understood by noting that the symmetry-breaking pattern $SU(2)_L \otimes SU(2)_R \to SU(2)_V$ is equivalent to $O(4) \to O(3)$ (apart from discrete groups), i.e., it is the same that characterizes transitions in the O(4) vector universality class.

We stress that these predictions are based on a number of assumptions, the main one being that the colored gauge modes are effectively decoupled from the critical modes at the transition. If this assumption is correct, then the effective LGW theory in terms of a gauge-invariant bilinear quark operator can provide reliable predictions. See, e.g., Ref. [227] for a report on the lattice numerical results obtained for the chiral transition.

3.3. LGW^{\times} transitions with a gauge-dependent order parameter

In Sec. 3.2 we discussed LGW transitions where only matter fields show a critical behavior and that admit a conventional LGW description in terms of a scalar gauge-invariant order parameter. In this Section, we discuss a second class of transitions, which we name LGW^{\times} transitions, which are also characterized by the fact that only scalar modes have a critical dynamics, but that do not admit a local gauge-invariant order-parameter field.

3D $O(N)^{\times}$ (Ising[×] and XY[×] for N=1 and 2, respectively) transitions are the simplest examples of this type of unconventional transitions. They admit an effective description in terms of the O(N)-symmetric Φ^4 theory with Lagrangian (2) and can be observed, e.g., in the lattice N-vector model minimally coupled with \mathbb{Z}_2 -gauge variables [233, 234]. On a cubic lattice its partition function is given by

$$Z = \sum_{\{\boldsymbol{s},\sigma\}} e^{-H/T}, \qquad H = -JN \sum_{\boldsymbol{x},\mu} \sigma_{\boldsymbol{x},\mu} \, \boldsymbol{s}_{\boldsymbol{x}} \cdot \boldsymbol{s}_{\boldsymbol{x}+\hat{\mu}} - K \sum_{\boldsymbol{x},\mu>\nu} \sigma_{\boldsymbol{x},\mu} \, \sigma_{\boldsymbol{x}+\hat{\mu},\nu} \, \sigma_{\boldsymbol{x}+\hat{\nu},\mu} \, \sigma_{\boldsymbol{x},\nu}, \tag{17}$$

where the site variables s_x are unit-length N-component real vectors (i.e., $s_x \cdot s_x = 1$), and the link variables $\sigma_{x,\mu}$ take the values ± 1 . The Hamiltonian parameter K plays the role of inverse gauge coupling. For $K \to \infty$ (small gauge-coupling limit) the variable $\sigma_{x,\mu}$ can be set equal to 1 (modulo gauge transformations) and the standard O(N) vector model is recovered. For N=1 the spin variables take the integer values $s_x=\pm 1$, and the model corresponds to the so-called \mathbb{Z}_2 -gauge Higgs model [41, 119, 235]. As we shall discuss in Sec. 7, $O(N)^\times$ transitions are observed along the transition line that separates the spin disordered phase from the spin ordered one, for sufficiently small values of the gauge coupling, i.e., for sufficiently large K.

In conventional N-vector systems with $N \geq 2$ the spontaneous breaking of the O(N) symmetry at the transition is driven by the condensation of the N-component fundamental vector field. However, in the gauge system with Hamiltonian (17), as a consequence of the \mathbb{Z}_2 -gauge symmetry, the local vector correlation $\langle s_x \cdot s_y \rangle$ trivially vanishes for $x \neq y$. Therefore, the spontaneous breaking of the O(N) symmetry can only be observed by considering correlations of composite gauge-invariant operators, such as the gauge-invariant bilinear operator $S_x^{ab} = s_x^a s_x^b - \delta^{ab}/N$, which transforms as a spin-two tensor under O(N) transformations. A distinctive feature of the $O(N)^{\times}$ transitions is that this bilinear operator, as well as all gauge-invariant operators, have the same critical behavior as in the conventional N-vector model without gauge invariance. The equivalent behavior of gauge-invariant correlations in O(N) and $O(N)^{\times}$ transitions implies that gauge modes do not drive the critical behavior. But, more importantly for the characterization of the effective critical behavior, this result allows us to exclude that the composite gauge-invariant operator S_x^{ab} can be taken as the fundamental field in a LGW effective theory. Indeed, if one identifies the LGW field Φ with the coarse-grained gauge-invariant spin-2 order parameter, the corresponding LGW theory turns out to be that of the RP^{N-1} models, cf. Eq. (15), which would predict a different universality class with a different

symmetry-breaking pattern [168], see also Sec. 7.2.2. On the contrary, we conclude that O(N) and $O(N)^{\times}$ transitions have the same effective description, which in turn implies that also $O(N)^{\times}$ transitions admit a LGW characterization in terms of a vector field Φ . The main issue here is the identification of the correct fundamental vector field Φ . As shown in Refs. [233, 234] and Sec. 7.3, this problem can be solved by identifying Φ as the coarse-grained analogue of the fundamental field s_x after an appropriate gauge-fixing procedure is considered. This implies that $O(N)^{\times}$ transitions can still be described by the O(N)-symmetric LGW theory (2), but with a gauge-dependent order-parameter field.

For N=1 there is no global symmetry group, since the global \mathbb{Z}_2 symmetry of the ungauged model has been turned into a local one. However, the global \mathbb{Z}_2 symmetry reemerges in the effective description of the large-K transitions. Their critical features are the same as in the LGW theory associated with the conventional Ising transitions. Therefore, we will name these transitions Ising \times transitions.

It is interesting to remark that, most probably, our interpretation of the transition as due to the condensation of a non-gauge-invariant local order parameter, is not the only one possible. Indeed, an alternative interpretation is that LGW[×] transitions are also controlled by a gauge-invariant order parameter. However, the order parameter is nonlocal, although it admits a local representation when some specific gauge-fixing condition is considered. An explicit realization of this mechanism occurs in noncompact LAH models and is discussed in Sec. 5.1.2.

 LGW^{\times} transitions do not only occur in O(N)-symmetric models, but are expected in generic spin models with more complex global symmetries, when they are coupled with discrete gauge variables. The discrete nature of the gauge group appears to be a crucial property for the existence of LGW^{\times} transitions. Indeed, if the gauge group is discrete it is possible that the pure spin FP remains stable in the presence of a small gauge coupling. If this occurs, in the weak gauge-coupling limit, continuous transitions should be of LGW^{\times} type.

3.4. GFT transitions described by effective field theories with gauge fields

LGW and LGW[×] transitions are both characterized by the fact that the critical behavior is completely determined by the behavior of the scalar variables. Here we consider transitions in which both scalar and gauge correlations are critical at the transition. In this case an appropriate effective field-theory description of the critical behavior requires a gauge field theory (GFT) with the explicit inclusion of gauge fields. Transitions of this type are observed in LAH models, as we shall discuss in Secs. 5 and 6. The corresponding field theory description is provided by the Abelian Higgs field theory (AHFT), or scalar QED. In the AHFT an N-component complex scalar field $\Phi(x)$ is minimally coupled with an electromagnetic field $A_{\mu}(x)$. The AHFT Lagrangian reads [17]

$$\mathcal{L}_{AH} = \frac{1}{4g^2} F_{\mu\nu}^2 + \overline{D_{\mu} \mathbf{\Phi}} \cdot D_{\mu} \mathbf{\Phi} + r \, \bar{\mathbf{\Phi}} \cdot \mathbf{\Phi} + u \, (\bar{\mathbf{\Phi}} \cdot \mathbf{\Phi})^2, \quad F_{\mu\nu} \equiv \partial_{\mu} A_{\nu} - \partial_{\nu} A_{\mu}, \quad D_{\mu} \equiv \partial_{\mu} + i A_{\mu}. \tag{18}$$

Beside the Abelian U(1) gauge invariance, the theory has a global SU(N) symmetry, $\Phi \to V\Phi$ with $V \in SU(N)$. Its RG flow will be discussed in Sec. 4. One expects that the stable charged FP of the RG flow of the AHFT, i.e., a stable FP with a nonvanishing gauge coupling, is the FP that controls the universal features of the charged critical transitions of lattice AH models, when both gauge and scalar fields are critical.

It is interesting to note that the effective description of GFT transitions requires non-gauge-invariant fundamental fields, like LGW^{\times} transitions. Thus, the issues we have discussed in Sec. 3.3 occur also here. In particular, vector correlations and gauge-field correlations are trivial in the gauge theory, because of gauge invariance. However, in GFTs the solution of these problems is well known: A gauge fixing should be added to the theory to be able to observe the critical correlations of the fundamental fields (this is a necessary step for perturbative calculations).

As we shall review in the next sections, critical behaviors consistent with the charged universality classes of the AHFT have been identified in lattice AH (LAH) models with noncompact gauge variables in the weak gauge-coupling regime, see Sec. 5, along the transition line that separates the Coulomb and Higgs phases [87, 91], for $N > N^*$, with $N^* = 7(2)$. On the other hand, in the strong gauge-coupling regime, transitions between the Coulomb and molecular phase have an effective LGW description. Charged universality classes have been identified also in compact formulations, again in the weak gauge-coupling limit, see Sec. 6.

It is interesting to note that in lattice gauge models the global symmetry group and the symmetry breaking pattern do not completely characterize the nature of the phase transition. The properties of the gauge modes are crucial to determine the critical behavior. Systems with global SU(N) symmetry, symmetry-breaking pattern $SU(N) \rightarrow SU(N-1)$, and local U(1) gauge symmetry provide an example of such behavior. If the gauge modes are not critical the transition is of LGW type. The corresponding Φ^4 theory is given in Eq. (10), which predicts first-order transitions for $N \geq 3$ and continuous transitions belonging to the O(3) vector universality class for N=2. On the other hand, if gauge modes are relevant, the transitions are described by the AHFT (18): they can be continuous for $N > N^* \approx 7$, and of first order in the opposite case, and in particular for N=2. Therefore, in the two cases the expected behavior at the transition is quite different.

3.5. Topological transitions in lattice gauge models

The first three types of transitions that we have discussed so far are all characterized by the spontaneous breaking of a global symmetry. In gauge models there are however also transitions that are not associated with a symmetry breaking and thus lie beyond the Landau paradigm. These transitions separate phases that only differ in the topological order of the gauge excitations. The scalar degrees of freedom, if present, play no role. Thus, they do not admit a LGW or LGW $^{\times}$ description, nor can they be described using a GFT with scalar matter, as in all these cases matter fields are critical. They therefore represent a novel class of transitions that do not obey the standard paradigm, see, e.g., Refs. [20, 21, 92, 93, 183, 236, 237].

Topological phase transitions are characterized by the divergence of the length scale ξ of the critical modes, as in more conventional cases. However, the absence of a local gauge-invariant order parameter forces one to define the length scale ξ from the behavior of extended objects, for instance Wilson loops in gauge theories. The presence of a divergent length allows one to define a universal critical exponent ν . Other exponents that are typically considered in conventional transitions, such as η and β , are instead not defined in the absence of a local order parameter. Topological transitions are also defined in the quantum setting, where one can use ν and the dynamic exponent z (defined in terms of the size dependence of the gap at the critical point) to characterize the critical behavior.¹⁴

Two important examples of models that undergo topological transitions are the inverted XY (IXY) model and the lattice \mathbb{Z}_Q -gauge model, which are reviewed below.

3.5.1. The three-dimensional inverted XY model

The inverted XY model (IXY) is a gauge model with Hamiltonian

$$H_{\rm IXY} = \frac{\kappa}{2} \sum_{\boldsymbol{x}, \mu > \nu} (\nabla_{\mu} A_{\boldsymbol{x}, \nu} - \nabla_{\nu} A_{\boldsymbol{x}, \mu})^2, \tag{19}$$

where the sum is over all lattice plaquettes, ∇_{μ} is the forward lattice derivative, $\nabla_{\mu} f(\mathbf{x}) = f(\mathbf{x} + \hat{\mu}) - f(\mathbf{x})$, and the field $A_{\mathbf{x},\mu}$ takes only values that are multiples of 2π , i.e., $A_{\mathbf{x},\mu} = 2\pi n_{\mathbf{x},\mu}$, with $n_{\mathbf{x},\mu} \in \mathbb{Z}$. The Hamiltonian H_{IXY} is invariant under the gauge transformations $n_{\mathbf{x},\mu} \to n_{\mathbf{x},\mu} + m_{\mathbf{x}+\hat{\mu}} - m_{\mathbf{x}}$, with $m_{\mathbf{x}} \in \mathbb{Z}$.

The free energy of the IXY model is related by duality to that of the XY model with Villain action [42, 65], which implies that the IXY model undergoes a transition (at $\kappa_c = 0.076051(2)$ [65, 87] when setting the temperature T=1) belonging to the XY universality class, but with inverted high- and low-temperature phases [42].

It is important to stress that the above identification of the universality classes is done using the duality between the gauge and the spin system, and that duality only maps the free energy and the related thermal observables. In particular, the magnetic sector present in the spin universality class has no counterpart in the

¹⁴We mention that topological transitions have also been associated with the breaking of higher-order symmetries, see, e.g., Refs. [238–242]. While conventional symmetries act on local objects defined on the entire system, higher-order symmetries act on extended objects associated with lower-dimensional submanifolds. Topological transitions can be interpreted as due to the spontaneous breaking of such generalized symmetries, somehow extending the Landau approach in which transitions are related to the spontaneous breaking of global symmetries.

gauge universality class. Viceversa, the charged sector that characterizes the IXY transition, see Secs. 5.1.2 and 5.2.2, is not present in the spin model. Thus, the XY FP that controls the behavior of the gauge model differs from the FP that is relevant in the XY model. Indeed, they represent FPs obtained by performing RG transformations on two different classes of Hamiltonians—those with local O(2) and global O(2) symmetry, respectively. Therefore, it is more appropriate to distinguish the IXY or gauge XY universality class from the spin XY universality class. ¹⁵

3.5.2. Three-dimensional lattice \mathbb{Z}_Q gauge theories

The lattice \mathbb{Z}_Q gauge theories with $Q \geq 2$ are paradigmatic models undergoing finite-temperature topological transitions [20], separating a high-temperature deconfined phase from a low-temperature confined phase, that have been investigated in several works, see, e.g., Refs. [119, 243–249]. Their lattice Hamiltonian reads¹⁶

$$H_{\mathbb{Z}_Q} = -2K \sum_{\boldsymbol{x}, \mu > \nu} \operatorname{Re} \left(\lambda_{\boldsymbol{x}, \mu} \lambda_{\boldsymbol{x} + \hat{\mu}, \nu} \bar{\lambda}_{\boldsymbol{x} + \hat{\nu}, \mu} \bar{\lambda}_{\boldsymbol{x}, \nu} \right), \quad \lambda_{\boldsymbol{x}, \mu} = \exp \left(i \frac{2\pi n_{\boldsymbol{x}, \mu}}{Q} \right), \quad n_{\boldsymbol{x}, \mu} \in 0, 1, \dots, Q - 1, \quad (20)$$

where $\lambda_{x,\mu}$ are \mathbb{Z}_Q -group variables associated with the links of a cubic lattice.

Their critical behavior can be inferred by using duality. The \mathbb{Z}_Q lattice gauge model is dual to a specific Q-state clock model [143], with \mathbb{Z}_Q spin variables $\exp(2\pi i n_x/Q)$ (where $n_x=1,...,Q$) associated with the lattice sites, and a Hamiltonian which is symmetric under global \mathbb{Z}_Q transformations. The 2-state clock model is equivalent to the Ising model, while the 3-state clock model is equivalent to the 3-state Potts model, which undergoes a first-order transition. The nature of the transitions for $Q \geq 4$ can be inferred by studying the RG flow of the LGW field theory associated with a \mathbb{Z}_Q -symmetric spin system [253]

$$\mathcal{L}_{\mathbb{Z}_Q} = |\partial_u \varphi|^2 + r |\varphi|^2 + u |\varphi|^4 + v (\varphi^Q + \bar{\varphi}^Q), \tag{21}$$

where $\varphi(\boldsymbol{x})$ is a complex field. The Q-dependent potential has dimension Q and is therefore irrelevant for Q>4. In this case we can thus set v=0, obtaining the standard U(1)-symmetric Φ^4 theory for a complex field. This implies an XY critical behavior and an effective enlargement of the symmetry of the critical modes at the transition: While the theory is \mathbb{Z}_Q -symmetric, critical modes are U(1)-symmetric. For Q=4, the Q-dependent potential has dimension four and represents a cubic anisotropy. The stable FP of its RG flow is again the XY FP with v=0 [95, 130, 150, 175, 254, 255].¹⁷

Using duality, the results for models with global \mathbb{Z}_Q symmetry allow us to infer the nature of the transitions in the \mathbb{Z}_Q gauge models. These arguments predict an Ising transition for Q=2, a first-order transition for Q=3, and an XY transition for any Q>4. For Q=4 the \mathbb{Z}_4 gauge model has a transition in the Ising universality class because its partition function can be written as that of two independent \mathbb{Z}_2 gauge models [92, 259] (this is analogous to what happens in the standard \mathbb{Z}_4 clock model, see footnote 17). However, this result is specific of the gauge formulation with Hamiltonian (20). Generic discrete models with \mathbb{Z}_4 gauge symmetry are instead expected to undergo transitions belonging to the XY universality class, or, more precisely, to the IXY universality class.

¹⁵The IXY or gauge XY universality class is also sometimes referred to as XY* universality class in the literature, see, e.g., Ref. [20].

 $^{^{16}}$ It is interesting to observe that, by means of the Fortuin-Kasteleyn representation [250], the \mathbb{Z}_Q gauge theory can be extended to any complex value of Q, see, e.g., Ref. [251]. Gauge models with real values of Q in the interval [0,1] have been studied, e.g., in Refs. [251, 252].

 $^{^{17}}$ For Q=4 the anisotropic interaction with coefficient v appearing in the Hamiltonian (21) gives only rise to scaling corrections. However, due to the small absolute value of the corresponding RG dimension [150, 175, 254] $y_v=-0.108(6)$, these scaling corrections decay slowly. Beside the stable FP with v=0, the LGW model also admits an unstable FP on the line w=u-6v=0, where the LGW Hamiltonian can be written as the sum of two identical LGW Hamiltonians with a real scalar field, so that this FP corresponds to an Ising critical behavior. The parameter w corresponds to a relevant perturbation of the decoupled Ising fixed point, with RG dimension $y_w=d-2/\nu_I=0.17475(2)$, where [256] $\nu_I=0.629971(4)$ is the Ising critical exponent. The standard \mathbb{Z}_4 clock model can be exactly rewritten as a sum of two Ising models [257, 258]. Thus, it corresponds to the LGW theory with w=0 and hence it undergoes an Ising transition. Generic four-state clock models, however, undergo XY transitions.

For $Q \to \infty$ we obtain the compact U(1) gauge theory in which the fields $\lambda_{x,\mu}$ are U(1) phases. This model does not have finite-K transitions because of the presence of topological excitations (monopoles) that keep the system always disordered [260]. The limit $K \to \infty$, $Q \to \infty$ at fixed K/Q^2 is more interesting [90]. In this case one obtains the IXY model defined in Sec. 3.5.1 with $\kappa = K/Q^2$.¹⁸ The IXY model is the relevant one for the behavior of the gauge model for $Q \ge 5$ (and also for Q = 4 in the generic case): For these values of Q transitions in the \mathbb{Z}_Q gauge model have the same critical behavior as the transition in the IXY model. It is interesting to give a RG interpretation of these results, considering the large- $Q \mathbb{Z}_Q$ gauge model as a perturbed IXY model, in which the inverse charge 1/Q plays the role of perturbation parameter. The IXY critical behavior of all \mathbb{Z}_Q gauge models with $Q \ge 4$ indicates that the 1/Q perturbation of the IXY critical behavior is irrelevant.

As already stressed above for the IXY model, the identification of the universality classes is done using duality, that only maps the free energy and the related thermal observables. Thus, we distinguish the gauge XY (a representative is the IXY transition) from the spin XY universality class and analogously, the gauge Ising from the spin Ising universality class.

Finally, we mention that the Wilson loops W_C , defined as the product of the link variables along a closed contour C within a plane, provide a nonlocal order parameter for the topological transition of the 3D lattice \mathbb{Z}_Q gauge models [119]. Indeed, their asymptotic size dependence for large contours changes at the transition, varying from the area law $W_C \sim \exp(-c_a A_C)$, where A_C is the area enclosed by the contour C and $c_a > 0$ is a constant, which is valid for small values of K, (this behavior can be easily checked in the strong-coupling regime for $K \ll 1$ [8, 262]), to the perimeter law $W_c \sim \exp(-c_p P_C)$, where P_C is the perimeter of the contour C and $c_p > 0$ is a constant, which is valid for large values of K. An analogous behavior is observed in 2D quantum formulations of the \mathbb{Z}_2 gauge theory, see, e.g., Ref. [20].

3.5.3. Topological transitions in low-temperature Higgs phases

Topological transitions, such as those arising in 3D \mathbb{Z}_Q gauge theories, also occur in theories with a larger gauge group if the reduced global symmetry of the low-temperature Higgs phase gives rise to an effective breaking of the gauge group to a residual smaller subgroup and, in particular, to the \mathbb{Z}_Q group. Topological transitions of this kind [20, 96, 98, 263] are realized in various lattice gauge systems, as we shall see in the following. For example, we mention LAH models with compact gauge variables and higher-charge scalar fields, see Sec. 6.1, and SU(N_c) gauge LNAH model with scalar matter in the adjoint representation, see Sec. 9.4.

In this context, the relevant gauge symmetry is the residual gauge symmetry G_R of the Higgs phase, which is defined as the group of gauge transformations that leave invariant a representative scalar field in the minimum-potential configuration. The representative scalar field is supposed to have been fixed to a specific value by using both the global and the local gauge symmetry. Note that the group G_R does not depend on the chosen representative of the scalar field in the Higgs phase, and it is determined by the global symmetry of the ordered phase. Therefore, it does not represent an additional characterization of the Higgs phase, and, more importantly, it has a gauge-independent relevance. The gauge modes associated with the residual gauge group G_R may give rise to gauge-independent topological transitions, as supported by the numerical results that we will present in the next sections. More precisely, topological transitions are possible if the gauge theory with gauge group G_R (and no scalar fields) has a topological transition, such as the \mathbb{Z}_Q gauge model in three dimensions.

To refer to the residual gauge symmetry G_R , we will usually speak of a formal breaking of the gauge symmetry G with gauge-symmetry breaking pattern $G \to G_R$, consistently with the common use of referring to the Higgs mechanism as realizing a gauge symmetry breaking (for example, the Standard Model of the electroweak interactions is often associated with the gauge symmetry breaking pattern $SU(2) \otimes U_Y(1) \to U_{em}(1)$ [1]). However, we should stress that the gauge symmetry cannot be spontaneously broken in the

¹⁸This result implies that the critical value $K_c(Q)$ for the Q-state gauge model scales as $K_c(Q) \simeq \kappa_{\rm nc}^{(c)} Q^2$ for large Q, where $\kappa_{\rm nc}^{(c)} = 0.076051(2)$ is the critical coupling of the IXY model. Using the existing estimates [247, 261] of $K_c(Q)$, Ref. [247] obtained $K_c(Q) \simeq w Q^2$ with w = 0.076053(4), in good agreement with the theoretical prediction, see also Ref. [90].

standard sense of statistical mechanics (i.e., the system cannot be forced in one specific minimum, for instance, by appropriately fixing the boundary conditions), as this is forbidden by well-known rigorous arguments [8, 43, 204, 205]. Thus, to identify uniquely the scalar fields in the low-temperature phase and the residual gauge symmetry, one can choose appropriate boundary conditions to fix the global symmetry, but one should also add an appropriate complete gauge fixing to eliminate the gauge redundancy.

4. Abelian Higgs gauge field theories

Many collective phenomena in condensed-matter physics [7, 12] are described by effective 3D U(1) gauge models in which scalar fields are coupled with an Abelian gauge field. We mention the transitions in superconductors [18, 19], in quantum SU(N) antiferromagnets [20, 27–32, 71, 72], and the unconventional quantum transitions between the Néel and the valence-bond-solid phases in two-dimensional antiferromagnetic SU(2) quantum systems [34–40, 264], which represent the paradigmatic models for the so-called deconfined quantum criticality [33]. The phase structure and the universal features of the transitions in scalar gauge models have been extensively studied [18–20, 27–93, 192–194, 196, 197, 202, 207, 210, 215, 264–276], and particular attention has been paid to the role of the gauge fields and of the related topological features, like monopoles and Berry phases, which cannot be captured by effective LGW theories with gauge-invariant scalar order parameters [2, 14, 20, 33, 95].

In this section we introduce the Abelian Higgs (AH) field theory (AHFT), or scalar QED, which describes a d-dimensional system of degenerate N-component scalar fields minimally coupled with an Abelian U(1) gauge field. By properly choosing the Lagrangian potential of the scalar fields, we can define models with different global symmetry: here we discuss SU(N) and SO(N) invariant models. We outline the known results for the renormalization-group (RG) flow of the models and the corresponding FPs, which are expected to describe the critical behavior of transitions in which both scalar and gauge field are critical (GFT transitions in the classification of Sec. 3.1).

4.1. SU(N)-symmetric Abelian Higgs field theory

4.1.1. The model

The SU(N)-symmetric AHFT is obtained by minimally coupling an N-component complex scalar field $\Phi(x)$ with an electromagnetic U(1) gauge field $A_{\mu}(x)$. The corresponding SFT (or Euclidean QFT) is formally defined by the functional path integral

$$Z = \int [d\mathbf{\Phi}] [d\mathbf{A}] e^{-S(\mathbf{\Phi}, \mathbf{A})}, \quad S(\mathbf{\Phi}, \mathbf{A}) = \int d^d x \left[\mathcal{L}_{AH}(\mathbf{\Phi}, \mathbf{A}) + \mathcal{L}_{gf}(\mathbf{A}) \right], \quad \mathcal{L}_{gf}(\mathbf{A}) = \frac{1}{2\zeta} (\partial_\mu A_\mu)^2, \quad (22)$$

where the gauge-invariant Lagrangian \mathcal{L}_{AH} is reported in Eq. (18). We have added here the Lorenz gauge-fixing term \mathcal{L}_{gf} , which is necessary to obtain a well-defined theory, see, e.g., Ref. [2]. As it stands here, the AHFT is only formally defined in perturbation theory. To go beyond perturbation theory, one must consider a nonperturbative regularization and show that the properly renormalized theory admits a finite limit when the regularization is eliminated. If we use the lattice regularization, this is possible only if the lattice model admits a continuous transition [2–4, 111, 131, 277].

The RG flow of the AHFT has been studied using the perturbative $\varepsilon \equiv 4-d$ expansion [18, 54, 83, 278, 279] and the functional RG approach [81]. The analysis of the corresponding FPs allows one to determine the nature of the transitions in this class of systems. In particular, if a stable FP exists, continuous transitions are possible in systems with analogous features. The model has also been studied using the large-N expansion, obtaining the expansion of some critical exponents for large N [18, 55, 64, 76, 207].

For $N \geq 2$, the pattern of the spontaneous breaking of the global symmetry is

$$SU(N) \to U(N-1).$$
 (23)

The ordered phase is characterized by the condensation of the local gauge-invariant bilinear operator

$$Q^{ab}(\mathbf{x}) = \bar{\Phi}^a(\mathbf{x})\Phi^b(\mathbf{x}) - \frac{1}{N}\delta^{ab}\bar{\Phi}(\mathbf{x})\cdot\Phi(\mathbf{x}). \tag{24}$$

Its two-point correlation function

$$G_O(x, y) = \langle \operatorname{Tr} Q(x)Q(y) \rangle,$$
 (25)

approaches a constant nonvanishing value for large distances (in the presence of symmetry-breaking boundary conditions) in the ordered phase, while at the critical point it behaves as

$$G_Q(x, y) \sim |x - y|^{-2y_q}, \qquad y_q = \frac{d - 2 + \eta_q}{2},$$
 (26)

where y_q is RG dimension of the operator Q, and η_q is the usual critical exponent. The approach to the critical point is controlled by the length-scale critical exponent ν , which can be defined from the power-law divergence of the length scale ξ of the critical modes, i.e. $\xi \sim |r - r_c|^{-\nu}$, where r is the coefficient of the quadratic term in Eq. (18) and r_c its critical value.

4.1.2. Renormalization-group flow in the perturbative ε -expansion

The RG flow of the SU(N)-symmetric AHFT field theory has been determined close to four dimensions in the ε -expansion framework. The RG scaling functions that are related with the diverging renormalization constants have been determined perturbatively [perturbative calculations are usually performed using the Lorenz gauge fixing as in Eq. (22)], in powers of $\varepsilon \equiv 4-d$ [18, 94]. In the perturbative calculations dimensional regularization and the minimal-subtraction (MS) renormalization scheme are generally used, see, e.g., Refs. [2, 95]. The corresponding MS β functions associated with the renormalized couplings $\alpha \equiv g^2$ and u have been computed to four loops [83]. The FPs of the RG flow are obtained from the common zeroes of the β function. Their stability is controlled by the eigenvalues of the matrix $\Omega_{ij} = \partial_{g_i} \beta_j$ (where g_i indicates the Lagrangian couplings, and β_i the corresponding β function) [2, 95]: a FP is stable if all eigenvalues λ_i of Ω , computed at the FP, are positive.

Here we report the one-loop β functions [18]

$$\beta_{\alpha} \equiv \mu \frac{\partial \alpha}{\partial \mu} = -\varepsilon \alpha + N\alpha^2, \qquad \beta_u \equiv \mu \frac{\partial u}{\partial \mu} = -\varepsilon u + (N+4)u^2 - 18u\alpha + 54\alpha^2.$$
 (27)

The normalizations of the renormalized couplings α and u have been chosen to simplify the formulas (they can be easily inferred from the above expressions). The analysis of the one-loop β functions shows that a stable FP exists for

$$N > N_4 = 90 + 24\sqrt{15} \approx 183. \tag{28}$$

It is given by

$$\alpha^* = \frac{\varepsilon}{N}, \qquad u^* = \frac{N + 18 + \sqrt{N^2 - 180N - 540}}{2N(N+4)} \varepsilon.$$
 (29)

We refer to this FP as *charged* FP, because α^* is nonzero, thus implying nontrivial critical correlations of the gauge field.

The value N^* above which the theory has a stable FP depends on the dimension d, thus, in the ε expansion approach one defines a function $N^*(d)$ such that a stable FP exists only for $N > N^*(d)$, with $N^*(4) = N_4$. 3D AH models may undergo a charged continuous transition only if $N > N^*(3)$. The critical number of components $N^*(d)$ has been determined to four loops [83]:

$$N^*(4-\varepsilon) = N^*(4) \left[1 - 1.752 \varepsilon + 0.789 \varepsilon^2 + 0.362 \varepsilon^3 + O(\varepsilon^4) \right]. \tag{30}$$

The determination of $N^*(3)$ from the asymptotic expansion (30) is quite difficult because of the large coefficients. Moreover, the perturbative expansions for gauge theories are not Borel summable, because of the presence of renormalons, see, e.g., Refs. [280–284], so it is not clear whether the resummation methods [2] that are successfully used for Φ^4 theories 19 may provide reasonably accurate estimates. In spite of these

¹⁹The ε-expansion for $Φ^4$ theories is conjectured to be Borel summable [2].

difficulties, by means of a resummation method that makes the reasonable assumption that $N^*(d)$ vanishes linearly for $d \to 2$ (this is suggested by the $D = 2 + \varepsilon$ perturbative results of Refs. [285, 286]), Ref. [83] obtained $N^*(3) = 12(4)$ in three dimensions, which confirms the absence of a stable FP—and therefore, of continuous transitions—for small values of N. The field-theoretical estimate is in reasonable agreement with the estimate [87, 90] $N^*(3) = 7(2)$ obtained by numerical analyses of the LAH models, see also Sec. 5.3.²⁰

It is interesting to observe that, to all orders of perturbation theory, the β function of the gauge coupling α can be expressed in terms of the anomalous dimension η_A of the scalar field in the Lorenz gauge [2, 53, 287]:

$$\beta_{\alpha} = \alpha \left[d - 4 + \eta_A(\alpha, u) \right], \qquad \eta_A(\alpha, u) = \frac{\mathrm{d} \log Z_A}{\mathrm{d} \log \mu},$$
 (31)

where Z_A is the MS renormalization constant associated with the gauge field. Therefore, at the charged FP $(\alpha^* \neq 0)$ the FP condition $\beta_{\alpha} = 0$ implies the exact relation [19, 53]

$$\eta_A \equiv \eta_A(\alpha^*, u^*) = 4 - d. \tag{32}$$

In particular, $\eta_A = 1$ in three dimensions.

The RG flow also presents an uncharged O(2N)-symmetric FP with vanishing gauge coupling, with $\alpha^* = 0$ and $u^* = u^*_{\mathrm{O}(2N)} = \varepsilon/(N+4)$. This FP exists for any N, including N=1, and it is always unstable against gauge fluctuations. Indeed, its stability matrix $\Omega_{ij} = \partial \beta_i/\partial g_j$ has a negative eigenvalue λ_{α} that satisfies the exact relation

$$\lambda_{\alpha} = \left. \frac{\partial \beta_{\alpha}}{\partial \alpha} \right|_{\alpha = 0} = -\varepsilon,\tag{33}$$

to all orders in perturbation theory [84]. Therefore, the addition of U(1) gauge interactions is a relevant RG perturbation of the ungauged O(2N)-vector theory, with RG dimension $y_{\alpha} = -\lambda_{\alpha} = 1$ in three dimensions. As a consequence, for small gauge couplings we always expect crossover effects with an apparent O(2N) behavior [2, 11, 92, 137], independently of the existence of the stable charged FP, which is only relevant for the eventual asymptotic behavior.

4.1.3. Role of the gauge fixing

As already mentioned above, the Lorenz gauge-fixing term \mathcal{L}_{gf} in Eq. (22) is necessary to obtain a well-defined functional path integral, and, in particular, a well-defined perturbative expansion, see, e.g., Ref. [2]. Appropriate Ward identities guarantee that the gauge-invariant observables do not depend on the parameter ζ appearing in the gauge-fixing term \mathcal{L}_{gf} . In particular, the MS perturbative β functions β_{α} and β_{u} , the corresponding FPs, and the critical exponents are independent of ζ . However, as discussed in Sec. 5.1, and, in more details, in Refs. [46–50, 91, 287], the gauge fixing plays an important role also in lattice AH models. In particular, different behaviors are observed for positive values of ζ (in this case we speak of a soft Lorenz gauge fixing) and in the limiting case $\zeta = 0$ (hard Lorenz gauge fixing). For instance, only in the second case the nonlocal gauge-invariant charge operators that condense in the low-temperature Higgs phase admit a local field representation [91, 287]. To better understand the role of the gauge fixing in the lattice theory, it is useful to discuss the RG flow of the Lorenz gauge parameter in the corresponding AHFT.

As a consequence of the Ward identities that follow from gauge invariance, which imply that the gauge-fixing term \mathcal{L}_{gf} in Eq. (22) does not renormalize, see, e.g., Ref. [2], the β function of the parameter ζ takes the simple form

$$\beta_{\zeta} \equiv \mu \frac{\partial \zeta}{\partial \mu} = -\zeta \, \eta_A(\alpha, u). \tag{34}$$

 $^{^{20}}$ A similar behavior has been observed [202] in quantum square-lattice SU(N) antiferromagnets at the transition between the SU(N) Néel phase and the valence-bond solid phase. The numerical FSS analyses of the Rényi entanglement entropy reported in Ref. [202] are apparently compatible with the CFT predictions appropriate for continuous transitions only for $N \geq 8$, leading to the conclusions that systems with $N \leq 7$ undergo (weak) first-order transitions. The N-component AHFT (22) is a candidate field theory for the critical behavior at these transitions, see, e.g., Refs. [27–30, 202]. If this is the case, then the results of Ref. [202] confirm the absence of a FP for small values of N.

Eq. (34) shows that the value $\zeta=0$ represents a FP of the RG flow in the theory with a Lorenz gauge fixing. Moreover, since $\eta_A>0$, this FP is unstable. If we start the RG flow from $\zeta>0$, then ζ increases towards infinity, and the fluctuations of the nongauge-invariant modes are expected to become unbounded in this limit: nongauge-invariant correlations are expected to become disordered on large scales as in the absence of a gauge fixing. Therefore, we expect to be able to observe a critical behavior in the nongauge invariant sector only for $\zeta=0$, i.e., in the presence of a hard Lorenz gauge fixing. This is confirmed by the numerical results discussed in Refs. [91, 287].

4.1.4. Three-dimensional Abelian Higgs field theory in the large-N limit

The existence of a critical transition for finite values of ε , and in particular in three dimensions, and for sufficiently large values of N is confirmed by nonperturbative (with respect to the couplings) computations in the large-N limit [18, 55, 64, 76]. These calculations provide 1/N expansions of some critical exponents. The correlation-length exponent ν and the exponent η_q defined in Eq. (26) are given by [18]:

$$\nu = 1 - \frac{48}{\pi^2 N} + O(N^{-2}), \tag{35}$$

$$\eta_q = 1 - \frac{32}{\pi^2 N} + O(N^{-2}). \tag{36}$$

In the presence of a gauge fixing one can also consider correlation functions that are not gauge invariant. For example, we may consider the correlation function $G_{\Phi}(x, y) \equiv \langle \bar{\Phi}(x) \cdot \Phi(y) \rangle$ of the Lagrangian field $\Phi(x)$. The anomalous dimension of $\Phi(x)$ depends on the gauge-fixing parameter ζ and is given by [18, 76]

$$\eta_{\phi} = -\frac{20 + 8\zeta}{\pi^2} \frac{1}{N} + O(N^{-2}). \tag{37}$$

As already discussed in Sec. 4.1.3, only in the presence of a hard Lorenz gauge fixing ($\zeta = 0$) nongauge invariant correlations can become critical. In particular, as we shall see in Sec. 5.1.2, only in this case the Higgs phase can be characterized by the condensation of the scalar field, reflecting the condensation of a nonlocal gauge-invariant charged operator. For $\zeta = 0$ we obtain

$$\eta_{\phi} = -\frac{20}{\pi^2} \frac{1}{N} + O(N^{-2}) \quad \text{for } \zeta = 0,$$
(38)

which allows one to compute the RG dimension of Φ in the hard Lorenz gauge: $y_{\phi} = (1 + \eta_{\phi})/2$.

4.2. Abelian Higgs field theories with multiparameter scalar potentials

We can also consider AHFTs with more general scalar potentials [278, 279, 288], that are invariant under a subgroup of SU(N), that is still large enough to ensure the presence of a single quadratic invariant term. If this were not the case, the model would describe multicritical behaviors, as already discussed in Sec. 2.2. In Secs. 4.2.1 and 4.2.2 we consider SO(N) invariant models. Further extensions are presented in Sec. 4.2.3.

4.2.1. SO(N)-symmetric Abelian Higgs field theories: Definition of the model

The simplest extension of the SU(N)-invariant AHFT is obtained by adding the quartic term $|\Phi \cdot \Phi|^2$ to the Lagrangian (18). We obtain

$$\mathcal{L}_{\mathcal{O}} = \frac{1}{4g^2} \sum_{\mu\nu} F_{\mu\nu}^2 + \overline{D_{\mu}} \overline{\Phi} \cdot D_{\mu} \Phi + r \, \overline{\Phi} \cdot \Phi + u \, (\overline{\Phi} \cdot \Phi)^2 + v \, |\Phi \cdot \Phi|^2, \tag{39}$$

with $u \geq 0$ and $u+v \geq 0$, to guarantee the stability of the potential. For N=1 the two quartic scalar terms are equivalent, thus one recovers the standard one-component AHFT. For N>1, the added term preserves the gauge invariance, but it breaks the global $\mathrm{SU}(N)$ symmetry, making the theory invariant under $\mathrm{SO}(N)$ transformations only. This symmetry group is large enough to guarantee that $\bar{\Phi} \cdot \Phi$ is the only quadratic invariant term allowed by the global and local symmetries.

To determine the possible ordered phases of the model with $N \geq 2$, one can use the mean-field approximation, since field fluctuations are only relevant along the transition lines. This amounts to analyzing the minima of the scalar potential [288]. One finds two ordered phases, with different symmetry, depending on the sign of v. For v < 0, the ordered phase is invariant under SO(N-1) transformations, so the symmetry-breaking pattern at the transition is the same as that of the O(N) vector model,

$$SO(N) \to SO(N-1)$$
 for $v < 0$. (40)

For v > 0 the ordered phase is invariant under SO(N-2) transformations, thus leading to the symmetry-breaking pattern

$$SO(N) \to SO(N-2)$$
 for $v > 0$. (41)

Of course, for v = 0 the model is SU(N) invariant and thus the ordered phase is U(N-1) invariant. The symmetry-breaking pattern is given in Eq. (23).

The appropriate order parameters for the two different types of transitions are [288]

$$R^{ab}(\mathbf{x}) = \operatorname{Re} Q^{ab}(\mathbf{x}), \qquad T^{ab}(\mathbf{x}) = \operatorname{Im} Q^{ab}(\mathbf{x}),$$
 (42)

which transform under different representations of the SO(N) group. Here Q^{ab} is the bilinear operator defined in Eq. (24).

As a final remark, it is important to note that the analysis of the possible phases and symmetry-breaking patterns only relies on the structure of the scalar potential. Therefore, it applies to any lattice model with SO(N) global invariance, independently of the presence or absence of gauge fields. Also the nature of the transition plays no role.

4.2.2. SO(N)-symmetric Abelian Higgs field theories: Renormalization-group flow

To determine the possible charged transitions in SO(N) invariant models, one can study the RG flow in the MS renormalization scheme close to four dimensions, as it was done for the SU(N) symmetric AHFT in Sec. 4.1.2. The one-loop β functions associated with the renormalized couplings α , u, and v, are given by [278, 279]

$$\beta_{\alpha} = -\varepsilon \alpha + N\alpha^{2},$$

$$\beta_{u} = -\varepsilon u + (N+4)u^{2} + 4uv + 4v^{2} - 18u\alpha + 54\alpha^{2},$$

$$\beta_{v} = -\varepsilon v + Nv^{2} + 6vu - 18v\alpha.$$
(43)

The normalizations of the renormalized couplings α, u, v have been again chosen to simplify the formulas (they can be easily inferred from the above expressions). For large values of N there is a stable FP, with $\alpha^* \approx \varepsilon/N$, $u^* \approx \varepsilon/N$, and $v^* \approx \varepsilon/N$. More precisely, a stable charged FP exists for $N > N_o^*(d)$, where [279]

$$N_o^*(d) = N_o^*(4) + O(\varepsilon)$$
 with $N_o^*(4) \approx 210$. (44)

Note that $v^* > 0$, so this FP is only relevant for charged transitions characterized by the symmetry-breaking pattern given in Eq. (41). There are no higher-order computations, that allow one to determine $N_o^*(d)$ in d dimensions and, in particular, for d = 3. However, by analogy with the SU(N)-symmetric case, one expects $N_o^*(d=3)$ to be of order ten [288].

These results allow us to predict the critical behavior of the transitions in generic SO(N)-invariant AH systems, when gauge fields are critical at the transition. If the symmetry-breaking pattern is the one given in Eq. (40), so that the system is effectively described by the SO(N)-symmetric AHFT with v < 0, no continuous transitions with critical gauge correlations are expected to occur. If, instead, the symmetry-breaking pattern is the one obtained for v > 0, see Eq. (41), then the behavior depends on the number of components of the scalar field. For $N > N_o^*(d=3)$, continuous charged transitions are possible, provided the lattice system is effectively inside the attraction domain of the stable charged FP. For smaller values of N, instead, transitions are of first order.

The RG analysis reported above shows that SO(N)-symmetric AH systems may undergo charged continuous phase transitions for sufficiently large values of N. Critical exponents in the large-N limit can be computed using the field-theoretical 1/N expansion. Ref. [278] computed the correlation-length exponent ν in a more general non-Abelian gauge theory with local O(M) and global O(N) invariance, which is equivalent to the SO(N)-symmetric AHFT for M=2. Using the results of Ref. [278] for M=2 one obtains

$$\nu = 1 - \frac{176}{3\pi^2 N} + O(N^{-2}). \tag{45}$$

4.2.3. Further extensions of the Abelian Higgs field theories

More general quartic scalar potential, with smaller global symmetry group, have also been considered. For instance, one may consider the model with Lagrangian [279]

$$\mathcal{L}_{P} = \frac{1}{4g^{2}} F_{\mu\nu}^{2} + \overline{D_{\mu}\Phi} \cdot D_{\mu}\Phi + r \,\bar{\Phi} \cdot \Phi + u \,(\bar{\Phi} \cdot \Phi)^{2} + v \,|\Phi \cdot \Phi|^{2} + w \sum_{a=1}^{N} (\bar{\Phi}^{a}\Phi^{a})^{2}, \tag{46}$$

which is invariant under the permutation group of N elements \mathbb{P}_N . For N=2 the quartic potential appearing in the Lagrangian (46) is the most general one that is gauge invariant and guarantees the uniqueness of the quadratic $\bar{\Phi} \cdot \Phi$ term. For N>2 there are other quartic terms satisfying these conditions. For instance, one can add $\sum_{a=1}^{N} \bar{\Phi}^a \Phi^a \bar{\Phi}^{a+1} \Phi^{a+1}$ (with the identification $\Phi^{N+1} = \Phi^1$), which is only invariant under global \mathbb{Z}_N transformations.

A one-loop $O(\varepsilon)$ analysis of the RG flow of the \mathbb{P}_N -symmetric AHFT (46) was reported in Ref. [279], showing that, close to four dimensions, a stable FP is present only for $N \geq 5494$.

4.3. Summary

The analysis of the RG flow in the SU(N) and SO(N) invariant AHFTs shows that a stable charged FP exists for sufficiently large N values. The existence of these FPs implies that statistical lattice systems with the same local and global symmetries may undergo continuous charged transitions, where both scalar and gauge fields are critical. In particular, SU(N)-symmetric and O(N)-symmetric AHFTs provide the effective description of charged continuous transitions characterized by the symmetry-breaking patterns $SU(N) \to U(N-1)$ and $SO(N) \to SO(N-2)$, respectively. As we shall see, such transitions are indeed observed in LAH models with noncompact gauge variables [87, 288], along the transition line separating the Coulomb and Higgs phases. They are characterized by the condensation of the local gauge-invariant bilinear tensor operators defined above and also of nonlocal charged vector operators [91, 93].

5. Lattice Abelian Higgs models with noncompact gauge variables

In this section we discuss the phase diagram and critical behavior of 3D lattice Abelian Higgs (LAH) models in which a noncompact Abelian gauge field is coupled with an N-component scalar field. We review results for a specific nearest-neighbor model, but the main features of the phase diagram and the universal properties of the transitions are expected to be the same in a large class of lattice gauge models characterized by a local U(1) gauge invariance. We first consider LAH models with global SU(N) symmetry, then we discuss the SO(N)-symmetric case.

5.1. N-component SU(N)-invariant lattice Abelian Higgs model

5.1.1. Definition of the model

In LAH models defined on a 3D cubic lattice the fundamental fields are N-component unit-length complex vectors z_x ($\bar{z}_x \cdot z_x = 1$) defined on the lattice sites x, and noncompact gauge variables $A_{x,\mu} \in \mathbb{R}$ ($\mu = 1, 2, 3$) defined on the lattice links. The simplest nearest-neighbor lattice model is defined by [46, 48, 50, 66, 87]²¹

$$Z = \int [dA_{\boldsymbol{x},\mu}d\bar{\boldsymbol{z}}_{\boldsymbol{x}}d\boldsymbol{z}_{\boldsymbol{x}}]e^{-H(\boldsymbol{A},\boldsymbol{z})}, \qquad H(\boldsymbol{A},\boldsymbol{z}) = \frac{\kappa}{2} \sum_{\boldsymbol{x},\mu>\nu} F_{\boldsymbol{x},\mu\nu}^2 - 2NJ \sum_{\boldsymbol{x},\mu} \operatorname{Re}\left(\lambda_{\boldsymbol{x},\mu}\,\bar{\boldsymbol{z}}_{\boldsymbol{x}}\cdot\boldsymbol{z}_{\boldsymbol{x}+\hat{\mu}}\right), \tag{47}$$

²¹We set T=1 and rescale the coupling J by a factor of N, to obtain a finite $N\to\infty$ limit at fixed J, see, e.g., Ref. [64].

where $\hat{\mu}$ is the unit spatial vector in the lattice direction μ , and

$$\lambda_{\boldsymbol{x},\mu} = e^{iA_{\boldsymbol{x},\mu}}, \qquad F_{\boldsymbol{x},\mu\nu} = \Delta_{\mu}A_{\boldsymbol{x},\nu} - \Delta_{\nu}A_{\boldsymbol{x},\mu}, \qquad \Delta_{\mu}A_{\boldsymbol{x},\nu} = A_{\boldsymbol{x}+\hat{\mu},\nu} - A_{\boldsymbol{x},\nu}. \tag{48}$$

The coupling $\kappa > 0$ plays the role of inverse (square) gauge coupling. The model is invariant under the global transformations $z_x \to V z_x$ with $V \in \mathrm{SU}(N)$ and under the local transformations

$$z_x \to e^{i\Lambda_x} z_x, \qquad A_{x,\mu} \to A_{x,\mu} + \Lambda_x - \Lambda_{x+\hat{\mu}}, \qquad \Lambda_x \in \mathbb{R}.$$
 (49)

Model (47) can be seen as a particular, quite straightforward, lattice regularization of the AHFT defined by the Lagrangian (18).

We should note that the partition function of the lattice gauge model (47) is not well defined. Indeed it diverges, even on a finite lattice, because of the zero modes due to the gauge invariance of the model. If periodic boundary conditions are used, this problem cannot be solved even when a maximal gauge fixing [131, 289] is added. This is due to the invariance of the Hamiltonian H under the noncompact group of transformations $A_{x,\mu} \to A_{x,\mu} + 2\pi n_{\mu}$ (where $n_{\mu} \in \mathbb{Z}$ depends on the direction μ but is independent of the point x), which is also (at least partially) present in the gauge-fixed theory, making the partition function Z ill-defined. In particular, the averages of functions of the noncompact gauge-invariant Polyakov operators, i.e., the sums of the fields $A_{x,\mu}$ along nontrivial paths winding around the lattice, are ill-defined [87]. To obtain a well-defined (rigorous) definition of the partition function of the finite-size gauge-fixed theory, without breaking translation invariance, one may consider the so-called C^* boundary conditions [87, 290, 291]. On a cubic lattice of size L, C^* boundary conditions are defined by

$$A_{\boldsymbol{x}+L\hat{\nu},\mu} = -A_{\boldsymbol{x},\mu}, \qquad \boldsymbol{z}_{\boldsymbol{x}+L\hat{\nu}} = \bar{\boldsymbol{z}}_{\boldsymbol{x}}. \tag{50}$$

These boundary conditions preserve the local gauge invariance of the Hamiltonian (47) provided Λ_x , defined in Eq. (49), is antiperiodic. They break the SU(N) global symmetry—they are only invariant under O(N) transformations—but, since the breaking only occurs on the boundaries, it is irrelevant for the bulk critical behavior.

As we shall see, some properties of the model can be best analyzed by adding a Lorenz gauge fixing. It is defined by requiring [287]

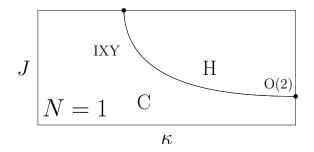
Lorenz gauge:
$$\sum_{\mu} \Delta_{\mu}^{-} A_{x,\mu} = 0, \quad \Delta_{\mu}^{-} A_{x,\nu} = A_{x,\nu} - A_{x-\hat{\mu},\nu},$$
 (51)

for all lattice sites x. In the presence of C* boundary conditions, the above Lorenz gauge condition represents a complete gauge fixing as it completely breaks gauge invariance and thus it makes gauge correlations well defined. As demonstrated in Ref. [287], the lattice Lorenz gauge fixing (51) has an important property. When computed in the Lorenz gauge, Fourier-transformed gauge correlations are also well defined in the infinite-volume limit for any nonvanishing momentum, at variance with what happens in other gauges. For instance, axial gauges suffer from the existence of an infinite two-dimensional family of quasizero modes for L large. These zero modes give rise to spurious divergences, unrelated to the presence of long-range physical correlations [287].

It is important to note that in the AHFT with action (22) gauge invariance is broken by adding $\mathcal{L}_{gf} \sim \zeta^{-1}(\partial_{\mu}A_{\mu})^2$ to the gauge-invariant Lagrangian. In the lattice case, this corresponds to adding

$$\frac{1}{2\zeta} \sum_{\boldsymbol{x},\mu} (\Delta_{\mu}^{-} A_{\boldsymbol{x},\mu})^{2} \tag{52}$$

to the lattice Hamiltonian, Eq. (47). We name this gauge-symmetry breaking a soft Lorenz gauge fixing. The gauge fixing condition (51) (hard Lorenz gauge fixing) is straightforwardly recovered in the $\zeta \to 0$ limit. As discussed in Ref. [287] soft gauge fixings are not appropriate for the nonperturbative analysis of the phase behavior of the LAH model, as they suffer from the presence of propagating unphysical longitudinal modes,



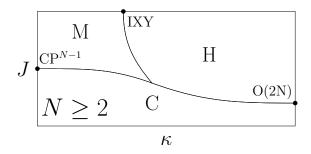


Figure 2: The κ -J phase diagram of the N-component LAH model (47), for N=1 (left), and generic $N\geq 2$ (right). For N=1, there are two phases, the Coulomb (C) and the Higgs (H) phase, characterized by the confinement and deconfinement of charged gauge-invariant excitations, respectively. For $N\geq 2$, the scalar field is disordered and gauge correlations are long ranged in the small-J Coulomb (C) phase. For large J two phases occur, the molecular (M) and Higgs (H) ordered phases, in which the global SU(N) symmetry is spontaneously broken. The two phases are distinguished by the behavior of the gauge modes: the gauge field is long ranged in the M phase (small κ), while it is gapped in the H phase (large κ). Moreover, while the C and M phases are confined phases, in the H phase charged gauge-invariant excitations are deconfined.

which may hide the physical signal. Similar conclusions are reached from the analysis of scalar correlation functions, see Ref. [91], and in field theory, see Sec. 4.1.3.

We finally mention that in the one-component (N=1) model one may integrate out the scalar field by choosing the so-called unitary gauge, that fixes $z_x = 1$ everywhere. This allows us to write the Hamiltonian in terms of the gauge variables only, as

$$H_{\text{ug}} = \frac{\kappa}{2} \sum_{\boldsymbol{x}, \mu > \nu} F_{\boldsymbol{x}, \mu \nu}^2 - 2J \sum_{\boldsymbol{x}, \mu} \cos A_{\boldsymbol{x}, \mu}. \tag{53}$$

The unitary gauge fixing is not complete, indeed the Hamiltonian $H_{\rm ug}$ is still invariant under gauge transformations in which $\Lambda_{\boldsymbol x}$ is a multiple of 2π . As discussed in Sec. 3.5.3, this residual gauge symmetry can induce topological transitions: The model (53) represents a soft version of the inverted XY (IXY) gauge model defined in Sec. 3.5.1, which is obtained for $J \to \infty$. Indeed, in this limit, we have $\cos A_{\boldsymbol x,\mu} = 1$, so $A_{\boldsymbol x,\mu}$ takes only values that are multiples of 2π , i.e., $A_{\boldsymbol x,\mu} = 2\pi n_{\boldsymbol x,\mu}$ with $n_{\boldsymbol x,\mu} \in \mathbb{Z}$.

The qualitative features of the phase diagram of the model depend on N, as sketched in Fig. 2. For N=1 there are only two phases, which differ in the topological properties of the gauge fields and in the confinement properties of the charged nonlocal excitations. For $N \geq 2$ the phase diagram is more complex, due to the possibility of the spontaneous breaking of the global SU(N) symmetry. Note that a Higgs phase is always present for large J and κ .

For N>1 a line of topological transitions is also present. The mechanism underlying these transitions is the one discussed in Sec. 3.5.3: in the broken-symmetry phase the minimum-energy configurations correspond (in the infinite-volume limit and up to gauge transformations) to $\mathbf{z}_{x}=\mathbf{z}_{x+\hat{\mu}}$ and $\lambda_{x,\mu}=1$. They are still invariant under gauge transformations in which Λ_{x} is a multiple of 2π , exactly for N=1, so we expect topological transitions analogous to the CH transitions for N=1.

5.1.2. Order parameters

The critical behavior in LAH models can be characterized by using three different types of order parameters. To characterize the Higgs phase one can consider nonlocal charged operators—charges are deconfined in the Higgs phase and confined in the other phases—or correlations of the gauge fields—they are gapped in the Higgs phase, long-ranged in the other cases. For $N \geq 2$, there are also transitions where the global symmetry is spontaneously broken, which can be signaled by appropriate gauge-invariant bilinear operators of the scalar fields.

The condensation of the charged excitations [46–50] can be monitored by looking at the correlation

functions of the nonlocal gauge-invariant operator [91, 292]

$$\Gamma_{x} = z_{x} \exp\left(i \sum_{y,\mu} E_{\mu}(y,x) A_{y,\mu}\right), \tag{54}$$

where $E_{\mu}(\boldsymbol{y}, \boldsymbol{x}) = V(\boldsymbol{y} + \hat{\mu}, \boldsymbol{x}) - V(\boldsymbol{y}, \boldsymbol{x})$, and $V(\boldsymbol{y}, \boldsymbol{x})$ is the lattice Coulomb potential associated with a unit charge located at \boldsymbol{x} . Note that this operator cannot be defined for periodic boundary conditions, as $V(\boldsymbol{y}, \boldsymbol{x})$ does not exist for these boundary conditions. A rigorous definition in a finite system is possible instead, if C^* boundary conditions are used.²² The operator $\Gamma_{\boldsymbol{x}}$ is invariant under local gauge transformations, but transforms as $\Gamma_{\boldsymbol{x}} \to e^{i\varphi}\Gamma_{\boldsymbol{x}}$ under a global U(1) transformation $\boldsymbol{z}_{\boldsymbol{x}} \to e^{i\varphi}\boldsymbol{z}_{\boldsymbol{x}}$, thus it behaves as a charged gauge-invariant operator.²³

The gauge-invariant nonlocal charged operator Γ_x simplifies in the Lorenz gauge (51). Indeed, since $\sum_{\boldsymbol{y},\mu} E_{\mu}(\boldsymbol{y},\boldsymbol{x}) A_{\boldsymbol{y},\mu} = -\sum_{\boldsymbol{y},\mu} V(\boldsymbol{y},\boldsymbol{x}) \Delta_{\mu}^{-} A_{\boldsymbol{y},\mu} = 0$, we obtain $\Gamma_x = \boldsymbol{z}_x$ and thus

$$G_{\Gamma}(x, y) \equiv \langle \bar{\Gamma}_x \cdot \Gamma_y \rangle = G_z(x, y) \equiv \langle \bar{z}_x \cdot z_y \rangle$$
 (Lorenz gauge). (55)

The Lorenz-gauge representation of the charged operator Γ_x in terms of the local scalar field z_x allows us to use the standard RG framework, which applies to local operators [6, 95, 113, 125, 135]. In particular, we can predict the critical behavior of its correlation functions. We define a critical exponent η_{Γ} from the critical-point relation

$$G_{\Gamma}(\boldsymbol{x}, \boldsymbol{y}) \sim \frac{1}{|\boldsymbol{x} - \boldsymbol{y}|^{d-2+\eta_{\Gamma}}}.$$
 (56)

In the Lorenz gauge η_{Γ} can be computed from the critical behavior of the correlation function of the local field z_x .

For N=1, in the unitary gauge the nonlocal scalar operator Γ_x becomes

$$\widetilde{\Gamma}_{x} = \exp\left(i\sum_{y,\mu} E_{\mu}(y,x)A_{y,\mu}\right),\tag{57}$$

which is invariant under gauge transformations in which Λ_x is a multiple of 2π , i.e., under the discrete gauge transformations that are appropriate for the IXY model or its soft version (53). The operator $\widetilde{\Gamma}_x$ is well-defined also in the IXY model (it only depends on the gauge fields), and therefore it represents a nonlocal order parameter for the topological IXY transition.

To determine the critical behavior of the gauge correlations, one can consider the gauge-invariant two-point correlation function of $F_{x,\mu\nu}$. In the Lorenz gauge, it can be expressed in terms of the correlation function

$$C_{\mu\nu}(\boldsymbol{x},\boldsymbol{y}) = \langle A_{\boldsymbol{x},\mu} A_{\boldsymbol{y},\nu} \rangle \tag{58}$$

of the gauge field [91, 93, 287]. At a critical transition

$$C_{\mu\nu}(\boldsymbol{x}, \boldsymbol{y}) \sim \frac{1}{|\boldsymbol{x} - \boldsymbol{y}|^{d-2+\eta_A}},$$
 (59)

which defines the critical exponent η_A .

²²The lattice Coulomb potential V(x, y) is the solution of the lattice Poisson equation $\sum_{\mu} \Delta_{\mu}^{-} \Delta_{\mu} V(x, y) = -\delta_{x,y}$, where the lattice derivatives act on the x variable. A consistent definition of Γ_{x} requires the use of boundary conditions for which the lattice Poisson equation has a unique solution. C^{*} boundary conditions, but not periodic boundary conditions, have this property.

 $^{^{23}}$ We are using here C^* boundary conditions, so $\mathbf{z}_{\boldsymbol{x}} \to e^{i\varphi} \mathbf{z}_{\boldsymbol{x}}$, $A_{\boldsymbol{x},\mu} \to A_{\boldsymbol{x},\mu}$ is not a gauge transformation (it would be for periodic boundary conditions). Indeed, if we define $\Lambda_{\boldsymbol{x}} = \varphi$, $A_{\boldsymbol{x},\mu}$ transforms nontrivially on the boundaries due the fact that $\Lambda_{\boldsymbol{x}}$ is antiperiodic.

Finally, in SU(N) invariant models with $N \ge 2$, to characterize the spontaneous breaking of the global symmetry, one can consider the gauge-invariant composite operator

$$Q_{\mathbf{r}}^{ab} = \bar{z}_{\mathbf{r}}^{a} z_{\mathbf{r}}^{b} - \delta^{ab}/N,\tag{60}$$

which transforms in the adjoint representation of the SU(N) global symmetry group. Its critical properties can be determined by studying the correlation function

$$G_Q(\boldsymbol{x}, \boldsymbol{y}) = \langle \operatorname{Tr} Q_{\boldsymbol{x}} Q_{\boldsymbol{y}} \rangle,$$
 (61)

which, at the critical point, scales as

$$G_Q(\boldsymbol{x}, \boldsymbol{y}) \sim \frac{1}{|\boldsymbol{x} - \boldsymbol{y}|^{d-2+\eta_q}},$$
 (62)

with the critical exponent η_a .

5.2. Phase diagram and critical behavior of the one-component lattice Abelian Higgs model

5.2.1. The Coulomb and Higgs phases

As shown in the left panel of Fig. 2, the one-component LAH model presents only two phases: a Coulomb (C) phase, in which gauge correlators are gapless, and a Higgs (H) phase in which gauge correlators are gapped; see, e.g., Ref. [50]. They can also be characterized by the confinement/deconfinement of charged gauge-invariant excitations [46, 47, 50], as we discuss below. The C and H phases are separated by a transition line connecting the transition points occurring in the $J \to \infty$ and $\kappa \to \infty$ limits, where the noncompact LAH model becomes equivalent to the 3D IXY model discussed in Sec. 3.5.1 and to the standard O(2)-vector spin model, respectively. As discussed in Ref. [93] and reviewed below, the critical behavior along the whole CH line is the same as that of the IXY model.

5.2.2. IXY critical behavior along the Coulomb-Higgs transition line

To characterize the behavior of the LAH model along the CH line, we first discuss the nature of the transitions in the two limiting cases, $J \to \infty$ and $\kappa \to \infty$.

For $J \to \infty$ scalar fields obey the relation $z_x = \lambda_{x,\mu} z_{x+\hat{\mu}}$. Iterating this condition along the sides of a plaquette we obtain

$$\lambda_{x,\mu} \lambda_{x+\hat{\mu},\nu} \bar{\lambda}_{x+\hat{\nu},\mu} \bar{\lambda}_{x,\nu} = 1. \tag{63}$$

By an appropriate gauge transformation, one can then set $A_{x,\mu} = 2\pi n_{x,\mu}$, where $n_{x,\mu} \in \mathbb{Z}$, thus obtaining the IXY model, see Sec. 3.5.1. Therefore, for $J \to \infty$ 3D LAH models undergo an IXY transition located at $\kappa_c(J \to \infty) = 0.076051(2)$ [65, 87].

In the limit $\kappa \to \infty$, all plaquettes $F_{x,\mu\nu}$ vanish. Thus, in infinite volume we can set $A_{x,\mu}=0$ everywhere up to a gauge transformation, obtaining the XY model. Therefore, the one-component LAH model is expected to undergo an XY transition at [293–295] $J_c(\kappa \to \infty)=0.22708234(9)$ for $\kappa \to \infty$ [this XY transition is denoted by O(2) in Fig. 2]. Note that, as discussed in Sec. 3.5.1, the continuous transitions at the two endpoints have a different nature and belong to two different universality classes, even if related by duality [42, 65]. Indeed, the duality transformations only relate thermal quantities.

The behavior along the CH line has been discussed in Ref. [93], finding that continuous transitions along the CH line belong to the same universality class as that of the IXY model, obtained for $J \to \infty$. Note that it is not possible to have finite- κ transitions with the same critical features as those of the spin XY model obtained in the limit $\kappa \to \infty$. Indeed, gauge interactions are a relevant perturbation of the spin XY model. As discussed in Sec. 4.1.2, the uncharged O(2) FP associated with the spin XY universality class is unstable with respect to a perturbation proportional to the gauge coupling [the corresponding eigenvalue of the stability matrix is negative, see Eq. (33)].

The IXY behavior of the transitions is confirmed by the FSS behavior of the energy cumulants [65, 93], see also Appendix A.3.2. Results for the third energy cumulant are shown in the left panel of Fig. 3. Data

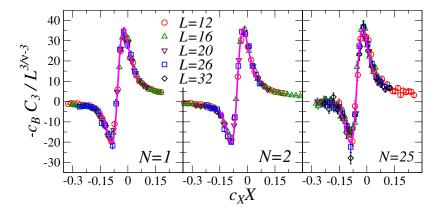


Figure 3: (Adapted from Ref. [93]) Scaling plot of the third energy cumulant, defined by $C_3 = -L^{-3}\langle (H - \langle H \rangle)^3 \rangle$, for N=1 (data across the CH line at fixed J=1), N=2 (data across the MH line at fixed J=1), and N=25 (data across the MH line at fixed J=0.4), from left to right. The FSS behavior of C_3 is discussed in Appendix A.3.2, see Eq. (A.13). We plot $c_B C_3 L^{3-3/\nu}$ versus $c_X X$, where $X=(\kappa-\kappa_c)L^{1/\nu}$, setting $\nu=\nu_{\rm XY}\approx 0.6717$, where $\nu_{\rm XY}$ is the XY value of the critical exponents (see Appendix B for a list of estimates of $\nu_{\rm XY}$) and κ_c is the critical-point value. The nonuniversal constants c_X and c_B are fixed by requiring the data to match the IXY curve (solid line). See Ref. [93] for details. The nice data collapse confirms that all transitions belong to the IXY universality class.

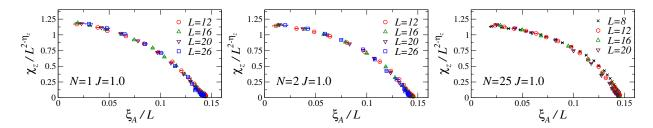


Figure 4: (Adapted from Ref. [93]). Scaling plot of the susceptibility $\chi_z = V^{-1} \sum_{x,y} G_z(x,y)$, $[G_z]$ is defined in (55)] as a function of the RG invariant ratio ξ_A/L , where ξ_A is the second-moment correlation length ξ_A defined in terms of the correlation function $C_{\mu\nu}(x,y)$ defined in Eq. (58) with $\mu=\nu$. All correlation functions are computed in the Lorenz gauge. Results at fixed J=1 for: a) N=1 (CH line); b) N=2 (MH line); c) N=25 (MH line); see the phase diagram in Fig. 2. We report $\chi_z/L^{2-\eta_z}$ against ξ_A/L [see the FSS relation, Eq. (A.24)] using $\eta_z=-0.74$. All data approach the same curve, apart from a multiplicative normalization and hence all systems belong to the same universality class.

nicely scale if the XY critical exponent $\nu_{XY} = 0.6717(1)$ is used. Moreover, the scaling curves match the curve obtained for the IXY model, reported as a solid line in the left panel of Fig. 3. These results confirm that all CH transitions belong to the IXY, or gauge XY, universality class.

Ref. [93] also studied the critical behavior of the charged operator $\Gamma_{\boldsymbol{x}}$ and of the gauge field $A_{\boldsymbol{x},\mu}$. A numerical analysis of the susceptibility $\chi_z = V^{-1} \sum_{\boldsymbol{x},\boldsymbol{y}} G_z(\boldsymbol{x},\boldsymbol{y})$ in the Lorenz gauge provides the estimate [93]

$$\eta_{\Gamma} = \eta_z = -0.74(4), \qquad y_{\Gamma} = \frac{d-2+\eta_{\Gamma}}{2} = 0.13(2),$$
(64)

where y_{Γ} is the RG dimension that can be associated with the nonlocal operator Γ_{x} . A scaling plot is reported in the left panel of Fig. 4.

The RG anomalous dimension η_A of the gauge field has been determined in Ref.[93], by performing a FSS analysis of the gauge correlation function $C_{\mu\nu}(\boldsymbol{x},\boldsymbol{y})$ defined in Eq. (58) in the Lorenz gauge. The numerical FSS analyses [93] confirm the exact result $\eta_A = 1$ that can be proved in the IXY model.²⁴

 $^{^{24}}$ This exact result follows from the correspondence between the zero-momentum $F_{x,\mu\nu}$ correlation function in the IXY

Note that the critical behavior of the charged scalar correlations along the CH line differs from that of the scalar correlations in the XY model obtained for $\kappa \to \infty$, see Fig. 2. Indeed, charged scalar correlations are characterized by the critical exponent $\eta_{\Gamma} \approx -0.7$ along the CH line at finite κ , definitely different from the XY value [95] $\eta_z \approx 0.038$ obtained for the limiting model at $\kappa = \infty$. Obviously, in a finite volume the Lorenz-gauge correlations of the field z_x along the CH line converge to the scalar correlations of the XY model for $\kappa \to \infty$. However, this result does not imply that their asymptotic infinite-size behavior is the same, since the $\kappa \to \infty$ and the $L \to \infty$ limits do not commute: as discussed in Sec. 4.1.2 the uncharged XY FP, which controls the critical behavior for $\kappa \to \infty$, is unstable with respect to gauge fluctuations, giving rise to a nonanalytic crossover behavior.

It is worth noting that the CH transitions are driven by the condensation of the two local fields z_x and $A_{x,\mu}$ if one considers the LAH model in the Lorenz gauge. This allows us to reinterpret the IXY transition as a conventional transition in a model without gauge invariance—the equivalence holds in the Lorenz gauge—with *local* order parameters. However, the effective model requires an additional XY scalar field: the topological properties of the IXY transition are now the result of the nontrivial interplay between the field $A_{x,\mu}$ and the additional XY scalar field z_x in the gauge-fixed N=1 LAH model.

We finally remark that, since the RG flow of the AHFT in the ε -expansion does not show any evidence of the existence of a stable charged FP for N=1, see Sec. 4.1.2, the IXY critical behavior along the CH transition line is apparently unrelated with the RG flow of the AHFT. However, as discussed above, the IXY model has an effective description in terms of a model which appears to be equivalent to the AHFT in the Lorenz gauge, with the same field content and global symmetries. To reconcile this interpretation of the IXY transition with the results of Sec. 4.1.2, one may conjecture that, for N=1, the 3D AHFT RG flow admits a stable FP that is not smoothly connected with the large-N and ε -expansion regimes: as N or the dimension d increases, the FP apparently disappears, so it cannot be identified in four dimensions or for large N. This field-theoretical interpretation is also consistent with the exact result $\eta_A=1$ for the IXY universality class, since $\eta_A=1$ holds at any charged FP of the 3D AHFT, see Eq. (32). An analogous conjecture has been put forward for other statistical systems, for example, for some frustrated spin systems. In that case 3D field-theoretical high-order perturbative analyses provided evidence of stable FPs not analytically connected with those appearing close to four dimensions and in the large-N limit of the 3D theory [95, 160, 163]. Field-theoretical approaches appropriate to describe the 3D critical behavior of N=1 systems (superconductors) were also discussed in Refs. [54, 60, 61, 297, 298].

5.3. Phase diagram and critical behavior of the multicomponent lattice Abelian Higgs model

5.3.1. The Coulomb, Molecular, and Higgs phases

The κ -J phase diagram of the LAH models for $N \geq 2$ (see Refs. [87, 192, 268]) is sketched in the right panel of Fig. 2. The model is invariant under $\mathrm{SU}(N)$ global transformations. Thus, transitions associated with the breaking of the $\mathrm{SU}(N)$ symmetry and phases characterized by standard, i.e., nontopological, order can be present.

The phase diagram is characterized by three different phases. For small J there is a Coulomb (C) phase, which is SU(N) symmetric and in which the gauge field is gapless and charged scalar modes are confined. For large J values there are two phases in which the SU(N) symmetry is broken. They are characterized by the different behavior of the gauge and nonlocal charged modes. In the molecular (M) phase the gauge field is long ranged and scalar charges are confined (as in the C phase), while in the Higgs (H) phase gauge fields are gapped and charges are deconfined, as it occurs in the one-component model.

The existence of these three phases is consistent with the analysis of the model behavior for $\kappa=0$, $J\to\infty$, and $\kappa\to\infty$. For $\kappa=0$ the LAH model reduces to the lattice CP^{N-1} model defined in Eq. (8), which undergoes a continuous O(3)-vector transition for N=2 and discontinuous transitions for $N\geq 3$ [82, 210]. For $J\to\infty$ the model behaves as the one-component LAH model. Indeed, for $J\to\infty$ the relation (63) holds for any N, therefore the gauge field $A_{x,\mu}$ takes only values which are multiples of 2π in all cases. As

model and the helicity modulus Υ computed in the dual XY model [65], and from the fact that Υ scales as L^{-1} in the XY model [296], see Ref. [93] for details.

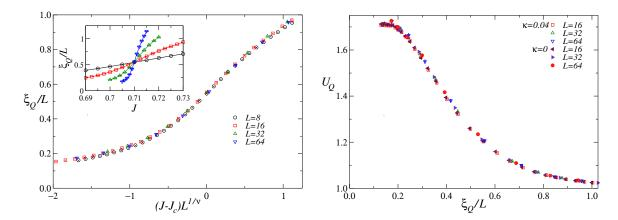


Figure 5: (Adapted from Ref. [87]). Numerical results for N=2 across the CM line. (Left) Plot of ξ_Q/L , where ξ_Q is the second-moment correlation length defined in terms of the correlation function (61) (the FSS behavior of ξ_Q/L is discussed in Appendix A.3.3), as a function of $(J-J_c)L^{1/\nu}$ (as a function of J in the inset), with $J_c=0.7099$ and $\nu=\nu_{O(3)}=0.7117$. Data are obtained by varying J for fixed $\kappa=0.04$. The good collapse of the data provides evidence that the transition belongs to the O(3) universality class, as expected. (Right) Plot of the Binder parameter U_Q of the operator Q_x^{ab} [defined in Eq. (60)] as a function of the ratio ξ_Q/L (the expected FSS behavior is discussed in Appendix A.3.4); we report data obtained by varying J for fixed $\kappa=0.04$ and $\kappa=0$. The excellent collapse of the data for $\kappa=0$ and $\kappa=0.04$ onto the same curve provides a robust evidence that both transitions belong to the same O(3) universality class.

a consequence, for $J \to \infty$ we have an IXY transition at $\kappa = \kappa_{c,IXY} = 0.076051(2)$ [65, 87], independently of N. For $\kappa = \infty$ all plaquettes vanish and the model reduces to the standard O(2N) vector model, up to a gauge transformation (more precisely, partition function and gauge-invariant correlations are the same).²⁵

The three phases of the multicomponent LAH model are separated by three different transition lines, the CM, CH, and MH transition lines, which start from the transition points located at $\kappa=0$, $J=\infty$ and $\kappa=\infty$, and are expected to meet at one point, as shown in Fig. 2. In particular, the phase diagram in the large-N limit is expected to have a simple shape [93]: The transition lines separating the C, M, and H phases become straight lines: the MH line is given by $\kappa=\kappa_c(J=\infty)$, while the CM and CH lines are given by $J=J_c(\kappa=0)=J_c(\kappa\to\infty)$.

The three different transition lines can be characterized by using the order parameters defined in Sec. 5.1.2. The CM transition line is uniquely determined by the spontaneous breaking of the global SU(N) symmetry. The appropriate order parameter is the gauge-invariant composite operator defined in Eq. (60). This order parameter is also relevant along the CH line, along which the global symmetry also breaks, but not along the MH line, which is purely topological and separates two phases with broken global symmetry.

The Higgs phase is a phase in which charges deconfine and gauge fields are gapped. Thus, the nonlocal gauge-invariant charged vector operator [91, 93, 287] Γ_x defined in Eq. (54) is critical along both the CH and the MH line. Analogously, along these two lines also gauge correlation functions (for instance, the correlation function defined in Eq. (58) computed in the Lorenz gauge) are critical.

The transitions along the CM, CH, and MH lines may be of first order or continuous and, in the latter case, belong to universality classes that may depend on the number N of scalar components. The continuous transitions are related to the stable (charged or uncharged) FP of the RG flow of the corresponding effective theory, each one with its own attraction domain in the model parameter space.

5.3.2. The Coulomb-Molecular transition line

Along the small- κ CM line separating the C and M phases, see the right panel of Fig. 2, we expect the transitions to have the same nature as the transition at $\kappa = 0$. For $\kappa = 0$, the LAH model reduces to the

This equivalence allows us to estimate the value of the J where the CH line ends for $\kappa = \infty$: $J_c(\kappa \to \infty) = 0.23396363(6)$ for N = 2 [299], and $J_c(\kappa \to \infty) = J_{c,\infty} + a_1 N^{-1} + O(N^{-2})$ in the large-N limit, with $J_{c,\infty} = 0.252731...$ and $a_1 \approx -0.234$ [300].

lattice formulation of the 3D CP^{N-1} model that has been extensively discussed in Sec. 3.2.1. Accordingly, along the CM line only gauge-invariant scalar modes are expected to be relevant, giving rise to an *uncharged* critical behavior. The critical features of the CM transitions can thus be discussed by using the same LGW model appropriate for the 3D CP^{N-1} model, see Sec. 3.2.1.

As discussed in Sec. 3.2.1, for $N \ge 3$ only first-order transitions are possible. Continuous transitions are possible for N = 2. In this case they belong to the Heisenberg universality class. This is supported by the FSS analyses of numerical results shown in Fig. 5.

5.3.3. The Coulomb-Higgs transition line

We now discuss the nature of the transitions along the large- κ line separating the Coulomb and Higgs phases. Numerical studies show that they can be of first order or continuous, depending on the number N of components of the scalar field [87, 192, 268]. In particular, Ref. [87] observed numerically continuous transitions for N=10,15,25 and first-order transitions for N=4. These results indicate that the transitions along the CH line can be continuous for $N>N_L^*$, and of first order in the opposite case, with $N_L^*=7(2)$.

At the continuous CH transitions scalar, charged, and gauge modes are all critical. As an example, in Fig. 6 we report the results [87, 91] of FSS analyses of numerical data (see Appendix A.3 for a summary of the relevant FSS relations used in the numerical analysis), that provide evidence of a continuous transition for N=25 with critical scalar modes. For instance, the left panel of Fig. 6 shows the scaling behavior of the correlation length ξ_Q computed in terms of the correlation function defined in Eq. (61), while the right panel shows the scaling behavior of the Binder parameter of the scalar field z_x versus the RG invariant ratio ξ_Q/L , computed in the Lorenz gauge (51), where the correlations of the local field z_x equal those of the nonlocal gauge-invariant charged operator Γ_x defined in Eq. (54), see Sec. 5.1.2. The excellent quality of the collapse of the data confirms that the transition is continuous and that correlations of both Q_x and Γ_x are critical. Similar results have been obtained for the gauge-field correlation functions.

It is important to note that the choice of the hard Lorenz gauge fixing (51) turns out to be crucial to observe the condensation of the scalar field z_x . If, instead of imposing the Lorenz constraint (51), we add the gauge-fixing term (52) to the Hamiltonian (soft Lorenz gauge fixing), then scalar-field correlations are always short ranged and the gauge-field correlations show the typical Coulomb behavior, for any positive value of the gauge parameter ζ , irrespective of the phase one is considering. As already noted in Sec. 4.1.3, the hard Lorenz gauge fixing, which is obtained in the limit $\zeta \to 0$, is also singled out by the AHFT. Since $\zeta = 0$ is an unstable FP of the RG flow, see Eq. (34), if we start the RG flow from any finite $\zeta > 0$, then ζ increases towards infinity, so the nongauge-invariant modes become unbounded. The instability of the $\zeta = 0$ FP, implies a nontrivial crossover behavior for small values of ζ , characterized by a length scale $\xi_{\zeta} \sim \zeta^{-1}$. This prediction has been verified numerically in Ref. [91] for the noncompact LAH model.

The simultaneous criticality of gauge, scalar, and charged correlations indicates that CH transitions are charged transitions. Therefore, one expects them to be controlled by the stable charged FP of the AHFT [87]. Thus, one may identify N_L^* with the number N^* of scalar components above which the RG flow of the N-component AHFT admits a stable FP in three dimensions, ²⁶ see Sec. 4.1.2. This conjecture has been checked by comparing the numerical estimates of the critical exponents along the CH transition line (obtained by numerical FSS analyses of MC data [87, 91]), with the 1/N results reported in Sec. 4.1.4 that have been computed in the AHFT.

In Fig. 7 the numerical estimates of the exponent ν and η_q are compared with the 1/N expressions reported in Sec. 4.1.4. The agreement is very good, thus providing a stringent check that the AHFT provides the correct effective description of the continuous transitions along the CH line. The same check has been performed for the exponent η_{Γ} , which has been determined by analyzing the susceptibility χ_z of the scalar field z_x computed in the Lorenz gauge (51). Ref. [91] estimated η_{Γ} for N=25, which, in turn provides an estimate of the RG dimension $y_{\Gamma}=(1+\eta_{\Gamma})/2$ of Γ_x . The result $y_{\Gamma}=0.4655(5)$ compares

Conly the relation $N_L^* \ge N^*$ is rigorously true, since for $N^* \le N < N_L^*$ the phase transition in the lattice model could be outside the attraction domain of the stable AHFT charged FP.

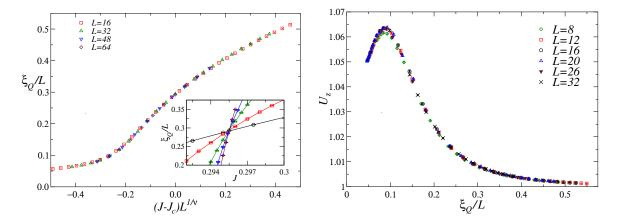


Figure 6: Data for N=25 obtained by varying J across the CH transition line, keeping $\kappa=0.4$ fixed. (Left)(Adapted from Ref. [87]) Plot of ξ_Q/L , where ξ_Q is the second-moment correlation length determined from the two-point correlation function of Q_x^{ab} , defined in Eq. (60); in the main panel data are plotted versus of $(J-J_c)L^{1/\nu}$, with $J_c=0.2955$ and $\nu=0.802$ (the best-fit estimate), in the inset versus J. (Right) (Adapted from Ref. [91]) Plot of the Binder parameter U_z of the scalar field \mathbf{z}_x computed in the Lorenz gauge as a function of the ratio ξ_Q/L , where ξ_Q is defined above (see Appendix A.3.4 for a discussion of the expected FSS behavior). The excellent data collapse signals that both the gauge-invariant correlation function G_Q and the correlation function G_z (computed in the Lorenz gauge) are critical along the CH transition line.

satisfactorily with the large-N field-theory formula [18, 76]

$$y_{\Gamma} = \frac{1}{2} - \frac{10}{\pi^2} \frac{1}{N} + O(N^{-2}), \tag{65}$$

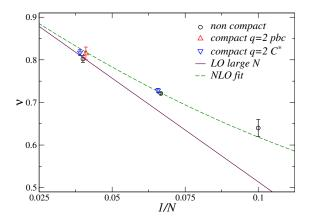
obtained from Eq. (38), which reports η_{ϕ} in the hard Lorenz gauge (in this case $\eta_{\phi} = \eta_{\Gamma}$). Indeed, for N = 25 the large-N formula (65) predicts $y_{\Gamma} \approx 0.459$. This result provides additional evidence of the charged nature of the FP controlling the critical behavior along the CH transition line for sufficiently large N.

Finally, let us discuss the gauge-field correlations. As discussed in Sec. 4.1.2, AHFT predicts $\eta_A=1$ at the charged FP. Numerical results along the CH line are in good agreement with this prediction. It is interesting to observe that the result $\eta_A=1$ also holds at IXY transitions, see Sec. 5.2.2. However, the IXY value cannot be explained by using the AHFT result, since the AHFT is apparently only relevant for the charged CH transitions and not for the topological IXY transition (see however the discussion reported at the end of Sec. 5.2.2).

5.3.4. The Molecular-Higgs transition line

The MH line separates two ordered phases in which the SU(N) symmetry is broken to U(N-1) [64]. MH transitions are characterized by the condensation of the charged nonlocal excitations and of the gauge modes. As shown in Ref. [93] the critical behavior along the MH line is the same as that along the CH line in the one-component LAH model, see Fig. 2. Therefore, along the MH line one expects IXY transitions. This is confirmed by the analyses of the energy cumulants and of the charged correlation functions (computed in the Lorenz gauge) reported in Ref. [93]. It is important to stress that the decoupling of the scalar modes is not obvious, because of the presence of 2N-2 massless Goldstone bosons related with the spontaneous breaking of the SU(N) symmetry [64]. These massless excitations turn out not to play any role in the critical behavior along the MH transitions.

As an example, in Fig. 3 we report a scaling plot of the third energy cumulant for N=2 and N=25. Their FSS behavior is the same as that at the CH transitions in the N=1 model, demonstrating that the transitions belong to the IXY universality class for any N. Charged excitations deconfine at the MH transitions. The RG dimension y_{Γ} of the charged operator Γ_{x} , estimated from the critical behavior of the vector variable z_{x} in the Lorenz gauge (see Sec. 5.1.2), turns out [93] to be independent of N and perfectly



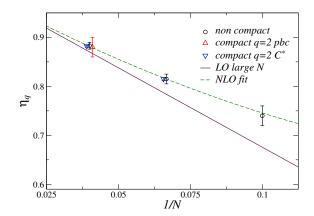


Figure 7: (Adapted from Ref. [90]) Summary of the results for the correlation-length critical exponent ν and for the anomalous dimension η_q of the operator Q_x^{ab} defined in Eq. (60). Results obtained in the noncompact (at CH transitions) and in the compact (at DC-OD transitions) model (these results will be discussed in Sec. 6). Data from Refs. [86, 87, 90]. (Left) We report the estimates of ν , the leading-order large-N estimate, Eq. (35) (LO large N), and an interpolation (NLO fit) obtained by adding a $1/N^2$ correction term to Eq. (35): $\nu = 1 - \frac{48}{\pi^2 N} + \frac{10.5(5)}{N^2}$. (Right) We report the estimates of η_q , the leading-order large-N estimate, Eq. (36) (LO large N), and an interpolation (NLO fit) obtained by adding a $1/N^2$ correction term to Eq. (36): $\eta_q = 1 - \frac{32}{\pi^2 N} + \frac{7.0(5)}{N^2}$.

consistent with the estimate (64) obtained along the CH line of the one-component LAH model, see Fig. 4. Finally, also the critical behavior of the gauge correlations (again computed in the Lorenz gauge) is consistent with an IXY critical behavior. For instance, one obtains $\eta_A = 1$ also along the MH line [93].

5.4. N-component SO(N)-invariant lattice Abelian Higgs model

The above results can be extended to SO(N)-symmetric LAH models, which are the lattice analogue of the SO(N)-symmetric AHFT discussed in Sec. 4.2.1. A lattice SO(N)-invariant LAH model is specified by the Hamiltonian [288, 301]

$$H_O(\boldsymbol{A}, \boldsymbol{z}) = \frac{\kappa}{2} \sum_{\boldsymbol{x}, \mu > \nu} F_{\boldsymbol{x}, \mu \nu}^2 - 2NJ \sum_{\boldsymbol{x}, \mu} \operatorname{Re} \left(\lambda_{\boldsymbol{x}, \mu} \bar{\boldsymbol{z}}_{\boldsymbol{x}} \cdot \boldsymbol{z}_{\boldsymbol{x} + \hat{\mu}} \right) + v \sum_{\boldsymbol{x}} |\boldsymbol{z}_{\boldsymbol{x}} \cdot \boldsymbol{z}_{\boldsymbol{x}}|^2, \tag{66}$$

where again we consider the unit-length constraint $\bar{z}_x \cdot z_x = 1$. One can easily check that, after relaxing the unit-length constraint for the scalar field, this Hamiltonian corresponds to the formal continuum limit of the SO(N)-symmetric AHFT with $\kappa = g^{-2}$.

The phase diagrams at fixed values of v are analogous to that of the SU(N)-symmetric LAH model, see the right panel of Fig. 2. The qualitative features of the three phases are the same, the only differences being the symmetry of the two ordered phases and the nature of the transitions that depend on the specific symmetry-breaking pattern. These two properties are determined by the specific form of the scalar potential and, in particular, by the sign of the Hamiltonian parameter v. The critical behaviors along the various transition lines have been investigated in Refs. [288, 301]. Here we summarize the main results.

The MH transitions are expected to always belong to the IXY universality class, as in SU(N)-invariant LAH models. This is due to the fact that MH transitions are topological transitions driven by the gauge modes, and scalar fields play no role at the transition, as discussed in Sec. 5.3.4. On the other hand, since the symmetry of the ordered phases depends on the parameter v (the ordered phases are symmetric under SO(N-2) and SO(N-1) transformations for v>0 and v<0, respectively), the nature of the CH and CM transitions depends on the sign of v. Correspondingly, also the relevant order parameter at the transition depends on the sign of the parameter. In particular, the transitions can be specified by the condensation of the lattice bilinear operators $R_{L,x}^{ab}$ and $T_{L,x}^{ab}$ defined as their field-theoretical counterparts, see Eq. (42).

The RG analysis of the SO(N)-symmetric AHFT, reported in Sec. 4.2.1, indicates that the LAH model (66) may undergo charged continuous transitions along the CH line for a large number N of components. Indeed, the continuous or first-order nature of the transitions is determined by the presence or absence of a stable FP in corresponding AHFT. As discussed in Sec. 4.2.1, a FP exists only for $N > N_o^*(d=3)$. Moreover, the attraction domain of the stable FP is limited to the parameter region v > 0, i.e., to systems in which the ordered phase is SO(N-2)-symmetric. Therefore, for $N < N_o^*(d=3)$ we expect only first-order transitions along the CH line. For $N > N_o^*(d=3)$, if the Higgs phase is symmetric under SO(N-1) transformations, then the CH line is again a line of first-order transitions. Instead, if the Higgs phase shows the spontaneous symmetry breaking $SO(N) \rightarrow SO(N-2)$, i.e., v is positive, then the CH transitions can be continuous, in the universality class associated with the stable charged FP of the SO(N)-symmetric AHFT.

Along the CM line gauge modes do not develop critical correlations, thus CM transitions admit a conventional LGW effective description in terms of a gauge-invariant order parameter [288]. For negative v, transitions are driven by the condensation of R_x^{ab} , defined in Eq. (42). A straightforward LGW analysis predicts first-order transitions for any $N \geq 3$. For N=2 continuous transitions in the XY universality class are possible. For positive v, the critical behavior can be effectively described by the O(N)-symmetric LGW theory for an antisymmetric rank-two tensor, which is the coarse-grained analogue of T_x^{ab} defined in Eq. (42). This allows us to predict that, for N=2, continuous CM transitions belong to the Ising universality class for all positive values of v. For N=3, instead, one expects the existence of a tricritical value $v^*>0$, such that the transition is of first order for $v< v^*$ and is continuous, in the Heisenberg universality class, for $v>v^*$. The existence of a tricritical value is due to the first-order nature of the CM transitions in SU(3) invariant AH models, i.e., for v=0. The same behavior, with critical Heisenberg transitions for large values of v, occurs also for N=4. For $N\geq 5$ transitions are always of first order. A numerical check of these predictions is reported in Ref. [301].

6. Lattice Abelian Higgs models with compact U(1) gauge variables

In this section we consider an alternative lattice discretization of the AHFT (18) based on compact gauge variables. In compact formulations there are topological features that are absent in noncompact formulations, like the presence of monopole configurations and a nontrivial dependence on the charge Q of the scalar field. As we shall see, these features give rise to notable differences with respect to the noncompact lattice formulation considered in Sec. 5. In particular, the relation with the continuum AHFT (18) turns out to be much less straightforward.

6.1. The compact formulation of lattice Abelian Higgs models

In the compact formulation on a cubic lattice the gauge fields are complex variables $\lambda_{x,\mu}$ satisfying $|\lambda_{x,\mu}|=1$, i.e., elements of the U(1) group, associated with the lattice links. The compact LAH model with N-component scalar fields z_x of integer charge Q is defined by the partition function and lattice Hamiltonian

$$Z = \sum_{\{\boldsymbol{z},\lambda\}} e^{-H_c}, \qquad H_c = -2 \kappa \sum_{\boldsymbol{x},\mu>\nu} \operatorname{Re} \left(\lambda_{\boldsymbol{x},\mu} \lambda_{\boldsymbol{x}+\hat{\mu},\nu} \bar{\lambda}_{\boldsymbol{x}+\hat{\nu},\mu} \bar{\lambda}_{\boldsymbol{x},\nu}\right) - 2NJ \sum_{\boldsymbol{x},\mu} \operatorname{Re} \left(\lambda_{\boldsymbol{x},\mu}^Q \bar{\boldsymbol{z}}_{\boldsymbol{x}} \cdot \boldsymbol{z}_{\boldsymbol{x}+\hat{\mu}}\right), \tag{67}$$

where the two sums in H_c run over all plaquettes and links of the cubic lattice, respectively, and the site variables satisfy the unit-length condition $\bar{z}_x \cdot z_x = 1$. The parameter $\kappa \geq 0$ plays the role of inverse (square) gauge coupling, as can be seen by taking the naive continuum limit in which the link variables are close to one. The compact formulation is well defined for all boundary conditions, since the Hamiltonian is bounded and the configuration space is compact. While in the noncompact case, the gauge group is the noncompact additive group of real numbers, in the compact case the model is invariant under U(1) gauge transformations. The nontrivial topology of the U(1) group allows one to define an integer charge Q and consider scalar fields that transform under a charge-Q representation of the U(1) group. The charge-Q model is invariant under the U(1) gauge transformations

$$z_x \to U_x^Q z_x, \qquad \lambda_{x,\mu} = U_x \lambda_{x,\mu} \bar{U}_{x+\hat{\mu}},$$
 (68)

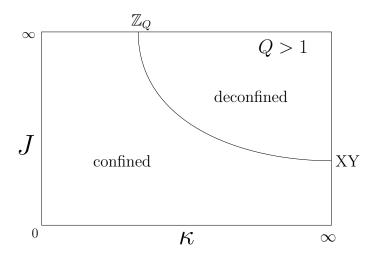


Figure 8: Sketch of the κ -J phase diagram of the 3D one-component CLAH model, in which a compact U(1) gauge field is coupled with a (unit-length) complex scalar field of charge $Q \geq 2$. A confined phase (for small J or small κ) and a deconfined phase (for large J and κ) are present, separated by a deconfinement transition line. For $\kappa \to \infty$ and $J \to \infty$ the model reduces to the XY vector model and to the lattice \mathbb{Z}_Q gauge model with Wilson action, respectively.

where U_x is an x-dependent phase, and under the global transformation $z_x \to V z_x$, where $V \in SU(N)$.

Unlike what happens in noncompact formulations of LAH models, the integer charge Q cannot be absorbed in the definition of the gauge field [302]. Therefore, it should be considered as an additional independent Hamiltonian parameter. As we shall see, the phase diagram of compact LAH models crucially depends on the charge Q. In particular, the κ -J phase diagram of models with Q=1 differs from that of models with $Q\geq 2$. Moreover, as in the noncompact case, the behavior for N=1 is qualitatively different from that obtained for $N\geq 2$.

For N=1 the Hamiltonian (67) can also be rewritten in terms of the gauge fields only. Indeed, in the unitary gauge we can set $z_x = 1$ for all x, obtaining the unitary-gauge Hamiltonian

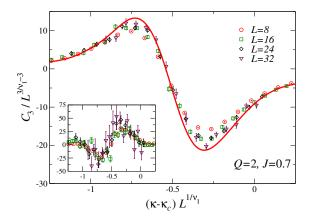
$$H_{\text{ug}} = -2 \kappa \sum_{\boldsymbol{x}, \mu > \nu} \operatorname{Re} \left(\lambda_{\boldsymbol{x}, \mu} \lambda_{\boldsymbol{x} + \hat{\mu}, \nu} \bar{\lambda}_{\boldsymbol{x} + \hat{\nu}, \mu} \bar{\lambda}_{\boldsymbol{x}, \nu} \right) - 2J \sum_{\boldsymbol{x} \mu} \operatorname{Re} \lambda_{\boldsymbol{x}, \mu}^{Q}.$$
 (69)

The unitary gauge is not complete and leaves a residual invariance under local \mathbb{Z}_Q gauge transformations, i.e., under the transformations $\lambda_{x,\mu} = V_x \lambda_{x,\mu} \bar{V}_{x+\hat{\mu}}$, where V_x are complex numbers satisfying $V_x^Q = 1$, i.e., elements of the \mathbb{Z}_Q group. For $Q \geq 2$ topological transitions can be present, as discussed in Sec. 3.5.3, since the model with Hamiltonian (69) is a soft version of the \mathbb{Z}_Q gauge theory defined in Sec. 3.5.2, which is obtained in the limit $J \to \infty$. Indeed, for $J \to \infty$, we should have $\lambda_{x,\mu}^Q = 1$ on all links, which implies that the fields $\lambda_{x,\mu}$ are elements of the discrete \mathbb{Z}_Q group. For Q = 1 the limit is obviously trivial.

6.2. The compact lattice Abelian Higgs model with one-component scalar fields

The phase diagram of the one-component CLAH model with Q=1 is trivial, as there is only one thermodynamic phase [41]. On the other hand, models with any $Q \geq 2$ show two different phases [41, 63, 92], as shown in Fig. 8. These two phases are distinguished by the confinement properties of the charged excitations with q < Q. Indeed, the transition line separating these two phases is related with the deconfinement transition of the charged degrees of freedom with q < Q, which can be probed by considering the behavior of the unit-charge Wilson loops $W_{\mathcal{C}} = \prod_{\ell \in \mathcal{C}} \lambda_{\ell}$, where \mathcal{C} is a closed lattice loop. For $Q \geq 2$, the unit-charge Wilson loops obey the area law in the confined phase and the perimeter law in the deconfined phase. For Q = 1 the area law never holds, due to the screening of the charged scalar modes.

The deconfinement transition line for $Q \geq 2$ is expected to connect the transition points of the models obtained for $J \to \infty$ and $\kappa \to \infty$ [41, 63]. As already mentioned, for $J \to \infty$ we obtain the \mathbb{Z}_Q gauge



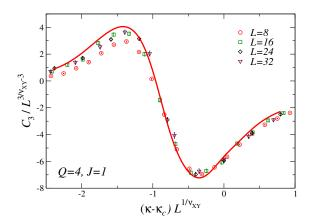


Figure 9: (From Ref. [92]) (Left) Plot of the third energy cumulant C_3 (its expected finite-size behavior is discussed in Appendix A.3.2) as a function of $(\kappa - \kappa_c)L^{1/\nu_I}$ for N=1 and Q=2, at fixed J=0.7. Here $\kappa_c=0.5880$ and ν_I is the Ising value $\nu_I=0.629971$ (see Appendix B for a collection of estimates of ν_I). The continuous curve is (up to nonuniversal rescaling constants) the scaling curve for C_3 in the \mathbb{Z}_2 gauge model (see Ref. [92] for a parametrization). Deviations can be explained by the presence of scaling corrections that vanish as $L^{-\omega_I}$ for large L, where $\omega_I=0.83$ is the universal leading scaling-correction exponent for Ising systems. This is confirmed by the plot shown in the inset, where the combination $L^{\omega_I}\left[L^{3-3/\nu_I}C_3(J,K,L)-\mathcal{C}_3(X)\right]$ is reported as a function of $(\kappa-\kappa_c)L^{1/\nu_I}$, where $\mathcal{C}_3(X)$ (solid curve) is the properly rescaled asymptotic curve computed in the \mathbb{Z}_2 gauge model. The collapse of the data onto a single curve indicates that the observed scaling corrections are consistent with those expected at an Ising transition. (Right) Plot of the third energy cumulant C_3 as a function of $(\kappa-\kappa_c)L^{1/\nu_{XY}}$, for the model with N=1 and Q=4, at fixed J=1. Here $\kappa_c=1.0205$ and ν_{XY} is the XY value $\nu_{XY}=0.6717$ (see Appendix B for estimates of ν_{XY}). The continuous curve is (up to nonuniversal rescaling constants) the scaling curve for C_3 in the IXY gauge model (see Ref. [92] for a parametrization).

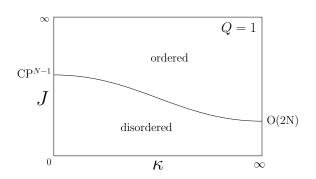
model with Wilson action discussed in Sec. 3.5.2. For $\kappa \to \infty$, we can set $\lambda_{x,\mu} = 1$ on all links, and thus we obtain the standard XY model. Given that the one-component model with charge Q is equivalent to the gauge model with Hamiltonian (69), which is a \mathbb{Z}_Q gauge-invariant model, the finite-J deconfinement transitions are expected to belong to the \mathbb{Z}_Q gauge universality class [92] (see, however, Ref. [63] for an alternative picture based on a line of FPs, thus leading to continuously varying critical exponents). As a consequence (see Sec. 3.5.2 for a discussion of the critical behavior of \mathbb{Z}_Q gauge-invariant models), the continuous transitions must belong to the Ising gauge universality class and to the XY gauge universality class for Q = 2 and $Q \ge 5$, respectively. For Q = 3 we expect first-order transitions. For Q = 4 the \mathbb{Z}_4 gauge theory that is obtained in the limit $J \to \infty$ has an Ising gauge transition, but, as discussed in Sec. 3.5.2, this is not the generic behavior expected for \mathbb{Z}_4 gauge invariant models. Generic \mathbb{Z}_4 gauge models should have continuous transitions in the XY gauge universality class. For finite J we therefore expect XY gauge transitions also for Q = 4.

Numerical FSS analyses of the energy cumulants [92] for Q=2, 4, 6, see Fig. 9, fully support the above predictions. It is worth mentioning that, for any value of the charge Q, there are significant crossover effects for relatively large values of κ , due to the presence of the XY spin FP that controls the critical behavior in the $\kappa \to \infty$ limit, which is unstable with respect to a nonzero gauge coupling $\alpha \equiv g^2 \sim 1/\kappa$, see Sec. 4.1.2.²⁷

6.3. The multicomponent compact lattice Abelian Higgs model

Multicomponent LAH models with compact gauge variables present a phase diagram that is more complex than that of the one-component model, because of the presence of transitions where the $\mathrm{SU}(N)$ symmetry spontaneously breaks. The phase diagrams for any $N\geq 2$ are sketched in the left and right panels of Fig. 10, for Q=1 and $Q\geq 2$, respectively.

²⁷The 3D RG dimension $y_{\alpha} = 1$ of the gauge coupling $\alpha \sim \kappa^{-1}$ provides the crossover exponent, which corresponds to the energy dimension of the gauge coupling α . Therefore, in the large- κ limit, the gauge field gives rise to an intrinsic crossover scale $\xi_{\alpha} \sim \kappa$. If the correlation length ξ or the size of the system L satisfies $\xi \lesssim \xi_{\alpha}$ or $L \lesssim \xi_{\alpha}$, significant crossover effects can be observed, with an apparent spin XY behavior.



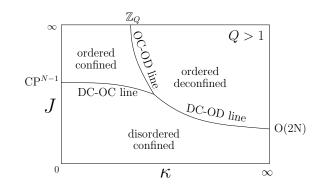


Figure 10: Sketch of the phase diagram of the 3D LAH model (67) with charge Q=1 (left panel) and $Q\geq 2$ (right panel), for generic $N\geq 2$. For Q=1 (left), the high-temperature (small J) and low-temperature (large J) phases are separated by a single transition line, characterized by the spontaneous breaking of the SU(N) symmetry. For $Q\geq 2$ (right), the phase diagram presents three phases, the disordered-confined (DC), the ordered-deconfined (OD), and the ordered-confined (OC) phase. The compact LAH model is equivalent to the \mathbb{CP}^{N-1} model for $\kappa=0$, to the O(2N) vector model for $\kappa\to\infty$, and to the lattice \mathbb{Z}_Q gauge model for $J\to\infty$.

6.3.1. Phase diagram for Q = 1

As sketched in the left panel of Fig. 10, only two phases are present for Q=1: a disordered phase for small J and an ordered phase for large J. They are separated by a single transition line, characterized by the breaking of the $\mathrm{SU}(N)$ symmetry, signaled by the condensation of the gauge-invariant bilinear operator Q_x^{ab} , defined in Eq. (60). At the transition, gauge fields only prevent gauge-dependent correlations, such as the vector correlations $\langle \bar{z}_x \cdot z_y \rangle$, from becoming critical (actually, due to gauge invariance $\langle \bar{z}_x \cdot z_y \rangle = \delta_{x,y}$). For $\kappa = 0$, the model is equivalent to the gauge CP^{N-1} model, whose critical behavior has been discussed

For $\kappa = 0$, the model is equivalent to the gauge \mathbb{CP}^{N-1} model, whose critical behavior has been discussed in Sec. 3.2.1. A natural hypothesis, that is confirmed by a detailed numerical study [84], is that the critical behavior does not depend on the value of κ . Thus, for any finite κ the Q = 1 model undergoes a LGW transition with gauge-invariant order parameter, as the \mathbb{CP}^{N-1} model. It follows, see Sec. 3.2.1, that continuous transitions (in the Heisenberg universality class) are only possible for N = 2. For larger values of N, we instead expect the transitions to be of first order. Note that the same critical behavior occurs in noncompact LAH models along the CM line (see the right panel of Fig. 2), as discussed in Sec. 5.3.2.

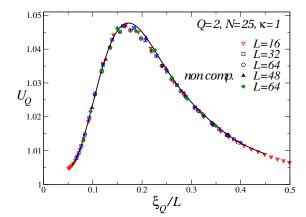
In the limit $\kappa \to \infty$, the model reduces to an O(2N) vector model, which presents a continuous transition at a finite value of J for any N. The corresponding FP is unstable with respect to a nonzero gauge coupling $\alpha \sim \kappa^{-1}$, see Sec. 4.1.2, but, as it occurs for the one-component compact LAH model discussed in Sec. 6.2, its presence gives rise to significant crossover effects for large values of κ .

6.3.2. Phase diagram for $Q \geq 2$

For $Q \geq 2$ the phase diagram is more complex, see the right panel of Fig. 10, with three different phases [41, 62, 63, 67, 70, 73, 75, 86]. They are characterized by the large-distance behavior of both scalar and gauge observables. Beside the gauge-invariant bilinear order parameter Q_x^{ab} [see. Eq. (60)], one may consider Wilson loops, which signal the confinement or deconfinement of external static sources with unit charge.

As shown in the right panel of Fig. 10, for small J and any $\kappa \geq 0$, there is a phase in which scalar-field correlations are disordered and single-charge modes are confined (the Wilson loop obeys the area law). For large values of J (low-temperature region) scalar correlations are ordered and the $\mathrm{SU}(N)$ symmetry is broken. Two different phases occur here: static single-charge test particles are confined for small κ and deconfined for large κ .

The three different phases are separated by three transition lines: the DC-OD transition line between the disordered-confined (DC) and the ordered-deconfined (OD) phases, the DC-OC line between the disordered-confined and ordered-confined (OC) phases, and the OC-OD line between the ordered-confined and ordered-deconfined phases. They are expected to meet at one point in the center of the phase diagram. The transition



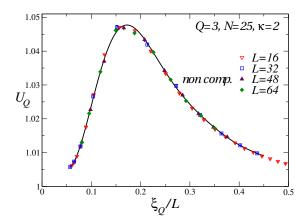


Figure 11: (Adapted from Ref. [90]) (Left) Plot of U_Q versus ξ_Q/L , where U_Q and ξ_Q are the Binder parameter and the second-moment correlation length defined in terms of the gauge-invariant operator Q_x^{ab} defined in Eq. (60). Results for the compact and noncompact model with N=25 and (compact model) Q=2. Data are obtained in MC simulations varying J across the DC-OD (compact) and CH (noncompact) line for $\kappa=1$. The solid line is an extrapolation of the data for the noncompact LAH model. Since U_Q and ξ_Q/L are RG invariant quantities, the collapse of the data signals that the transitions in the two models belong to the same universality class (see Appendix A.3.4 for a discussion of the FSS behavior). (Right) Same plot as in the left panel for the compact model with Q=3, fixing $\kappa=2$.

lines have different features that depend on the number N of components and on the charge Q of the scalar field

The transitions along the DC-OC line are analogous to those occurring along the unique transition line present for Q=1, see Sec. 6.3.1, and along the CM line in noncompact models. In particular, they have the same nature as in the 3D lattice CP^{N-1} model obtained for $\kappa=0$. Therefore, continuous transitions are only expected for N=2, with a critical behavior belonging to the O(3) vector universality class.

In the limit $J \to \infty$, the model (67) becomes equivalent to a \mathbb{Z}_Q gauge model with Wilson action [86], as it occurs for N=1, see Sec. 6.2. A natural hypothesis is that the transitions along the OC-OD line belong to the universality class of the \mathbb{Z}_Q gauge model, as in the N=1 compact LAH model, see Sec. 6.2. This prediction has been verified numerically for Q=2. Ref. [86] computed the energy cumulants, finding that they have the same FSS behavior as in the \mathbb{Z}_2 gauge model. These results confirm that the OC-OD transitions belong to the Ising gauge universality class for this value of Q.

The transitions along the large- κ DC-OD line have been investigated numerically in Ref. [86], which focused on the compact model for N=15 and 25 and two charge values, Q=2 and Q=3, and analyzed the finite-size behavior of the correlation function of the operator Q_x^{ab} (some data are reported in Fig. 11). The analysis shows that the continuous DC-OD transitions belong to the same universality as the transitions along the CH line in the noncompact models discussed in Sec. 5.3.3, for all values of N and Q investigated. Some results taken from Ref. [86] are reported in Fig. 11, which shows that the data for the compact and the noncompact model have the same FSS behavior. Moreover, the estimated critical exponents computed in the compact and in the noncompact model for the same value of N are consistent within errors, see Fig. 7. Therefore, the stable charged FP point of the RG flow of the AHFT, see Sec. 4.1.2, which exists for $N \gtrsim 7$, controls the continuous transitions in multicomponent LAH models with both noncompact and compact gauge variables for large values of κ ; more precisely, along the CH line in noncompact models and along the DC-OD line in compact models with any charge Q satisfying $Q \ge 2$.

6.3.3. Relation between the compact and the noncompact lattice Abelian Higgs models

The previous results show that noncompact and compact $(Q \geq 2)$ LAH models have similar phase diagrams. For $N \geq 2$, the compact DC-OC line and the noncompact CM line have the same nature, and so have the compact DC-OD and noncompact CH line for any $Q \geq 2$. The MH line and the OC-OD line both correspond to topological transitions. These results may appear unexpected. Therefore, it is

worth discussing the relation between the compact and noncompact models in more detail, to explain the similarities of their phase diagram.

For this purpose, we note that the compact formulation of LAH models is equivalent to the noncompact one in the limit $Q \to \infty$, $\kappa \to \infty$ at fixed κ/Q^2 . Indeed, if we rewrite the compact field $\lambda_{x,\mu}$ as $\lambda_{x,\mu} = e^{iA_{x,\mu}/Q}$ with $A_{x,\mu} \in [-\pi Q, \pi Q]$, the compact-field Hamiltonian (67) becomes

$$H_c = -2\kappa \sum_{\boldsymbol{x}, \mu > \nu} \operatorname{Re} \exp \left[-\frac{i}{Q} (\Delta_{\hat{\mu}} A_{\boldsymbol{x}, \nu} - \Delta_{\hat{\nu}} A_{\boldsymbol{x}, \mu}) \right] - JN \sum_{\boldsymbol{x}, \mu} 2 \operatorname{Re} \left(\bar{\boldsymbol{z}}_{\boldsymbol{x}} \cdot e^{iA_{\boldsymbol{x}, \mu}} \, \boldsymbol{z}_{\boldsymbol{x} + \hat{\mu}} \right). \tag{70}$$

For $Q \to \infty$, the gauge real variables $A_{x,\mu}$ become unbounded, and the Hamiltonian becomes equivalent to that of the noncompact formulation with $\kappa_{\rm nc} = 2\kappa/Q^2$, where $\kappa_{\rm nc}$ is the gauge coupling of the resulting noncompact gauge-field Hamiltonian. Note that this equivalence trivially holds as long as the fluctuations of $A_{x,\mu}$ on each plaquette are bounded and uncorrelated for $Q \to \infty$, i.e., for any point of the phase diagram. In particular, in Sec. 3.5.2 it has already been discussed for the \mathbb{Z}_Q gauge model (the limiting model of the compact LAH model for $J \to \infty$), which is equivalent to the IXY model (the limiting model of the noncompact LAH model for $J \to \infty$) in the limit considered above.

The argument presented above shows that the compact model converges to the noncompact one as $Q, \kappa \to \infty$, at fixed $\kappa_{\rm nc} = 2\kappa/Q^2$. Therefore, also their phase diagrams must become identical for large Q. As far as the nature of the critical lines, the numerical evidence reported in Sec. 6.3.2 shows that the compactification of the model is an irrelevant perturbation of the noncompact model obtained for $Q = \infty$, as already discussed for the IXY model in Sec. 3.5.2. Thus, the critical behavior should become identical for $Q \to \infty$. In practice, it is not really required to take large values of Q to observe the same IXY critical behavior, as in the noncompact model. As we have already mentioned, the behavior along the DC-OC and DC-OD is the same as that on the corresponding CM and CH lines for any $Q \ge 2$, while the behavior along the OC-OD and MH lines is the same for any $Q \ge 4$. Thus, differences only occur along the line of topological transitions that end at $J = \infty$ for Q = 2 and 3. While in the noncompact model these topological transitions belong to the IXY universality class, in the compact one the IXY critical behavior is only observed for $Q \ge 4$. For Q = 3 transitions are of first order, while for Q = 2 they belong to the Ising gauge universality class.

6.3.4. Relevance of monopole configurations

In compact gauge models, the nontrivial topology of the gauge fields allows one to define topological objects. Their role has been investigated in several studies, see, e.g., Refs. [66, 85, 89, 215, 303, 304], which indicate that their presence may significantly affect the nature of the phase transitions and their critical behavior. Refs. [85, 89] performed a numerical study to understand the role of monopole configurations, which naturally emerge in LAH models with compact gauge fields, using the monopole definition of Ref. [305].

In lattice systems with periodic boundary conditions one can define monopoles and antimopoles using the prescription proposed in Ref. [305]. This prescription starts from the noncompact lattice curl $\Theta_{\boldsymbol{x},\mu\nu} = \theta_{\boldsymbol{x},\mu} + \theta_{\boldsymbol{x}+\hat{\mu},\nu} - \theta_{\boldsymbol{x},\nu} - \theta_{\boldsymbol{x}+\hat{\nu},\mu}$ associated with each plaquette, where $\theta_{\boldsymbol{x},\mu} \in [-\pi,\pi)$ is the phase associated with the compact lattice variable $\lambda_{\boldsymbol{x},\mu}$, $\lambda_{\boldsymbol{x},\mu} = e^{i\theta_{\boldsymbol{x},\mu}}$. Note that $\Theta_{\boldsymbol{x},\mu\nu}$ is antisymmetric in μ and ν , so this definition provides two different quantities that differ by a sign for each plaquette, depending on the orientation. One can easily verify that, for any closed lattice surface S made of elementary plaquettes, the naively defined outgoing magnetic flux across S vanishes, i.e., $\sum_{P \in S} \Theta_{\boldsymbol{x},\mu\nu} = 0$, where the sum extends to all plaquettes in S, $\Theta_{\boldsymbol{x},\mu\nu}$ is associated with plaquette $P = (\boldsymbol{x},\mu\nu)$, and the plaquette orientation is chosen in such a way that the unit vector $\hat{\mu} \times \hat{\nu}$ points outward with respect to the surface.²⁸ To define a nontrivial net number of monopoles (i.e., the difference between the number of monopoles and of antimonopoles) within the surface S, one must isolate the singular contribution from the smooth background corresponding to

²⁸These rules are a discrete version of the integration rules of a differential two-form on a two-dimensional surface, which can be formalized using the formalism of lattice differential forms, see, e.g., Ref. [306].

small values of $|\Theta_{x,\mu\nu}|$. This can be done by defining

$$N_{\text{mono}}(S) = \sum_{P \in S} M\left(\frac{\Theta_{\boldsymbol{x},\mu\nu}}{2\pi}\right), \qquad M(x) = x - \lfloor x + 1/2 \rfloor, \tag{71}$$

where $\lfloor \rfloor$ denotes the floor function. The function M(x) satisfies $-1/2 \leq M(x) < 1/2$, M(x) = x for any x in the interval [-1/2, 1/2); moreover, M(x) - x is always an integer. The fact that N_{mono} is an integer number easily follows from these properties. Note that $|\Theta_{\boldsymbol{x},\mu}|$ has to be larger than π on some plaquettes for $N_{\text{mono}}(S)$ to be nonvanishing.

A topic that has been investigated in the literature is whether the suppression of the monopole configurations in the partition function changes the nature of the transition, or whether it gives rise to new universality classes somehow related to those found in noncompact formulations, in which analogous monopole configurations are absent. These issues have been addressed in Refs. [85, 89]. In the lattice CP^{N-1} model defined by the Hamiltonian reported in Eq. (8), a finite density of monopoles is observed in the disordered low-J phase up to the critical point, while in the low-temperature regime $J > J_c$ only isolated pairs of monopoles and anti-monopoles are typically present, whose number decreases rapidly with increasing J, since $\Theta_{x,\mu\nu}$ approaches zero in the large-J limit. Thus, the monopole density is an appropriate order parameter of the transition. As a consequence, by considering only monopole-free configurations, one is changing the nature of the small-J phase, and therefore one expects a different critical behavior or even the absence of any transition.

To define a monopole-free version of the \mathbb{CP}^{N-1} model (MFCP^{N-1}), one may change the configuration space, considering only configurations for which $N_{\text{mono}}(C)=0$ on any elementary lattice cube C [85, 89]. The numerical analyses of Refs. [85, 89] show that the MFCP^{N-1} models, as well as some extensions obtained by relaxing the unit-length condition on the scalar fields, undergo finite-J transitions. However, the features of these transitions are apparently unrelated with those of the transitions in the standard \mathbb{CP}^{N-1} model. In particular, there is no O(3) continuous transition for N=2. Moreover, the numerical data definitely exclude that the MFCP^{N-1} model has a transition associated with the AHFT for large values of N [85, 89]. Ref. [86] also studied the critical behavior of monopole-free "higher-charge" \mathbb{CP}^{N-1} models, obtained by

Ref. [86] also studied the critical behavior of monopole-free "higher-charge" \mathbb{CP}^{N-1} models, obtained by setting $\kappa=0$ in Eq. (67).²⁹ The results show that, for $Q\geq 2$ the monopole-free model has the same behavior as the standard \mathbb{CP}^{N-1} model. This means that in the compact LAH model the topological properties of the gauge field are inessential for any $Q\geq 2$, which is consistent with the fact that the compact and noncompact model have analogous phase diagrams for $Q\geq 2$, and in particular with the appearance (for $N\gtrsim 7$) of an AHFT critical behavior both in the noncompact LAH model along the CH line and in the compact LAH model with $Q\geq 2$ along the DC-OD line, see the discussion in Sec. 6.3.2.

7. Lattice spin systems with discrete gauge symmetries

In this section we review the phase diagram and critical behavior of gauge spin systems with discrete gauge group, focusing mainly on lattice \mathbb{Z}_2 -gauge N-vector models, obtained by minimally coupling N-component real fields with \mathbb{Z}_2 -gauge fields [233]. As discussed in Sec. 3.3 they are paradigmatic models undergoing LGW $^{\times}$ phase transitions. They display different phases, characterized by the spontaneous breaking of the global O(N) symmetry and by the different topological properties of the \mathbb{Z}_2 -gauge correlations, see, e.g., Refs. [20, 41]. They are relevant in several different contexts, see, e.g., Refs. [307–319]. In particular, they are relevant for transitions in nematic liquid crystal [313, 315, 316, 320–322] and for systems with fractionalized quantum numbers, see, e.g., Refs. [309, 318].

 $^{^{29}}$ If we set $\kappa=0$ in Eq. (67) we obtain a charge-Q CP^{N-1} model. In the absence of the monopole-free condition, this model is equivalent to the standard Q=1 CP^{N-1} model (it is enough to redefine the gauge fields). This equivalence does not hold in the monopole-free version, as in this case it is not possible to replace $\lambda_{x,\mu}^Q$ with $\lambda_{x,\mu}$, as the gauge fields also appear in the monopole-free condition. Thus, we obtain a different monopole-free model for each Q.

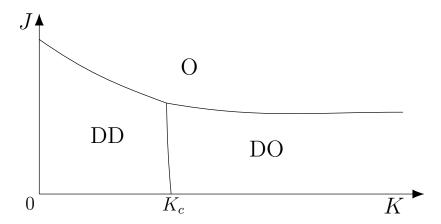


Figure 12: Sketch of the K-J phase diagram of the 3D \mathbb{Z}_2 -gauge N-vector model with $N \geq 2$. There are two spin-disordered phases for small J: a small-K phase, in which both spin and \mathbb{Z}_2 -gauge variables are disordered (we indicate it by DD), and a large-K phase, in which the \mathbb{Z}_2 -gauge variables order (we indicate it by DO). For large J there is a single phase, in which both spins and gauge variables are ordered (we indicate it by O).

7.1. The \mathbb{Z}_2 -gauge N-vector models

The \mathbb{Z}_2 -gauge N-vector model is a lattice N-vector model with local \mathbb{Z}_2 gauge invariance. From the point of view of the symmetries, it can be interpreted as an N-vector model, which is symmetric under $O(N) = \mathbb{Z}_2 \otimes SO(N)$ transformations, in which the \mathbb{Z}_2 symmetry is gauged, giving rise to a \mathbb{Z}_2 -gauge theory coupled with scalar vector fields. Its lattice Hamiltonian is reported in Eq. (17). It is invariant under global SO(N) transformations $s_x \to V s_x$ with $V \in SO(N)$, and local \mathbb{Z}_2 gauge transformations,

$$s_{x} \to w_{x} s_{x}, \qquad \sigma_{x,\nu} \to w_{x} \sigma_{x,\nu} w_{x+\hat{\nu}}, \qquad w_{x} = \pm 1.$$
 (72)

Due to the \mathbb{Z}_2 gauge invariance, the correlation function of the vector variables \mathbf{s}_x , $G_s(\mathbf{x}, \mathbf{y}) = \langle \mathbf{s}_x \cdot \mathbf{s}_y \rangle$, trivially vanishes for $\mathbf{x} \neq \mathbf{y}$. For $N \geq 2$, the spontaneous breaking of the global SO(N) symmetry is signaled by the condensation of the gauge-invariant bilinear operator R_x^{ab} ,

$$R_{\boldsymbol{x}}^{ab} = s_{\boldsymbol{x}}^{a} s_{\boldsymbol{x}}^{b} - \frac{1}{N} \delta^{ab}, \tag{73}$$

which is the analogue of the operator Q_x^{ab} defined in the LAH model, see Eq. (60). Its correlation function

$$G_R(\boldsymbol{x}, \boldsymbol{y}) \equiv \langle \operatorname{Tr} R_{\boldsymbol{x}} R_{\boldsymbol{y}} \rangle$$
 (74)

orders at the transition. If the transition is continuous, at the critical point it behaves as

$$G_R(\boldsymbol{x}, \boldsymbol{y})|_{T=T_c} \sim |\boldsymbol{x} - \boldsymbol{y}|^{-2Y_R},$$
 (75)

where Y_R is the RG dimension of R_x^{ab} , which may depend on the number N of components of the scalar field and also on the specific transition line (as we shall see, this occurs for N=2).

7.2. Phase diagram and critical behavior of \mathbb{Z}_2 -gauge N-vector models with $N \geq 2$

The phase diagram for $N \geq 2$ is sketched in Fig. 12, see, e.g., Refs. [20, 41, 233]. Two spin-disordered phases are present for small J: a small-K phase, in which both spin and \mathbb{Z}_2 -gauge variables are disordered (DD), and a large-K phase in which the \mathbb{Z}_2 -gauge variables order (DO). For large J there is a single ordered phase in which both spins and gauge variables order (O). These phases are separated by three transition lines, which meet at one point, see Fig. 12.³⁰ Note that in the ordered phase, once a representative of the

³⁰An estimate of the intersection point (K_{\star}, J_{\star}) of the three lines for small values of N $(N \lesssim 5 \text{ say})$ is reported in Ref. [233]: $K_{\star} \approx 0.761 - 0.003N \approx 0.75$, $J_{\star} \approx 0.23$.

minimum energy configuration is chosen, i.e., $s_x = s_{x+\hat{\mu}}$ and $w_{x,\mu} = 1$ (up to gauge transformations and in the thermodynamic limit), there is no residual gauge symmetry. Therefore, we do not expect the presence of topological phases or transitions, see the discussion reported in Sec. 3.5.3.

In the following we review the existing theoretical and numerical results for the nature of the transitions along the three transition lines. More details can be found in Refs. [233, 234].

7.2.1. Topological \mathbb{Z}_2 -gauge transitions along the DD-DO transition line

For J=0 the model reduces to the \mathbb{Z}_2 gauge model [119], reviewed in Sec. 3.5.2, for any N. Therefore, there is a continuous topological phase transition [86, 323] at J=0, $K_{\mathbb{Z}_2}=0.761413292(11)$, separating a small-K confined phase from a large-K deconfined phase. The J=0 critical point is the starting point of a transition line, which separates two phases in which the spin variables are disordered. For J>0 these phases can no longer be characterized by the size behavior of the Wilson loops, which always obey the perimeter law because of the screening of the charged fields. Nonetheless, they can still be distinguished by the different topological properties of the gauge modes [20, 41]. In particular, the gauge field is disordered for small K and ordered for large K. This result follows from the observation that, since the spin variables are not critical for sufficiently small values of J, they can be integrated out. For the values of J for which the strong-coupling expansion converges, one obtains an effective \mathbb{Z}_2 gauge theory with local couplings, which is expected to have the same critical behavior as the model for $J=0.^{31}$

7.2.2. RP^{N-1} -like transitions along the DD-O transition line

The transitions along the DD-O line have the same nature as the transition in the RP^{N-1} model obtained for K=0 [233]. As discussed in Sec. 3.2.2, the RP^{N-1} model undergoes a LGW transition, which may be continuous only for N=2—in this case it belongs to the XY universality class. For $N\geq 3$ the transitions are of first order.

The order parameter of the DD-O transitions is the bilinear operator R_x^{ab} defined in Eq. (73). For N=2, if the transition is continuous, it behaves as an XY vector field, so its RG dimension Y_R coincides with the RG dimension $Y_{V,XY} = (1 + \eta_{XY})/2$ of the vector field in the standard XY model. Thus, at continuous transitions along the DD-O line for N=2, we have $Y_R=Y_{V,XY}=0.519088(22)$ (using the estimates of η_{XY} reported in Appendix B). The transitions along the DD-O line for N=2 have been also investigated numerically [233], confirming that continuous transitions behave as predicted by the LGW approach, but also observing that the continuous transitions turn into first-order ones for $K=K_{\rm tri}$, with $K_{\rm tri} < K^*$, i.e., before the intersection point (at $K=K^*$) of the transition lines. Some numerical results are reported in the left panel of Fig. 13.

7.2.3. $O(N)^{\times}$ transitions along the DO-O transition line

The transitions along the DO-O line, at least for large enough values of K, belong to the $O(N)^{\times}$ universality class [21, 234, 324, 325].³² As the standard O(N) vector transitions, they are characterized by the symmetry-breaking pattern $SO(N) \rightarrow O(N-1)$. However, the vector field that is supposed to be the order parameter of the transition is not gauge invariant. They are therefore LGW[×] transitions in the classification of Sec. 3.1.

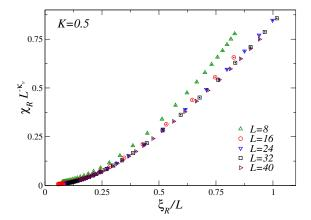
For $K \to \infty$ the plaquette term in the Hamiltonian (17) converges to one. Therefore, in infinite volume, we can set $\sigma_{x,\mu} = 1$ modulo gauge transformations, obtaining the same partition function as that of the standard N-vector model. It follows that the model undergoes a continuous transition at a finite $J_c(K = \infty)$ belonging to the O(N) vector universality class.³³

As discussed in Sec. 7.1, the breaking of the SO(N) symmetry along the DO-O line is signaled by the condensation of the operator R_x^{ab} defined in Eq. (73). Along the DO-O line this operator, as well as all gauge-invariant operators, have the same critical behavior as in the conventional N-vector model without gauge

³¹At leading order in J, one again obtains the \mathbb{Z}_2 gauge model [41, 119, 235, 313], with renormalized gauge coupling $K+NJ^4$. This implies $K_c(J) = K_c(J=0) - NJ^4 + O(J^6)$.

³²Note that in these references the $O(N)^{\times}$ universality class was denoted by the symbol $O(N)^*$.

 $^{^{33}}$ Estimates of the critical point of the standard N-vector models defined in Eq. (1)—therefore, of $J_c(K=\infty)$ —can be found in Refs. [209, 293, 295, 299, 300, 326, 327].



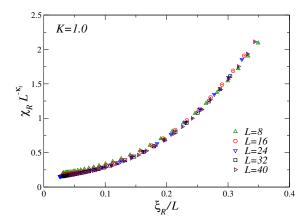


Figure 13: (Adapted from Ref. [233]) Plot of the rescaled susceptibility χ_R versus ξ_R/L , where χ_R and the second-moment correlation length ξ_R are defined in terms of two-point function $G_R(x,y)$ defined in Eq. (75). Results for N=2. Left: results for K=0.5 (DD-O line); we set $\kappa_v=3-2Y_{V,XY}=1.96182$. Right: results for K=1.0 (DO-O line); we set $\kappa_t=3-2Y_{T,XY}=0.5274$. The nice data collapse shows that $Y_{V,XY}$ and $Y_{T,XY}$ are the correct scaling dimensions of the operator R_x^{ab} along the DD-O and DO-O transition lines, respectively.

invariance [233]. The equivalence of the gauge-invariant correlations in O(N) models and along the DO-O line implies that the gauge modes do not drive the critical behavior for finite large values of K. Moreover, these transitions have the same effective description as the conventional O(N) ones, although there is no appropriate gauge-invariant order parameter. These transitions are therefore $O(N)^{\times}$ transitions, according to the classification reported in Sec. 3.1. Note that these transitions differ from the RP^{N-1} transitions that occur along the DD-O line, which are also LGW transitions but with a different, gauge-invariant, order parameter, see Sec. 7.2.2.

The existence of the DO-O $O(N)^{\times}$ transition line implies the stability, against gauge fluctuations, of the O(N) vector transition occurring for $K \to \infty$. Note that this is only possible if the gauge group is discrete and is related to the fact that the DO-O line separates two phases, in which the gauge variables are topologically ordered. Indeed, gauge fluctuations are expected to be generally relevant in models with continuous Abelian and non-Abelian gauge symmetries. In that case, gauge interactions destabilize the vector critical behavior, leading to transitions of different nature, as discussed in Section 4.1.2.

In $O(N)^{\times}$ transitions, the main issue is the identification of the non-gauge-invariant order parameter. In noncompact models, local order parameters are identified by introducing an appropriate gauge fixing, the Lorenz gauge, see Sec. 5 and, particular, Sec. 5.1.2. In the context of compact models, one can exploit a stochastic gauge-fixing procedure [233, 234], as discussed below in Sec. 7.3. The introduction of this peculiar gauge fixing allows one to identify the spin variable s_x as the order parameter of the transition, as in standard N-vector systems. Numerical results for N=1,2,3 reported in Refs. [233, 234] fully confirm this scenario. In the gauge-fixed theory, along the DO-O line the vector field s_x behaves as in the standard N-vector model.

Let us finally focus on the \mathbb{Z}_2 -gauge XY (N=2) model, which is the only case in which continuous transitions may occur along all three transition lines. It is interesting to note that the continuous transitions along the DD-O and DO-O lines are all expected to belong to the 3D XY universality class. However, this does not imply that the critical behavior is the same, as the two transition lines have different effective LGW descriptions. This is clearly demonstrated by the different critical behavior of the operator R_x^{ab} defined in Eq. (73). As discussed in Sec. 7.2.2, the bilinear operator R_x^{ab} is the effective XY order parameter at continuous DD-O transitions, so its RG dimensions is the same as that of the vector field in the XY model: $Y_R = Y_{V,XY} = (1 + \eta_{XY})/2 \approx 0.519$. On the other hand, along the DO-O line, gauge-invariant quantities behave as in the O(N) vector model. Therefore, the operator R_x^{ab} behaves as a spin-two tensor operator at a standard XY transition. It follows that its RG dimension equals the RG dimension $Y_{T,XY}$ of the spin-2 operator in the XY model (numerical estimates of this quantity are reported in Refs. [175, 254, 328, 329]):

 $Y_R = Y_{T,XY} = 1.23629(11)$. These predictions have been verified numerically in Ref. [233]. As an example, some results are reported Fig. 13, which confirm the identification of the DO-O transitions as $O(N)^{\times}$ continuous transitions with a gauge-dependent vector order parameter, and of the DD-O as LGW transitions with a gauge-invariant spin-two order parameter.

7.3. The stochastic gauge fixing

In noncompact LAH models the critical behavior of gauge and charged excitations can be determined by studying local correlation functions in an appropriately gauge-fixed theory, see Sec. 5.1.2. Moreover, as discussed in Refs. [91, 287] not all gauge fixings can be used: local gauge-dependent operators may be used to uncover the critical behavior of charged excitations in the Lorenz gauge, but not, e.g., in the axial gauge.

By analogy, one expects that the identification of the vector order parameter of $O(N)^{\times}$ transitions with a local operator requires the introduction of a gauge fixing in the theory. A standard way of fixing the gauge in compact models consists in setting the bond variables on a maximal lattice tree equal to the identity [262, 289]. A particular case of this procedure is the axial gauge, in which all bonds in a given lattice direction are set equal to the identity (paying attention to the boundary conditions and adding some additional constraints on the boundaries). However, as discussed in Ref. [234], these gauge fixings do not solve the problem, i.e., they do not allow one to identify the critical vector modes that characterize the $O(N)^{\times}$ universality class. As we already mentioned, this is not unexpected, as the axial gauge is also not appropriate in noncompact gauge models [91, 287]. We also mention that Ref. [234] also considered a Lorenz-like complete gauge fixing, again with no success.

To define a local $O(N)^{\times}$ order parameter, a novel procedure, which is conceptually different from the usual gauge-fixing strategies, was proposed in Refs. [233, 234]. It generalizes the variational approach that is used in the context of lattice gauge theories and is usually called Landau gauge fixing.³⁴ We review it below, in the context of the \mathbb{Z}_2 -gauge N-vector model.

The basic idea is to average non-gauge invariant quantities over all possible gauge transformations with a properly chosen, not gauge-invariant, weight. This is achieved by introducing \mathbb{Z}_2 fields $w_x = \pm 1$ defined on the lattice sites, and an ancillary Hamiltonian H_w that generally depends on w_x , s_x , and $\sigma_{x,\mu}$. If $A(s_x, \sigma_{x,\mu})$ is a function of the fields, one defines its weighted average over the gauge transformations as

$$[A(\boldsymbol{s}_{\boldsymbol{x}}, \sigma_{\boldsymbol{x}, \mu})] = \frac{\sum_{\{w\}} A(\hat{\boldsymbol{s}}_{\boldsymbol{x}}, \hat{\sigma}_{\boldsymbol{x}, \mu}) e^{-H_w}}{\sum_{\{w\}} e^{-H_w}}, \qquad \hat{\boldsymbol{s}}_{\boldsymbol{x}} = w_{\boldsymbol{x}} \boldsymbol{s}_{\boldsymbol{x}}, \qquad \hat{\sigma}_{\boldsymbol{x}, \mu} = w_{\boldsymbol{x}} \sigma_{\boldsymbol{x}, \mu} w_{\boldsymbol{x} + \hat{\mu}}, \tag{76}$$

where \hat{s}_{x} and $\hat{\sigma}_{x,\mu}$ correspond to the fields obtained by performing a gauge transformation with gauge function w_{x} as in Eq. (72). The average $[A(s_{x}, \sigma_{x,\mu})]$ is then averaged over the fields s_{x} and $\sigma_{x,\mu}$ using the original Hamiltonian (17), i.e.,

$$\langle [A(\boldsymbol{s}_{\boldsymbol{x}}, \sigma_{\boldsymbol{x}, \mu})] \rangle = \frac{\sum_{\{\boldsymbol{s}, \sigma\}} [A(\boldsymbol{s}_{\boldsymbol{x}}, \sigma_{\boldsymbol{x}, \mu})] e^{-H}}{\sum_{\{\boldsymbol{s}, \sigma\}} e^{-H}}.$$
 (77)

One can easily see that gauge-invariant observables are invariant under this gauge-fixing procedure. In this approach, we can define the vector correlation function as

$$G_V(\boldsymbol{x}, \boldsymbol{y}) = \langle [\boldsymbol{s}_{\boldsymbol{x}} \cdot \boldsymbol{s}_{\boldsymbol{y}}] \rangle. \tag{78}$$

The choice of the ancillary Hamiltonian H_w is a crucial point. To obtain critical vector correlations, one would like to work in a gauge which maximizes the number of bonds with $\sigma_{x,\mu} = 1$. Indeed, this implies

 $^{^{34}}$ In a lattice gauge theory with gauge fields $U_{x,\mu}$, the Landau gauge is defined as the set of gauge fields that maximize $\sum_{x\mu}$ Re Tr $U_{x,\mu}$, see, e.g., Ref. [330]. This approach is numerically difficult to apply and, in general, it suffers from the so-called Gribov problem [331, 332]: there may be several degenerate or quasidegenerate maxima. In the continuum limit, it goes over to the gauge-fixing condition $\partial_{\mu}A_{\mu}=0$, that we have named Lorenz gauge, but which is also referred to as Landau gauge. In continuum theories Landau gauge and Lorenz gauge are often used interchangeably, although the name "Landau gauge" is often preferred for Euclidean field theories, "Lorenz gauge" for theories defined in Minkowski space. To be consistent with the definitions of Sec. 5, we would call it Lorenz gauge.

that the Hamiltonian for the gauge-transformed fields \hat{s}_x is almost ferromagnetic. Therefore, these fields display the same critical behavior as vector fields in the O(N) model. With this idea in mind, an optimal choice is provided by the simple Hamiltonian

$$H_w(\gamma) = -\gamma \sum_{\boldsymbol{x},\mu} \hat{\sigma}_{\boldsymbol{x},\mu} = -\gamma \sum_{\boldsymbol{x},\mu} w_{\boldsymbol{x}} \sigma_{\boldsymbol{x},\mu} w_{\boldsymbol{x}+\hat{\mu}}, \tag{79}$$

where γ is a positive number that should be large enough to ensure that the minima of $H_w(\gamma)$ dominate in the average over the gauge transformations. It is worth noting that the global theory including the quenched stochastic gauge fixing is invariant under an extended set of local transformations with \mathbb{Z}_2 -gauge parameter $v_x = \pm 1$ given by³⁵

$$s_{x} \to v_{x} s_{x}, \qquad \sigma_{x,\mu} \to v_{x} \sigma_{x,\mu} v_{x+\hat{\mu}}, \qquad w_{x} \to v_{x} w_{x}.$$
 (80)

Thus, only observables that are invariant under this set of transformations, such as \hat{s}_{x} and $\hat{\sigma}_{x,\mu}$, have nonvanishing correlation functions and a nontrivial critical behavior.

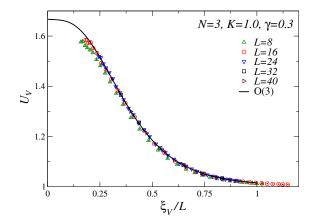
The stochastic gauge-fixing procedure mimics what is done in random systems with quenched disorder, for instance in spin glasses. The variables s_x and $\sigma_{x,\mu}$ are the disorder variables and e^{-H}/Z represents the disorder distribution, while w_x are the system variables that are distributed with Gibbs weight e^{-H_w}/Z_w at fixed disorder. In the language of disordered systems, the average $[\cdot]$ therefore represents the thermal average at fixed disorder, while $\langle \cdot \rangle$ is the average over the different disorder realizations.³⁶ This analogy allows one to exploit known results for the properties of quenched random systems. In particular, the present procedure is thermodynamically consistent and, when the low-temperature (large γ) phase is not a spin-glass phase, it admits a local field-theory representation, see, Refs. [152, 333]. Thus, the standard RG machinery can be applied to correlations computed in the gauge-fixed theory.

The resulting model with the added variables w_x is a quenched random-bond Ising model [151, 334] with a particular choice of bond distribution. Quenched random-bond Ising models have various phasesdisordered, ferromagnetic, and glassy phases—depending on the temperature (whose role is played here by $1/\gamma$), the amount of randomness of the bond distribution, and its spatial correlations, see, e.g., Refs. [151, 334-348]. In particular, the present model is expected to undergo a quenched transition at $\gamma = \gamma_c(J, K)$ for any J and K. The transition separates a disordered phase for $\gamma < \gamma_c(J,K)$ from a large- γ phase, which a priori can be ferromagnetic or glassy. If J and K belong to the DO-O transition line, the large- γ phase turns out to be ferromagnetic. 37 Thus, the long-distance behavior of the variables w_x is the same for all $\gamma > \gamma_c(J, K)$: The variables w_x simply make uncorrelated short-range fluctuations around the minimum configurations obtained for $\gamma \to \infty$. It is thus natural to conjecture that γ is an irrelevant parameter, i.e., that the critical behavior of the gauge-fixed quantities is the same for any $\gamma > \gamma_c(J, K)$ along the DO-O transition line. In RG language, $1/\gamma$ represents an irrelevant perturbation of the $\gamma = \infty$ fixed point. The irrelevance of γ is conjectured to be a general feature of the stochastic gauge fixing, which holds for any N (the numerical analyses of Refs. [233, 234] confirm this conjecture). It is important to stress the significant advantage of the stochastic gauge fixing with respect to traditional gauge-fixing approaches. As we can work at fixed γ , there is no need to determine the minima or maxima of some gauge-fixing function, bypassing the problem of the Gribov copies [331, 332].

 $^{^{35}}$ For N=1 i.e., in the \mathbb{Z}_2 -gauge Higgs model, one can fix this gauge invariance by working in the unitary gauge, $s_{\boldsymbol{x}}=1$ for all points $\boldsymbol{x}.$

 $^{^{36}}$ To avoid confusion, note that symbols [·] and $\langle \cdot \rangle$ have typically the opposite meaning in the random-system literature: the former represents the disorder average and the latter the thermal average.

³⁷Note that the two-point function of w_x vanishes for non-coincident points, due to the generalized gauge invariance, Eq. (80). The nature of the large- γ phase can be determined by considering correlation functions of the so-called overlap $O_x = w_x^{(1)} w_x^{(2)}$, where $w_x^{(1)}$ and $w_x^{(2)}$ represent two different configurations sampled with the same probability e^{-H_w}/Z_w , i.e. corresponding to the same values of $\sigma_{x,\mu}$ and s_x . Along the DO-O line, for $\gamma > \gamma_c(J,K)$ the Binder cumulant of the overlap variable approaches 1, and the overlap susceptibility diverges linearly with the volume, indicating that the large- γ phase is a standard ferromagnetic phase.



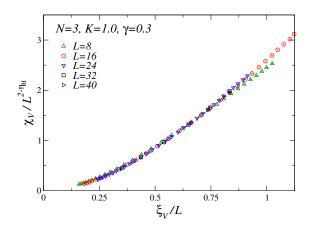


Figure 14: (Adapted from Ref. [234]) FSS analyses (see Appendix A.3 for a discussion of the expected scaling behavior) of MC data for the \mathbb{Z}_2 -gauge N-vector model with N=3, using the stochastic gauge fixing with parameter $\gamma=0.3$. Simulations at fixed K=1 across the DO-O transition line. (Left) Plot of the vector Binder parameter U_V defined in terms of s_x , versus ξ_V/L , where ξ_V is the second-moment correlation length computed by using the vector correlation function G_V . Data collapse on the N-vector (N=3) universal curve (see Ref. [276] for a parametrization), showing that the vector degrees of freedom behaves as at a standard O(3) transition. (Right) Plot of the vector susceptibility χ_V defined in terms of G_V versus the ratio ξ_V/L . The susceptibility is rescaled according to Eq. (A.24), using the exponent $\eta_H=0.03784$ of the Heisenberg O(3) universality class (see Appendix B for a list of estimates of η_H). The nice collapse of the data supports the O(3) nature of the vector modes in the presence of a stochastic gauge fixing.

The ancillary Hamiltonian H_w given in Eq. (79) is simple and allows us to reinterpret the gauge-fixed model as a quenched random-bond model. However, other choices may work as well. It is important to note that the emerging critical behavior of the vector field is expected to be universal, i.e., independent of the ancillary Hamiltonian H_w , provided that H_w has been properly chosen to make the spin-spin interactions ferromagnetic. This is essentially due to the fact that the critical behavior of all gauge invariant quantities—for instance, the spin-two operator R_x^{ab} or the gauge-invariant energy—is independent of H_w : they all behave as in the N-vector model. Therefore, along the DO-O line, $G_V(x-y)$ should also behave as in the N-vector model, if it is critical.

The theoretical predictions have been confirmed numerically in Refs. [233, 234]. For both N=2 and 3, the stochastically gauge-fixed correlation function G_V defined in Eq. (78), as well as other vector observables like the vector Binder parameter, show the same critical behavior as in the N-vector model. Some data for N=3 are reported in Fig. 14.

We finally mention that the above ideas can be straightforwardly extended to lattice gauge models with other discrete groups or with continuous compact gauge variables.

7.4. Phase diagram and critical behavior of the \mathbb{Z}_2 -gauge Higgs model

We now focus on the phase diagram of the \mathbb{Z}_2 -gauge Higgs model, i.e., of the lattice model (17) for N=1. In this case the spin variables take the integer values $s_x=\pm 1$, as the link variables.

The model satisfies an exact duality relation [349]. If we redefine the Hamiltonian parameters as

$$(J', K') = \left(-\frac{1}{2}\ln\tanh K, -\frac{1}{2}\ln\tanh J\right),\tag{81}$$

the free-energy density $F(J,K) = -\frac{T}{L^d} \ln Z$ satisfies the relation

$$F(J', K') = F(J, K) - \frac{3}{2} \ln[\sinh(2J)\sinh(2K)]. \tag{82}$$

One can also define a self-dual line, requiring J' = J and K' = K, which can be parametrized by one of the two equivalent equations

$$D(J,K) = J + \frac{1}{2}\ln\tanh K = 0,$$
 $D'(J,K) = K + \frac{1}{2}\ln\tanh J = 0.$ (83)

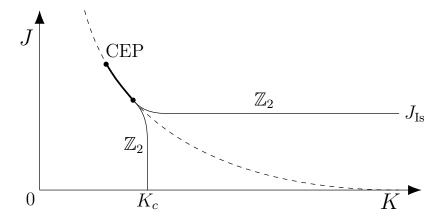


Figure 15: Sketch of the phase diagram of the 3D \mathbb{Z}_2 gauge Higgs model, see, e.g., Refs. [176, 351, 353]. The dashed line is the self-dual line, the thick line is a finite stretch of the self-dual line corresponding to first-order transitions. The two lines labeled " \mathbb{Z}_2 " are related by duality, and correspond to Ising continuous transitions. They end at $[J=J_{\rm Is}\approx 0.221655, K=\infty]$ and at $[J=0,K=K_{\mathbb{Z}_2}\approx 0.761413]$. The three lines meet at a MCP [176, 351–353, 355, 356] at $[K_\star=0.7525(1),J_\star=0.22578(5)]$. The corresponding multicritical behavior turns out to be controlled by the multicritical XY FP [176, 356, 357]. The second endpoint (CEP) of the first-order transition line, at $[K\approx 0.688,J\approx 0.258]$, is expected to be an Ising critical endpoint.

7.4.1. The phase diagram of the three-dimensional \mathbb{Z}_2 -gauge Higgs model

A sketch of the phase diagram is shown in Fig. 15. For $K \to \infty$ an Ising transition occurs at [323] $J_{\rm Is} = 0.221654626(5)$. By duality, in the pure \mathbb{Z}_2 gauge model a transition occurs in the corresponding point, J = 0 and $K_c = -\frac{1}{2}\ln\tanh J_{\rm Is} = 0.761413292(11)$. Two Ising continuous transition lines, related by the duality transformation (81), start from these points [41, 350] (the argument is analogous to that discussed in Sec. 7.2.3) and intersect on the self-dual line [176, 351] at $K_{\star} = 0.7525(1)$, $J_{\star} = 0.22578(5)$. Note that the transitions along both lines are Ising-like transitions and that in both cases there is no global symmetry. Nonetheless, as we shall discuss, the two lines have different nature: the line that starts at J = 0 is a topological transition line, while the line that starts at $K = \infty$ is an Ising[×] line, i.e., it admits an Ising order parameter that can only be identified once a proper gauge fixing is introduced. Note that, in the absence of a gauge fixing, only the cumulants of the energy density (see Sec. Appendix A.3.2 for definitions) can be used to characterize these transitions in a gauge-invariant way [176, 351] (note that the tensor R^{ab} defined in Eq. (73) trivially vanishes for N = 1).

Finally, numerical studies [352–354] have provided evidence of first-order transitions along the self-dual line, in the relatively small interval starting from the MCP and ending at $J_{\star} \approx 0.258$ and $\kappa_{\star} \approx 0.688$. This endpoint is expected to correspond to a continuous transition belonging to the Ising universality class (see Ref. [351] for a numerical study).

Since the first-order transition line is limited to a finite interval along the self-dual line, only two thermodynamic phases exist, see Fig. 15. For small J and large K there is a topological deconfined phase. The remaining part of the phase diagram corresponds to a single phase that extends from the disordered small-J, K region to the whole large-J region. In particular, no phase transition occurs along the line K=0, where the model becomes trivial, as can be seen in the unitary gauge $s_x=1$. We may only distinguish two different regimes: a Higgs-like regime in the large J and K region, and a confined regime in the small J and K region (see, e.g., Ref. [358]). However, these two regions are connected by continuous paths in the phase diagram, along which all local gauge-invariant operators (more precisely the gauge invariant operators depending on a finite number of s_x and $\sigma_{x,\mu}$ variables) are analytic functions of the Hamiltonian parameters [41, 350].

7.4.2. Order parameters driving the Ising[×] transitions

Along the two transition lines that start at J=0 and $K=\infty$ and are related by duality, thermal observables behave as in the Ising universality class. However, as already discussed in Sec. 3.5.2, the corresponding universality classes are different. Even if there is no \mathbb{Z}_2 global symmetry, the transitions

along the line that starts at $K=\infty$ are Ising[×] transitions and admit, as we shall describe below, an effective description in terms of a standard LGW theory with \mathbb{Z}_2 global invariance, once an appropriate gauge fixing has been introduced. On the other hand, along the line that starts at J=0, transitions are topological as in the pure \mathbb{Z}_2 gauge model.³⁸

To verify the Ising[×] critical behavior, Ref. [234] studied the \mathbb{Z}_2 -gauge Higgs model with the stochastic gauge fixing introduced in Sec. 7.3, using the ancillary Hamiltonian H_w defined in Eq. (79). Numerical FSS analyses [234] along the large-K transition line show that the critical behavior of the correlation function $G_V(x,y)$ defined in Eq. (78) is the same as in the standard Ising model, with the large-J, large-K region corresponding to the magnetized phase. Therefore, as in multicomponent models the stochastic gauge fixing allows us to identify the universal gauge-dependent spin correlations which characterize standard Ising transitions. The same conclusions were reached in Ref. [366], in what was called Landau gauge (see footnote 34), which essentially corresponds to taking the limit $\gamma \to \infty$ in the stochastic gauge fixing approach (but note that the multiplicity of the minima, the so-called Gribov copies, could not be taken into account). The same analysis, using the stochastic gauge fixing, was also performed along the small-J transition line. In this case the correlation function $G_V(x,y)$ is not critical at the transition. As expected, these transitions are not LGW[×] transitions.

In the stochastic gauge-fixed theory, the spin s_x magnetizes along the Ising[×] transition line, i.e., there is a ferromagnetic phase in the large-J, large-K Higgs phase. On the other hand, for small values of J, s_x is always disordered. This implies the presence of an additional transition line in the gauge-fixed theory, which separates the single phase [41] in which the confining and the Higgs regime both occur. The line most probably starts at the CEP, see Fig. 15, and necessarily ends on the K=0 axis.³⁹ This is confirmed by numerical analyses [367], which observe continuous transitions in the small-K region, on the left of the first-order transition line, see Fig. 15. This line, which separates the Higgs regime, in which the gauge-fixed spin correlations (in the generalized unitary gauge they are equivalent to correlations of the ancillary fields) magnetize, from the confined regime, is related to the specific form of the ancillary model and therefore does not have a direct physical significance. However, it signals that the thermodynamic description does not provide the full picture.

To distinguish the confinement/deconfinement properties of the model, several nonlocal order parameters have been proposed, see, e.g., Refs.[20, 356, 359–365, 368]. Note that the size dependence of Wilson loops does not provide a good order parameter. In the presence of dynamical matter fields transforming in the fundamental representation, charge screening is present and Wilson loops always scale with the perimeter law. Only for J=0 does the transition at $K=K_{\mathbb{Z}_2}$ separate regions characterized by the area law and the perimeter law. A possible order parameter is the so-called Fredenhagen-Marcu [45, 369] order parameter, which is defined by using a gauge-invariant two-point function built by joining two spins s_x with a staple-shaped string of gauge fields, normalized by the square root of a Wilson loop. The behavior of this order parameter in the \mathbb{Z}_2 -gauge Higgs model has been studied in Refs. [356, 370]. It correctly identifies the confinement/deconfinement transition in the model and its Ising $^{\times}$ universality class. A different order

 $^{^{38}}$ Note that the topological transitions along the transition line starting from the J=0 critical point cannot be characterized by the size behavior of the Wilson loops, at variance with what occurs in the 3D \mathbb{Z}_2 gauge model, see Sec. 3.5.2, because Wilson loops satisfy the perimeter law for any J>0, due to the screening of the site spin variables. A more general interpretation of these topological transitions is discussed in Ref. [20] in a quantum setting, see also Refs. [359–365]. They correspond to topological transitions between a small-K trivial phase and a large-K phase with topological order. These two phases correspond to the confined and deconfined phases at J=0, respectively. We also mention that these transitions are sometimes referred to as Ising* transitions; see, e.g., Refs. [176, 324, 351, 353]. As discussed in Sec. 3.5.2, we name them Ising gauge transitions.

 $^{^{39}}$ For K=0 the gauge-fixed model is equivalent to the so-called $\pm J$ Ising model [151, 334–348], with spatially-independent random links (it is immediate to verify it in the so-called unitary gauge $s_x=1$, see footnote 35). In the notation of Refs. [342–344], the probability p of the random link variable $J_{\rm xy}$ ($\sigma_{x,\mu}$ in our model in the unitary gauge) is $P(J_{\rm xy})=p\delta(J_{\rm xy}-1)+(1-p)\delta(J_{\rm xy}+1)$ with $p=e^J/(e^J+e^{-J})$. The temperature T in the $\pm J$ Ising model corresponds to $T=\gamma^{-1}$, so the line $J=\gamma$ corresponds to the so-called Nishimori line [339]. Neglecting the small reentrance of the ferromagnetic-glassy transition line—see Refs. [342–344] for a discussion of the phase diagram of the $\pm J$ Ising model—,the ancillary model has a large- γ ferromagnetic phase only for $J>1/T_{\rm N}=J_N=0.5991(1)$ (T_N is the Nishimori temperature). Moreover, in the ferromagnetic phase the correlation function G_V orders (note that the ancillary model has a ferromagnetic phase also close to the small-J topological line, but here G_V does not order). This implies that the transition line ends in K=0, $J=J_N$ [367].

parameter has been advocated in Ref. [371] (see also Ref. [368]), defined by using a properly normalized correlator between a Wilson and 't Hooft loop, and studied numerically in Ref. [370]. Another order parameter, whose definition is strictly related with the strong-coupling surface formulation of the \mathbb{Z}_2 -gauge Higgs model (see, e.g., Refs. [351, 372]), has been proposed and numerically tested in Ref. [373]. The possibility that the crossover between the confinement and the Higgs regime could induce superficial phase transitions in quantum many-body systems has instead been investigated in Refs. [374, 375].

7.4.3. Multicritical behavior at the intersection point of the transition lines

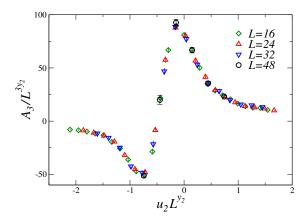
The first-order and the two continuous Ising transition lines intersect in a multicritical point (MCP) located along the self-dual line [176, 351, 353].⁴⁰. Critical exponents have been numerically computed at the MCP [176, 351, 355, 356], obtaining results consistent with a multicritical XY behavior.

The apparent XY nature of the multicritical behavior can be naturally explained [176] by assuming that the effective description of the transition is provided by the multicritical $\mathbb{Z}_2 \oplus \mathbb{Z}_2$ LGW theory presented in Sec. 2.2.4, describing the competition of two one-component $(N_1 = N_2 = 1)$ scalar fields. This conjecture is made plausible by the following arguments. The multicritical behavior arises from the competition of the order parameters that characterize the critical behavior along the two Ising-like lines. As we have discussed in the previous section, along the large-K transition line, we have Ising[×] transitions, with a scalar order parameter. Thus, they admit a LGW description in terms of a scalar nongauge-invariant field ϕ_1 . The transitions along the small-J line are instead topological transitions, characterized by an order parameter that is a nonlocal function of the gauge degrees of freedom. Assuming that duality can be extended from thermodynamic quantities to operators, Ref. [176] argued that the nonlocal order parameter is dual to a local order parameter, since the topological transition line is mapped onto an Ising[×] transition line under duality. Thus, as a working hypothesis, one may associate a scalar field ϕ_2 with the topological Ising gauge transitions, which locally interacts with the Ising[×] order-parameter field ϕ_1 . If this conjecture holds, the multicritical behavior has an effective description in terms of a local Lagrangian for the two fields ϕ_1 and ϕ_2 . We thus obtain the LGW Lagrangian (5) discussed in Sec. 2.2.4 with $N_1 = N_2 = 1$.

The multicritical model defined in Sec. 2.2.4 has been extensively studied [95, 172, 173, 175, 176, 254]. In particular, for $N_1 = N_2 = 1$ it admits a bicritical point (see the left panel of Fig. 1) with a critical behavior controlled by a stable fixed point with enlarged O(2) global symmetry. The main conjecture put forward in Ref. [176] is that this stable multicritical XY FP is the one that controls the multicritical XY behavior in the \mathbb{Z}_2 -gauge Higgs theory. In this scenario, the two relevant operators at the MCP are the quadratic spin-2 and spin-0 field combinations, whose RG dimensions are [175, 254] $y_1 = 1.7639(11)$ and [294] $y_2 = 1/\nu_{\rm XY} = 1.4888(2)$ respectively. The numerical estimates [176, 351, 355, 356] of y_1 and y_2 are in good agreement (errors are of the order of 1%) with the more accurate XY estimates reported above. To give an idea of the accuracy of the multicritical XY scenario, in Fig. 16 we show the FSS behavior of some particular third- and fourth-order energy cumulants using the XY critical exponent $y_2 = 1/\nu_{\rm XY}$. The agreement with the multicritical XY scenario is globally very good and strongly supports it. However, we also note that the multicritical XY theory is based on some unproved assumptions, the main one being the existence of a (dual) local order parameter for the topological transitions. We should also mention that this assumption is still controversial: Refs. [351, 355, 373] consider it implausible, and interpret the agreement between numerical results and XY estimates as a mere coincidence.

⁴⁰See Appendix A.4 for a brief review of the main universal features of the scaling behavior close to a MCP

 $^{^{41}}$ We do not have sound arguments to argue that these considerations can also be applied to the \mathbb{Z}_2 -gauge N-vector models with N>1, to determine the behavior at the intersection point of the three transition lines, see Fig. 12. Nevertheless, if, in analogy with the \mathbb{Z}_2 -gauge Higgs model, we assume that the competition of the Ising critical modes (DD-DO line) and the N-vector critical modes (DO-O line) can somehow be represented by the competition of corresponding local order parameters, we can use the multicritical LGW theory (5) with $N_1=1$ and $N_2=N>1$ to understand the behavior close to the intersection point of the transition lines. Under this assumption, the results for the 3D RG flow of the multicritical $O(N_1) \oplus O(N_2)$ LGW theory, outlined in Sec. 2.2.4, predict that the intersection point would generally correspond to a first-order transition for any N>1, with a phase diagram analogous to the one shown in the right panel of Fig. 1.



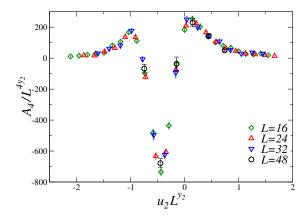


Figure 16: (From Ref. [176]) FSS behavior of the third and fourth cumulant of an energy-like variable that scales with critical exponent y_2 when measured along the self-dual line (see Appendix A.4 for a discussion of FSS at MCPs). See Ref. [176] for details. The nice collapse of the data when using the XY critical exponent $y_2 = 1/\nu_{\rm XY}$ provides an accurate check of the conjectured multicritical XY behavior at the MCP point.

7.5. Other models with discrete symmetries

In Secs. 5 and 6 we discussed the phase diagram and critical properties of U(1) gauge theories with global U(N) symmetry, while in this section we considered gauge models with discrete \mathbb{Z}_2 gauge symmetry and O(N) global symmetry. We now present some additional models with discrete gauge and/or global symmetry, in which the gauge and/or the scalar fields take only a discrete set of values. These models can be considered as approximations of models with continuous groups. However, classical theorems by Jordan and Turing [376] show that the only continuous groups of transformations that can be approximated with arbitrary precision by using their discrete subgroups are the Abelian ones. Thus, in the compact case, the only possibility is replacing the U(1) group with the cyclic finite group \mathbb{Z}_N . In the noncompact case, the additive group \mathbb{R} can be replaced by the discrete, but still infinite, additive group \mathbb{Z} . As we shall see, in some cases these discretized models undergo transitions that are analogous to those occurring in models with continuous fields and symmetry groups, with an enlargement of the global and/or local gauge symmetry.

7.5.1. Compact models with $\mathbb{Z}_{\mathcal{N}}$ local symmetry

We consider a model with global \mathbb{Z}_q symmetry and local $\mathbb{Z}_{\mathcal{N}}$ gauge symmetry. We assume that q is an integer multiple of \mathcal{N} and we define $p=q/\mathcal{N}$. The scalar fields are complex phases $z_{\boldsymbol{x}}$, which take q different values, $z_{\boldsymbol{x}}=\exp(2\pi i m/q)$ with $m=1,\ldots q-1$, while gauge fields are complex phases $\lambda_{\boldsymbol{x},\nu}=\exp(2\pi n i/\mathcal{N})$, $n=0,\ldots,\mathcal{N}-1$. The Hamiltonian and the partition function are given by

$$H = -2J \sum_{\boldsymbol{x},\mu} \operatorname{Re} \bar{z}_{\boldsymbol{x}} \lambda_{\boldsymbol{x},\mu} z_{\boldsymbol{x}+\hat{\mu}} - 2\kappa \sum_{\boldsymbol{x},\mu>\nu} \operatorname{Re} \lambda_{\boldsymbol{x},\mu} \lambda_{\boldsymbol{x}+\hat{\mu},\nu} \bar{\lambda}_{\boldsymbol{x}+\hat{\nu},\mu} \bar{\lambda}_{\boldsymbol{x},\nu}, \qquad Z = \sum_{\{z,\lambda\}} e^{-H/T}. \tag{84}$$

In the following we conventionally set T=1. For $\mathcal{N}=q=2$ this model is the \mathbb{Z}_2 -gauge Higgs model discussed in Sec. 7.4. Here we review the results of Ref. [253], where these models for $p=q/\mathcal{N}>1$ were studied, obtaining the phase diagram reported in Fig. 17.

The nature of the different transition lines can be understood by looking at the critical behavior when κ or J are zero or infinity. In the limit $\kappa \to \infty$ all plaquettes approach one, and (in the thermodynamic limit) one can set $\sigma_{x,\mu}=1$ on all links using a gauge transformation, thus obtaining the ferromagnetic \mathbb{Z}_q clock model. The critical properties of this model have been discussed in Sec. 3.5.2. We summarize here the conclusions: for q=2 and 4 the \mathbb{Z}_q clock model undergoes a transition in the Ising universality class, for q=3 it undergoes a first-order transition, while for $q\geq 5$ its critical behavior is the same as in the XY model.

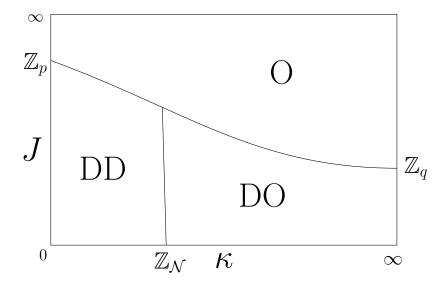


Figure 17: Sketch of the phase diagram of the 3D model with Hamiltonian Eq. (84), for $p = q/\mathcal{N} > 1$. For small J there are two phases: a spin- and gauge-disordered phase (DD) for small κ (corresponding to the confined phase for J = 0) and a spin- and gauge-ordered phase (DO) for large κ (corresponding to the deconfined phase for J = 0). For large J a single spin- and gauge-ordered phase is present (O).

For J=0, there are no scalar fields and one obtains the pure gauge $\mathbb{Z}_{\mathcal{N}}$ model with Wilson action, see Eq. (20), whose critical properties have already been discussed in Sec. 3.5.2. We thus expect an Ising gauge transition for $\mathcal{N}=2$ and 4, a discontinuous transition for $\mathcal{N}=3$, and XY gauge transitions for $\mathcal{N}\geq 5$.

For $J \to \infty$ no transition is expected (fixing the global and local invariance we can set $z_x = \lambda_{x,\mu} = 1$ on all links), while for $\kappa = 0$ one can show, using universality arguments, the transition to be a LGW transition in the \mathbb{Z}_p universality class, see Ref. [253] for more details. Thus, no transition occurs for p = 1. The model undergoes an Ising and XY transitions for p = 2 and $p \geq 5$, respectively, and a first-order transition for p = 3. An XY transition is also expected for p = 4. Indeed, in the latter case the model obtained for $\kappa = 0$ is a generic model with \mathbb{Z}_4 global symmetry, and thus it should have an XY transition, as discussed in Sec. 3.5.2 and, in particular, in footnote 17. The order parameter at these transitions is the gauge-invariant operator $s_x^{\mathcal{N}}$. This quantity transforms nontrivially only under the \mathbb{Z}_p subgroup of the global invariance group, so the effective description is given by the LGW Lagrangian (21) with Q = p.

From the discussion of the limiting cases it follows that the phase diagram for p > 1 has the form sketched in Fig. 17, while the phase diagram for p = 1 is qualitatively similar to the one reported in Fig. 15, with no transition for $\kappa = 0$. It is reasonable to assume the transitions along the DD-O line to be analogous to those occurring for $\kappa = 0$, while the transitions along the DD-DO are expected to be topological transitions as for J = 0. Again, the case $\mathcal{N} = 4$ should be discussed separately. Indeed, while the transition for J = 0 is an Ising gauge transition, for $J \neq 0$ we expect an XY gauge phase transition (see the discussion in Sec. 3.5.2 and, in particular, footnote 17).

The behavior along the DO-O line is similar to what is observed in the \mathbb{Z}_2 -gauge N-vector model. Gauge fluctuations, due to the discrete nature of the gauge group, are not able to destabilize the \mathbb{Z}_q critical behavior observed for $\kappa = \infty$. The scalar field—the order parameter in \mathbb{Z}_q transitions—is not gauge invariant, so the transition is of the LGW[×] type. We thus expect $\operatorname{Ising}^{\times}$ transitions for q=2, discontinuous transitions for q=3, and XY[×] transitions for $q\geq 5$. For q=4 we expect an XY[×] transition if the gauge fluctuations are strong enough to destabilize the decoupled Ising transition at $\kappa=\infty$, and an $\operatorname{Ising}^{\times}$ transition if this is not the case.

These predictions have been confirmed in Ref. [253] by numerical simulations, studying the behavior of the gauge-invariant correlation function

$$G_{\mathcal{N}}(\boldsymbol{x}, \boldsymbol{y}) = \operatorname{Re} \langle (\bar{z}_{\boldsymbol{x}} z_{\boldsymbol{y}})^{\mathcal{N}} \rangle$$
 (85)

In particular, for q=4 the transitions along the DO-O line are numerically compatible with an Ising[×] behavior. Thus, gauge interactions do not destabilize the accidental symmetry that is present in the \mathbb{Z}_4 clock model at $\kappa \to \infty$.

It is interesting to note that the model with $\mathcal{N}=2$ and any $p\geq 5$ has the same phase diagram and critical behaviors as the \mathbb{Z}_2 -gauge N-vector model with N=2, which can be obtained by performing a naive limit $q\to\infty$ of the Hamiltonian (84).⁴² Thus, for $p\geq 5$ we observe a symmetry enlargement of the global symmetry along the DD-O and DO-O lines, while, for $\mathcal{N}\geq 4$, correlation functions display an enlarged gauge symmetry along the topological DD-DO transition line.

7.5.2. Gauge symmetry enlargement

As we have already discussed several times, see, e.g., Sec. 7.5.1, at transitions of LGW and LGW[×] type, gauge models may display an enlargement of the global symmetry. Analogously, at topological transitions, one may observe an enlargement of the gauge symmetry—this occurs in \mathbb{Z}_Q gauge models, see Sec. 3.5.2. The models we are now going to discuss have instead been investigated to understand whether there are transitions showing a gauge-symmetry enlargement, which can be effectively described by a continuum GFT. In the present context, one is looking for models with discrete gauge symmetry that undergo charged transitions that are associated with the AHFT, with an enlarged U(1) gauge symmetry.

Charged transitions controlled by the AHFT occur in the N-component LAH model with noncompact Abelian gauge field (along the CH line) and in the higher-charge (Q>1) N-component LAH model with compact Abelian gauge field (along the DC-OD line). In both cases the gauge group can be approximated with arbitrary accuracy by considering discrete compact or noncompact subgroups and one can define models that are only invariant under these discrete subgroups. The question is whether these discrete models also have charged transitions as their continuous counterparts.

We begin discussing the discretized version [377] of the noncompact N-component LAH model with Hamiltonian (47) defined in Sec. 5.1. The discretized model is defined in the same way, the only difference being the set of values that the gauge field $A_{x,\mu}$ takes. In the discretized model, the gauge field takes only the values $2\pi m/q$, with $m \in \mathbb{Z}$. The model is invariant under a restricted set of gauge transformations (we indicate with $\mathbb{Z}_q^{(nc)}$ the corresponding group)

$$\mathbf{z}_{x} \to e^{i\Lambda_{x}} \mathbf{z}_{x}, \qquad A_{x,\mu} \to A_{x,\mu} + \Lambda_{x} - \Lambda_{x+\hat{\mu}}, \qquad \Lambda_{x} = 2\pi m/q, \quad m \in \mathbb{Z}.$$
 (86)

The original noncompact U(1) gauge theory is formally recovered in the limit $q \to \infty$. Note that the gauge group is discrete, but infinite. As already discussed in Sec. 5.1, a proper definition of the model requires the introduction of C^* boundary conditions.

The model is invariant under global $\mathrm{SU}(N)$ transformations as the usual LAH model, the order parameter being the operator Q_x^{ab} defined in Eq. (60). Moreover, because of the smaller local gauge symmetry, it is also invariant under an additional set of global transformations with $\mathbb{R}/\mathbb{Z}_q^{(nc)} = \mathrm{U}(1)/\mathbb{Z}_q$ symmetry group. A gauge-invariant order parameter associated with this symmetry is the operator $\Sigma_x^{i_1\cdots i_q} = z_x^{i_1}\cdots z_x^{i_q}$, where z_x^i denotes the *i*-th component of the complex *N*-vector z_x . Note that this order parameter transforms nontrivially under the global $\mathrm{SU}(N)$ symmetry—thus, it acquires a nonvanishing expectation value only if both symmetries are broken—while the order parameter Q_x^{ab} is invariant under the $\mathrm{U}(1)/\mathbb{Z}_q$ symmetry, and thus it is only sensitive to the breaking of the $\mathrm{SU}(N)$ symmetry. As a consequence, we expect the $\mathrm{U}(1)/\mathbb{Z}_q$ symmetry to be spontaneously broken only in a phase in which the $\mathrm{SU}(N)$ symmetry is also broken.

Due to its larger global symmetry, the phase diagram of the discrete N-component LAH model is significantly more complex than that of the N-component LAH with U(1) gauge symmetry. A sketch is shown in Fig. 18. Using the same arguments presented in Sec. 6.2, it is possible to show (see Ref. [377] for more details) that an IXY transition occurs both for $J = \infty$ (as in the noncompact U(1) gauge AH model)

⁴²For $\mathcal{N}=2$ the correlation function $G_{\mathcal{N}}(\boldsymbol{x},\boldsymbol{y})$ defined in Eq. (85) is equal to $2G_{R}(\boldsymbol{x},\boldsymbol{y})$ [see Eq. (74)] for N=2, if we identify $\boldsymbol{s}_{\boldsymbol{x}}=(\operatorname{Re} z_{\boldsymbol{x}},\operatorname{Im} z_{\boldsymbol{x}})$ in Eq. (73). Therefore, for $q\to\infty$ the function $G_{\mathcal{N}}(\boldsymbol{x},\boldsymbol{y})$ is equivalent to $G_{R}(\boldsymbol{x},\boldsymbol{y})$ in the \mathbb{Z}_2 -gauge XY model.

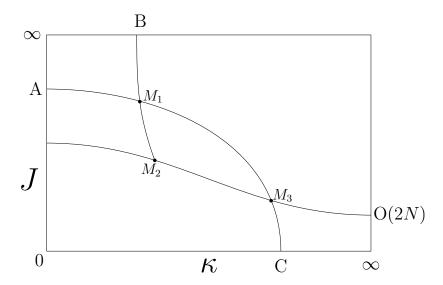


Figure 18: Sketch of the phase diagram of the 3D N-component LAH model with discrete gauge symmetry. In the noncompact case the transition in A belongs to the XY universality class, while the transitions at points B and C belong to the IXY universality class [377]. In the compact case the transition in A is in the XY universality class, while the transitions at points B and C are in the \mathbb{Z}_Q and \mathbb{Z}_q universality class, respectively [214]. Both in the compact and in the noncompact case, we have $J_c(A), \kappa_c(C) \to \infty$ in the limit $q \to \infty$.

and for J=0. Moreover, the transition on the J=0 axis occurs at $\kappa_c(J=0)=q^2\kappa_c(J=\infty)$, where $\kappa_c(J=\infty)=0.076051(2)$, so $\kappa_c(J=0)\to\infty$ for $q\to\infty$. This should not come as a surprise, since we should recover the phase diagram of the model with U(1) symmetry with no transition on the J=0 line, see Fig. 2, for $q\to\infty$. Moreover, two transitions are present on the $\kappa=0$ axis: a transition for $J=J_{\mathrm{SU}(N)}$, where the global $\mathrm{SU}(N)$ symmetry is spontaneously broken, and a transition at $J=J_q$, associated with the spontaneous breaking of the U(1)/ \mathbb{Z}_q symmetry. As discussed above, we expect the latter symmetry to break in a phase in which the $\mathrm{SU}(N)$ symmetry is already broken, implying $J_q>J_{\mathrm{SU}(N)}$ (therefore the point A in Fig. 18 corresponds to $J=J_q$). Note that $J_q\to\infty$ as $q\to\infty$, since this transition is not present in the phase diagram of the noncompact U(1) gauge model, see Fig. 2.

In Ref. [377] the phase diagram of the N-component $\mathbb{Z}_q^{(nc)}$ gauge model has been numerically investigated, studying in detail the critical behavior along the transition line M_2M_3 in Fig. 18. Indeed, for $q \to \infty$, this line corresponds to the CH line (see Fig. 2) of the noncompact U(1) gauge model, which is the line where the AHFT critical behavior emerges if the number N of scalar components is large enough, as discussed in Sec. 5.3.3. The numerical results show that, for N=25 and $q \geq 5$, the transitions along the line M_2M_3 are continuous, and that their critical behavior is the same as along the CH line in the noncompact U(1) gauge model. Thus, for $q \geq 5$ and large values of N, the transitions along the line M_2M_3 are effectively associated with the stable charged FP of the AHFT, with a corresponding enlargement of the gauge symmetry. On the right of the intersection point M_3 we instead have $O(2N)^{\times}$ critical transitions.

A similar analysis [214] can be performed for the compact model defined in Sec. 6.3.2. One considers the multicomponent LAH model with charge-Q scalar fields and Hamiltonian (67) and defines a discretized version by requiring the gauge fields to take the values $\lambda_{x,\mu} = \exp(i2\pi n/q)$, $n = 0, \dots q - 1$. Since $\lambda_{x,\mu}^q = 1$ and the theory is invariant under charge conjugation, it is sufficient to consider values of Q satisfying $1 \le Q \le q/2$. The model is invariant under the local \mathbb{Z}_q transformations

$$z_x \to \alpha_x^Q z_x, \quad \lambda_{x,\mu} \to \alpha_x \lambda_{x,\mu} \bar{\alpha}_{x+\hat{\mu}},$$
 (87)

where $\alpha_{\boldsymbol{x}} \in \mathbb{Z}_q$, and under the global transformation $\boldsymbol{z_x} \to V \boldsymbol{z_x}$, where $^{43} V \in \mathrm{SU}(N)$. As in the noncompact $\mathbb{Z}_q^{(nc)}$ model, also in the \mathbb{Z}_q gauge model there is an additional $\mathrm{U}(1)/\mathbb{Z}_q$ global symmetry.

 $^{^{43}}$ If q/Q=2 the global symmetry is larger: the invariance group is $O(2N_f)$, see Ref. [214].

The phase diagram of the N-component \mathbb{Z}_q -gauge model has been studied in Ref. [214]. For Q>1 it is the same as the phase diagram for the noncompact model reported in Fig. 18. Only the nature of some transition lines differs. For $J\to\infty$ and J=0 the model is equivalent to a \mathbb{Z}_Q and \mathbb{Z}_q model, respectively, so the transitions along the BM_2 (the numerical results of Ref. [214] show that the behavior along M_1M_2 is the same as along the BM_1 line) and CM_3 lines are expected to belong to the gauge \mathbb{Z}_Q and \mathbb{Z}_q universality classes, respectively. The transitions along the AM_1 line are instead expected to be in the XY universality class, as in the $\mathbb{Z}_q^{(nc)}$ model.

In Ref. [214] the universality class of the transitions along the line M_2M_3 has been investigated for Q=2 and N=15. In the U(1) invariant model, recovered for $q\to\infty$, these transitions are charged transitions associated with the stable FP of the AHFT, see Sec. 6.3.2. On the other hand, only discontinuous transitions were identified along the M_2M_3 line for values of q up to q=10. Apparently, in the discretized model there are no charged transitions. It is still an open issue to understand why the two apparently similar discretized models, the compact and the noncompact model, behave differently. The origin may lie in the fact that in the noncompact model the gauge group is discrete but still infinite, while in the compact case the gauge group is discrete and finite.

8. Non-Abelian Higgs field theories

Non-Abelian gauge symmetries play a fundamental role in the construction of quantum and statistical field theories that describe phenomena in various physical contexts. In high-energy physics they provide the framework to formulate the fundamental theories of the strong and electroweak interactions, see, e.g., Refs. [1, 2, 378], while in condensed-matter physics they provide an effective description of classical and quantum critical phenomena characterized by the emergence of non-Abelian gauge fields, see, e.g., Refs [16, 20, 96, 379, 380]. In the presence of low-energy modes associated with scalar fields, they give rise to the non-Abelian Higgs mechanism [103–105], which, for instance, is one of the main features of the theory of electroweak interactions [1, 2, 378]. The emerging Higgs phases in non-Abelian Higgs (NAH) theories crucially depend on the interplay between local and global symmetries, and on the spontaneous breaking patterns of the global symmetry, see, e.g., Refs. [33, 41, 62, 64, 65, 96–99, 262, 263, 278, 381–384].

Three-dimensional non-Abelian gauge models can be used to effectively describe the critical behavior of 3D statistical non-Abelian gauge models at finite-temperature phase transitions [385–394], and to investigate some aspects of fundamental mechanisms, such as confinement [260, 381, 395, 396]. The peculiar critical behaviors developed by 3D NAH models also provide additional possible scenarios for finite-temperature continuous transitions in D=3+1 non-Abelian gauge QFTs, in which temperature is related to the (inverse) finite size along the fourth Euclidean direction in the corresponding path-integral formulation, see, e.g., Refs. [23, 25, 26, 170, 171, 225, 226, 385–391, 397]. NAH theories have also been considered as effective theories of phenomena involving emerging non-Abelian gauge fields interacting with scalar modes, see, e.g., Refs. [96, 379], which are meant to explain some aspects of the phenomenology of high-temperature cuprate superconductors, see, e.g., Refs. [398–400].

In this section we introduce the NAH field theories (NAHFTs), i.e. field theories in which multiflavor scalar fields are coupled with non-Abelian gauge fields. In particular, we discuss statistical field theories with local $SU(N_c)$ and $SO(N_c)$ gauge symmetry, and scalar fields transforming according to different representations of the gauge group (we consider the fundamental and the adjoint representation). We outline the known features of their RG flow, whose stable infrared FPs are expected to describe the charged critical behaviors of the corresponding statistical systems.

8.1. $SU(N_c)$ gauge Higgs theory with scalar fields in the fundamental representation

8.1.1. The statistical field theory

We consider the NAHFT in which $\mathrm{SU}(N_c)$ gauge fields interact with N_f degenerate scalar fields in the fundamental representation of the gauge group. The fundamental fields are a complex scalar field $\Phi^{af}(\boldsymbol{x})$, where $a=1,...,N_c$ and $f=1,...,N_f$, and the gauge fields $A_{\mu}^c(\boldsymbol{x})$ where $c=1,...,N_c^2-1$, associated with the Hermitean generators T^c of the $\mathrm{SU}(N_c)$ algebra, normalized as $\mathrm{Tr}(T^aT^b)=\frac{1}{2}\delta^{ab}$. The most general

renormalizable Lagrangian that is invariant under local $SU(N_c)$ color transformations and under global $U(N_f)$ flavor transformations reads [99, 278]

$$\mathcal{L}_{SU} = \frac{1}{2g^2} \text{Tr } \mathcal{F}_{\mu\nu}^2 + \text{Tr} \left[(D_{\mu} \Phi)^{\dagger} (D_{\mu} \Phi) \right] + V(\Phi),$$

$$V(\Phi) = r \text{Tr } \Phi^{\dagger} \Phi + u (\text{Tr } \Phi^{\dagger} \Phi)^2 + v \text{Tr } (\Phi^{\dagger} \Phi)^2,$$
(88)

where $\mathcal{F}_{\mu\nu} = \partial_{\mu}\mathcal{A}_{\nu} - \partial_{\nu}\mathcal{A}_{\mu} - i[\mathcal{A}_{\mu}, \mathcal{A}_{\nu}]$ and $\mathcal{A}_{\mu} = \sum_{c} A_{\mu}^{c} T^{c}$, D_{μ} is the covariant derivative associated with the fundamental representation, i.e., $D_{\mu,ab} = \partial_{\mu}\delta_{ab} - i\sum_{c} T_{F,ab}^{c} A_{\mu}^{c}$ where T_{F}^{c} are the $N_{c}^{2} - 1$ generators in the fundamental representation of $SU(N_{c})$. The global $U(N_{f})$ group acts as $\Phi(\mathbf{x}) \to \Phi(\mathbf{x})W$, with $W \in U(N_{f})$, while the local $SU(N_c)$ gauge group acts as

$$\Phi(\mathbf{x}) \to V(\mathbf{x})\Phi(\mathbf{x}), \qquad \mathcal{A}_{\mu}(\mathbf{x}) \to V(\mathbf{x})\mathcal{A}_{\mu}(\mathbf{x})V^{\dagger}(\mathbf{x}) - i(\partial_{\mu}V(\mathbf{x}))V^{\dagger}(\mathbf{x}), \qquad V(\mathbf{x}) \in SU(N_c).$$
 (89)

Since the group $U(N_f)$ is not simple, we may separately consider $SU(N_f)$ and U(1) transformations, that correspond to $\Phi^{af} \to \sum_g V^{fg} \Phi^{ag}$, $V \in SU(N_f)$, and $\Phi^{af} \to e^{i\theta} \Phi^{af}$, $\theta \in [0, 2\pi)$, respectively. For $N_f < N_c$ the U(1) symmetry is only apparent, as a generic U(1) global transformation of the field Φ_x can be reabsorbed by composing an $SU(N_f)$ global transformation and an $SU(N_c)$ local transformation, see Ref. [169] for details. For $N_f \ge N_c$, since the diagonal matrices $e^{2\pi i/N_c}$ are elements of the $SU(N_c)$ group (they correspond to its center), θ can be restricted to $[0, 2\pi/N_c)$, and the global symmetry group is actually $U(N_f)/\mathbb{Z}_{N_c}$.

For $N_c = 2$, because of the pseudoreality of the SU(2) gauge group, the NAHFT (88) with v = 0 turns out to be invariant under transformations associated with a symmetry group that is larger than $U(N_f)$, i.e. the $Sp(N_f)/\mathbb{Z}_2$ group [32, 97, 99, 169, 378, 383, 387]. In particular, it is invariant under $Sp(2)/\mathbb{Z}_2 = SO(5)$ transformations for $N_f = 2$ [97, 169]. Therefore, the $N_c = 2$ NAHFT (88) with v = 0 is stable under RG transformations, defining a distinct theory characterized by the global symmetry $\operatorname{Sp}(N_f)/\mathbb{Z}_2$.

We finally recall that the standard Faddeev-Popov quantization [401] of a non-Abelian gauge field theory requires the addition of a gauge fixing. If we consider the Lorenz gauge fixing used in the AHFT defined in Eq. (22), one should also introduce appropriate scalar fields with fermionic statistics (ghosts), see, e.g., Refs. [1, 2].

8.1.2. Higgs phases and breaking patterns of the global symmetry

The global symmetry of the Higgs phases, which is nontrivial only for $N_f \geq 2$, can be studied by performing an analysis of the minima of the scalar potential. We report here the main results. See Ref. [99] for more details, and Appendix C for a sketch of the derivations in the corresponding lattice models. The results of these analyses depend on the sign of v and, for v > 0, also on the number of colors N_c and flavors N_f .

For v < 0 the Higgs phase is invariant under $U(1) \oplus U(N_f - 1)$ transformations, leading to the spontaneous symmetry breaking pattern

$$U(N_f) \to U(1) \oplus U(N_f - 1).$$
 (90)

Note that the U(1) symmetry is not broken, so only the $SU(N_f)$ symmetry plays a role. The relevant symmetry breaking pattern is therefore

$$SU(N_f) \to U(N_f - 1).$$
 (91)

For v > 0 one should distinguish three different cases. For $N_f < N_c$ there is no symmetry breaking and therefore no Higgs ordered phase. For $N_f \geq N_c$ we have instead

$$U(N_f) \to SU(N_f)$$
 for $N_f = N_c$, (92)

$$U(N_f) \to SU(N_f) \qquad \text{for } N_f = N_c,$$

$$U(N_f) \to SU(N_c) \otimes U(N_f - N_c) \qquad \text{for } N_f > N_c.$$

$$(92)$$

It is important to note that for $N_f = N_c$ the Higgs phase is symmetric under $SU(N_f)$ transformations. In this case transitions in the corresponding lattice models are only associated with the breaking of the U(1) symmetry. On the other hand, for $N_f > N_c$, in the Higgs phase both the U(1) and the SU(N_f) symmetry are broken.

8.1.3. Renormalization-group flow

A nonperturbative formulation of the NAHFT is provided by the continuum (critical) limit of corresponding lattice models with the same local gauge and global symmetries, as it is done for the strong-interaction theory, quantum chromodynamics (QCD) [3, 100]. For this purpose it is crucial that the corresponding lattice discretizations has a continuous charged transition where the gauge fields play a relevant role. Therefore, it is important to identify the universality classes of the charged transitions in this class of systems. They must be related to the RG flow of the NAHFT, and in particular to its stable FPs.

The RG flow of the NAHFT (88) can be investigated perturbatively, in powers of $\varepsilon \equiv 4-d$ [94], using dimensional regularization and the minimal-subtraction (MS) renormalization scheme, see, e.g., Ref. [2, 95]. The RG flow close to four dimensions is determined by the MS β functions associated with the Lagrangian couplings $\alpha = g^2$, u, and v. At one-loop order, we have [99, 278]

$$\beta_{\alpha} \equiv \mu \frac{\partial \alpha}{\partial \mu} = -\varepsilon \alpha + (N_f - 22N_c) \alpha^2,$$

$$\beta_{u} \equiv \mu \frac{\partial u}{\partial \mu} = -\varepsilon u + (N_f N_c + 4) u^2 + 2(N_f + N_c) uv + 3v^2 - \frac{18(N_c^2 - 1)}{N_c} u\alpha + \frac{27(N_c^2 + 2)}{N_c^2} \alpha^2,$$

$$\beta_{v} \equiv \mu \frac{\partial v}{\partial \mu} = -\varepsilon v + (N_f + N_c) v^2 + 6uv - \frac{18(N_c^2 - 1)}{N_c} v\alpha + \frac{27(N_c^2 - 4)}{N_c} \alpha^2.$$

$$(94)$$

Some numerical factors have been reabsorbed in the normalizations of the renormalized couplings, in order to simplify the previous expressions.

The analysis of the common zeroes of the β functions shows that the RG flow close to four dimensions has a stable charged FP with a nonzero FP value of the gauge coupling α , for a sufficiently large number of flavors; more precisely, for $N_f > N_f^*$, with, e.g., $N_f^* = 375.4 + O(\varepsilon)$ for $N_c = 2$, and $N_f^* = 638.9 + O(\varepsilon)$ for $N_c = 3$. The values of N_f^* are large in four dimensions, but they are expected to decrease significantly in three dimensions for any N_c , as it also happens in the AHFT, where N_f^* varies from $N_f^* \approx 183$ in four dimensions to $N_f^* \approx 7$ in three dimensions. In particular, for $N_c = 2$ numerical studies based on MC simulations of lattice SU(2)-gauge Higgs models [402] indicate $N_f^* = 25(4)$ in three dimensions, see Sec. 9.3. We also mention that in the case of the SU(2)-gauge NAHFT (88) for v = 0, for which the global symmetry enlarges to $\mathrm{Sp}(N_f)/\mathbb{Z}_2$, a charged FP exists for $N_f > N_f^* \approx 359 + O(\varepsilon)$ [97]. This FP turns out to be unstable in the full theory, i.e, with respect to nonzero values of the Lagrangian coupling v.

The stable charged FP of this class of NAHFTs is located in the positive v region for any N_c . This result indicates that only transitions characterized by the $\mathrm{U}(N_f) \to \mathrm{SU}(N_c) \otimes \mathrm{U}(N_f - N_c)$ symmetry-breaking pattern may correspond to charged continuous transitions. Those characterized by the symmetry-breaking pattern $\mathrm{U}(N_f) \to \mathrm{U}(1) \oplus \mathrm{U}(N_f - 1)$, corresponding to v < 0, instead cannot be charged continuous transitions. As we have already discussed for the AH models, it is crucial to note that the FPs of the NAHFTs are relevant for the existence of charged continuous transitions, i.e., of continuous transitions where both scalar and gauge fields are critical. As discussed in Sec. 3.1, gauge models can also undergo other types of transitions that admit different effective descriptions. Therefore, it is a priori possible to have further continuous transitions, which may be LGW or topological transitions, also for $N_f < N_f^*$ and for v < 0. Some examples will be discussed in Sec. 9.

As it occurs in models with Abelian gauge symmetry, the uncharged FP with vanishing gauge coupling $\alpha = 0$ is unstable with respect to the gauge coupling, since its stability matrix $\Omega_{ij} = \partial \beta_i / \partial g_j$ has a negative eigenvalue [99]

$$\lambda_{\alpha} = \left. \partial \beta_{\alpha} / \partial \alpha \right|_{\alpha = 0} = -\varepsilon + O(\varepsilon^2). \tag{95}$$

This result suggests that also in three dimensions gauge fluctuations make the uncharged FP unstable, as also confirmed by the numerical studies of 3D SU(2)-gauge LNAH models [99], see also Sec. 9. Note that continuous transitions described by the uncharged FP of the NAHFT for $\alpha=0$ would be characterized by an asymptotic critical behavior in which gauge-field correlations are not critical, thus they would correspond to LGW[×] transitions, effectively described by a LGW theory with a gauge-dependent complex order-parameter field $\Phi^{af}(\boldsymbol{x})$ with $a=1,...,N_c$ and $f=1,...,N_f$.

An alternative approach to the study of the $SU(N_c)$ -gauge NAHFT is provided by the $1/N_f$ expansion at fixed N_c [278]. These computations confirm the existence of a charged critical behavior in three dimensions. For example, a $O(1/N_f)$ computation of the length-scale critical exponent ν predicts [278]

$$\nu = 1 + \frac{a_1}{N_f} + O(N_f^{-2}), \qquad a_1 = -\frac{48N_c}{\pi^2 N_f}, \tag{96}$$

in the 3D $SU(N_c)$ -gauge NAHFT with Lagrangian (88).

8.2. $SO(N_c)$ gauge Higgs theory with scalar fields in the fundamental representation

The NAHFT with gauge group $SO(N_c)$ and multiflavor scalar fields in the fundamental representation is obtained by considering a real scalar field $\Phi^{af}(\boldsymbol{x})$ (with $a=1,...,N_c$ and $f=1,...,N_f$) and the gauge fields $A^c_{\mu}(\boldsymbol{x})$ associated with the generators T^c of the $SO(N_c)$ algebra. The most general renormalizable Lagrangian is [157, 278, 384]

$$\mathcal{L}_{SO} = \frac{1}{2g^2} \operatorname{Tr} \mathcal{F}_{\mu\nu}^2 + + \operatorname{Tr} \left[(D_{\mu} \Phi)^{\dagger} (D_{\mu} \Phi) \right] + V(\Phi), \tag{97}$$
$$V(\Phi) = \frac{r}{2} \operatorname{Tr} \Phi^t \Phi + u (\operatorname{Tr} \Phi^t \Phi)^2 + v \left[\operatorname{Tr} (\Phi^t \Phi)^2 - (\operatorname{Tr} \Phi^t \Phi)^2 \right],$$

where $\mathcal{F}_{\mu\nu}$ is the non-Abelian field strength of the gauge field $\mathcal{A}_{\mu} = \sum_{c} A_{\mu}^{c} T^{c}$, and D_{μ} is the covariant derivative associated with the fundamental representation of $SO(N_c)$. For any value of N_c and N_f , the Lagrangian (97) is invariant under the local $SO(N_c)$ gauge transformations,

$$\Phi(\mathbf{x}) \to V(\mathbf{x})\Phi(\mathbf{x}), \qquad A_{\mu}(\mathbf{x}) \to V(\mathbf{x})A_{\mu}(\mathbf{x})V^{t}(\mathbf{x}) - (\partial_{\mu}V(\mathbf{x}))V^{t}(\mathbf{x}), \qquad V(\mathbf{x}) \in SO(N_{c}),$$
 (98)

and under the global $O(N_f)$ transformations, $\Phi(x) \to \Phi(x)W$ with $W \in O(N_f)$. For $N_c = 2$, we have an Abelian O(2) gauge model with $SO(N_f)$ global symmetry, which is equivalent to the one discussed in Sec. 4.2.1 ⁴⁴

The RG flow determined by the β functions associated with the Lagrangian quartic couplings provides information on the nature of the transitions described by the continuum $SO(N_c)$ gauge theory (97). In the ε -expansion framework, the one-loop MS β functions are [98, 278, 384]

$$\beta_{\alpha} \equiv \mu \frac{\partial \alpha}{\partial \mu} = -\varepsilon \alpha + \frac{N_f - 22(N_c - 2)}{12} \alpha^2,$$

$$\beta_u \equiv \mu \frac{\partial u}{\partial \mu} = -\varepsilon u + \frac{N_c N_f + 8}{6} u^2 + \frac{(N_f - 1)(N_c - 1)}{6} (v^2 - 2uv) - \frac{3}{2} (N_c - 1)u\alpha + \frac{9}{8} (N_c - 1)\alpha^2,$$

$$\beta_v \equiv \mu \frac{\partial v}{\partial \mu} = -\varepsilon v + \frac{N_c + N_f - 8}{6} v^2 + 2uv - \frac{3}{2} (N_c - 1)v\alpha + \frac{9}{8} (N_c - 2)\alpha^2,$$
(99)

where the renormalized couplings $\alpha = g^2$, u, and v have been normalized to simplify the expressions.⁴⁵

The RG flow of the theory does not have stable charged FPs with $\alpha > 0$, unless $N_f > N_f^*(d)$, where $N_f^*(d)$ is very large in four dimensions. Indeed, we find $N_f^*(4) = 210.5$ for $N_c = 2$, and $N_f^*(4) \approx 443.8$, for $N_c = 3$. The stable FPs always lie in the region u, v > 0. More precisely, one finds $v^* \approx 6\varepsilon/N_f$, $u^* \approx 6\varepsilon/N_f$, and $\alpha^* = 12\varepsilon/N_f$ for large values of N_f . Note that the existence of a critical theory for large values of N_f is also confirmed by the analysis of the model using the large- N_f expansion [278].

The results reviewed above show that continuous transitions with the effective field-theory description (97) are only possible for a large number of components. Again, we remind the reader that this result does not exclude the presence of other types of continuous transitions (see Sec. 3.1) for small values of N_f .

⁴⁴If we define $\Phi_A^f = (\Phi^{1f} + i\Phi^{2f})/\sqrt{2}$, $u_A = 4u - 2v$, $v_A = 2v$, $r_A = r$, the Lagrangian (97) takes the form given in Eq. (39), provided we indicate with Φ_A the complex field and with r_A , u_A , and v_A the Hamiltonian parameters of the AHFT. Note that for v = 0 its global symmetry enlarges to $U(N_f)$, see Sec. 4.2.1.

⁴⁵Because of the equivalence of the present model with $N_c = 2$ with the SO(N)-symmetric AHFT, their β functions are related. If we redefine the couplings in Eq. (99) as $\alpha \to 12\alpha$, $u \to 3(u+v)$ and $v \to 6v$, we obtain the β functions reported in Eq. (43).

8.3. $SU(N_c)$ gauge Higgs theory with scalar fields in the adjoint representation

We now consider the $SU(N_c)$ gauge NAHFT with scalar fields in the adjoint representation. As argued in Ref. [96], 3D SU(2)-gauge theories with adjoint scalar fields with $N_f = 1$ or $N_f = 4$ are expected to describe some aspects of the optimal doping criticality in cuprate superconductors, as emerging from experiments, see, e.g., Refs. [398–400].

To define the model we consider real scalar fields $\Phi^{af}(\boldsymbol{x})$ with $a=1,...,N_c^2-1$ (color index) and $f=1,...,N_f$ (flavor index), and N_c^2-1 real gauge fields $A_{\mu}^c(\boldsymbol{x})$. The most general renormalizable Lagrangian is

$$\mathcal{L}_{\text{SUadj}} = \frac{1}{2g^2} \operatorname{Tr} \mathcal{F}_{\mu\nu}^2 + \operatorname{Tr} \left[(D_{\mu} \Phi)^{\dagger} (D_{\mu} \Phi) \right] + V(\Phi), \tag{100}$$

$$V(\Phi) = \frac{r}{2} \operatorname{Tr} \Phi^t \Phi + u (\operatorname{Tr} \Phi^t \Phi)^2 + v \left[\operatorname{Tr} (\Phi^t \Phi)^2 - (\operatorname{Tr} \Phi^t \Phi)^2 \right],$$

where $\mathcal{F}_{\mu\nu}$ is the field strength of the gauge field $\mathcal{A}_{\mu} \equiv \sum_{c} A^{c}_{\mu} T^{c}$, and D_{μ} is the covariant derivative associated with the adjoint representation, i.e., $\partial_{\mu} + i \sum_{c} A^{c}_{\mu} T^{c}_{A}$ and $T^{abc}_{A} = -i f^{abc}$ are the Hermitian SU(N_{c}) generators in the adjoint representation (f^{abc} are the structure constants of the SU(N_{c}) group). The model is invariant under left SU(N_{c}) local transformations and under right O(N_{f}) global transformations.

For $N_c = 2$ the model is equivalent to the SO(3) gauge model (97) with N_f flavor, which allows one to use the results reported in Sec. 8.2. For instance, the β functions of the SU(2) gauge theory with adjoint scalar matter are [96]

$$\beta_{\alpha} = -\varepsilon \alpha + \frac{N_f - 22}{12} \alpha^2,$$

$$\beta_u = -\varepsilon u + \frac{3N_f + 8}{6} u^2 + \frac{N_f - 1}{3} (v^2 - 2uv) - 3u\alpha + \frac{9}{4} \alpha^2,$$

$$\beta_v = -\varepsilon v + \frac{N_f - 5}{6} v^2 + 2uv - 3v\alpha + \frac{9}{8} \alpha^2.$$
(101)

They have a stable FP for sufficiently large N_f , more precisely for $N_f > N^* + O(\varepsilon)$ with $N^* \approx 443.8$. In particular, in the large- N_f limit the stable FP of the β functions is located at $\alpha^* \approx 12\varepsilon/N_f$, $u^* \approx 6\varepsilon/N_f$, $v^* \approx 6\varepsilon/N_f$. Note that, also in this case, the stable large- N_f charged FP is located in the region v > 0.

9. Lattice non-Abelian Higgs models

In this section we consider 3D lattice non-Abelian Higgs (LNAH) models, i.e., 3D lattice non-Abelian gauge models with multicomponent degenerate scalar fields, and review the known results regarding their phase diagram, the main properties of their low-temperature Higgs phases, and the nature of their phase transitions and critical behaviors. We mainly consider $SU(N_c)$ gauge models with scalar fields transforming in the fundamental and adjoint representations of the gauge group. We also briefly discuss $SO(N_c)$ gauge models with multicomponent scalar fields in the fundamental representation.

Like LAH theories, see Secs. 5 and 6, one of the main issues is the identification of the effective field-theoretical description of the phase transitions present in LNAH models. Their phase diagrams exhibit transitions of various types, as discussed in Sec. 3.1. There are transitions that admit a LGW description in terms of a gauge-invariant order-parameter field—this is appropriate when gauge modes are not critical—and GFT transitions with critical gauge modes, associated with the stable charged FPs of the NAHFTs discussed in Sec. 8. Moreover, when scalar fields transform in the adjoint representation of the $SU(N_c)$ gauge group, also topological transitions appear, which are not associated with the breaking of the global symmetry. Note that, to define nonperturbatively the NAHFT as the continuum limit of a lattice model, it is crucial that the corresponding LNAH models, with analogous local and global symmetries, undergo charged continuous transitions where both scalar and gauge modes develop a critical behavior.

9.1. Lattice $SU(N_c)$ gauge Higgs models with multiflavor scalar fields

We consider LNAH models with multiflavor scalar fields, which are invariant under $SU(N_c)$ gauge transformations and $U(N_f)$ global transformations. Scalar fields transform under the fundamental representation of the local and global symmetry groups. The Hamiltonian can be straightforwardly obtained by taking a lattice discretization of the Lagrangian (88), using the compact Wilson formulation in which gauge fields are replaced by link variables taking values in the gauge group [100]. In the lattice model—for simplicity we consider cubic lattices—the fundamental fields are complex matrices Φ_x^{af} , with $a=1,...,N_c$ (color index) and $f=1,...,N_f$ (flavor index), defined on the lattice sites, and $SU(N_c)$ matrices $U_{x,\mu}$, defined on the lattice links. The partition function is

$$Z = \sum_{\{\Phi, U\}} e^{-\beta H}, \qquad \beta = 1/T, \qquad H = H_K(\Phi, U) + H_V(\Phi) + H_G(U). \tag{102}$$

The Hamiltonian H is the sum of the scalar-field kinetic term H_K , of the local scalar potential H_V , and of the pure-gauge Hamiltonian H_G . As usual, we set the lattice spacing equal to one, so that all lengths are measured in units of the lattice spacing. The kinetic term H_K is given by

$$H_K(\Phi, U) = -JN_f \sum_{\boldsymbol{x}, \mu} \operatorname{Re} \operatorname{Tr} \Phi_{\boldsymbol{x}}^{\dagger} U_{\boldsymbol{x}, \mu} \Phi_{\boldsymbol{x} + \hat{\mu}}.$$
(103)

In the following we set J = 1, so that energies are measured in units of J. The local scalar potential H_V is given by

$$H_V(\Phi) = \sum_{\boldsymbol{x}} V(\Phi_{\boldsymbol{x}}), \qquad V(\Phi) = \frac{r}{2} \operatorname{Tr} \Phi^{\dagger} \Phi + \frac{u}{4} \left(\operatorname{Tr} \Phi^{\dagger} \Phi \right)^2 + \frac{v}{4} \operatorname{Tr} (\Phi^{\dagger} \Phi)^2, \tag{104}$$

where $V(\Phi)$ is the most general quartic polynomial that is symmetric under $[\mathrm{U}(N_f)\otimes\mathrm{U}(N_c)]/\mathrm{U}(1)$ transformations. Note that for $N_f=1$ the two quartic terms in $V(\Phi)$ are equivalent. Finally, the pure-gauge Hamiltonian $H_G(U)$ is the sum of plaquette terms [100],

$$H_G(U) = -\frac{\gamma}{N_c} \sum_{\boldsymbol{x}, \mu > \nu} \operatorname{Re} \operatorname{Tr} \Pi_{\boldsymbol{x}, \mu \nu}, \qquad \Pi_{\boldsymbol{x}, \mu \nu} = U_{\boldsymbol{x}, \mu} U_{\boldsymbol{x} + \hat{\mu}, \nu} U_{\boldsymbol{x} + \hat{\nu}, \mu}^{\dagger} U_{\boldsymbol{x}, \nu}^{\dagger}, \tag{105}$$

where the parameter γ plays the role of inverse gauge coupling.

The Hamiltonian H is invariant under global $U(N_f)$ transformations that only act on the scalar field, $\Phi \to \Phi W$, $W \in U(N_f)$, and under local $SU(N_c)$ gauge transformations

$$\Phi_{\boldsymbol{x}} \to V_{\boldsymbol{x}} \Phi_{\boldsymbol{x}}, \qquad U_{\boldsymbol{x},\mu} \to V_{\boldsymbol{x}} U_{\boldsymbol{x},\mu} V_{\boldsymbol{x}+\hat{\mu}}^{\dagger}, \qquad V_{\boldsymbol{x}} \in \mathrm{SU}(N_c).$$
(106)

The lattice model (102) can be simplified by considering the fixed-length limit of the scalar field, i.e., by requiring $\operatorname{Tr} \Phi_{\boldsymbol{x}}^{\dagger} \Phi_{\boldsymbol{x}} = 1$, which can be formally obtained by considering the limit $u, r \to \infty$ keeping the ratio r/u = -1 fixed. In the unit-length limit the lattice potential (104) reduces to

$$V(\Phi) = \frac{v}{4} \operatorname{Tr} (\Phi^{\dagger} \Phi)^{2}, \qquad \operatorname{Tr} \Phi^{\dagger} \Phi = 1.$$
 (107)

The model in the unit-length limit is generally expected to have the same features as models with generic r and u.

As already discussed in Sec. 8.1.2, phase transitions can be characterized by the breaking of the global $SU(N_f)$ symmetry or by the breaking of the U(1) symmetry. The spontaneous breaking of the global $SU(N_f)$ symmetry is signaled by the condensation of the gauge-invariant bilinear operator

$$P_{\boldsymbol{x}}^{fg} = \sum_{a} \bar{\Phi}_{\boldsymbol{x}}^{af} \Phi_{\boldsymbol{x}}^{ag} - \frac{1}{N_{f}} \delta^{fg}, \qquad G_{P}(\boldsymbol{x}, \boldsymbol{y}) \equiv \langle \operatorname{Tr} P_{\boldsymbol{x}} P_{\boldsymbol{y}} \rangle.$$
 (108)

The bilinear operator P_x^{fg} is invariant under the U(1) global transformations and satisfies Tr $P_x = 0$ (because of the unit-length constraint of Φ_x). To monitor the breaking of the U(1) global symmetry, one may consider gauge-invariant operators that transform nontrivially under U(1) transformations. For example, for $N_c = 2$, one may consider the bilinear operator

$$Y_{\boldsymbol{x}}^{fg} = \epsilon^{ab} \, \Phi_{\boldsymbol{x}}^{af} \, \Phi_{\boldsymbol{x}}^{bg}, \qquad G_Y(\boldsymbol{x}, \boldsymbol{y}) \equiv \langle \operatorname{Tr} Y_{\boldsymbol{x}}^{\dagger} Y_{\boldsymbol{y}} \rangle,$$
 (109)

where e^{ab} is the completely antisymmetric tensor in the color space, with $e^{12} = 1$. Note that, if $N_f > N_c = 2$, the composite operator Y_x^{fg} transforms nontrivially under the $SU(N_f)$ group, therefore the U(1) symmetry can be spontaneously broken only in phases characterized by a broken $SU(N_f)$ symmetry. Instead, for $N_f = N_c = 2$, the operator Y_x^{fg} can be rewritten as $Y_x^{fg} = e^{fg} \det \Phi_x$, and is therefore invariant under SU(2) global transformations. If $N_f = N_c$, the U(1) symmetry can thus be broken irrespectively of the breaking of the $SU(N_f)$ symmetry. Analogous results hold for generic values of N_c , see Refs. [99, 169].

9.2. Phase diagram and critical behaviors of lattice $SU(N_c)$ gauge Higgs models

We now outline the main features of the phase diagram of the LNAH models (102), discussing the nature of their phase transitions and critical behaviors. We mainly focus on the LNAH models subject to the unit-length limit (107). Qualitatively similar phase diagrams are expected when relaxing the unit-length constraint, i.e. for generic $SU(N_c)$ gauge LNAH models defined by the Hamiltonian (102).

9.2.1. General considerations related to the low-temperature Higgs phases

For $N_f=1$, the phase diagram of the SU(N_c) gauge LNAH models is trivial: there is a single thermodynamic phase for any N_c [41, 43, 382], without transitions. In this case we may only distinguish two different regimes: a confined regime for small values of βJ and $\beta \gamma$, and a Higgs regime for large βJ and $\beta \gamma$, which are analytically connected. For $\gamma=0$ it is easy to realize that no transitions are possible. Indeed, using the gauge and global symmetry, we can set (unitary gauge) $\Phi=(1,0,\ldots)$, obtaining a model of decoupled gauge fields. The same result holds for finite γ [41].

For $N_f \geq 2$, as we have discussed in Sec. 8.1.2, there are various Higgs phases characterized by different spontaneous breakings of the global symmetry [99]. For $\beta \to \infty$, the symmetry of the ordered Higgs phases can be determined by looking at the minima of the scalar potential. Thus, results analogous to those presented in Sec. 8.1.2 are obtained. For $N_f \geq N_c$ there are two Higgs phases, one corresponding to negative values of v for large β , and a second one corresponding to positive values of v. For $N_f < N_c$, there is instead a single ordered phase in the negative-v region. Indeed, for large values of β the system is always disordered for v > 0.

The transitions between the disordered phase and the negative-v Higgs phase are characterized by the symmetry-breaking pattern $U(N_f) \to U(1) \oplus U(N_f - 1)$, cf. Eq. (90). On the basis of the RG flow of the NAHFT close to four dimensions, see Sec. 8.1.3, these transitions are not expected to be charged continuous transitions, because of the absence of a corresponding stable charged FP. However, LGW transitions are still possible. Since the U(1) symmetry is not broken, the relevant symmetry-breaking pattern is $SU(N_f) \to U(N_f - 1)$, cf. Eq. (91), which is the symmetry-breaking pattern of the CP^{N_f-1} transitions discussed in Sec. 3.2.1. This is not unexpected, as the order parameter of the transition is the operator P_x^{ab} , defined in Eq. (108), which is a bilinear Hermitian traceless field as the CP^{N_f-1} order parameter defined in Eq. (9). Using the results presented in Sec. 3.2.1, we thus conclude that continuous transitions only occur for $N_f = 2$ —they belong to the O(3) universality class. First-order transitions are expected for larger values of N_f .

For $N_f \geq N_c$ a second Higgs phase occurs, since the system orders for v > 0 when β is increased. The nature of this phase depends on N_f and N_c . For $N_f = N_c$ the global symmetry breaking pattern is $\mathrm{U}(N_f) \to \mathrm{SU}(N_f)$, cf. Eq. (92). In this case the $\mathrm{SU}(N_f)$ symmetry is not broken in the Higgs phase, so the transition is only related to the breaking of the U(1) symmetry, the order parameter being det Φ , as discussed in Sec. 8.1.2. Thus, the system can develop continuous LGW transitions belonging to the XY universality class. No charged continuous transitions described by the corresponding NAHFT are expected, since charged FPs exist only for $N_f \gg N_c$ (unless some new features emerge in three dimensions, as it occurs for the one-component LAH model with noncompact gauge variables; see the discussion at the end of Sec. 5.2.2). Finally,

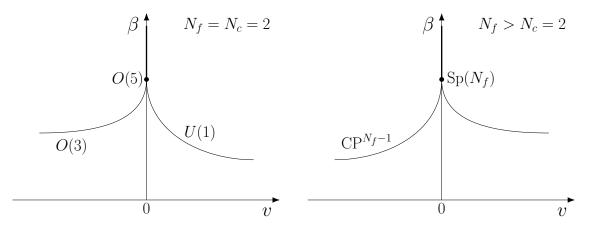


Figure 19: Sketch of the phase diagram of 3D SU(2) gauge LNAH models with N_f scalar flavors in the fundamental representation, for $N_f = N_c = 2$ (left) and $N_f > N_c = 2$ (right) in the β -v plane for finite values of $\gamma \ge 0$ (the qualitative behavior should not depend on γ). Left $(N_f = N_c = 2)$: there are two transition lines for $v \ne 0$, intersecting at a MCP located at $(v = 0, \beta = \beta_{\rm mc})$ with O(5) symmetry; continuous transitions belong to the O(3) and U(1) = SO(2) vector universality classes for v < 0 and v > 0, respectively; first-order transitions are expected on the line $(v = 0, \beta > \beta_{\rm mc})$. Right $(N_f > N_c = 2)$: for v < 0 transitions are of first order (as in the ${\rm CP}^{N_f-1}$ model); for v > 0 the nature of the transitions might depend on γ for sufficiently large values of N_f ; in particular, for large values of N_f the system is expected to undergo charged continuous transitions associated with the stable charged FP of the corresponding NAHFT; for v = 0 we have a first-order line ending at the intersection of the transition lines (the transitions are expected to be of first order close to the intersection).

for $N_f > N_c$ and v > 0 we have transitions with symmetry-breaking pattern $U(N_f) \to SU(N_c) \otimes U(N_f - N_c)$, cf. Eq. (93). In this case, charged continuous transitions corresponding to the stable FP of the corresponding NAHFT can be observed for $N_f > N_f^*(3)$, where $N_f^*(3)$ is the $(N_c$ -dependent) critical flavor number defined in Sec. 8.1.3.⁴⁶

9.2.2. Lattice SU(2) gauge Higgs models

We now focus on LNAH models with SU(2) gauge symmetry, which present some peculiar features that are not present for $N_c \geq 3$. The phase diagrams of multicomponent LNAH models with $N_c = 2$ are sketched in Fig. 19 for a generic value of γ . For any $N_f \geq 2$ there are two low-temperature Higgs phases separated by a first-order transition line. Since the LNAH model (102) with v=0 is invariant under a larger group of transformations, the $\text{Sp}(N_f)/\mathbb{Z}_2$ group [97, 169], the first-order line always lies on the line v=0. At the intersection point of the three transition lines, the behavior can be critical only for $N_f=2$, with a MCP belonging to the $\text{Sp}(N_2)/\mathbb{Z}_2 = \text{O}(5)$ universality class (see Sec. 9.2.3 for a more extensive discussion). For $N_f \geq 3$, RG arguments based on a multicritical LGW theory predict the intersection point to correspond to a first-order transition [97, 169].

The behavior along the transition lines that separate the disordered phase from the ordered Higgs phases has been discussed in Sec. 9.2.1. For v < 0, continuous transitions are only possible for $N_f = 2$. They belong to the CP¹, i.e., vector O(3), universality class (this has been numerically checked for $\gamma = 0$ in Ref. [99]). For larger values of N_f , transitions are always of first order. For v > 0, XY transitions are expected for $N_f = 2$ (numerical results confirm this prediction [99]). For larger values of N_f , we may have charged continuous transitions associated with the stable charged FPs of the NAHFT, see Sec. 8.1.3. Numerical studies [99, 402] for relatively large values of N_f confirm this scenario. Indeed, for a sufficiently large number N_f of flavors

 $^{^{46}}$ It is worth noting that a LGW field-theoretical description in terms of a gauge-invariant order-parameter field does not exist, since the Higgs phase symmetry $SU(N_c) \otimes U(N_f - N_c)$ depends on the number of colors. Therefore, any effective description should somehow take into account some specific properties of the gauge interaction. In principle, this color-dependent symmetry breaking may be realized in LGW $^{\times}$ transitions with a gauge-dependent order-parameter field. However, the latter scenario is quite unlikely in 3D systems, because gauge fluctuations are expected to be generally relevant at the uncharged FP of theories with continuous gauge groups, see Sec. 8.1.3.

the SU(2) gauge LNAH models undergo continuous transitions for finite (sufficiently large) values of γ , with a critical behavior consistent with that predicted by the 3D SU(2) gauge Higgs field theory. This is confirmed by the comparison of numerical lattice results and large- N_f field-theoretical predictions, see also Sec. 9.3.

9.2.3. O(5) multicritical behavior of the two-flavor SU(2) gauge Higgs model

We now focus on a particular region of the phase diagram of SU(2) gauge LNAH models with N_f flavors. We discuss the nature of the transition point that lies on the v=0 axis, where the transition lines intersect, see Fig. 19 (we discuss the behavior at fixed γ ; in the full phase diagram, we have a γ dependent line of such intersection points). Note that the global symmetry of the model enlarges to $\operatorname{Sp}(N_f)/\mathbb{Z}_2$ for v=0.

The behavior at the intersection point depends on N_f . For $N_f > 2$, the intersection point is expected to be a first-order transition point, as predicted by an analysis based on the corresponding multicritical LGW theory [97, 169].⁴⁷ Therefore, we expect the three transition lines to be of first order close to the intersection. More precisely, the discussion presented in Sec. 9.2.1 implies that for $N_f < N_f^*(3)$ the transitions are of first order for any value of v. On the other hand, for $N_f > N_f^*(3)$, charged continuous transitions are possible for v > 0. Even in this case, we however expect first-order transitions for any v < 0, and also for sufficiently small positive values of v.

For $N_f = 2$, see the left panel of Fig. 19, it is possible to observe a multicritical behavior on the v = 0 line, arising from the competition of the O(3) order parameter, driving the negative-v transitions, and the U(1), i.e., O(2), order parameter, associated with the positive-v transitions. Because of the exact symmetry under Sp(2)/ \mathbb{Z}_2 =O(5) transformations of the model with v = 0, the multicritical behavior belongs to the multicritical O(5) vector universality class. Correspondingly, at the MCP the two order-parameter operators P_x and Y_x defined in Sec. 9.1 can be combined [97, 169] into a five-component real order parameter—the magnetization—for O(5) vector systems [97, 169]. Note that all transitions are uncharged—gauge modes do not play any role—and thus the multicritical behavior can be effectively described by the LGW multicritical theory with O(2) \oplus O(3) symmetry discussed in Sec. 2.2.4.

As discussed in Appendix A.4, the multicritical behavior is controlled by two relevant RG perturbations, represented by two scaling fields u_1 and u_2 that are functions of the model parameters and have positive RG dimensions y_1 and y_2 . In the case of the O(5)-symmetric MCP we can identify $u_1 \approx v$ and $u_2 \approx 1 - \beta/\beta_{\rm mc}$, whose RG dimensions are determined by the O(5) vector universality class [175, 178]. They are given by $y_1 = y_{2,2} = 1.832(8)$ [175], where $y_{2,2}$ is the RG scaling dimension of the coupling associated to the spin-two perturbation of the O(5)-vector FP, and $y_2 = 1/\nu_{\rm O(5)} = 1.2818(10)$ (using the best available estimate [299] $\nu_{\rm O(5)} = 0.7802(6)$ for the length-scale exponent of the O(5) vector universality class).

It is important to remark that MCPs arising from the competition of O(3) and U(1) order parameters do not generally belong to the O(5) vector universality class [175, 178]. Indeed, the analysis of the RG flow of the O(3) \oplus O(2) LGW theory (5) shows that the multicritical O(5) FP is unstable against the quartic spin-4 perturbation, whose coupling has a positive RG scaling dimension [178], given by $y_{4,4} = 0.23(2)$. Therefore, the observation of an O(5) multicritical behavior generally requires a further tuning of the model parameters to decouple the spin-4 perturbation of the O(5) FP. In the case at hand, the O(5) symmetry enlargement is guaranteed by the fact that the LNAH model for v=0 is exactly invariant under the larger group $\operatorname{Sp}(2)/\mathbb{Z}_2 = \operatorname{SO}(5)$. The presence of the SU(2) gauge invariance thus provides a robust mechanism—no fine tuning is needed— to obtain an O(5) multicritical behavior in O(3) \oplus U(1) systems, effectively canceling the spin-4 relevant perturbation of the O(5) FP [175, 178]. It is also interesting to note that, by fixing

⁴⁷We should also mention that the field-theory model with v = 0 admits a charged FP for large values of N_f . Thus, in this case a charged multicritical behavior can also appear.

⁴⁸The only stable FP in the $O(3) \oplus O(2)$ LGW theory is the decoupled FP [175, 403, 404] Therefore, if the system is in its attraction domain, a decoupled critical behavior should be observed at the MCP, with a tetracritical phase diagram as that show in the central panel of Fig. 1.

 $^{^{49}}$ It is worth mentioning that an effective O(5) symmetry enlargement at multicritical transitions driven by the competition of O(3) and U(1) critical modes has been suggested, and apparently observed, in various physical contexts, e.g., in systems with deconfined criticality [31, 203, 273, 405–409] and in high- T_c superconductors [178, 410–414].

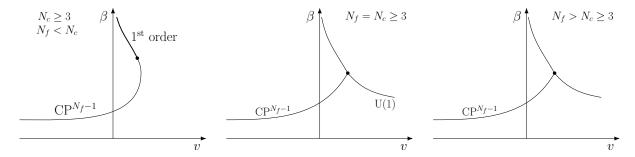


Figure 20: Sketches of the phase diagrams of 3D SU(N_c) gauge LNAH models with N_f scalar fields in the fundamental representation, at fixed $\gamma \geq 0$ expected for $N_c \geq 3$, and $N_f < N_c$ (left), $N_f = N_c$ (middle), $N_f > N_c$ (right).

 $\beta = \beta_{\rm mc}$ ($\beta_{\rm mc}$ corresponds to the location of the MCP) and by varying v from v < 0 to v > 0, the system goes from an O(3) ordered phase to a U(1) ordered phase across a continuous transition, the O(5) MCP.

9.2.4. Lattice $SU(N_c)$ gauge Higgs models with $N_c \geq 3$

We now discuss the possible phase diagrams of the $SU(N_c)$ gauge LNAH model for $N_c \ge 3$, see Fig. 20, distinguishing three cases, $N_f < N_c$, $N_f = N_c$, and $N_f > N_c$.

For $N_f < N_c$, see the left panel of Fig. 20, as discussed in Sec. 9.2.1, there is a single negative-v Higgs phase. Along the transition line, the system behaves as the \mathbb{CP}^{N_f-1} model, so continuous transitions are only possible for $N_f = 2$, see Sec. 3.2.1. For $N_f \geq 3$ the boundary of the Higgs phase is a first-order transition line. For $N_f = 2$, the behavior along the boundary is the one reported in the left panel of Fig. 20, see Refs. [97, 169]. For large β the boundary corresponds to a first-order transition line, then it turns into a continuous $\mathrm{O}(3)$ transition line, with the presence of a tricritical point. Note that for $N_c \geq 3$, the line v = 0 does not play any role, and therefore the boundary does not lie on the line v = 0. It starts at v = 0 for $\beta \to \infty$, then it lies in the v > 0 plane before bending and moving in the v < 0 half plane.

Possible phase diagrams for $N_f = N_c$ and $N_f > N_c$ are shown in the central and right panels of Fig. 20, respectively. The behavior is qualitatively similar to that observed for $N_c = 2$. The only difference is the absence of an enlarged symmetry for v = 0, so that the v = 0 axis does not play any particular role at finite β . Therefore, the intersection point of the transition lines should be located in a generic point. Analogously, the first-order transition line that separates the two low-temperature Higgs phases will be a generic line in the $\beta - v$ plane for each value of γ . Concerning the nature of transition lines, we may apply considerations similar to those reported in Sec. 9.2.2 for $N_c = 2$, so we do not repeat them. See Ref. [99] for a more detailed description.

9.3. Critical behaviors associated with the charged fixed point of the SU(N_c) gauge Higgs field theory

An important issue is the relation between the statistical lattice gauge model (102) and the corresponding NAHFT (88), which is the field theory with the same field content and the same local and global symmetries. In particular, one would like to identify the continuous transitions that can be described by the stable charged FP of the RG flow of the continuum $SU(N_c)$ gauge Higgs field theory, see Sec. 8.1.3. The analogous problem for charged transitions in AH models has been discussed in Secs. 5 and 6.

As we have discussed in Sec. 8.1.3, the RG flow of the NAHFT (88) has a stable charged FP in the domain v > 0—therefore, the symmetry-breaking pattern is given in Eq. (93)—for $N_f > N_f^*(d)$. The presence of a stable FP indicates that lattice models can undergo charged continuous transitions for sufficiently large values of N_f . Phase transitions with symmetry-breaking pattern $U(N_f) \to SU(N_c) \otimes U(N_f - N_c)$ are expected to occur along the surface separating the disordered phase from the positive-v Higgs phase (see the right panel of Fig. 19). Moreover, since charged continuous transitions are characterized by the presence of critical gauge fluctuations, they are expected to occur for sufficiently large values of γ (they are not expected for small values of γ , given that for $\gamma = 0$ gauge fields can be integrated out).

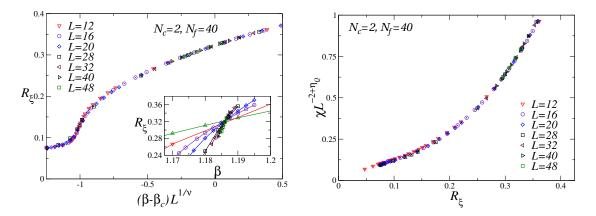


Figure 21: FSS behavior of the 3D SU(2) gauge LNAH model along the disorder-Higgs transition line. Results for $N_f=40$, v=1, and $\gamma=1$, varying the inverse temperature β . The left panel shows data for ξ_P/L , where ξ_P is the second-moment correlation length computed from the correlation function G_P defined in Eq. (108), versus $X=(\beta-\beta_c)L^{1/\nu}$, using the best estimates $\beta_c=1.18625$ and $\nu=0.745$. The excellent collapse of the data confirms that the transition is continuous. The inset shows the same data versus β . The right panel shows the rescaled susceptibility χ_P associated with G_P , which asymptotically behaves as $\chi_P\approx L^{2-\eta_P}\chi_P(\xi_P/L)$, see Eq. (A.24), with $\eta_P=0.87(1)$.

Refs. [99, 402] report a numerical study of the SU(2) gauge model ($N_c=2$) aiming at identifying possible charged transitions for large values of N_f . Continuous transitions are observed for $N_f=30,40$, and 60, keeping v=1 and $\gamma=1$ fixed and varying β . Some numerical FSS results are shown in Fig. 21 for $N_f=40$; they clearly show that the transition is continuous. We also mention that the universal FSS associated with the charged critical behavior for $N_f=40$ and $\gamma=1$, shown in Fig. 21, differs from that observed for the same value of N_f ($N_f=40$) in the limit $\gamma\to\infty$ [99], confirming that gauge fluctuations are relevant along the large- γ charged transition line.

To confirm that these large- N_f transitions have a critical behavior associated with the stable charged FP of the NAHFT, one may compare the numerical estimates of the correlation-length exponent ν with the field-theoretical $1/N_f$ result reported in Eq. (96). Such a comparison is reported in Fig. 22, which shows that numerical data and large- N_f field-theoretical predictions are in nice agreement. In particular, the estimate $\nu=0.745(10)$ for $N_f=40$ appears in reasonable agreement (the small difference can be interpreted as a $1/N_f^2$ correction, see Ref. [402]) with the value $\nu\approx0.757$ obtained from the $O(N_f^{-1})$ formula reported in Eq. (96). The results of Refs. [99, 402] allow one to estimate N_f^* in three dimensions for $N_c=2$. Since only first-order transitions are observed for $N_f=20$ for different values of v and v, and continuous transitions are found for $N_f=30$, one may conclude that $N_f^*=25(4)$ [402]. Note that this value is significantly smaller than $N_f^*\approx375$, the result in four dimensions. This difference is not surprising, since a similar difference was observed for the AHFT, see Sec. 4.1.2.

The agreement between the NAHFT results and the lattice numerical estimates nicely supports the conjecture that the continuous transitions observed in the lattice model can be associated with the stable charged FP of the RG flow of the SU(2) gauge NAHFT formally defined by the Lagrangian (88) and its corresponding functional path integral. We expect that analogous results hold for $N_c \geq 3$, although larger values of N_f are likely required to observe charged continuous transitions. We finally remark that the existence of these 3D charged universality classes implies the existence of a well-defined nonperturbative continuum limit of the SU(N_c) gauge NAHFTs, for a sufficiently large number of scalar components.

9.4. Lattice $SU(N_c)$ gauge Higgs models with scalar fields in the adjoint representation

We now consider $SU(N_c)$ gauge LNAH models with scalar fields transforming in the adjoint representation of the gauge group. We discuss their phase diagram and the nature of their Higgs phases, which qualitatively differ from what is observed in models in which the scalar fields transform in the fundamental representation.

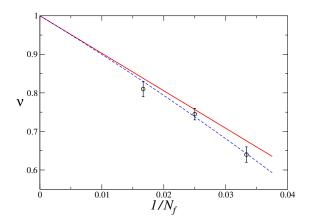


Figure 22: (Adapted from Ref. [402]) Numerical estimates of the critical exponent ν versus $1/N_f$ for the SU(2) gauge LNAH model (102). For comparison we also report the $O(1/N_f)$ theoretical prediction, Eq. (96) (solid line) and a next-to-leading interpolation including a $1/N_f^2$ term, i.e. $\nu=1+a_1/N_f+a_2/N_f^2$ (dashed line), with $a_2\approx -30$.

9.4.1. Lattice Hamiltonian

To construct representatives of this class of models, we may consider lattice gauge models defined on cubic lattices that are invariant under local $SU(N_c)$ and global $O(N_f)$ transformations, with scalar fields that transform under the adjoint representation of $SU(N_c)$ and under the fundamental representation of the $O(N_f)$ group.

The fundamental variables are real matrices Φ_x^{af} , with $a=1,...,N_c^2-1$ (color index) and $f=1,...,N_f$ (flavor index), defined on the lattice sites, and gauge fields $U_{x,\mu} \in \mathrm{SU}(N_c)$ associated with the lattice links [100]. The Hamiltonian and the corresponding partition function are [98, 263, 385, 391–394]

$$H = H_K(\Phi, U) + H_V(\Phi) + H_G(U), \qquad Z = \sum_{\{\Phi, U\}} e^{-\beta H},$$
 (110)

where the lattice Hamiltonian H is the sum of the scalar kinetic term H_K , of the local scalar potential H_V , and of the pure-gauge Hamiltonian H_G . As usual, we set the lattice spacing equal to one, so all lengths are measured in units of the lattice spacing. The scalar kinetic term H_K is given by

$$H_K(\Phi, U) = -\frac{1}{2} J N_f \sum_{\boldsymbol{x}, \mu} \operatorname{Tr} \Phi_{\boldsymbol{x}}^t \widetilde{U}_{\boldsymbol{x}, \mu} \Phi_{\boldsymbol{x} + \hat{\mu}}, \tag{111}$$

where the matrix $\widetilde{U}_{\boldsymbol{x},\mu}^{ab}$ is the adjoint representation of the original link variable $U_{\boldsymbol{x},\mu}$. The matrix $\widetilde{U}_{\boldsymbol{x},\mu}^{ab}$ is explicitly given by $\widetilde{U}_{\boldsymbol{x},\mu}^{ab} = 2 \operatorname{Tr}(U_{\boldsymbol{x},\mu}^{\dagger} T^a U_{\boldsymbol{x},\mu} T^b)$, where $a,b=1,...,N_c^2-1$, and T^a are the N_c^2-1 generators in the fundamental representation, with normalization $\operatorname{Tr} T^a T^b = \frac{1}{2} \delta^{ab}$. In the following we fix J=1, so that energies are measured in units of J. The scalar potential term H_V is written as

$$H_V(\Phi) = \sum_{\mathbf{x}} V(\Phi_{\mathbf{x}}), \qquad V(\Phi) = \frac{r}{2} \operatorname{Tr} \Phi^t \Phi + \frac{u}{4} \left(\operatorname{Tr} \Phi^t \Phi \right)^2 + \frac{v}{4} \operatorname{Tr} (\Phi^t \Phi)^2, \tag{112}$$

which is the most general quartic potential invariant under $O(N_f) \otimes O(N_c^2 - 1)$ transformations. For v = 0, the symmetry group of $H_V(\Phi)$ is larger, namely, the O(M) group with $M = N_f(N_c^2 - 1)$. Finally, the pure-gauge plaquette term reads

$$H_G(U) = -\frac{\gamma}{N_c} \sum_{\boldsymbol{x}, \mu > \nu} \operatorname{Re} \operatorname{Tr} \Pi_{\boldsymbol{x}, \mu \nu}, \qquad \Pi_{\boldsymbol{x}, \mu \nu} = U_{\boldsymbol{x}, \mu} U_{\boldsymbol{x} + \hat{\mu}, \nu} U_{\boldsymbol{x} + \hat{\nu}, \mu}^{\dagger} U_{\boldsymbol{x}, \nu}^{\dagger}, \tag{113}$$

where the parameter γ plays the role of inverse gauge coupling.

The model is invariant under global $O(N_f)$ transformations, $\Phi_{\boldsymbol{x}}^{af} \to \sum_g O^{fg} \Phi_{\boldsymbol{x}}^{ag}$, and under local $SU(N_c)$ transformations

$$U_{x,\mu} \to V_x U_{x,\mu} V_{x+\hat{\mu}}^{\dagger}, \qquad \Phi_x^{af} \to \sum_b \widetilde{V}_x^{ab} \Phi_x^{bf},$$
 (114)

where $V_{\boldsymbol{x}}$ is a $\mathrm{SU}(N_c)$ matrix and $\widetilde{V}_{\boldsymbol{x}}$ is the corresponding matrix in the adjoint representation. The Hamiltonian is also invariant under the transformations $U_{\boldsymbol{x},\mu} \to z(x_\mu)U_{\boldsymbol{x},\mu}$, where $z(x_\mu)$ is an element of the gauge-group center \mathbb{Z}_{N_c} that depends only on x_μ (the μ -th component of the position vector). When this symmetry is not spontaneously broken, Wilson loops obey the area law and color charges transforming in the fundamental representation are confined.

One may again consider a simplified model, requiring the scalar fields to obey the fixed length constraint $\operatorname{Tr} \Phi_{\boldsymbol{x}}^t \Phi_{\boldsymbol{x}} = 2$. Formally, this model can be obtained by taking the limit $u, r \to \infty$ keeping the ratio r/u = -2 fixed. The corresponding lattice Hamiltonian reads

$$H = -\frac{N_f}{2} \sum_{\boldsymbol{x},\mu} \operatorname{Tr} \Phi_{\boldsymbol{x}}^t \widetilde{U}_{\boldsymbol{x},\mu} \Phi_{\boldsymbol{x}+\hat{\mu}} + \frac{v}{4} \sum_{\boldsymbol{x}} \operatorname{Tr} (\Phi_{\boldsymbol{x}}^t \Phi_{\boldsymbol{x}})^2 - \frac{\gamma}{N_c} \sum_{\boldsymbol{x},\mu>\nu} \operatorname{Re} \operatorname{Tr} \Pi_{\boldsymbol{x},\mu\nu}, \qquad \operatorname{Tr} \Phi_{\boldsymbol{x}}^t \Phi_{\boldsymbol{x}} = 2.$$
 (115)

Models with generic values of r and u are expected to have the same qualitative behavior as this simplified model.

The critical properties of the scalar fields can be monitored by using the correlation function G_P of the gauge-invariant bilinear operator

$$P_{\boldsymbol{x}}^{fg} = \frac{1}{2} \sum_{a} \Phi_{\boldsymbol{x}}^{af} \Phi_{\boldsymbol{x}}^{ag} - \frac{1}{N_f} \delta^{fg}, \qquad G_P(\boldsymbol{x}, \boldsymbol{y}) \equiv \langle \operatorname{Tr} P_{\boldsymbol{x}} P_{\boldsymbol{y}} \rangle, \tag{116}$$

which satisfies $\operatorname{Tr} P_x = 0$ due to the fixed-length constraint. The bilinear scalar operator P_x provides the natural order parameter for the breaking of the global $O(N_f)$ symmetry.

9.4.2. Higgs phases and phase transitions

 $\mathrm{SU}(N_c)$ gauge models with a single $(N_f=1)$ adjoint scalar field have been the subject of several studies, see, e.g., Refs. [385, 415, 416], since they are the lattice analogues of the Georgi-Glashow model, in which magnetic monopoles are responsible for confinement [260, 381, 395, 396]. The single-flavor adjoint model has also been considered to describe some features of electron-doped cuprates [96]. Its phase diagram is trivial, as it presents a single thermodynamic phase, with two continuously connected regimes, a high-temperature disordered regime and a low-temperature Higgs-like regime [96, 415]. Indeed, the existence of a distinct low-temperature Higgs phase requires the breaking of a global symmetry, which is only possible for $N_f \geq 2$. In the following we mostly focus on the multiflavor models, which present a complex phase diagram, with several different phases and transition lines.

For $N_f \geq 2$ the lattice models show different Higgs phases associated with different symmetry-breaking patterns. The symmetries of the Higgs phases can be inferred by means of a mean-field analysis [96, 98, 263]—critical fluctuations are only relevant along the transition lines. The symmetries of the Higgs phases are indeed the symmetries of the minima of the local scalar potential $V(\Phi) = \frac{v}{4} \operatorname{Tr} (\Phi^t \Phi)^2$ in the fixed-length limit $\operatorname{Tr} \Phi^t \Phi = 2$. In the following we summarize the main properties of these phases, which depend on the number of colors N_c , of flavors N_f , and on the parameter v [96, 98, 263]. Moreover, their nature also depends on the behavior of the gauge modes, which may undergo topological transitions due to the fluctuations of variables associated with the gauge-group center \mathbb{Z}_{N_c} . Numerical studies for $N_c = 2$ and $N_c = 3$ have been reported in Refs. [98, 263, 417].

Two qualitatively different phase diagrams are found, depending on the number of colors N_c and of flavors N_f . For $N_f \leq N_c^2 - 1$, independently of the specific value of N_c , there is a single Higgs phase that lies in the half-space v < 0 for large values of β . Indeed, the mean-field analysis shows that for $\beta \to \infty$ the model orders only for v < 0. For v > 0, the system is disordered for $\beta \to \infty$.

For any N_f and N_c satisfying $N_f > N_c^2 - 1$, instead, there are two different low-temperature Higgs phases [96, 98, 263]. For $\beta \to \infty$, they correspond to the minima of the lattice potential for v < 0 and

v>0, respectively, and thus we again refer to these two phases as the negative-v and positive-v phases, respectively, although, this characterization does not hold for finite β . The two Higgs phases have different global symmetries and also different residual gauge symmetries, as defined in Sec. 3.5.3. Some details can be found in Refs. [96, 98], and in Sec. 9.4.3 for the specific case $N_c=2$ and $N_f=4$. In particular, the positive-v Higgs phase has a residual \mathbb{Z}_{N_c} gauge symmetry, so topological \mathbb{Z}_{N_c} gauge transitions can occur when varying the inverse gauge coupling γ , as discussed in Sec. 3.5.3.

The possible existence of topological transitions associated with the gauge-group center \mathbb{Z}_{N_c} can also be inferred by looking at the behavior of the model in the limit $\beta \to \infty$ keeping $\kappa \equiv \beta \gamma$ fixed, see Ref. [98] for details. For v>0 the relevant configurations, i.e., those that minimize the scalar potential and the scalar kinetic energy H_K , are characterized by $\tilde{U}_{x,\mu}=1$, so $U_{x,\mu}=\lambda_{x,\mu}\in\mathbb{Z}_{N_c}$. Therefore, in this limit the model (115) reduces to the lattice \mathbb{Z}_Q gauge theory with $Q=N_c$ discussed in Sec. 3.5.2. In three dimensions, this lattice discrete gauge model undergoes a transition at a finite value of the gauge coupling K. For example, the lattice \mathbb{Z}_2 gauge theory [119] presents a small-K confined phase and a large-K deconfined phase (which may carry topological order at the quantum level [20]), separated by a critical point at $K_c=0.761413292(11)$ [86, 323]. If the \mathbb{Z}_{N_c} gauge transition persists for finite values of β , then, when varying γ or κ , one may have different low-temperature Higgs phases, which have the same global symmetry but differ in the large-scale behavior of the \mathbb{Z}_{N_c} modes.

These arguments indicate that there are two different positive-v Higgs phases, which differ for the behavior of the topological modes associated with the gauge-group center \mathbb{Z}_{N_c} [96, 263]. Some numerical evidence of the existence of topological \mathbb{Z}_2 transitions in the SU(2) gauge LNAH models with four adjoint scalar fields is presented in Ref. [98].

9.4.3. The adjoint SU(2) gauge Higgs model with four flavors

Let us now focus on the model with $N_c=2$ and $N_f=4$, which is expected to describe some aspects of the optimal doping criticality in cuprate high- T_c superconductors [96]. Since $N_f>N_c^2-1$, there are several Higgs phases characterized by different global and gauge symmetry-breaking patterns. For finite β the two Higgs phases are divided by a transition line that ends at v=0, $\beta=\infty$, which is expected to be generically of first order, as it is the boundary of two different ordered phases.

In the negative-v region, the global symmetry-breaking pattern is $O(4) \rightarrow O(3) \oplus \mathbb{Z}_2$ and the gauge symmetry-breaking pattern is $SU(2) \rightarrow U(1)$. Since the remnant gauge-invariance group of the Higgs phase is U(1), and the three dimensional U(1) lattice gauge theory does not undergo phase transitions [260, 418], ⁵⁰ no topological transition is expected, so the gauge coupling should be irrelevant. Therefore, this suggests that there is a single negative-v Higgs phase, irrespective of the value of γ (of course we cannot exclude the existence of first-order transitions due to the greater complexity of the adjoint LNAH model). The transition line separating the negative-v Higgs phase from the disordered phase is expected to have the same nature as the transition in the 3D RP³ model (for v < 0 one can establish a correspondence between the behavior of the $SU(N_c)$ gauge model and the 3D RP^{N_f-1} model [419]), which undergoes a first-order transition, see Sec. 3.2.2.

The structure of the positive-v Higgs phase is more interesting. The global symmetry-breaking pattern of the positive-v Higgs phase is $O(4) \rightarrow O(3)$. Thus, uncharged continuous transitions between the positive-v Higgs phase and the disordered phase are expected to belong to the O(4) vector universality class, provided that gauge modes are irrelevant. The gauge symmetry-breaking pattern along the disorder-Higgs transition line is $SU(2) \rightarrow \mathbb{Z}_2$, so the Higgs phase is invariant under the center of the gauge group, opening the possibility of \mathbb{Z}_2 topological transitions controlled by the gauge coupling γ , as discussed in Sec. 3.5.3.

In the left panel of Fig. 23 we report a sketch of the phase diagram for $\gamma = 0$, based on the theoretical expectations just discussed and the numerical simulations reported in Ref. [98]. Note that the negative-v phase extends in the positive-v region for intermediate values of β . The transitions between the two low-temperature phases and between the negative-v and the disordered phase are of first order, as expected.

⁵⁰Confinement is present in the 3D U(1) gauge model also at weak coupling, see Refs. [260, 418], on the contrary of what happens in four-dimensional models, see Ref. [306].

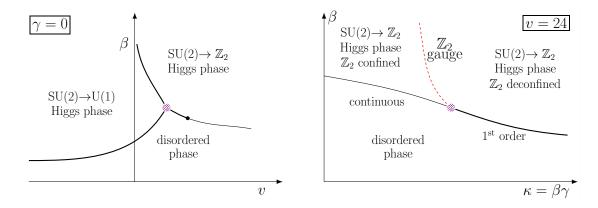


Figure 23: Sketches of the phase diagram of 3D SU(2) gauge LNAH models with four scalar fields in the adjoint representation [98], at fixed $\gamma=0$ (left) and at fixed v=24 (right). Thick lines denote first-order transitions, while thin lines correspond to continuous transitions. Left panel: the shaded point is a first-order intersection point; the filled black point that separates first-order from continuous transitions occurs at $v=v^*$ with $6< v^*<12$. Right panel: the \mathbb{Z}_2 -gauge transition line (dashed line) starts at $\kappa_c\approx 0.761$, $\beta=\infty$ and ends at a multicritical point (shaded point) at $\kappa=\kappa_{mc}$ with $1<\kappa_{mc}<2$. In each Higgs phase we also report the gauge-symmetry-breaking pattern associated with the transition that divides the Higgs phase from the disordered phase.

The nature of the transitions between the positive-v and the disordered phase depends instead on v, and for large values of v, they become apparently continuous.

For larger values of γ it is possible to have topological transitions in the positive-v region. Indeed, one may have two different positive-v Higgs phases, which differ for the behavior of the topological modes associated with the gauge-group center \mathbb{Z}_2 [96, 263]. Numerical evidence of the existence of such topological transitions in the Higgs phase has been reported in Ref. [98], looking at the scaling behavior of the energy cumulants, as described in Appendix A.3.2.

To monitor the role played by the gauge fluctuations for v>0, one may focus on the phase diagram for a specific positive value of v>0, as a function of $\kappa=\beta\gamma$ and β , see the right panel of Fig. 23, where a sketch of the phase diagram at fixed v=24 is shown. The nature of the transition changes significantly with increasing κ . While a continuous transition occurs for $\kappa \lesssim 1$, for $\kappa \geq 2$ transitions are of first order, their strength decreasing with increasing κ . A natural hypothesis is that this abrupt change is due to the different nature of the Higgs phase: Up to $\kappa \simeq 1$ the low-temperature phase is characterized by confined \mathbb{Z}_2 gauge excitations, while for $\kappa \geq 2$ the \mathbb{Z}_2 gauge modes are deconfined. This requires the existence of the \mathbb{Z}_2 gauge transition line.

To summarize, the phase diagram shown in the right panel of Fig. 23 appears to be characterized by three phases, a small- β disordered phase, and two large- β Higgs phases, which are distinguished by the behavior of gauge-group center modes. These phases are separated by three transition lines: (i) a disordered-Higgs transition line for small κ , which appears to be continuous; (ii) a disordered-Higgs transition line for large κ , which is of first order; (iii) a continuous \mathbb{Z}_2 gauge transition line, which separates the two low-temperature Higgs phases.

We also mention the numerical study of Ref. [417] on the confinement/deconfinement properties of the different Higgs phases, looking at the behavior of the Polyakov loops. The disordered symmetric phase is confining, so Wilson loops obey the area law, due to the fact that the adjoint scalar field cannot screen the gauge fluctuations. On the other hand, in the Higgs phase, in which the topological \mathbb{Z}_2 gauge excitations deconfine, Polyakov loops take a nonvanishing value.

As a final remark, we note that the identification of continuous transitions associated with the stable charged FP of the RG flow of the adjoint NAHFT, see Sec.8.3, remains an open issue. We believe that further numerical investigations of the phase diagram and of the critical behaviors of $SU(N_c)$ gauge LNAH models with adjoint scalar fields is needed to achieve a satisfactory characterization of their main features.

9.5. Lattice $SO(N_c)$ gauge models with multiflavor scalar fields

A lattice $SO(N_c)$ gauge model with N_f degenerate scalar fields in the fundamental representation can be derived by gauging the most general $O(N_c)\otimes O(N_f)$ -symmetric φ^4 model defined on a cubic lattice. We associate $N_c\times N_f$ real matrix variables $\varphi^{af}_{\boldsymbol{x}}$ with each site \boldsymbol{x} and $SO(N_c)$ group elements $O_{\boldsymbol{x},\mu}$ with each link. The lattice Hamiltonian [384] is

$$H = -J N_f \sum_{\boldsymbol{x},\mu} \operatorname{Tr} \left[\varphi_{\boldsymbol{x}}^t O_{\boldsymbol{x},\mu} \varphi_{\boldsymbol{x}+\hat{\mu}} \right] + \sum_{\boldsymbol{x}} V(\varphi_{\boldsymbol{x}}) - \frac{\gamma}{N_c} \sum_{\boldsymbol{x},\mu>\nu} \operatorname{Tr} \left[O_{\boldsymbol{x},\mu} O_{\boldsymbol{x}+\hat{\mu},\nu} O_{\boldsymbol{x}+\hat{\nu},\mu}^t O_{\boldsymbol{x},\nu}^t \right], \quad (117)$$

$$V(\varphi_{\boldsymbol{x}}) = r \operatorname{Tr} \varphi_{\boldsymbol{x}}^t \varphi_{\boldsymbol{x}} + u \left(\operatorname{Tr} \varphi_{\boldsymbol{x}}^t \varphi_{\boldsymbol{x}} \right)^2 + v \left[\operatorname{Tr} \varphi_{\boldsymbol{x}}^t \varphi_{\boldsymbol{x}} \varphi_{\boldsymbol{x}}^t \varphi_{\boldsymbol{x}} - \left(\operatorname{Tr} \varphi_{\boldsymbol{x}}^t \varphi_{\boldsymbol{x}} \right)^2 \right].$$
(118)

For any value of N_c and N_f , the lattice gauge theory is invariant under the local gauge transformation $\varphi_{\boldsymbol{x}} \to G_{\boldsymbol{x}} \varphi_{\boldsymbol{x}}$ and $O_{\boldsymbol{x},\mu} \to G_{\boldsymbol{x}} O_{\boldsymbol{x},\mu} G_{\boldsymbol{x}+\hat{\mu}}^t$ with $G_{\boldsymbol{x}} \in \mathrm{SO}(N_c)$, and under the global transformation $\varphi_{\boldsymbol{x}} \to \varphi_{\boldsymbol{x}} W$ and $O_{\boldsymbol{x},\mu} \to O_{\boldsymbol{x},\mu}$ with $W \in \mathrm{O}(N_f)$.

One may again consider the unit-length limit of the scalar field, formally obtained by taking the limit $r, u \to \infty$ keeping r/u = -1 fixed, leading to the constraint $\operatorname{Tr} \varphi_x^t \varphi_x = 1$. In the one-flavor case, $N_f = 1$, the phase diagram of the lattice $\operatorname{SO}(N_c)$ gauge model (117) is expected to show only one phase. This can be easily verified for $\gamma = 0$, where the model becomes trivial in the unitary gauge, and cannot have any phase transition. For $N_c = 2$ the gauge group is equivalent to the Abelian group U(1), and the model is equivalent to LAHMs with compact gauge variables discussed in Sec. 6. New critical behaviors are expected only in the non-Abelian case, $N_c \geq 3$. The natural order parameter for the breaking of the $\operatorname{SO}(N_f)$ global symmetry is the gauge-invariant real traceless and symmetric bilinear operator

$$R_{\boldsymbol{x}}^{fg} = \sum_{a} \varphi_{\boldsymbol{x}}^{af} \varphi_{\boldsymbol{x}}^{ag} - \frac{\delta^{fg}}{N_f}, \qquad (119)$$

which is a rank-2 operator with respect to the global $O(N_f)$ symmetry group.

The field-theoretical ε -expansion analysis of the RG flow of the NAHFT (97) predicts the existence of charged universality classes for a sufficiently large number N_f of components, controlled by the stable charged FP appearing for positive values of v. No stable FPs emerge for v < 0, at least close to four dimensions. Beside charged transitions statistical systems may also develop other critical behaviors described by appropriate LGW field theories, in which the gauge correlations are not critical, as is the case in the strong-coupling ($\gamma \to 0$) gauge limit.

An analysis of the phase diagram of the model with v=0 was reported in Ref. [384]. For $N_f \geq 2$ the phase diagram is characterized by two phases: a low-temperature phase in which the order parameter R_x^{fg} defined in Eq. (119) condenses, and a high-temperature disordered phase. The two phases are separated by a transition line, where the $SO(N_f)$ symmetry is broken. The gauge parameter γ , corresponding to the inverse gauge coupling, is not expected to play any particular role, at least for sufficiently small values. This scenario has been checked numerically for several values of γ . Along the disorder-order transition line only the correlations of the gauge-invariant operator R_x^{fg} are critical, while gauge modes are not critical. This is consistent with the predictions of the continuum gauge model (97): since stable FPs exist only for $N_f \gg 1$, one expects only uncharged transitions for small N_f . Since the gauge modes do not show critical behaviors, one may predict the critical behavior by using an effective $O(N_f)$ -invariant LGW theory based on a gauge-invariant order parameter associated with the rank-two symmetric real traceless tensor R_x^{ab} . This analysis is reported in Sec. 3.2.2. It predicts first-order transitions for $N_f \geq 3$ and continuous transitions for $N_f = 2$, which belong to the XY universality class for any $N_c \geq 3$.

Note that charged continuous transitions are possible for large values of N_f according to the RG flow of the SO(N_c) gauge NAHFT, see Sec. 8.2, because of the presence of a stable large- N_f charged FP [157, 278, 384]. As it occurs in SU(N_c) gauge LNAH models with scalar fields in the fundamental representation, continuous charged transitions are expected to appear for positive values of v, sufficiently large values of γ , and a sufficiently large number N_f of components.

10. Two-dimensional lattice Abelian and non-Abelian gauge Higgs models

In the previous sections we discussed 3D Abelian and non-Abelian Higgs models, to investigate the role of the gauge and global symmetries in determining their main thermodynamic properties, such as the Higgs phases, the nature of the phase transitions, and the continuum limits associated with their critical behaviors. Analogous issues can be addressed in lower-dimensional models.

In two dimensions the phase diagram of lattice models with short-range interactions (such as the nearest-neighbor models considered in the previous sections) and continuous global symmetries are generally characterized by a single disordered phase. Indeed, according to the Mermin-Wagner theorem [420, 421], they cannot have magnetized phases characterized by the condensation of an order parameter, and therefore they do not undergo phase transitions driven by the spontaneous breaking of a continuous global symmetry.

However, in the zero-temperature limit they can develop an asymptotic critical behavior, whose universal features are determined by the symmetries of the system and are generally associated with 2D nonlinear σ models defined on symmetric spaces, see, e.g., Refs. [2, 95, 422]. The O(N) σ model with $N \geq 3$ and the CP^{N-1} model with $N \geq 2$ are paradigmatic models that show this type of behavior. Indeed, the lattice O(N) model behaves as the nonlinear σ model defined on the O(N)/O(N-1) symmetric space, while the CP^{N-1} lattice model is related to the nonlinear σ model defined on the $U(N)/[U(1)\times U(N-1)]$ symmetric space, see, e.g., Ref. [2]. In this type of models, the correlation functions in the thermodynamic limit are characterized by a length scale ξ that diverges as $T^p e^{c/T}$ for $T \to 0$, where p and c are universal coefficients that only depend on the universality class and that can be determined in perturbation theory (the coefficient c also depends on the normalization of T, which can be uniquely fixed perturbatively), see Appendix A.5 for details.

Systems with an Abelian O(2) global symmetry are peculiar in this respect, since they may undergo a finite-temperature topological Berezinskii-Kosterlitz-Thouless (BKT) transition [423–425], which separates the high-T disordered phase from the low-temperature nonmagnetized spin-wave phase characterized by correlation functions that decay algebraically.

In this section we discuss how the interplay of global and gauge symmetries determine the effective lowenergy field theory realized in the zero-temperature continuum limit (critical behavior) of 2D lattice gauge models using the standard Wilson formulation of gauge variables [3, 100].

10.1. General conjecture for the zero-temperature continuum limit

In the case of models characterized by both global and gauge symmetries, the asymptotic zero-temperature critical behavior (equivalently, continuum limit) is expected to arise from the interplay between the two different symmetries. For the purpose of understanding which features are relevant and which continuum limits are effectively realized, several 2D lattice Abelian and non-Abelian gauge models have been investigated [223, 419, 426–430]. The results of these analyses have led to the following general conjecture:

The zero-temperature critical behavior, and therefore the continuum limit, of 2D lattice gauge models with scalar fields belongs to the universality class associated with a 2D theory defined on a symmetric space [2, 422] with the same global symmetry.

2D field-theoretical models defined on symmetric spaces have been largely investigated, see, e.g., Ref. [2], and several high-order perturbative computations, in particular of their β functions, have been reported in the literature [2, 95, 278, 285, 422, 431–446]. The O(N) σ and the CP^{N-1} models are the simplest examples. Other examples of lattice gauge models with critical behavior corresponding to a symmetric-space field theory will be discussed in the following of this section.

10.2. Continuum limits of multiflavor lattice gauge theories

We now summarize the main results obtained for several 2D multiflavor lattice Abelian and non-Abelian gauge models [419, 426–430]. They support the conjecture on the nature of their continuum limit presented in Sec. 10.1. The analysis of the zero-temperature behavior requires the determination of the relevant low-energy degrees of freedom, which correspond to the minimum configurations of the Hamiltonian, and of

the residual global symmetry, which essentially determines the appropriate corresponding field-theoretical σ model. These analyses are then supplemented by MC nonperturbative studies based on FSS analyses of the numerical data.

10.2.1. Lattice U(1) gauge models

We first consider 2D lattice multiflavor Abelian U(1) gauge models with compact gauge variables and N-component scalar fields. On a square lattice the Hamiltonian reads

$$H = -N \sum_{\boldsymbol{x},\mu} \left(\bar{\boldsymbol{z}}_{\boldsymbol{x}} \cdot \lambda_{\boldsymbol{x},\mu} \, \boldsymbol{z}_{\boldsymbol{x}+\hat{\mu}} + \text{c.c.} \right) - \gamma \sum_{\boldsymbol{x},\mu>\nu} \left(\lambda_{\boldsymbol{x},\mu} \, \lambda_{\boldsymbol{x}+\hat{\mu},\nu} \, \bar{\lambda}_{\boldsymbol{x}+\hat{\nu},\mu} \, \bar{\lambda}_{\boldsymbol{x},\nu} + \text{c.c.} \right), \tag{120}$$

where z_x is a unit-length N-component complex vector, $\lambda_{x,\mu}$ are U(1) link variables, γ plays the role of inverse gauge coupling, and $\hat{\mu} = \hat{1}, \hat{2}$ are unit vectors along the lattice directions. As usual, the partition function is defined as $Z = \sum_{\{z,\lambda\}} e^{-\beta H}$ with $\beta = 1/T$.

For some particular values of γ the model (120) becomes equivalent to simpler well-known models. In the limit $\gamma \to \infty$, the gauge link variables are all equal to one modulo gauge transformations, so model (120) becomes equivalent to the standard 2D O(2N)-symmetric vector model, whose properties are reviewed in Appendix A.5. For $\gamma=0$ the AH model (120) is a particular lattice formulation of the CP^{N-1} model [2, 206–208, 441, 442].⁵¹ For both $\gamma=0$ and $\gamma=\infty$, the lattice model shows a universal critical behavior for $\beta\to\infty$. In this limit, the correlation length ξ increases exponentially, $\xi\sim\beta^{-p}e^{c\beta}$. Of course, the critical behaviors for $\gamma=0$ and $\gamma\to\infty$ differ, belonging to the universality class of the 2D CP^{N-1} σ model for $\gamma=0$ and to that of the 2D O(2N) σ model for $\gamma\to\infty$.

As in the 3D LAH models discussed in Sec. 6, the zero-temperature critical behavior can be investigated by analyzing the correlations of the gauge-invariant bilinear $Q_x^{ab} = \bar{z}_x^a z_x^b - \delta^{ab}/N$. The FSS analyses of the MC results reported in Ref. [426] show that the asymptotic behavior is independent of γ , and corresponds to that found for $\gamma=0$. Therefore, the zero-temperature critical behavior of the 2D lattice U(1) model with an N-component complex scalar field belongs to the universality class of the 2D CP^{N-1} model, thus corresponding to the symmetric space U(N)/[U(1)×U(N-1)]. The independence of the critical behavior on γ is related to the subleading behavior of the gauge modes.

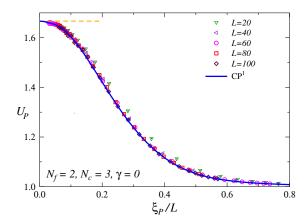
10.2.2. Lattice $SU(N_c)$ gauge models

We now consider 2D non-Abelian $SU(N_c)$ models defined on square lattices, with multiflavor matter fields in the fundamental and adjoint representations, analogous to those defined in Secs. 9.1 and 9.4.1 in the unit-length limit, respectively.

The zero-temperature critical behavior of the $\mathrm{SU}(N_c)$ gauge model with N_f scalar fields in the fundamental representation was analyzed in Ref. [427] for the particular value v=0 of the Hamiltonian parameter, see Eq. (107). In this more symmetric case, the numerical results show that the asymptotic low-temperature behavior belongs to the universality class of the 2D CP^{N_f-1} field theory when $N_c \geq 3$, and to that of the 2D $\mathrm{Sp}(N_f)$ field theory for $N_c=2$. This suggests that their RG flows are associated with the coset $S^M/\mathrm{SU}(N_c)$, where S^M is the M-dimensional sphere and $M=2N_fN_c$, thus they are asymptotically controlled by the 2D SFTs associated with the symmetric spaces that have the same global symmetry, i.e., $\mathrm{U}(N_f)$ for $N_c \geq 3$ and $\mathrm{Sp}(N_f)$ for $N_c=2$.

 $SU(N_c)$ gauge models with N_f scalar fields in the adjoint representation were investigated in Ref. [419], focusing on systems with $N_f \geq 3$. For these models the zero-temperature critical behavior, and therefore their continuum limit, depends on the sign of the parameter v appearing in the scalar potential, see Eq. (112). For $v \leq 0$ the lattice gauge model has the same continuum limit as the RP^{N_f-1} model [217–221, 223], for any value of N_c . For positive v instead, the critical behavior depends on both N_c and N_f . For $N_f \leq N_c^2 - 1$, there

 $^{^{51}}$ 2D CP^{N-1} models have been much studied in the literature, both analytically and numerically, because they provide a theoretical laboratory to understand some of the mechanisms of quantum field theories of fundamental interactions. In particular, they share some notable features with QCD, the theory of the hadronic strong interactions, such as the asymptotic freedom and the so-called θ dependence related to topology, see, e.g., Refs. [435, 436, 440, 447–449].



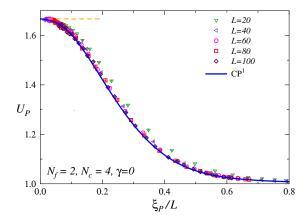


Figure 24: (Adapted from Ref. [427]) We show numerical results for the 2D SU(N_c) gauge LNAH models with $N_c=3$ (left) and $N_c=4$ (right); $N_f=2$ and $\gamma=0$ in both cases. We plot the Binder parameter U_P associated with the operator $P_{\bf x}^{fg}$, defined in Eq. (108), versus ξ_P/L , where ξ_P is the second-moment correlation length associated with the correlation function G_P , defined as in Eq. A.16. In both panels, with increasing L, data approach the solid line representing the universal scaling curve of the 2D CP¹ model (see Ref. [426] for a parameterization), associated with the symmetric space that has the same global symmetry, thus supporting the conjecture reported in Sec. 10.1. As discussed in Sec. Appendix A.3.4), this comparison does not involve any nonuniversal normalization.

is no continuum limit: correlation functions are always short ranged. On the other hand, for $N_f > N_c^2 - 1$ the system develops long-range correlations for $T \to 0$. The corresponding continuum limit is the same as that of the σ model defined on the symmetric space $\mathrm{O}(N_f)/\mathrm{O}(q) \otimes \mathrm{O}(N_f - q)$ with $q = N_c^2 - 1$. Indeed, the correlation functions of the bilinear operator P_x^{ab} in the two models have the same critical behavior in the zero-temperature continuum limit. In particular, for $N_f = N_c^2$, the gauge model is equivalent to the $\mathrm{O}(N_f)$ vector σ model. Numerical data support these predictions. Some of them are shown in Fig. 24. Again, these results support the conjecture outlined in Sec. 10.1.

10.2.3. Lattice $SO(N_c)$ gauge models

We finally consider 2D square-lattice models with non-Abelian $SO(N_c)$ gauge symmetry and $O(N_f)$ global symmetry, which are defined by the same Hamiltonian reported in Eq. (117) in the unit-length limit. Again for $N_c = 2$, these lattice gauge models are equivalent to the 2D Abelian U(1) gauge models discussed in Sec. 10.2.1. Therefore, here we assume $N_c \geq 3$. Analytical and numerical studies of their critical behavior are reported in Refs. [428–430].

For $N_f \geq 3$ the models show a zero-temperature critical behavior. By studying the minimum-energy configurations, which are the relevant ones in the zero-temperature limit, and the structure of their fluctuations, two different low-temperature regimes are identified. If the Hamiltonian parameter v is negative, see Eq. (118), then the model shares the same low-temperature critical behavior as that of the 2D RP^{N_f-1} models [217–221, 223]. Gauge degrees of freedom do not play any active role in the critical domain, and indeed the low-temperature effective theory is independent of the number of colors N_c . For positive values of v, the nature of the low-temperature regime depends on the number of colors and flavors. If $N_f \leq N_c$ the configurations minimizing the Hamiltonian do not show any residual global symmetry, and no diverging correlation length and critical behavior is present. If instead $N_f > N_c$, the minimizing configurations maintain a residual nontrivial global symmetry, and the low-temperature behavior is expected to be described by the non-linear σ model defined on the real Grassmannian manifold $SO(N_f)/[SO(N_c) \times SO(N_f - N_c)]$. This identification was also supported by numerical results reported in Refs. [428, 430] for several values of N_f and N_c . They show the emergence of a color-reflection symmetry in the critical domain, since the results obtained using $SO(N_c)$ and $SO(N_f - N_c)$ groups, keeping fixed N_f , approach the same asymptotic curve in the FSS limit [430].

We finally consider the model with $N_f = 2$, in which the global symmetry group is the Abelian O(2)

group. Two-flavor $SO(N_c)$ -gauge models behave differently, in that they undergo a finite-temperature topological BKT transition [423–425, 450–455], between the high-temperature disordered phase and a low-temperature spin-wave phase characterized by quasi-long range order with vanishing magnetization.⁵² The FSS analyses of the MC results reported in Ref. [429] confirm the existence of the finite-temperature BKT transitions.

11. Effects of perturbations breaking the local gauge symmetry

Gauge symmetries can emerge as low-energy effective symmetries of many-body systems [20, 21, 456, 457]. However, because of the presence of microscopic gauge-symmetry violations, it is crucial to understand the effects of perturbations that explicitly break gauge invariance. One would like to understand whether, and when, gauge-symmetry breaking (GSB) perturbations destabilize the emergent gauge model—consequently, a gauge-invariant dynamics would be observed only if an appropriate tuning of the model parameters is performed—, or whether, and when, GSB perturbations do not effectively change the low-energy dynamics—in this case the gauge-symmetric theory would describe the asymptotic dynamics even in the presence of some (possibly small) violations. This issue is also crucial in the context of analog quantum simulations, for example when controllable atomic systems are engineered to effectively reproduce the dynamics of gauge-symmetric theoretical models. Indeed, in the proposed artificial gauge-symmetry realizations [458–460], the gauge symmetry in not exact and it is only expected to effectively emerge in the low-energy dynamics, see, e.g., Refs [461–466] for some experimental results.

In this section we discuss GSB effects in LAH models with noncompact and compact gauge fields. The gauge symmetry can be broken by adding different nongauge invariant terms to the gauge-invariant LAH Hamiltonian. A first peculiar class of GSB terms is that of gauge fixings: they leave gauge-invariant correlations invariant, without changing the physical gauge-invariant behavior of the model, although they may allow one to observe gauge degrees of freedom that are relevant in the RG description of the critical behavior, see, e.g., Secs. 5 and 6. Here we discuss GSB perturbations that also affect gauge-invariant correlations. Specifically, we consider operators analogous to photon-mass terms, which break the gauge invariance of LAH models introduced in Secs. 5 and 6, respectively. However, we expect the main features of the results reviewed here to be valid also in the presence of more general GSB terms.

11.1. Gauge-symmetry breaking in lattice Abelian Higgs models with noncompact gauge fields

Let us consider the LAH model with noncompact gauge variables introduced in Sec. 5.1, in the presence of a GSB perturbation obtained by adding a photon-mass term

$$H_m = \frac{m^2}{2} \sum_{x,\mu} A_{x,\mu}^2 \tag{121}$$

to the Hamiltonian (47). To understand the phase diagram of the combined model as a function of the parameters J, κ , and m^2 , it is convenient to first discuss some specific subcases.

For $\kappa = 0$, the global Hamiltonian can be written as

$$H = -2NJ \sum_{\boldsymbol{x},\mu} \operatorname{Re} \left(e^{iA_{\boldsymbol{x},\mu}} \, \bar{\boldsymbol{z}}_{\boldsymbol{x}} \cdot \boldsymbol{z}_{\boldsymbol{x}+\hat{\mu}} \right) + \frac{m^2}{2} \sum_{\boldsymbol{x},\mu} A_{\boldsymbol{x},\mu}^2.$$
 (122)

For $m^2 \to \infty$, one has $A_{\boldsymbol{x},\mu} = 0$, so one obtains a simple scalar Hamiltonian with enlarged O(2N) symmetry. Indeed, if we set $z_{\boldsymbol{x}}^a = \sigma_{\boldsymbol{x}}^a + i\sigma_{\boldsymbol{x}}^{a+N}$, where $\sigma_{\boldsymbol{x}}^a$ is a real 2N-component vector, we obtain

$$H = -JN \sum_{x,\mu} \sigma_x \cdot \sigma_{x+\hat{\mu}}.$$
 (123)

⁵²We recall that BKT transitions are characterized by a finite critical temperature with an exponentially divergent correlation length ξ : ξ behaves as $\xi \sim \exp(c/\sqrt{T-T_c})$ approaching the BKT critical temperature T_c from the high-temperature phase.

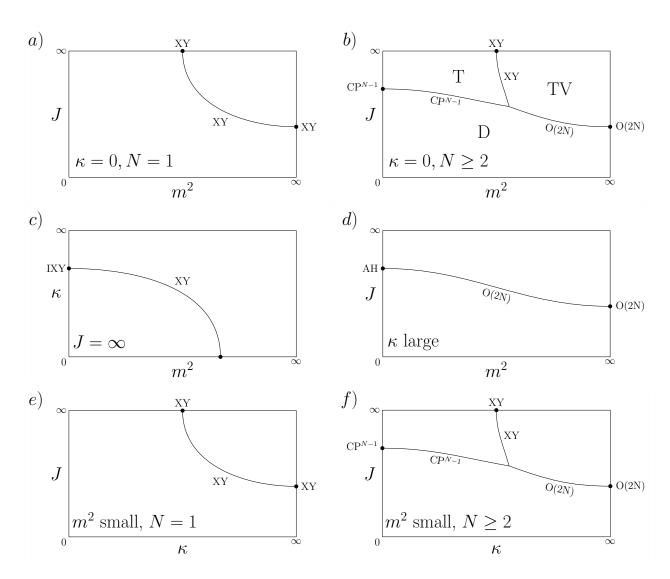


Figure 25: Sketch of the phase diagrams for the noncompact Higgs model with GSB perturbation (121). (Top panels) Phase diagram for $\kappa=0$ (it also holds for the compact model, with w replacing m^2): (a) N=1 and (b) $N\geq 2$; scalar correlations are disordered in the D phase, tensor correlations are ordered in the T and TV phase, while vector correlations are ordered only in the TV phase. (Central panels) Phase diagram (c) for $J=\infty$ as a function of κ and m^2 , and (d) for κ large as a function of J and J0. (Bottom panels) Phase diagrams for small J1. (e) J2. Along each transition line we report the expected corresponding universality class.

This is the 2N-vector model defined in Eq. (1) (rescaling the coupling J by a factor N), which undergoes a continuous transition at a finite value of J in the O(2N) universality class, see Sec. 2.2.1. Note that the presence of an enlarged symmetry at the transition is a general property of U(N) invariant scalar models, as discussed in Sec. 2.2.2.

For $\kappa = 0$ and $J \to \infty$, the gauge fields are constrained to be multiples of 2π modulo gauge transformations, see Sec. 5.2.2, i.e.,

$$A_{x,\mu} = 2\pi n_{x,\mu} + \nabla_{\mu} \phi_{x}, \tag{124}$$

where ϕ_x is a real scalar field and $n_{x,\mu}$ is an integer-valued link variable. The GSB Hamiltonian (121) becomes

$$H_m = \frac{m^2}{2} \sum_{x,\mu} (\nabla_{\mu} \phi_x + 2\pi n_{x,\mu})^2, \tag{125}$$

where ϕ_{x} and $n_{x,\mu}$ play the role of independent dynamic variables. This is the Villain formulation of the XY model, so there must be an XY transition at a finite value of m^{2} .

Taking into account the fact that for $\kappa = 0$ and $m^2 = 0$ the LAH model reduces itself to a lattice \mathbb{CP}^{N-1} model, see Sec. 3.2.1, and therefore there is a corresponding finite-temperature transition for $N \geq 2$, and no transition for N=1, one arrives at the phase diagrams reported in the two upper panels of Fig. 25. For N=1 [phase diagram (a)] there is a single transition line, while for $N\geq 2$ [phase diagram (b)], there are three different transition lines intersecting in a single point. For small values of m^2 the GSB perturbation is not strong enough to induce long-range order in the vector correlations of $\boldsymbol{z_x}$, while the gauge invariant spin-2 tensor operator in Eq. (60) is ordered, as for $m^2 = 0$. We expect the \mathbb{CP}^{N-1} behavior to extend along the D-T transition line, which starts at $m^2 = 0$, as shown in Ref. [467] for a general GSB perturbation of the compact model, and verified numerically in Ref. [276]. In particular, for N=2, continuous transitions should belong to the O(3) universality class. The irrelevance of the GSB perturbation for small m^2 is not unexpected, since gauge modes do not play any active role at the \mathbb{CP}^{N-1} transition. For large m^2 values, in the low-temperature phase also vector correlations become long ranged. A natural hypothesis is that the critical behavior observed along the T-TV and D-TV transition lines, for finite values of J and m^2 , is the same as that observed for $J \to \infty$ and $m^2 \to \infty$, respectively. Thus, continuous transitions should belong to the XY and O(2N) universality classes, respectively. The phase diagrams reported in the two upper panels of Fig. 25 are supposed to hold also for small values of κ . On the other hand, for large values of κ , we expect a different behavior.

Before discussing the large- κ behavior, let us consider the limit $J \to \infty$ for generic κ and m^2 . Since in this limit the gauge fields take the form (124), the effective Hamiltonian is equivalent to an IXY model (discussed in Sec. 3.5.1) coupled with the Villain XY model (125). In panel (c) of Fig. 25 we show the expected phase diagram, showing a transition line connecting the Villain XY model transition for $\kappa = 0$ with the transition of the IXY model on the $m^2 = 0$ axis. Continuous transitions should belong to the XY vector universality class for $m^2 \neq 0$. While there is an XY transition if m^2 is varied for fixed small κ , no transition occurs when κ is fixed to a large value. Thus, for large κ we expect a single transition line, see panel (d) of Fig. 25, connecting the $m^2 = 0$ transition to the O(2N) transition occurring for $m^2 \to \infty$. It is natural to expect that continuous transitions along the whole line belong to the O(2N) universality class for $m^2 > 0$. In particular, the charged transitions that occur for $m^2 = 0$ and $N > N^*$ should be unstable with respect to the addition of the GSB term.

We finally consider the expected phase diagrams for fixed small values of m^2 , see panels (e) and (f) of Fig. 25. They are qualitatively similar to the phase diagrams occurring for $m^2 = 0$, see Fig. 2. However, the nature of the phases, and therefore of the transitions, is different. The Coulomb phase is replaced by a disordered phase, in which both scalar and gauge modes are gapped, while in the low-temperature phase both scalar and gauge fields are ordered. Note that, in the latter phase, because of the absence of gauge invariance, both the gauge-invariant tensor correlations and the non-gauge-invariant vector correlations are long ranged for $N \geq 2$. In the molecular phase (which is present only for $N \geq 2$), the addition of the GSB term changes the nature of the gauge excitations—the Coulomb phase is replaced by a gapped gauge-field phase—but not that of the scalar modes: tensor correlations display long range order and vector correlations are disordered, as in the gauge-invariant model. As for the transition lines, the small- κ transition line (which

is only present for $N \ge 2$) corresponds to \mathbb{CP}^{N-1} transitions as for $m^2 = 0$: the GSB term is an irrelevant perturbation. On the other hand, the nature of the other two transitions changes. The topological IXY transitions are now replaced by standard XY vector transitions, while the continuous charged transitions that occur for large values of N become $\mathbb{O}(2N)$ vector transitions.

11.2. Gauge-symmetry breaking in lattice Abelian Higgs models with compact gauge fields

The effect of adding a GSB perturbation to the unit-charge (Q = 1) LAH model with compact gauge variables, see Sec. 6.1, is discussed in Refs. [276, 467]. We consider a GSB term that is analogous to the photon-mass term in the small gauge limit, i.e.,

$$H_m = -w \sum_{\boldsymbol{x},\mu} \operatorname{Re} \, \lambda_{\boldsymbol{x},\mu}. \tag{126}$$

Since for Q=1 the plaquette term proportional to κ , cf. Eq. (67), is irrelevant—the critical behavior is the same for any finite κ , see Sec. 6.3.1—it is enough to discuss the behavior for $\kappa=0$, considering the simplified lattice model with Hamiltonian

$$H = -2NJ \sum_{\boldsymbol{x},\mu} \operatorname{Re} \left(\lambda_{\boldsymbol{x},\mu} \, \bar{\boldsymbol{z}}_{\boldsymbol{x}} \cdot \boldsymbol{z}_{\boldsymbol{x}+\hat{\mu}} \right) - w \sum_{\boldsymbol{x},\mu} \operatorname{Re} \, \lambda_{\boldsymbol{x},\mu}. \tag{127}$$

The behavior of this combined model is analogous to the one presented in the noncompact case. Indeed, for $w \to \infty$, we can set $\lambda_{x\mu} = 1$, and thus we obtain again the O(2N) vector model (123). On the other hand, for $J \to \infty$, $\lambda_{x,\mu} = 1$ modulo gauge transformations, i.e., $\lambda_{x,\mu} = e^{i(\phi_x - \phi_{x+\hat{\mu}})}$. Substituting this expression in the GSB term (126), we obtain the effective Hamiltonian

$$H_m = -w \sum_{\boldsymbol{x},\mu} \cos(\phi_{\boldsymbol{x}} - \phi_{\boldsymbol{x}+\hat{\mu}}), \tag{128}$$

which is the standard XY Hamiltonian. Thus, also in this case we obtain the phase diagrams reported in the upper panels of Fig. 25, with m^2 replaced by w.

We now present an argument—it rephrases a similar argument of Ref. [41]—that shows that the phase behavior discussed above generally holds for generic GSB perturbations at transitions where gauge fields are not critical. Indeed, let us consider the partition function of a generic model with a GSB perturbation that only depends on the gauge fields:

$$Z = \int [dU_{\boldsymbol{x},\mu}] [d\Phi_{\boldsymbol{x}}] \exp[-\beta H(U_{\boldsymbol{x},\mu},\Phi_{\boldsymbol{x}})], \qquad H(U_{\boldsymbol{x},\mu},\Phi_{\boldsymbol{x}}) = H_{GI}(U_{\boldsymbol{x},\mu},\Phi_{\boldsymbol{x}}) + H_{GSB}(U_{\boldsymbol{x},\mu}), \qquad (129)$$

where $H_{\rm GI}$ is the gauge-invariant Hamiltonian, and $H_{\rm GSB}$ is a generic Hamiltonian term breaking the gauge symmetry, depending only on the link gauge variables $U_{x,\mu}$. We now perform a change of variables on the scalar and gauge fields that corresponds to a gauge transformation—thus Z, or any expectation value of gauge-invariant operators, does not change. In particular, we redefine $U_{x,\mu} \to V_x U_{x,\mu} V_{x+\mu}^{\dagger}$. As $H_{\rm GI}$ is gauge invariant, the partition function becomes

$$Z = \int [dU_{\boldsymbol{x},\mu}][d\Phi_{\boldsymbol{x}}] \exp\left[-\beta H_{\text{GI}}(U_{\boldsymbol{x},\mu},\Phi_{\boldsymbol{x}}) - \beta H_{\text{GSB}}(V_{\boldsymbol{x}}U_{\boldsymbol{x},\mu}V_{\boldsymbol{x}+\mu}^{\dagger})\right]. \tag{130}$$

The partition function does not depend on the set of variables V_x and thus we can integrate over them without changing the partition function. We define a new Hamiltonian \hat{H} so that

$$\widehat{H} = H_{\text{GI}} + \widehat{H}_{\text{GSB}}, \qquad \widehat{H}_{\text{GSB}}(U_{\boldsymbol{x},\mu}) = -\ln \int [dV_{\boldsymbol{x}}] \exp[-\beta H_{\text{GSB}}(V_{\boldsymbol{x}}U_{\boldsymbol{x},\mu}V_{\boldsymbol{x}+\mu}^{\dagger})]. \tag{131}$$

The new Hamiltonian \hat{H} is clearly gauge invariant, and equivalent to the original one, if we consider the partition function and, more generally, any gauge-invariant correlation function. The Hamiltonian \hat{H} contains interactions between the gauge variables $U_{x,\mu}$ and $U_{y,\nu}$ at any distance |x-y|. However, if these

interactions are exponentially suppressed for $|x-y| \to \infty$, then \widehat{H} represents a gauge-invariant model with effective short-range interactions. This is the general scenario that we expect to emerge when the gauge fields are not critical. This can be verified by performing a strong-coupling expansion assuming βw small. For example, in the case of the GSB perturbation (126), \widehat{H} can be written as a sum of lattice loops. In the strong-coupling expansion, a lattice loop of length L is weighted by a factor that behaves as $(\beta w)^L$ for $\beta w \to 0$. For instance, the leading term is the plaquette, with a weight of order $(\beta w)^4$, which renormalizes the value of γ . The next term corresponds to the 2×1 plaquette, with a coefficient proportional to $(\beta w)^6$, and so on. Couplings therefore scale as $\exp(-a|x-y|)$ with $a \sim -\ln(\beta w)$, showing the short-range nature of the interactions.

This argument proves that, for sufficiently small, but finite, values of the GSB parameter w, the partition function and the gauge-invariant correlation functions can be computed in an equivalent gauge-invariant theory, without GSB terms, with short-range interactions. Finally, to conclude the argument, let us note that we are considering a model in which gauge fields do not play any role, i.e., the critical behavior is independent of the gauge-field interactions, and therefore it is the same as in the original model with w=0. We conclude that the phase structure is independent of w for sufficiently small values. Note that the argument does not rely on the Abelian nature of the theory and thus is should also hold in non-Abelian gauge models.

We finally mention that the same arguments also apply to a different model without gauge fields. Indeed, for $\kappa = 0$, one can integrate out the link variables λ , obtaining an effective Hamiltonian

$$H_{\text{eff}} = -\sum_{\boldsymbol{x},\mu} \ln I_0 \left(2JN | \hat{w} + \bar{\boldsymbol{z}}_{\boldsymbol{x}} \cdot \boldsymbol{z}_{\boldsymbol{x}+\hat{\mu}} | \right), \tag{132}$$

with $\widehat{w} = w/(2JN)$. As it occurs in the \mathbb{CP}^{N-1} model, we expect the Hamiltonian H_{eff} to have the same critical behavior as the Hamiltonian obtained by replacing the Bessel function $I_0(x)$ with its small-x expansion. Since

$$|\widehat{w} + \bar{z}_{x} \cdot z_{x+\hat{\mu}}|^{2} = \widehat{w}^{2} + 2\widehat{w}\operatorname{Re}\left(\bar{z}_{x} \cdot z_{x+\hat{\mu}}\right) + |\bar{z}_{x} \cdot z_{x+\hat{\mu}}|^{2},$$
(133)

an equivalent compact model is

$$H = -N^2 \widetilde{J} \sum_{\boldsymbol{x},\mu} |\bar{\boldsymbol{z}}_{\boldsymbol{x}} \cdot \boldsymbol{z}_{\boldsymbol{x}+\hat{\mu}}|^2 + \widetilde{w} \sum_{\boldsymbol{x},\mu} \operatorname{Re} \,\bar{\boldsymbol{z}}_{\boldsymbol{x}} \cdot \boldsymbol{z}_{\boldsymbol{x}+\hat{\mu}}.$$
(134)

The term proportional to \widetilde{J} is the standard formulation of the U(N)-invariant \mathbb{CP}^{N-1} model without gauge fields, see Eq. (7), while the second term is the O(2N) invariant vector model, which represents here the GSB perturbation. The phase diagram of this model is similar to the one presented in panel (b) of Fig. 25, with three different phases characterized by the different behavior of the scalar fields. The only qualitative difference is the shape of the D-TV transition line that ends on the J=0 axis at the critical point w_c of the O(2N) vector model.

12. Conclusions and outlook

We have reviewed the statistical properties of Abelian and non-Abelian Higgs theories, describing multicomponent scalar fields coupled with Abelian and non-Abelian gauge fields, mostly in three dimensions. As remarked several times, the interplay between local gauge and global symmetries determines the nature of the Higgs phases and of the phase transitions of these lattice gauge systems. Their nature also crucially depends on the role played by gauge modes at criticality, whether they are critical at the transition or not. In the latter case, their role is that of selecting the critical scalar modes, so that only critical correlations associated with gauge-invariant scalar modes can be observed. The topological properties of the gauge modes can also give rise to topological transitions between Higgs phases with the same scalar global symmetry. These transitions are related to the breaking pattern of the gauge symmetry in the Higgs phase. We discuss examples with a residual \mathbb{Z}_Q gauge symmetry, leading to topological \mathbb{Z}_Q gauge transitions when varying the gauge coupling.

The results reviewed here show that the possible critical behaviors observed in 3D lattice gauge Higgs systems are quite varied, showing also features that cannot be explained by the standard LGW paradigm. The continuous transitions of the statistical Abelian and non-Abelian gauge systems considered in this review can be classified as follows (see Sec. 3.1): (i) LGW transitions with gauge-invariant order parameter and noncritical gauge modes; (ii) LGW^{\times} transitions, where gauge modes are also not critical, but where the effective order-parameter field is gauge dependent; (iii) GFT transitions, where gauge modes are critical and that require an effective description that includes the gauge fields; (iv) topological transitions driven only by topological gauge modes, without any local gauge-invariant scalar order parameter.

We have focused on the equilibrium thermodynamic behavior of classical statistical systems, whose partition function is defined as a path-integral functional, by integrating over continuum or lattice configurations. However, the results for classical statistical systems in (d+1) dimensions also apply to quantum transitions in d dimensions, using the quantum-to-classical mapping. Indeed, they are relevant for the d-dimensional quantum transitions that can be related with classical thermal transitions in (d+1)-dimensional isotropic systems. In particular, this requires that the critical exponent z, associated with the vanishing gap $\Delta \sim \xi^{-z}$ at the quantum critical point, satisfies z=1. However, further interesting developments may come from a thorough analysis of quantum transitions in the presence of emerging gauge symmetries with $z \neq 1$ [14, 101]. This issue definitely calls for further studies.

Another interesting issue is the critical dynamics of statistical systems with gauge symmetries. On one side, one would like to understand if the presence of gauge symmetries gives rise to distinctive new features for the different types of dynamics that are usually considered for standard statistical systems [114, 468, 469]. A systematic study of the critical dynamics in the presence of gauge symmetries may provide further interesting characterizations of the different types of transitions that we have outlined in Sec. 3.1. On the other side, it would be interesting to understand whether it is possible to define dynamics that are not considered in the standard classification of systems without gauge symmetries. As an example, one may consider the purely relaxational dynamics with only dissipative couplings and no conservation laws, usually called dynamic model A [468]. This dynamics can be realized by considering a relaxational stochastic Langevin dynamics, which is also at the basis of the stochastic quantization of gauge theories [10, 470–474]. It would be interesting to understand how the expected critical slowing down, signalled by the critical divergence of the relaxation time τ of the critical modes (at criticality, $\tau \sim \xi^z$, where z is a dynamic critical exponent), depends on type of transition, and how the nonperturbative results compare with the field-theoretical predictions that are typically obtained in the presence of a gauge fixing. Some studies of the critical dynamics have been already reported, see, e.g., Refs. [244, 248, 475-482], most of them addressing the dynamics at superconducting phase transitions. However, a systematic analysis of dynamic phenomena is still missing.

We finally mention that new scenarios may arise from the inclusion of fermionic fields in AH and NAH systems. This topic is relevant in condensed-matter physics as many field-theoretical models with emerging gauge symmetries include both fermionic and scalar excitations, see, e.g., Refs. [20, 96, 237, 380, 483, 484]. The study of the corresponding lattice gauge systems may extend the phenomenology of phase transitions in the presence of gauge symmetries. As for LAH and LNAH systems with only scalar matter, one key issue would be that of identifying the 3D transitions where both matter and gauge fields are critical, allowing one to define the continuum limit of the corresponding SFTs. The same issue is also important in lattice gauge models with fermionic matter only. Some studies of the phase diagram and critical behavior of 3D models including fermionic fields can be found in Refs. [76, 485–508].

Appendix A. Renormalization-group theory of critical phenomena

In this appendix we report an overview of the RG theory, which provides a general framework to explain the observed scaling behavior at continuous phase transitions [2, 6, 8, 9, 11, 94, 95, 113, 114, 124, 125, 127, 129, 130, 132–137]. We present the RG scaling relations in the thermodynamic (infinite-volume) limit and in the FSS limit and, in particular, we discuss the leading scaling behavior and the scaling corrections characterizing the deviations from the asymptotic relations. We only consider classical transitions, generally driven by thermal fluctuations; the extension to quantum transitions driven by quantum fluctuations is discussed in Refs. [14, 101, 118, 138]. FSS behaviors also emerge at first-order transitions [115, 117]. These

phenomena for classical and quantum transitions are discussed in Refs. [115, 117, 509, 510]. In the following we do not discuss the critical dynamics at thermal and quantum transitions. Reviews can be found in Refs. [101, 468, 469].

Appendix A.1. Universal power laws at the critical point

To fix the ideas, we consider a prototypical d-dimensional statistical system undergoing a continuous transition. The behavior of the system is controlled by two relevant Hamiltonian parameters r and h, which can be defined so as to vanish at the critical point. Thus, the critical point is located at r = h = 0. We also assume the presence of a \mathbb{Z}_2 -symmetry, as it occurs, e.g., in Ising transitions, which is unbroken in the phase with r > 0 (paramagnetic phase in magnetic systems) and spontaneously broken in the (ferromagnetic) phase with r < 0. The parameter r is associated with a RG perturbation that is invariant under the global symmetry and is usually identified with the reduced temperature $r \sim T/T_c - 1$. The parameter h is assumed to be odd with respect to the \mathbb{Z}_2 -symmetry, thus it can be identified with an external homogeneous field coupled with the order parameter driving the symmetry breaking.

In the thermodynamic limit, when approaching the critical point from the disordered phase keeping h=0, the length scale ξ of the critical modes diverges as $\xi \sim r^{-\nu}$, where ν is a universal length-scale critical exponent. Another universal critical exponent η is traditionally introduced to characterize the space dependence at criticality of the two-point function of the order parameter: $G(\boldsymbol{x}_1, \boldsymbol{x}_2) \sim |\boldsymbol{x}_1 - \boldsymbol{x}_2|^{-(d-2+\eta)}$ for r=h=0. The RG dimensions of the perturbations associated with r and h are related with the critical exponents ν and η , as [95, 125]

$$y_r = 1/\nu, \qquad y_h = \frac{d+2-\eta}{2}.$$
 (A.1)

Using scaling and hyperscaling arguments (see, e.g., Refs. [2, 95, 114]), the exponents associated with the scaling behavior of other observables, like the magnetization or the critical equation of state, can be expressed in terms of the two independent exponents ν and η . The corrections to the asymptotic power laws behave as $\xi^{-\omega}$ for $\xi \to \infty$, where $\omega > 0$ is another universal exponent characterizing the critical behavior [2, 95], which is generally associated with the leading irrelevant RG perturbation.

Appendix A.2. Scaling laws in the thermodynamic limit

We consider the free-energy density of a statistical system,

$$F = -\frac{T}{V} \ln Z, \qquad Z = \sum_{\{\varphi\}} e^{-\beta H}, \qquad \beta = 1/T, \qquad V = L^d,$$
 (A.2)

where the summation is over all configurations $\{\varphi\}$ of the system. According to the RG theory, F obeys a general scaling law. Indeed, we can write F in terms of the nonlinear scaling fields associated with the RG eigenoperators at the FP of the RG flow [95, 125]. Therefore, close to a continuous transition, the free-energy density in the infinite-volume limit can be written in terms of scaling fields [125], as

$$F(r,h) = F_{\text{reg}}(r,h^2) + F_{\text{sing}}(u_r, u_h, \{v_i\}). \tag{A.3}$$

Here $F_{\rm reg}$ is a nonuniversal function, which is analytic at the critical point and must be even with respect to the parameter h related to the odd perturbation (for a general symmetry group it should depend on a combination of h that is invariant under the symmetry transformations). The singular contribution, $F_{\rm sing}$, bears the nonanalyticity of the critical behavior and its universal features. The arguments of $F_{\rm sing}$ are the so-called nonlinear scaling fields [125]: they are analytic nonlinear functions of the model parameters, related to the eigenoperators that diagonalize the RG flow close to the FP, and transform multiplicatively under the RG flow. We have singled out the relevant scaling fields u_r and u_h that are associated with the model parameters r and h, and have positive RG dimensions y_r amd y_h . The scaling fields $\{v_i\}$ (there is an infinite number of them) are RG irrelevant, i.e., their RG dimensions y_i are negative. They give rise to scaling corrections to the asymptotic critical behavior in the infinite-volume limit. Assuming that they are ordered

so that $|y_1| \le |y_2|, \le \ldots$, the RG dimension $y_1 < 0$ generally determines the leading scaling corrections, thus we identify $\omega = -y_1$.

In general, the nonlinear scaling fields depend on the control parameters r and h. Taking into account the assumed \mathbb{Z}_2 symmetry and the respectively even and odd properties of r and h, close to the critical point the relevant scaling fields u_r and u_h can be generally expanded as

$$u_r = r + c_r r^2 + O(r^3, h^2 r), u_h = h + c_h r h + O(h^3, r^2 h),$$
 (A.4)

where c_r and c_h are nonuniversal constants. As for the irrelevant scaling fields v_i , they are generally nonvanishing at the critical point.

The singular part of the free energy (A.3) is expected to satisfy the homogeneous scaling law

$$F_{\text{sing}}(u_r, u_h, \{v_i\}) = b^{-d} F_{\text{sing}}(b^{y_r} u_r, b^{y_h} u_h, \{b^{y_i} v_i\}), \tag{A.5}$$

where b is an arbitrary scale factor and y_r and y_h are given in Eq. (A.1). To obtain more explicit scaling relations, one can fix the arbitrariness of the scale parameter b, setting $b = u_r^{-1/y_r} = u_r^{-\nu}$, which diverges in the critical limit $r, h \to 0$. The following asymptotic behavior of the free-energy density emerges:⁵³

$$F_{\text{sing}} = u_r^{d\nu} \mathcal{F}(u_h/u_r^{y_h\nu}, \{v_i/u_r^{y_i\nu}\}) = u_r^{d\nu} \left[\mathcal{F}_0(u_h/u_r^{y_h\nu}) + u_r^{\omega\nu} \mathcal{F}_\omega(u_h/u_r^{y_h\nu}) + \cdots \right], \tag{A.6}$$

where \mathcal{F}_0 and \mathcal{F}_ω are universal scaling functions, and we kept only the leading correction to scaling, which is relatively suppressed as $u_r^{\omega\nu}$ with $\omega=-y_1$. Note, however, that, since the scaling fields have arbitrary normalization, the universality of the scaling functions \mathcal{F}_0 and \mathcal{F}_ω holds apart from a normalization of each argument and an overall constant. By differentiating the free-energy density, one can straightforwardly derive analogous scaling relations for other observables, such as the energy density and the magnetization. To eventually obtain the scaling relations in terms of the external parameters r and h controlling the approach to the critical point, one needs to expand the scaling fields as in Eq. (A.4). The subleading terms in these expansions give rise to analytic scaling corrections.

Analogous scaling relations can be obtained for the correlation functions of local operators. For example, the two-point correlation function of the local operator O(x), whose RG dimension is y_o , is expected to asymptotically behave as

$$G_O(\mathbf{x}, \mathbf{y}) = \langle O(\mathbf{x})O(\mathbf{y})\rangle \approx \xi^{-2y_o} \mathcal{G}_O(\mathbf{x}/\xi, \mathbf{y}/\xi, h \, \xi^{y_h}), \qquad \xi \sim r^{-\nu}, \tag{A.7}$$

when approaching the critical point from the disordered phase r > 0.

Appendix A.3. Finite-size scaling

The RG scaling relations reported in Appendix A.2 hold in the thermodynamic limit, which is well defined for any $r \neq 0$ or $h \neq 0$, since the correlation length ξ is finite. Nonetheless, for practical purposes, both experimentally and numerically, one typically has to face with systems of finite size L. Also in this case, for large values of L, it is possible to observe a universal scaling behavior.

Finite-size effects in critical phenomena have been the object of many theoretical studies [95, 134–136, 511, 512]. The FSS theory describes the critical behavior around a critical point, when the correlation length ξ of the critical modes becomes comparable with the size L of the system. The FSS approach is one of the most effective techniques to determine the universal features of continuous phase transitions, such as the critical exponents. While infinite-volume methods require the condition $\xi \ll L$ to be satisfied, FSS methods apply in the less demanding regime $\xi \sim L$. The FSS theory provides the asymptotic scaling behavior when both $L, \xi \to \infty$, keeping their ratio ξ/L fixed. This regime presents universal features, shared by all systems whose transition belongs to the same universality class.

⁵³Note that the expansion (A.6) is only possible below the upper critical dimension [113]. Above it, the failure of this expansion causes a breakdown of the hyperscaling relations, allowing one to recover the mean-field exponents.

Appendix A.3.1. Free-energy density

In the FSS framework, the finite size of the system is taken into account by adding the length scale L in the scaling laws [95, 101, 118, 125, 135, 136, 138, 513, 514]. In the following we focus for concreteness on finite-size systems without boundaries, such as systems with periodic or antiperiodic boundary conditions. In these cases the scaling laws, and in particular the corrections to the asymptotic scaling behavior, are simpler. The corrections to the bulk scaling laws due to the presence of boundaries are discussed in, e.g., Refs. [101, 135, 136, 138, 514]. In the FSS limit the free-energy density can be written as

$$F(L, r, h) = F_{\text{reg}}(r, h^2) + F_{\text{sing}}(L, u_r, u_h, \{v_i\}), \tag{A.8}$$

where F_{reg} is again a nonuniversal analytic function, which is assumed to be independent of L, or, more plausibly, to depend on L only through exponentially small corrections [135, 136, 138, 514]. According to the RG theory, the singular part F_{sing} satisfies the homogeneous scaling law

$$F_{\text{sing}}(L, u_r, u_h, \{v_i\}) = b^{-d} F_{\text{sing}}(L/b, u_r b^{y_r}, u_h b^{y_h}, \{v_i b^{y_i}\}), \tag{A.9}$$

where b is an arbitrary constant. To derive the FSS behavior, we fix b = L, thus obtaining

$$F_{\text{sing}} = L^{-d} \mathcal{F}(L^{y_r} u_r, L^{y_h} u_h, \{L^{y_i} v_i\}). \tag{A.10}$$

The arguments $\{L^{y_i}v_i\}$, corresponding to the irrelevant scaling fields with $y_i < 0$, vanish for $L \to \infty$. Thus, provided that F_{sing} is finite and nonvanishing in this limit, and neglecting the analytic corrections arising from the higher-order terms of the polynomial expansion of the scaling fields u_r and u_h , see Eq. (A.4), we can expand the singular part of the free energy as

$$F_{\text{sing}} \approx L^{-d} \left[\mathcal{F}_0(W, Z) + v_1 L^{-\omega} \mathcal{F}_\omega(W, Z) + \ldots \right], \qquad W = L^{y_r} r, \quad Z = L^{y_h} h, \tag{A.11}$$

where we only retain the contribution of the dominant (least) irrelevant scaling field of RG dimension $y_1 = -\omega$. The scaling behavior in the thermodynamic limit can be recovered from the FSS homogenous law (A.9), by choosing $b = u_r^{-\nu}$ and taking the limit $L/b \to \infty$. The scaling laws of several interesting quantities can be obtained by taking derivatives of the free energy with respect of r and h, such as the energy density, the specific heat, the magnetization, the magnetic susceptibility, etc...

The above scaling laws hold in generic systems. However, in some cases the scaling behavior is more complex, due to the appearance of logarithmic terms [125]. They may be induced by the presence of marginal RG perturbations, as it happens for the Berezinskii-Kosterlitz-Thouless (BKT) transitions that occur in 2D U(1)-symmetric systems [423, 454, 455, 515, 516], or by resonances between the RG eigenvalues, as it occurs in 2D Ising transitions [125, 517], or in 3D O(N)-vector models in the large-N limit [518–520].

The FSS limit, which corresponds to taking $r \to 0$, thus $\xi \to \infty$, and $L \to \infty$ at fixed ξ/L , definitely differs from the critical limit in the thermodynamic limit, which is generally obtained by first taking the large-L limit keeping r or ξ fixed, and then the critical limit $r \to 0$ or, equivalently $\xi \to \infty$. However, assuming that the FSS and infinite-volume behavior asymptotically match, one may straightforwardly derive the infinite-volume scaling behavior from the FSS relations, by taking the limit $\xi/L \to 0$.

We finally remark that, in numerical and experimental investigations of finite-size systems, the knowledge of the leading asymptotic behavior may not be enough to estimate the critical parameters, because data are generally available only for limited ranges of parameter values and system sizes, which are often relatively small. Under these circumstances, the asymptotic FSS predictions may be affected by sizable scaling corrections. Accurate estimates of the critical parameters thus require a robust control of the corrections to the asymptotic scaling behavior. This is also important for a conclusive identification of the universality class of a continuous transition, when there are no solid theoretical arguments to predict it. Moreover, an understanding of the finite-size effects is relevant for experiments, when relatively small systems are considered (see, e.g., Ref. [521]), or in particle systems trapped by external (usually harmonic) forces, as in cold-atom setups (see, e.g., Refs. [522–527]).

Appendix A.3.2. Energy cumulants

As discussed in this review, statistical models with gauge symmetries also undergo topological transitions characterized by the absence of a local order parameter, such as those belonging to the 3D \mathbb{Z}_Q gauge and IXY universality classes (see Sec. 3.5), which are also found in LAH and LNAH models (see Secs. 5 and 6). The numerical study of the critical properties at these topological transitions can be performed by analyzing the scaling properties of the gauge-invariant energy cumulants, which are always gauge invariant and well defined, see, e.g., Refs. [63, 86, 92, 176].

The gauge-invariant energy cumulants C_k are intensive quantities that can be defined by taking inverse-temperature derivatives of the free-energy density, more precisely

$$C_k = \frac{1}{V} \left(\frac{\partial}{\partial \beta}\right)^k \log Z(\beta), \tag{A.12}$$

where Z is the partition function defined in Eq. (A.2).⁵⁴ Note that $C_1 = -E$ where $E = \langle H \rangle / V$ is the energy density, and C_2 is proportional to the specific heat.

At continuous transitions, the cumulant C_k is expected to show the FSS behavior (we assume h = 0 in the following)

$$C_k(r,L) \approx L^{k/\nu - d} \left[\mathcal{U}_k(W) + O(L^{-\omega}) \right] + B_k(r), \qquad W = rL^{y_r},$$
 (A.13)

where $B_k(r)$ is a regular function—the so-called analytic background [86, 95]. Note that the relation $C_{k+1} = \partial C_k/\partial \beta$ implies $\mathcal{U}_{k+1}(W) \sim -\partial_W \mathcal{U}_k(W)$. Further properties of the scaling functions \mathcal{U}_{k+1} are derived in Ref. [92].

As one can easily check, the first cumulant $C_1 = -E$ is dominated by the analytic background contribution B_1 , due to the relation $\nu > 1/d > 0$, which is generally satisfied at continuous transitions [95]. This makes the scaling behavior of the energy density subleading, and therefore rather difficult to observe (this issue has been addressed in Refs. [528, 529]). Also the second cumulant C_2 , which is proportional to the specific heat, is dominated by the analytic background when the specific-heat exponent $\alpha = 2\nu - d$ is negative. The singular scaling part is always the dominant term in the higher energy cumulants C_k , i.e., for $k \geq 3$. Taking into account that their numerical computation becomes harder and harder with increasing k, due to significant cancellations which make their relative error quite large and increasing with k, optimal results are obtained by focusing on C_3 and C_4 .

Appendix A.3.3. The order-parameter correlation function

For vanishing magnetic field, h = 0, the leading scaling behavior of the two-point correlation function of the order-parameter field $\phi(\mathbf{x})$ is given by

$$G(\boldsymbol{x}, L, r) \equiv \langle \phi(\boldsymbol{x}_1) \phi(\boldsymbol{x}_2) \rangle \approx L^{-2y_{\phi}} \left[\mathcal{G}(\boldsymbol{x}/L, W) + O(L^{-\omega}) \right], \qquad y_{\phi} = \frac{d - 2 + \eta}{2}, \quad W = L^{y_r} r, \quad (A.14)$$

where y_{ϕ} is the RG dimension of the field $\phi(\mathbf{x})$, $\mathbf{x} \equiv \mathbf{x}_1 - \mathbf{x}_2$ and we assumed translation invariance (i.e., the absence the boundaries). The integral of $G(\mathbf{x}, L, r)$ over the whole finite volume L^d provides the magnetic susceptibility

$$\chi(L,r) = L^{2-\eta} \left[\mathcal{X}(W) + O(L^{-\omega}) \right] + B_{\chi}(r). \tag{A.15}$$

The scaling function \mathcal{X} is universal, apart from a multiplicative factor and a normalization of the argument. The function B_{χ} is an analytic background term, see, e.g., Ref. [95].

The length scale associated with the critical modes can be obtained from the correlation function G. For this purpose different definitions can be considered. In the infinite-volume limit, or if at least one of

⁵⁴The cumulants C_k can be related to the energy central momenta $M_k = \langle (H - \langle H \rangle)^k \rangle$, by $C_1 = -\langle H \rangle/V$, $C_2 = M_2/V$, $C_3 = -L^{-3}M_3$, $C_4 = (M_4 - 3M_2^2)/V$, etc.

the spatial dimensions is infinite, one may define a correlation length ξ_e from the large-distance exponential decay of the two-point correlation function (A.14), i.e., $G(x) \sim \exp(-|x|/\xi_e)$, provided the system is not at a critical point. An alternative definition, particularly useful for the analysis of finite systems, relies on the second moment of the order-parameter correlation function. More precisely, on a lattice one defines

$$\xi^2 \equiv \frac{1}{4\sin^2(p_{\min}/2)} \frac{\widetilde{G}(\mathbf{0}) - \widetilde{G}(\mathbf{p})}{\widetilde{G}(\mathbf{p})},\tag{A.16}$$

where $p_{\min} \equiv 2\pi/L$, p is a vector with only one nonvanishing component equal to p_{\min} , and $\widetilde{G}(p)$ is the Fourier transform of G(x). This definition is particularly convenient when using periodic boundary conditions, but it can also be used in other cases, at least as far as $2\pi/L$ is a legitimate lattice momentum.

Appendix A.3.4. Renormalization-group invariant quantities

Dimensionless RG invariant quantities are particularly useful for the investigation of the critical behavior. Examples of such quantities are the ratio

$$R_{\mathcal{E}} \equiv \xi/L,\tag{A.17}$$

where ξ is any length scale related to the critical modes, for example the one defined in Eq. (A.16), and the so-called Binder parameter associated with the order-parameter field, defined as

$$U = \frac{\langle \mu_2^2 \rangle}{\langle \mu_2 \rangle^2}, \qquad \mu_2 = \frac{1}{V^2} \sum_{\boldsymbol{x}, \boldsymbol{y}} \phi_{\boldsymbol{x}} \phi_{\boldsymbol{y}}. \tag{A.18}$$

In the FSS limit, at zero external field h, RG invariant quantities (we denote them generically with R) behave as

$$R(L,r) \approx \mathcal{R}(W) + L^{-\omega} \mathcal{R}_{\omega}(W) + \dots$$
 (A.19)

The scaling function $\mathcal{R}(W)$ is universal, apart from a normalization of the argument. In particular, the limit

$$\lim_{L \to \infty} R(L, 0) = \mathcal{R}(0) \tag{A.20}$$

is universal. It depends on the universality class but not on the microscopic details of the model. It also depends on the shape of the finite lattice and on the boundary conditions.

The FSS behavior of the RG-invariant quantities R can be exploited to determine the critical point [95, 530]. Indeed, when the following inequalities hold

$$\lim_{r \to 0^-} \lim_{L \to \infty} R(L, r) > \lim_{L \to \infty} R(L, 0) > \lim_{r \to 0^+} \lim_{L \to \infty} R(L, r)$$
(A.21)

(or the analogous ones with < replacing >), one can define $r_{\rm cross}$ by requiring

$$R(L, r_{\text{cross}}) = R(2L, r_{\text{cross}}). \tag{A.22}$$

The crossing point r_{cross} converges to r=0, with corrections that are typically suppressed as $L^{-1/\nu-\omega}$.

We finally note that, if a RG invariant quantity R_m is monotonic with respect to the relevant parameter r, as is generally the case for $R_{\xi} = \xi/L$, one may write for a second generic RG invariant quantity R_i the scaling relation

$$R_i(L,r) = \widehat{\mathcal{R}}_i(R_m) + O(L^{-\omega}), \tag{A.23}$$

where \widehat{R}_i depends on the universality class only, without any nonuniversal normalization of the argument. This is true once the boundary conditions and the shape of the lattice have been fixed. The scaling relation (A.23) is particularly convenient to test universality-class predictions, since it allows one to compare the results for different models without the need of tuning nonuniversal parameters. One may write the FSS behavior of any other quantity in terms of R_{ξ} . For example, the asymptotic FSS behavior of the susceptibility χ defined in Eq. (A.15) can be rewritten as

$$\chi(L,r) \approx L^{2-\eta} \widehat{\mathcal{X}}(R_{\xi}),$$
(A.24)

where the FSS function $\hat{\mathcal{X}}$ is now expected to be universal apart from a multiplicative factor only.

Appendix A.4. Scaling behavior at a multicritical point

We now briefly outline the FSS behavior at a multicritical point (MCP), see Fig. 1, which is generally characterized by the presence of two relevant RG perturbations, which are both invariant under the global symmetry of the model and which must be both tuned to approach the MCP. We indicate with r_1 and r_2 the corresponding Hamiltonian parameters, normalized so that $r_1 = r_2 = 0$ at the MCP. At a MCP, the singular part of the free-energy density can be written as [95, 172–176]

$$F_{\text{sing}}(r_1, r_2, L) \approx L^{-d} \mathcal{F}(u_1 L^{y_1}, u_2 L^{y_2}),$$
 (A.25)

where u_1 and u_2 are the nonlinear scaling fields associated with the two relevant parameters r_1 and r_2 (they are analytic functions of r_1 and r_2 , that satisfy $u_1 \approx r_1$ and $u_2 \approx r_2$), $y_1 > 0$ and $y_2 > 0$ are the corresponding RG dimensions (we assume $y_1 > y_2$), and we neglected corrections to the multicritical behavior due to the irrelevant scaling fields.

In the infinite-volume limit and neglecting subleading corrections, we can rewrite the singular part of the free-energy density as

$$F_{\text{sing}}(r_1, r_2) = |u_2|^{d/y_2} \mathcal{F}_{\pm}(X), \qquad X \equiv u_1 |u_2|^{-\phi}, \qquad \phi \equiv y_1/y_2 > 1,$$
 (A.26)

where the functions $\mathcal{F}_{\pm}(X)$ apply to the parameter regions in which $\pm u_2 > 0$, respectively, and ϕ is the so-called crossover exponent associated with the MCP. Close to the MCP, the transition lines follow the equation $X = u_1|u_2|^{-\phi} = \text{const}$ with a different constant for each transition line. Since $\phi > 1$, they are tangent to the line $u_1 = 0$.

Appendix A.5. Two-dimensional spin models with continuous symmetry

According to the Mermin-Wagner theorem [420, 421], 2D statistical models with short-range interactions and continuous symmetries cannot have low-temperature magnetized phases characterized by the condensation of an order parameter, and therefore they do not undergo phase transitions driven by the spontaneous breaking of the global symmetry. Examples of such 2D models are the N-vector models defined by the Hamiltonian (1) on a square lattice (setting the external magnetic field h to zero), the 2D CP^{N-1} and RP^{N-1} models, defined Sec. 3.2.1 and Sec. 3.2.2, respectively. Their phase diagrams are generally characterized by a single disordered phase with the notable exception of systems with Abelian O(2) symmetry. They show a critical behavior only in the zero-temperature limit, with universal features that are determined by the symmetries of the system. An effective description is provided by the 2D nonlinear σ models defined on symmetric spaces, see, e.g., Refs. [2, 95].

These statistical systems are asymptotically free with a nonperturbatively generated mass gap. Such a property is also present in QCD, the theory of strong interactions, and thus these 2D theories have often been used as toy models to understand some of the nonperturbative mechanisms characterizing QCD, see, e.g., Refs. [2, 95, 446, 449]. We mention that the 2D N-vector model is also important in condensed-matter physics. For N=3 it describes the zero-temperature behavior of the 2D spin-S Heisenberg quantum antiferromagnet [439]. Indeed, at finite temperature T this quantum spin system is described by a (2+1)-dimensional O(3) classical theory in which the Euclidean time direction has a finite extent 1/T. In the critical limit the relation $1/T \ll \xi$ is satisfied, therefore the system becomes effectively two-dimensional, and thus its critical behavior is described by the 2D O(3)-vector model.

The long-distance critical behavior in the zero-temperature limit can be predicted by performing perturbative computations in powers of T, see, e.g., Refs. [2, 95, 285, 431–446]. In particular, the T-dependence of the correlation length ξ can be inferred from the perturbative expansion of the lattice β function, related with the derivative of the correlation length ξ with respect to T,

$$\beta(T) = \left(\frac{1}{\xi} \frac{d\xi}{dT}\right)^{-1} = -T^2 \sum_{n=0} \beta_n T^n. \tag{A.27}$$

Indeed, one obtains, see, e.g., Refs. [2, 95],

$$\xi(T) = \xi_0 \left(\beta_0 T\right)^{\beta_1/\beta_0^2} \exp\left(\frac{1}{\beta_0 T}\right) \exp\left[\int_0^T dt \left(\frac{1}{\beta(t)} + \frac{1}{\beta_0 t^2} - \frac{\beta_1}{\beta_0^2 t}\right)\right],\tag{A.28}$$

where ξ_0 is a nonperturbative model-dependent constant (depending also on the actual definition of ξ). More specifically, using the first known terms of the β functions, the asymptotic behavior of the length scale in the zero-temperature limit is (see, e.g., Refs. [2, 95])

$$\xi(T) \sim B^{-\frac{1}{N-2}} e^B, \qquad B = \frac{2\pi}{(N-2)T},$$
 (A.29)

for N-vector models (with $N \geq 3$), and [441]

$$\xi(T) \sim B^{-\frac{2}{N}} e^B, \qquad B = \frac{2\pi}{T},$$
 (A.30)

for lattice CP^{N-1} models $(N \ge 2)$.

The asymptotic behaviors (A.29) and (A.30) are quite difficult to observe because the neglected corrections decay as inverse powers of $\ln \xi$ in the large- ξ limit. It is important to observe that these logarithmic corrections are not present when considering RG invariant dimensionless quantities R(T). In this case, scaling corrections are proportional to negative integer powers of ξ , multiplied by powers of $\ln \xi$ (equivalently powers of T). In particular, for the N-vector and \mathbb{CP}^{N-1} models we have

$$R(T) = R^* + O\left[T^p/\xi(T)^2\right],$$
 (A.31)

where p is a model-dependent power. Therefore, apart from logarithmic corrections (due to $T \sim 1/\ln \xi$), the leading scaling-correction exponent is $\omega = 2$. Such a behavior has been verified explicitly in the large-N limit, see, e.g., Ref. [531].

We also mention that the nature of the asymptotic low-temperature behavior of the 2D RP^{N-1} models has been long debated, see, e.g., Refs. [217–221, 223]. Refs. [219–221] reported arguments that support the claim that RP^{N-1} and N-vector models belong to the same universality class, implying the irrelevance of the \mathbb{Z}_2 gauge symmetry. They are essentially related to the fact that N-vector and RP^{N-1} have the same asymptotic perturbative behavior. However, extensive numerical results for several variant RP^{N-1} models [223] show substantial differences in the nonperturbative scaling functions, which may be explained by the nonperturbative relevance of the topological \mathbb{Z}_2 defects characterizing the RP^{N-1} models, giving rise to distinct universality classes.

We finally mention that 2D systems with an Abelian O(2) global symmetry, such as the N=2 XY vector model and the RP¹ model, are peculiar in this respect, since they can undergo a finite-temperature topological BKT transition [423–425], which separates the high-T disordered phase from the low-temperature nonmagnetized phase characterized by spin waves and quasi-long range order with vanishing magnetization. At BKT transitions the correlation length ξ scales as $\xi \sim \exp(c/\sqrt{T-T_c})$ approaching the BKT critical temperature T_c from the high-temperature phase. The scaling behavior at BKT transitions has been extensively discussed in the literature, see, e.g., Refs. [95, 171, 423–425, 450–454].

Appendix A.6. Finite-size scaling at first-order transitions

The behaviors emerging at first-order phase transitions are more complex than those observed at continuous transitions, see, e.g., Refs.[115, 117]. Critical phenomena at continuous phase transitions are essentially related with the presence of critical correlations, which decay as a power of the distance at the critical point, and with a diverging length scale ξ . When approaching the critical point, the long-distance behavior, i.e., on distances of the order of the scale ξ , shows universal features that only depend on few global properties of the microscopic short-distance interactions. The behavior at first-order transitions is instead more complex. Indeed, we typically observe the coexistence of different phases, with one or more phases that

are ordered on all length scales, apart from some short-range local fluctuations. The presence of coexisting phases gives rise to peculiar competing phenomena in the phase-coexistence region, such as metastability, nucleation, droplet formation, coarsening, etc. [115, 532]. Moreover, the observed bulk behavior crucially depends on the nature of the boundary conditions, at variance with what happens at continuous transitions, where boundary conditions only affect some finite-size properties of the system, but are irrelevant in the thermodynamic limit. The sensitivity to the boundary conditions represents one of the main qualitative differences between continuous and first-order phase transitions [117].

First-order transitions are characterized by the discontinuity of thermodynamic quantities. In d-dimensional finite systems these discontinuities are smeared out, but they still give rise to easily identifiable properties. A nontrivial FSS behavior have been also established at first-order classical and quantum transitions [115, 117, 509, 510, 533–540], generalizing the ideas that had been previously developed in the context of critical transitions. For instance, the specific heat and the magnetic susceptibility show a sharp maximum that diverges as a power of the volume and the same is true for the cumulants of the order parameter in magnetic transitions.

To distinguish continuous from first-order transitions in numerical studies of systems with limited size, one can exploit the substantial differences of their FSS behavior. A possible approach consists in considering the large-L behavior of the specific heat or of the susceptibility of the order parameter, that should have a maximum that diverges as L^d . [541–544] In practice, one should compute the maximum of the susceptibility $\chi_{A,\max}(L)$ of a local operator A_x for each value of L and then fit the results to a power law aL^p . If one obtains $p \approx d$, the transition is of first order; otherwise, the transition is continuous, p being related to standard critical exponents. If A is the energy density, then χ_A is the specific heat that diverges as $L^{\alpha/\nu}$ (if α is positive), while if A is the magnetization, then $\chi_A \sim L^{2-\eta}$. This approach works nicely for strongly discontinuous transitions. In the case of weakly discontinuous transition, however, the asymptotic behavior $\chi_A \sim L^d$ may set in for values of L that are much larger than those considered in the simulations. Thus, data may show an effective scaling $\chi_{A,\max}(L) \sim L^p$, with p significantly smaller than d, effectively mimicking a continuous transition (the Potts model [545, 546] in two and three dimensions is a good example, see Refs. [541–544]).

At order-disorder magnetic transitions, the Binder cumulant U_m associated with the magnetization usually provides a better indicator [540]. Indeed, it diverges at first-order transitions, while it is smooth and finite at continuous transitions. Thus, the observation that $U_{m,\max}(L)$ increases with L is an evidence of the discontinuous nature of the transition, even if the maximum does not scale as L^d , as it should do asymptotically. This idea have been exploited to determine the nature of the transitions in several models, including systems with gauge symmetries, such as the LAH and LNAH model, see, e.g., Refs. [82, 87, 97, 99].

An extended review of the FSS behavior at thermal and quantum first-order transitions and of its dependence on the boundary conditions can be found in Ref. [117].

Appendix B. Critical exponents of some O(N)-vector universality classes

In this appendix we report the presently most accurate estimates of the critical exponents for the most common 3D N-vector universality classes, the Ising (N=1), XY (N=2), and Heisenberg (N=3) universality classes. An effective LGW model is the Φ^4 field theory for an N-component real field, while a lattice representative is the standard N-vector model defined by the Hamiltonian (1). The estimates are reported in Tables B.1, B.2, and B.3 for N=1, N=2, and N=3, respectively. A more complete list of theoretical and experimental results can be found in Ref. [95] (at least up to 2002); those reported here are the most accurate in the various approaches. We recall that the critical exponents controlling the asymptotic exponents of other observables can be obtained from ν and η by using scaling and hyperscaling relations (see, e.g., Refs. [2, 114]). Accurate estimates of the critical exponents of the O(N) vector universality classes for $N \geq 4$ can be found in Refs. [95, 299].

	3D Ising	ν	η	ω	Ref.
SFT	6-loop 3D expansion	0.6304(13)	0.0335(25)	0.799(11)	[547]
	6-loop ε expansion	0.6292(5)	0.0362(6)	0.820(7)	[548]
	Functional RG	0.63012(16)	0.0361(11)	0.832(14)	[549]
	CFT bootstrap	0.629971(4)	0.036298(2)	0.8297(2)	[256]
Lattice	High-T expansion	0.63012(16)	0.0364(2)	0.82(4)	[550]
	MC	0.63020(12)	0.0372(10)	0.82(3)	[551]
	MC	0.63002(10)	0.03627(10)	0.832(6)	[552]

Table B.1: Estimates of the critical exponents of the 3D Ising universality class (characterized by a global \mathbb{Z}_2 symmetry). We report the correlation-length exponent ν , the order-parameter exponent η , and the exponent ω associated with the leading scaling corrections. We report: SFT results obtained by resumming high-order perturbative expansions (6-loop calculations in the fixed-dimension scheme [547, 553–557] and in the ε -expansion scheme [548, 558–560]), by using functional RG approaches [549], and the conformal field theory (CFT) bootstrap [256, 561] approach; results obtained in lattice models by resumming high-temperature expansions [550] and in MC simulations [551, 552, 562, 563]. We note that there is an overall agreement among the results obtained by the different approaches. Moreover, there is also a good agreement with experiments in physical systems that undergo continuous transitions in the Ising universality class (liquid-vapor systems, binary systems, uniaxial magnetic systems, Coulombic systems, etc.) see, e.g., Ref. [95] for a list of experimental results.

	3D XY	ν	η	ω	Ref.
SFT	6-loop 3D expansion	0.6703(15)	0.035(3)	0.789(11)	[547]
	6-loop ε expansion	0.6690(10)	0.0380(6)	0.804(3)	[548]
	Functional RG	0.6716(6)	0.0380(13)	0.791(8)	[549]
	CFT bootstrap	0.67175(10)	0.038176(44)	0.794(8)	[328]
Lattice	$\operatorname{High-}T + \operatorname{MC}$	0.6717(1)	0.0381(2)	0.785(20)	[294]
	MC	0.6717(3)			[564]
	MC	0.67169(7)	0.03810(8)	0.789(4)	[293]

Table B.2: Estimates of the critical exponents of the 3D XY universality class (characterized by a global O(2) symmetry). We report the correlation-length exponent ν , the order-parameter exponent η , and the exponent ω associated with the leading scaling corrections. We report: SFT results obtained by resumming high-order perturbative expansions [547, 548] (6-loop calculations in the fixed-dimension and in the ε -expansion scheme), by using functional RG approaches [549] and the conformal field theory (CFT) bootstrap [328] approach; results obtained in lattice models by combining high-temperature and MC results [294] and in MC simulations [293, 564]. We also mention that experimental estimates in a microgravity environment have been obtained for the ⁴He superfluid transition [565–567]. See Ref. [95] for a more complete list of theoretical and experimental results.

	3D O(3)	ν	η	ω	Ref.
SFT	6-loop 3D expansion	0.7073(35)	0.0355(25)	0.782(13)	[547]
	6-loop ε expansion	0.7059(20)	0.03663(12)	0.795(7)	[548]
	Functional RG	0.7114(9)	0.0376(13)	0.769(11)	[549]
	CFT bootstrap	0.7117(4)	0.03787(13)		[568]
Lattice	$\operatorname{High-}T + \operatorname{MC}$	0.7112(5)	0.0375(5)		[569]
	$\operatorname{High-}T + \operatorname{MC}$	0.7117(5)	0.0378(5)		[254]
	$\operatorname{High-}T + \operatorname{MC}$	0.7116(2)	0.0378(3)		[570]
	MC	0.71164(10)	0.03784(5)	0.759(2)	[570]

Table B.3: Estimates of the critical exponents of the 3D Heisenberg universality class (characterized by a global O(3) symmetry). We report the correlation-length exponent ν , the order-parameter exponent η , and the exponent ω associated with the leading scaling corrections. We report: SFT results obtained by resumming high-order perturbative expansions [547, 548] (6-loop calculations in the fixed-dimension and in the ε -expansion scheme), by using functional RG approaches [549], and the conformal field theory (CFT) bootstrap [568] approach; results obtained in lattice models by combining high-temperature and MC results [254, 569] and in MC simulations [570]. See Refs. [95, 570] for a more complete list of theoretical and experimental results.

Appendix C. Mean-field analysis of the low-temperature Higgs phases

In this appendix we present a mean-field analysis of the low-temperature Higgs phases of the LNAH model with $SU(N_c)$ gauge symmetry and N_f degenerate scalar flavors in the fundamental representation. This model has been discussed in Sec. 9.1. For more details see Ref. [99]. This analysis allows one to infer the symmetry properties of the low-temperature Higgs phases, which depend on the parameter v, the number of colors N_c and of flavors N_f . It is worth noting that this discussion applies to generic d-dimensional systems, therefore also to 4D space-time systems that may be relevant in the context of high-energy physics. Analogous analyses can be performed for $SU(N_c)$ theories with scalar matter in the adjoint representation [96, 98, 263], and $SO(N_c)$ gauge LNAH models [384].

The $SU(N_c)$ gauge model has different Higgs phases, whose symmetry corresponds to the symmetry of the minimum-energy configurations that dominate the partition function for $\beta \to \infty$. As discussed in Ref. [99] they are obtained by considering separately the minima of the scalar kinetic energy term (103) and of the scalar potential $V(\Phi)$, defined in Eq. (104).

The kinetic term (103) is minimized by the condition $\Phi_{\boldsymbol{x}} = U_{\boldsymbol{x},\mu} \Phi_{\boldsymbol{x}+\hat{\mu}}$, which implies $V(\Phi_{\boldsymbol{x}}) = V(\Phi_{\boldsymbol{x}+\hat{\mu}})$. It follows that minimum configurations are obtained by minimizing the potential energy on each lattice site. Therefore, below we neglect the \boldsymbol{x} dependence of the field. One can easily verify that the symmetry properties of the minimum-potential configurations do not depend on r and u, and therefore we only report explicit results for the unit-length limit in which $\operatorname{Tr} \Phi^{\dagger} \Phi = 1$.

To determine the minima of $V(\Phi)$, one may use the singular-value decomposition that allows one to rewrite the field Φ as $\Phi^{af} = \sum_{bg} C^{ab} W^{bg} F^{gf}$, where $C \in \mathrm{U}(N_c)$ and $F \in \mathrm{U}(N_f)$ are unitary matrices, and W is an $N_c \times N_f$ rectangular matrix. Its nondiagonal elements vanish $(W^{ij} = 0 \text{ for } i \neq j)$, while the diagonal elements are real and nonnegative, $W^{ii} = w_i > 0$ (i = 1, ..., q), with $q = \mathrm{Min}[N_f, N_c]$. Substituting the above expression in $V(\Phi)$, one obtains

$$V(\Phi) = \frac{v}{4} \text{Tr} (\Phi^{\dagger} \Phi)^2 = \frac{v}{4} \sum_{i=1}^{q} w_i^4, \qquad \text{Tr } \Phi^{\dagger} \Phi = \sum_{i=1}^{q} w_i^2 = 1.$$
 (C.1)

A straightforward minimization of the potential, subject to the unit-length constraint, gives two different solutions, depending on the sign of v, which are:

$$w_1 = 1, \quad w_2 = \dots = w_q = 0, \quad \text{for } v < 0;$$
 (C.2)

$$w_1 = \dots = w_q = 1/\sqrt{q}, \quad \text{for } v > 0, \quad \text{where } q = \text{Min}[N_f, N_c].$$
 (C.3)

The solution (C.2) for v < 0 allows one to rewrite the field as

$$\Phi^{af} = s^a z^f, \tag{C.4}$$

where s and z are unit-length complex vectors with N_c and N_f components, respectively, satisfying $\bar{s} \cdot s = 1$ and $\bar{z} \cdot z = 1$. Modulo gauge transformations, these solutions are invariant under $U(1) \oplus U(N_f - 1)$ transformations, leading to the global-symmetry breaking pattern $U(N_f) \to U(1) \oplus U(N_f - 1)$.

As discussed in Sec. 9.2.1, the model has a global U(1) symmetry that is not broken, so the relevant symmetry-breaking pattern is $SU(N_f) \to U(N_f-1)$, which is the same as for the \mathbb{CP}^{N_f-1} transition. Thus, if the gauge dynamics is not relevant at the transition, for v<0 we expect the non-Abelian gauge model with $U(N_f)$ global symmetry and the \mathbb{CP}^{N_f-1} model to have the same critical behavior, for any N_c . The correspondence between the two models can also be established by noting that the relevant order parameter at the transition is the bilinear operator P_x^{fg} defined in Eq. (108), which assumes the simple form $P_x^{fg} = \bar{z}_x^f z_x^g - \delta^{fg}/N_f$ on the minimum configurations. It is thus equivalent to a local projector $\bar{z}_x^f z_x^g$ onto a one-dimensional space. If we assume that the critical behavior of the gauge model is only determined by the fluctuations that preserve the minimum-energy structure, the effective scalar model that describes the critical fluctuations can be identified with the \mathbb{CP}^{N_f-1} model.

To exclude the possible presence of topological transitions, one should determine the gauge symmetry breaking pattern, as discussed in Sec. 3.5.3. If we repeatedly apply the relation $\Phi_x = U_{x,\mu}\Phi_{x+\hat{\mu}}$ along a

plaquette, we obtain the equation $\Phi_{\boldsymbol{x}} = \Pi_{\boldsymbol{x},\mu\nu}\Phi_{\boldsymbol{x}}$, where $\Pi_{\boldsymbol{x},\mu\nu}$ is the plaquette operator defined in Eq. (105). For minimum configurations of type (C.2), using Eq. (C.4), we have $s_{\boldsymbol{x}}^a = \sum_b \Pi_{\boldsymbol{x},\mu\nu}^{ab} s_{\boldsymbol{x}}^b$, i.e., the plaquette $\Pi_{\boldsymbol{x},\mu\nu}$ has one unit eigenvalue. Thus, for $\beta \to \infty$ there is still a residual $\mathrm{SU}(N_c-1)$ symmetry, independently of the flavor number N_f . Since $\mathrm{SU}(N_c-1)$ gauge models are always disordered, no topological transitions are expected.

The solution (C.3) for v > 0 implies more complex symmetry-breaking patterns. In particular, we must distinguish three different cases: $N_f < N_c$, $N_f = N_c$, and $N_f > N_c$. The minimum-potential configurations take the form:

$$\Phi^{af} = \frac{1}{\sqrt{q}} \delta^{af}, \quad \text{for } N_f < N_c; \tag{C.5}$$

$$\Phi^{af} = \frac{1}{\sqrt{q}} \delta^{af} \phi, \quad \phi \in U(1), \quad \text{for } N_f = N_c.$$
 (C.6)

$$\Phi^{af} = \frac{1}{\sqrt{N_c}} F^{af}, \qquad F \in U(N_f), \qquad \text{for } N_f > N_c.$$
 (C.7)

If we substitute these expressions in the relation $\Phi_{\boldsymbol{x}} = \Pi_{\boldsymbol{x},\mu\nu}\Phi_{\boldsymbol{x}}$ that follows from the minimization of the kinetic energy, one can verify that the plaquette $\Pi_{\boldsymbol{x},\mu\nu}$ has q unit eigenvalues. Thus, for $N_f \geq N_c$, $\Pi_{\boldsymbol{x},\mu\nu} = 1$ and the gauge variables are gauge equivalent to the trivial configuration, i.e., $U_{\boldsymbol{x},\mu} = V_{\boldsymbol{x}}^{\dagger}V_{\boldsymbol{x}+\hat{\mu}}$ where $V_{\boldsymbol{x}} \in \mathrm{SU}(N_c)$. These results allow us to exclude the presence of topological transitions, related to the residual gauge symmetry in the Higgs phase, see Sec. 3.5.3. Indeed, for $N_f \geq N_c$ there is no residual gauge symmetry, while for $N_f < N_c$, gauge modes are controlled by a residual $\mathrm{SU}(N_c - N_f)$ gauge theory that does not undergo finite-temperature transitions.

For $N_f \leq N_c$ the SU(N_f) symmetry cannot be broken. Indeed, if we compute the bilinear operator P_x^{fg} defined in Eq. (108) on the minimum configurations, it vanishes trivially. Equivalently, any SU(N_f) transformation leaves the minimum-potential configurations invariant. Thus, there is no global SU(N_f) symmetry breaking. As discussed in Sec. 9.2.1, this implies that no transition is expected for $N_f < N_c$. For $N_f = N_c$, as discussed in Sec. 9.2.1, the minimum configurations break the U(1) symmetry, and thus U(1) transitions are possible.

For $N_f > N_c$, the minimum-potential configurations take the form (C.7). In the ordered phase the relevant fluctuations are supposed to be those that preserve this structure. Therefore, the field Φ_x^{af} can be parameterized as in Eq. (C.7), with a site-dependent unitary matrix F_x . The link variable can be expressed as $U_{x,\mu} = V_x^{\dagger} V_{x+\hat{\mu}}$ with $V_x \in \mathrm{SU}(N_c)$ as all plaquettes are equal to the identity. Substituting this parametrization in the kinetic term (103) of the Hamiltonian, we obtain

$$H_K = -\frac{N_f}{N_c} \sum_{\boldsymbol{x}\mu} \operatorname{Re} \operatorname{Tr} \left(F_{\boldsymbol{x}}^{\dagger} \widehat{V}_{\boldsymbol{x}}^{\dagger} Y \widehat{V}_{\boldsymbol{x}+\hat{\mu}} F_{\boldsymbol{x}+\hat{\mu}} \right), \tag{C.8}$$

where $Y = I_{N_c} \oplus 0$ is an $N_f \times N_f$ diagonal matrix in which the first N_c elements are one and the other $N_f - N_c$ elements are zero, and $\hat{V} = V \oplus I_{N_f - N_c}$. This Hamiltonian is invariant under the global transformations $F_{\boldsymbol{x}} \to F_{\boldsymbol{x}} M$, with $M \in \mathrm{U}(N_f)$, and under the local transformations $F_{\boldsymbol{x}} \to W_{\boldsymbol{x}} F_{\boldsymbol{x}}$ and $\hat{V}_{\boldsymbol{x}} \to \hat{V}_{\boldsymbol{x}} G_{\boldsymbol{x}}$, with $W_{\boldsymbol{x}} = W_{\boldsymbol{x}}^{(1)} \oplus W_{\boldsymbol{x}}^{(2)}$ and $G_{\boldsymbol{x}} = W_{\boldsymbol{x}}^{(1)} \oplus I_{N_f - N_c}$, where $W_{\boldsymbol{x}}^{(1)} \in \mathrm{SU}(N_c)$, $W_{\boldsymbol{x}}^{(2)} \in \mathrm{U}(N_f - N_c)$ ($F_{\boldsymbol{x}}$ is unitary so that $F_{\boldsymbol{x}}^{\dagger} F_{\boldsymbol{x}} = I_{N_f}$). Therefore the global symmetry of the effective model that describes the critical fluctuations is $\mathrm{SU}(N_f)/[\mathrm{SU}(N_c) \otimes \mathrm{SU}(N_f - N_c)]$, which corresponds to the global symmetry-breaking pattern $\mathrm{U}(N_f) \to \mathrm{SU}(N_c) \otimes \mathrm{U}(N_f - N_c)$, where we have also included the unbroken U(1) symmetry.

References

- [1] S. Weinberg, The Quantum Theory of Fields, Cambridge University Press, Cambridge (UK), 2005.
- [2] J. Zinn-Justin, Quantum Field Theory and Critical Phenomena, Clarendon Press, Oxford (UK), 2002.
- [3] I. Montvay, G. Munster, Quantum Fields on a Lattice, Cambridge University Press, Cambridge (UK), 1994.
- [4] H. J. Rothe, Lattice Gauge Theories. An Introduction, World Scientific, Singapore (Singapore), 2005.

- [5] L. D. Landau, E. M. Lifshitz, Course of Theoretical Physics, vol. 5: Statistical Physics (Part 1), Elsevier Butterworth-Heinemann, Oxford (UK) Burlingto(MA), 1980.
- [6] K. G. Wilson, The renormalization group and critical phenomena, Rev. Mod. Phys. 55 (1983) 583. doi:10.1103/ RevModPhys.55.583.
- [7] P. W. Anderson, Basic Notions of Condensed Matter Physics, The Benjamin/Cummings Publishing Company, Menlo Park (CA), 1976.
- [8] C. Itzykson, J.-M. Drouffe, Statistical field theory: Volume 1. From Brownian motion to renormalization and lattice gauge theory, Cambridge University Press, Cambridge, 1989. doi:10.1017/CB09780511622779.
- [9] C. Itzykson, J.-M. Drouffe, Statistical field theory: Volume 2. Strong coupling, Monte Carlo methods, conformal field theory and random systems, Cambridge University Press, Cambridge, 1989. doi:10.1017/CB09780511622786.
- [10] G. Parisi, Statistical Field Theory, Addison-Wesley Publishing Company, Menlo Park (CA), 1994.
- [11] D. J. Amit, V. Martín-Mayor, Field theory, the renormalization group, and critical phenomena: Graphs to computers, 3rd Edition, World Scientific, Singapore, 2005. doi:10.1142/5715.
- [12] X. G. Wen, Quantum field theory of many-body systems: from the origin of sound to an origin of light and electrons, Oxford University Press, Oxford (UK), 2004.
- [13] E. H. Fradkin, Field theories of condensed matter physics, Cambridge University Press, Cambridge (UK), 2013.
- [14] S. Sachdev, Quantum Phase Transitions, Cambridge University Press, Cambridge (UK), 199.
- [15] B. Zeng, X. Chen, D.-L. Zhou, X.-G. Wen, Quantum information meets quantum matter: From quantum entanglement to topological phases of many-body systems, Springer-Verlag, New York, 2019. doi:10.1007/978-1-4939-9084-9.
- [16] S. Sachdev, Quantum Phases of Matter, Cambridge University Press, Cambridge (UK), 2023.
- [17] V. L. Ginzburg, L. D. Landau, On the Theory of superconductivity, Zh. Eksp. Teor. Fiz. 20 (1950) 1064. doi:10.1016/b978-0-08-010586-4.50078-x.
- [18] B. I. Halperin, T. C. Lubensky, S.-k. Ma, First-Order Phase Transitions in Superconductors and Smectic-A Liquid Crystals, Phys. Rev. Lett. 32 (1974) 292. doi:10.1103/PhysRevLett.32.292.
- [19] I. F. Herbut, A Modern Approach to Critical Phenomena, Cambridge University Press, Cambridge (UK), 2007.
- [20] S. Sachdev, Topological order, emergent gauge fields, and Fermi surface reconstruction, Rept. Prog. Phys. 82 (1) (2019) 014001. arXiv:1801.01125, doi:10.1088/1361-6633/aae110.
- [21] T. Senthil, Deconfined quantum critical points: a review, in: A. Aharony, O. Entin-Wohlman, D. Huse, L. Radzihovsky (Eds.), 50 years of the renormalization group, dedicated to the memory of Michael. E. Fisher, World Scientific, Singapore (Singapore), 2024. arXiv:2306.12638.
- [22] E. W. Kolb, M. S. Turner, The early universe, Addison-Wesley Publishing Company, Menlo Park (CA), 1994.
- [23] D. Boyanovsky, H. J. de Vega, D. J. Schwarz, Phase transitions in the early and the present universe, Ann. Rev. Nucl. Part. Sci. 56 (2006) 441. arXiv:hep-ph/0602002, doi:10.1146/annurev.nucl.56.080805.140539.
- [24] D. J. Gross, R. D. Pisarski, L. G. Yaffe, QCD and Instantons at Finite Temperature, Rev. Mod. Phys. 53 (1981) 43. doi:10.1103/RevModPhys.53.43.
- [25] R. D. Pisarski, F. Wilczek, Remarks on the Chiral Phase Transition in Chromodynamics, Phys. Rev. D 29 (1984) 338. doi:10.1103/PhysRevD.29.338.
- [26] J. Adams, et al., Experimental and theoretical challenges in the search for the quark gluon plasma: The STAR Collaboration's critical assessment of the evidence from RHIC collisions, Nucl. Phys. A 757 (2005) 102. arXiv:nucl-ex/0501009, doi:10.1016/j.nuclphysa.2005.03.085.
- [27] N. Read, S. Sachdev, Spin-Peierls, valence-bond solid, and Néel ground states of low-dimensional quantum antiferromagnets, Phys. Rev. B 42 (1990) 4568. doi:10.1103/PhysRevB.42.4568.
- [28] R. K. Kaul, Quantum phase transitions in bilayer SU(N) antiferromagnets, Phys. Rev. B 85 (2012) 180411. arXiv: 1203.6677, doi:10.1103/PhysRevB.85.180411.
- [29] R. K. Kaul, A. W. Sandvik, Lattice Model for the SU(N) Néel to Valence-Bond Solid Quantum Phase Transition at Large N, Phys. Rev. Lett. 108 (2012) 137201. arXiv:1110.4130, doi:10.1103/PhysRevLett.108.137201.
- [30] M. S. Block, R. G. Melko, R. K. Kaul, Fate of \mathbb{CP}^{N-1} Fixed Points with q Monopoles, Phys. Rev. Lett. 111 (2013) 137202. arXiv:1307.0519, doi:10.1103/PhysRevLett.111.137202.
- [31] A. Nahum, J. T. Chalker, P. Serna, M. Ortuño, A. M. Somoza, Deconfined Quantum Criticality, Scaling Violations, and Classical Loop Models, Phys. Rev. X 5 (2015) 041048. arXiv:1506.06798, doi:10.1103/PhysRevX.5.041048.
- [32] C. Wang, A. Nahum, M. A. Metlitski, C. Xu, T. Senthil, Deconfined quantum critical points: symmetries and dualities, Phys. Rev. X 7 (2017) 031051. arXiv:1703.02426, doi:10.1103/PhysRevX.7.031051.
- [33] T. Senthil, L. Balents, S. Sachdev, A. Vishwanath, M. P. A. Fisher, Quantum criticality beyond the Landau-Ginzburg-Wilson paradigm, Phys. Rev. B 70 (2004) 144407. arXiv:cond-mat/0312617, doi:10.1103/PhysRevB.70.144407.
- [34] A. W. Sandvik, Evidence for Deconfined Quantum Criticality in a Two-Dimensional Heisenberg Model with Four-Spin Interactions, Phys. Rev. Lett. 98 (2007) 227202. arXiv:cond-mat/0611343, doi:10.1103/PhysRevLett.98.227202.
- [35] R. G. Melko, R. K. Kaul, Scaling in the Fan of an Unconventional Quantum Critical Point, Phys. Rev. Lett. 100 (2008) 017203. arXiv:0707.2961, doi:10.1103/PhysRevLett.100.017203.
- [36] F. J. Jiang, M. Nyfeler, S. Chandrasekharan, U. J. Wiese, From an Antiferromagnet to a Valence Bond Solid: Evidence for a First-Order Phase Transition, J. Stat. Mech. 2008 (02) (2008) P02009. arXiv:0710.3926, doi:10.1088/1742-5468/ 2008/02/P02009.
- [37] A. W. Sandvik, Continuous quantum phase transition between an antiferromagnet and a valence-bond-solid in two dimensions: evidence for logarithmic corrections to scaling, Phys. Rev. Lett. 104 (2010) 177201. arXiv:1001.4296, doi:10.1103/PhysRevLett.104.177201.
- [38] K. Harada, T. Suzuki, T. Okubo, H. Matsuo, J. Lou, H. Watanabe, S. Todo, N. Kawashima, Possibility of deconfined

- criticality in SU(N) Heisenberg models at small N, Phys. Rev. B 88 (2013) 220408. arXiv:1307.0501, doi:10.1103/PhysRevB.88.220408.
- [39] K. Chen, Y. Huang, Y. Deng, A. B. Kuklov, N. V. Prokof'ev, B. V. Svistunov, Deconfined Criticality Flow in the Heisenberg Model with Ring-Exchange Interactions, Phys. Rev. Lett. 110 (2013) 185701. arXiv:1301.3136, doi:10. 1103/PhysRevLett.110.185701.
- [40] S. Pujari, K. Damle, F. Alet, Néel-State to Valence-Bond-Solid Transition on the Honeycomb Lattice: Evidence for Deconfined Criticality, Phys. Rev. Lett. 111 (2013) 087203. arXiv:1302.1408, doi:10.1103/PhysRevLett.111.087203.
- [41] E. H. Fradkin, S. H. Shenker, Phase Diagrams of Lattice Gauge Theories with Higgs Fields, Phys. Rev. D 19 (1979) 3682. doi:10.1103/PhysRevD.19.3682.
- [42] C. Dasgupta, B. I. Halperin, Phase Transition in a Lattice Model of Superconductivity, Phys. Rev. Lett. 47 (1981) 1556. doi:10.1103/PhysRevLett.47.1556.
- [43] J. Fröhlich, G. Morchio, F. Strocchi, Higgs phenomenon without symmetry breaking order parameter, Nucl. Phys. B 190 (1981) 553. doi:10.1016/0550-3213(81)90448-X.
- [44] J. Bricmont, J. Fröhlich, An order parameter distinguishing between different phases of lattice gauge theories with matter fields, Phys. Lett. B 122 (1983) 73. doi:10.1016/0370-2693(83)91171-1.
- [45] K. Fredenhagen, M. Marcu, Charged States in Z₂ Gauge Theories, Commun. Math. Phys. 92 (1983) 81. doi:10.1007/BF01206315.
- [46] T. Kennedy, C. King, Symmetry Breaking in the Lattice Abelian Higgs Model, Phys. Rev. Lett. 55 (1985) 776. doi: 10.1103/PhysRevLett.55.776.
- [47] T. Kennedy, C. King, Spontaneous Symmetry Breakdown in the Abelian Higgs Model, Commun. Math. Phys. 104 (1986) 327. doi:10.1007/BF01211599.
- [48] C. Borgs, F. Nill, Symmetry Breaking in Landau Gauge A comment to a paper by T. Kennedy and C. King, Commun. Math. Phys. 104 (1986) 349. doi:10.1007/BF01211600.
- [49] C. Borgs, F. Nill, No Higgs Mechanism in Scalar Lattice QED With Strong Electromagnetic Coupling, Phys. Lett. B 171 (1986) 289. doi:10.1016/0370-2693(86)91550-9.
- [50] C. Borgs, F. Nill, The Phase Diagram of the Abelian Lattice Higgs Model. A Review of Rigorous Results, J. Stat. Phys. 47 (1987) 877. doi:10.1007/BF01206163.
- [51] M. Kiometzis, H. Kleinert, A. M. J. Schakel, Critical Exponents of the Superconducting Phase Transition, Phys. Rev. Lett. 73 (1994) 1975. arXiv:cond-mat/9503019, doi:10.1103/PhysRevLett.73.1975.
- [52] B. Bergerhoff, F. Freire, D. F. Litim, A. Lola, C. Wetterich, Phase diagram of superconductors from nonperturbative flow equations, Phys. Rev. B 53 (1996) 5734. arXiv:hep-ph/9503334, doi:10.1103/PhysRevB.53.5734.
- [53] I. F. Herbut, Z. Tešanović, Critical fluctuations in superconductors and the magnetic field penetration depth, Phys. Rev. Lett. 76 (1996) 4588. arXiv:cond-mat/9605185, doi:10.1103/PhysRevLett.76.4588.
- [54] R. Folk, Y. Holovatch, On the critical fluctuations in superconductors, J. Phys. A 29 (1996) 3409. doi:10.1088/ 0305-4470/29/13/014.
- [55] V. Y. Irkhin, A. A. Katanin, M. I. Katsnelson, 1/N expansion for critical exponents of magnetic phase transitions in the CP^{N-1} model for 2 < d < 4, Phys. Rev. B 54 (1996) 11953. doi:10.1103/PhysRevB.54.11953.
- [56] K. Kajantie, M. Karjalainen, M. Laine, J. Peisa, Masses and phase structure in the Ginzburg-Landau model, Phys. Rev. B 57 (1998) 3011. arXiv:cond-mat/9704056, doi:10.1103/PhysRevB.57.3011.
- [57] P. Olsson, S. Teitel, Critical Behavior of the Meissner Transition in the Lattice London Superconductor, Phys. Rev. Lett. 80 (1998) 1964. arXiv:cond-mat/9710200, doi:10.1103/PhysRevLett.80.1964.
- [58] C. de Calan, F. S. Nogueira, Scaling critical behavior of superconductors at zero magnetic field, Phys. Rev. B 60 (1999) 4255. arXiv:cond-mat/9903247, doi:10.1103/PhysRevB.60.4255.
- [59] J. Hove, A. Sudbø, Anomalous Scaling Dimensions and Stable Charged Fixed Point of Type-II Superconductors, Phys. Rev. Lett. 84 (2000) 3426. arXiv:cond-mat/0002197, doi:10.1103/PhysRevLett.84.3426.
- [60] H. Kleinert, F. S. Nogueira, A. Sudbø, Deconfinement transition in three-dimensional compact U(1) gauge theories coupled to matter fields, Phys. Rev. Lett. 88 (2002) 232001. arXiv:hep-th/0201168, doi:10.1103/PhysRevLett.88. 232001.
- [61] S. Mo, J. Hove, A. Sudbø, The Order of the metal to superconductor transition, Phys. Rev. B 65 (2002) 104501. arXiv:cond-mat/0109260, doi:10.1103/PhysRevB.65.104501.
- [62] A. Sudbø, E. Smorgrav, J. Smiseth, F. S. Nogueira, J. Hove, Criticality in the (2+1)-dimensional compact Higgs model and fractionalized insulators, Phys. Rev. Lett. 89 (2002) 226403. arXiv:cond-mat/0207501, doi:10.1103/PhysRevLett. 89.226403.
- [63] J. Smiseth, E. Smorgrav, F. S. Nogueira, J. Hove, A. Sudbø, Phase structure of d = 2+1 compact lattice gauge theories and the transition from Mott insulator to fractionalized insulator, Phys. Rev. B 67 (2003) 205104. arXiv:cond-mat/0301297, doi:10.1103/PhysRevB.67.205104.
- [64] M. Moshe, J. Zinn-Justin, Quantum field theory in the large N limit: A Review, Phys. Rept. 385 (2003) 69. arXiv: hep-th/0306133, doi:10.1016/S0370-1573(03)00263-1.
- [65] T. Neuhaus, A. Rajantie, K. Rummukainen, Numerical study of duality and universality in a frozen superconductor, Phys. Rev. B 67 (2003) 014525. arXiv:cond-mat/0205523, doi:10.1103/PhysRevB.67.014525.
- [66] O. I. Motrunich, A. Vishwanath, Emergent photons and new transitions in the O(3) sigma model with hedgehog suppression, Phys. Rev. B 70 (2004) 075104. arXiv:cond-mat/0311222, doi:10.1103/PhysRevB.70.075104.
- [67] F. S. Nogueira, J. Smiseth, E. Smorgrav, A. Sudbø, Compact U(1) gauge theories in (2+1)-dimensions and the physics of low dimensional insulating materials, Eur. Phys. J. C 33 (2004) S885. arXiv:hep-th/0310100, doi:10.1140/epjcd/ s2003-03-1004-y.

- [68] J. Smiseth, E. Smorgrav, A. Sudbø, Critical properties of the N component Ginzburg-Landau model, Phys. Rev. Lett. 93 (2004) 077002. arXiv:cond-mat/0403417, doi:10.1103/PhysRevLett.93.077002.
- [69] M. B. Hastings, X.-G. Wen, Quasi-adiabatic continuation of quantum states: The Stability of topological ground state degeneracy and emergent gauge invariance, Phys. Rev. B 72 (2005) 045141. arXiv:cond-mat/0503554, doi:10.1103/ PhysRevB.72.045141.
- [70] M. N. Chernodub, R. Feldmann, E.-M. Ilgenfritz, A. Schiller, The Compact Q = 2 Abelian Higgs model in the London limit: Vortex-monopole chains and the photon propagator, Phys. Rev. D 71 (2005) 074502. arXiv:hep-lat/0502009, doi:10.1103/PhysRevD.71.074502.
- [71] S. Takashima, I. Ichinose, T. Matsui, CP¹ + U(1) lattice gauge theory in three dimensions: Phase structure, spins, gauge bosons, and instantons, Phys. Rev. B 72 (2005) 075112. arXiv:cond-mat/0504193, doi:10.1103/PhysRevB.72.075112.
- [72] S. Takashima, I. Ichinose, T. Matsui, Deconfinement of spinons on critical points: Multi-flavor CP1 + U(1) lattice gauge theory in three dimensions, Phys. Rev. B 73 (2006) 075119. arXiv:cond-mat/0511107, doi:10.1103/PhysRevB.73.075119.
- [73] M. N. Chernodub, E.-M. Ilgenfritz, A. Schiller, Phase structure of an Abelian two-Higgs model and high temperature superconductors, Phys. Rev. B 73 (2006) 100506. arXiv:cond-mat/0512111, doi:10.1103/PhysRevB.73.100506.
- [74] A. B. Kuklov, N. V. Prokof'ev, B. V. Svistunov, M. Troyer, Deconfined criticality, runaway flow in the two-component scalar electrodynamics and weak first-order superfluid-solid transitions, Ann. Phys. 321 (2006) 1602. arXiv:cond-mat/0602466, doi:10.1016/j.aop.2006.04.007.
- [75] S. Wenzel, E. Bittner, W. Janke, A. M. J. Schakel, Percolation of Vortices in the 3D Abelian Lattice Higgs Model, Nucl. Phys. B 793 (2008) 344. arXiv:0708.0903, doi:10.1016/j.nuclphysb.2007.10.024.
- [76] R. K. Kaul, S. Sachdev, Quantum criticality of U(1) gauge theories with fermionic and bosonic matter in two spatial dimensions, Phys. Rev. B 77 (2008) 155105. arXiv:0801.0723, doi:10.1103/PhysRevB.77.155105.
- [77] T. Ono, S. Doi, Y. Hori, I. Ichinose, T. Matsui, Phase structure and critical behavior of multi-Higgs U(1) lattice gauge theory in three dimensions, Annals Phys. 324 (2009) 2453. arXiv:0712.2291, doi:10.1016/j.aop.2009.09.002.
- [78] G. Chen, J. Gukelberger, S. Trebst, F. Alet, L. Balents, Coulomb gas transitions in three-dimensional classical dimer models, Phys. Rev. B 80 (2009) 045112. arXiv:0903.3944, doi:10.1103/PhysRevB.80.045112.
- [79] T. A. Bojesen, A. Sudbø, Berry phases, current lattices, and suppression of phase transitions in a lattice gauge theory of quantum antiferromagnets, Phys. Rev. B 88 (2013) 094412. arXiv:1306.2949, doi:10.1103/PhysRevB.88.094412.
- [80] G. J. Sreejith, S. Powell, Scaling dimensions of higher-charge monopoles at deconfined critical points, Phys. Rev. B 92 (2015) 184413. arXiv:1504.02278, doi:10.1103/PhysRevB.92.184413.
- [81] G. Fejős, T. Hatsuda, Renormalization group flows of the N-component Abelian Higgs model, Phys. Rev. D 96 (5) (2017) 056018, arXiv:1705.07333, doi:10.1103/PhysRevD.96.056018.
- [82] A. Pelissetto, E. Vicari, Three-dimensional ferromagnetic CP(N-1) models, Phys. Rev. E 100 (2019) 022122. arXiv: 1905.03307, doi:10.1103/PhysRevE.100.022122.
- [83] B. Ihrig, N. Zerf, P. Marquard, I. F. Herbut, M. M. Scherer, Abelian Higgs model at four loops, fixed-point collision and deconfined criticality, Phys. Rev. B 100 (2019) 134507. arXiv:1907.08140, doi:10.1103/PhysRevB.100.134507.
- [84] A. Pelissetto, E. Vicari, Multicomponent compact Abelian-Higgs lattice models, Phys. Rev. E 100 (2019) 042134. arXiv: 1909.04137, doi:10.1103/PhysRevE.100.042134.
- [85] A. Pelissetto, E. Vicari, Three-dimensional monopole-free CP^{N-1} models, Phys. Rev. E 101 (2020) 062136. arXiv: 2003.14075, doi:10.1103/PhysRevE.101.062136.
- [86] C. Bonati, A. Pelissetto, E. Vicari, Higher-charge three-dimensional compact lattice Abelian-Higgs models, Phys. Rev. E 102 (2020) 062151. arXiv:2011.04503, doi:10.1103/PhysRevE.102.062151.
- [87] C. Bonati, A. Pelissetto, E. Vicari, Lattice Abelian-Higgs model with noncompact gauge fields, Phys. Rev. B 103 (2021) 085104. arXiv:2010.06311, doi:10.1103/PhysRevB.103.085104.
- [88] D. Weston, E. Babaev, Composite order in SU(N) theories coupled to an Abelian gauge field, Phys. Rev. B 104 (2021) 075116. arXiv:1908.10847, doi:10.1103/PhysRevB.104.075116.
- [89] C. Bonati, A. Pelissetto, E. Vicari, Three-dimensional monopole-free CP^{N-1} models: behavior in the presence of a quartic potential, J. Stat. Mech. 2206 (2022) 063206. arXiv:2202.04614, doi:10.1088/1742-5468/ac7795.
- [90] C. Bonati, A. Pelissetto, E. Vicari, Critical behaviors of lattice U(1) gauge models and three-dimensional Abelian-Higgs gauge field theory, Phys. Rev. B 105 (2022) 085112. arXiv:2201.01082, doi:10.1103/PhysRevB.105.085112.
- [91] C. Bonati, A. Pelissetto, E. Vicari, Coulomb-Higgs phase transition of three-dimensional lattice Abelian Higgs gauge models with noncompact gauge variables and gauge fixing, Phys. Rev. E 108 (2023) 044125. arXiv:2305.15236, doi: 10.1103/PhysRevE.108.044125.
- [92] C. Bonati, A. Pelissetto, E. Vicari, Deconfinement transitions in three-dimensional compact lattice Abelian Higgs models with multiple-charge scalar fields, Phys. Rev. E 109 (2024) 044146. arXiv:2402.06374, doi:10.1103/PhysRevE.109. 044146.
- [93] C. Bonati, A. Pelissetto, E. Vicari, Diverse universality classes of the topological deconfinement transitions of three-dimensional noncompact lattice Abelian Higgs models, Phys. Rev. D 109 (2024) 034517. arXiv:2308.00101, doi:10.1103/PhysRevD.109.034517.
- [94] K. G. Wilson, J. B. Kogut, The Renormalization group and the epsilon expansion, Phys. Rept. 12 (1974) 75. doi: 10.1016/0370-1573(74)90023-4.
- [95] A. Pelissetto, E. Vicari, Critical phenomena and renormalization group theory, Phys. Rept. 368 (2002) 549. arXiv: cond-mat/0012164, doi:10.1016/S0370-1573(02)00219-3.
- [96] S. Sachdev, H. D. Scammell, M. S. Scheurer, G. Tarnopolsky, Gauge theory for the cuprates near optimal doping, Phys. Rev. B 99 (2019) 054516. arXiv:1811.04930, doi:10.1103/PhysRevB.99.054516.
- [97] C. Bonati, A. Pelissetto, E. Vicari, Phase diagram, symmetry breaking, and critical behavior of three-dimensional lattice

- multiflavor scalar chromodynamics, Phys. Rev. Lett. 123 (2019) 232002. arXiv:1910.03965, doi:10.1103/PhysRevLett. 123.232002.
- [98] C. Bonati, A. Franchi, A. Pelissetto, E. Vicari, Three-dimensional lattice SU(Nc) gauge theories with multiflavor scalar fields in the adjoint representation, Phys. Rev. B 104 (2021) 115166. arXiv:2106.15152, doi:10.1103/PhysRevB.104. 115166.
- [99] C. Bonati, A. Franchi, A. Pelissetto, E. Vicari, Phase diagram and Higgs phases of three-dimensional lattice SU(Nc) gauge theories with multiparameter scalar potentials, Phys. Rev. E 104 (2021) 064111. arXiv:2110.01657, doi:10.1103/PhysRevE.104.064111.
- [100] K. G. Wilson, Confinement of Quarks, Phys. Rev. D 10 (1974) 2445. doi:10.1103/PhysRevD.10.2445.
- [101] D. Rossini, E. Vicari, Coherent and dissipative dynamics at quantum phase transitions, Phys. Rept. 936 (2021) 1. arXiv:2103.02626, doi:10.1016/j.physrep.2021.08.003.
- [102] P. W. Anderson, Plasmons, Gauge Invariance, and Mass, Phys. Rev. 130 (1963) 439. doi:10.1103/PhysRev.130.439.
- [103] F. Englert, R. Brout, Broken Symmetry and the Mass of Gauge Vector Mesons, Phys. Rev. Lett. 13 (1964) 321. doi: 10.1103/PhysRevLett.13.321.
- [104] P. W. Higgs, Broken Symmetries and the Masses of Gauge Bosons, Phys. Rev. Lett. 13 (1964) 508. doi:10.1103/ PhysRevLett.13.508.
- [105] G. S. Guralnik, C. R. Hagen, T. W. B. Kibble, Global Conservation Laws and Massless Particles, Phys. Rev. Lett. 13 (1964) 585. doi:10.1103/PhysRevLett.13.585.
- [106] E. Farhi, L. Susskind, Technicolor, Phys. Rept. 74 (1981) 277. doi:10.1016/0370-1573(81)90173-3.
- [107] R. K. Kaul, Technicolor, Rev. Mod. Phys. 55 (1983) 449. doi:10.1103/RevModPhys.55.449.
- [108] K. D. Lane, Technicolor 2000, Frascati Phys. Ser. 18 (2000) 235. arXiv:hep-ph/0007304.
- [109] R. Contino, The Higgs as a Composite Nambu-Goldstone Boson, in: Theoretical Advanced Study Institute in Elementary Particle Physics: Physics of the Large and the Small, 2011, p. 235. arXiv:1005.4269, doi:10.1142/9789814327183_0005.
- [110] G. Cacciapaglia, C. Pica, F. Sannino, Fundamental Composite Dynamics: A Review, Phys. Rept. 877 (2020) 1. arXiv: 2002.04914, doi:10.1016/j.physrep.2020.07.002.
- [111] D. J. E. Callaway, Triviality Pursuit: Can Elementary Scalar Particles Exist?, Phys. Rept. 167 (1988) 241. doi: 10.1016/0370-1573(88)90008-7.
- [112] M. E. Fisher, The nature of critical points, in: W. E. Brittin (Ed.), Lecture notes in Theoretical Physics, vol. 7c, University of Colorado Press, Boulder (Colorado), 1965.
- [113] M. E. Fisher, The renormalization group in the theory of critical behavior, Rev. Mod. Phys. 46 (1974) 597, [Erratum: Rev. Mod. Phys. 47, 543 (1975)]. doi:10.1103/RevModPhys.46.597.
- [114] S.-k. Ma, Modern theory of critical phenomena, Rourledge, New York (USA), 2001.
- [115] K. Binder, Theory of first-order phase transitions, Rep. Prog. Phys. 50 (1987) 783. doi:10.1088/0034-4885/50/7/001.
- [116] M. E. Fisher, Excursions In The Land Of Statistical Physics, World Scientific, Singapore (Singapore), 2016.
- [117] A. Pelissetto, E. Vicari, Scaling behaviors at quantum and classical first-order transitions, in: A. Aharony, O. Entin-Wohlman, D. Huse, L. Radzihovsky (Eds.), 50 years of the renormalization group, dedicated to the memory of Michael. E. Fisher, World Scientific, Singapore (Singapore), 2024. arXiv:2302.08238.
- [118] S. L. Sondhi, S. M. Girvin, J. P. Carini, D. Shahar, Continuous quantum phase transitions, Rev. Mod. Phys. 69 (1997) 315. arXiv:cond-mat/9609279, doi:10.1103/RevModPhys.69.315.
- [119] F. J. Wegner, Duality in Generalized Ising Models and Phase Transitions Without Local Order Parameters, J. Math. Phys. 12 (1971) 2259. doi:10.1063/1.1665530.
- [120] S. Sachdev, Emergent gauge fields and the high temperature superconductors, Phil. Trans. Roy. Soc. Lond. A 374 (2016) 20150248. arXiv:1512.00465, doi:10.1098/rsta.2015.0248.
- [121] D. Ruelle, Classical statistical mechanics of a system of particles, Helv. Phys. Acta 36 (1963) 183. URL https://www.e-periodica.ch/digbib/view?pid=hpa-001:1963:36::1128#187
- [122] D. Ruelle, Statistical mechanics of quantum systems of particles, Helv. Phys. Acta 36 (1963) 789. URL https://www.e-periodica.ch/digbib/view?pid=hpa-001:1963:36::1167#793
- [123] M. E. Fisher, The free energy of a macroscopic system, Arch. Rational Mech. Anal. 17 (1964) 377. doi:10.1007/ BF00250473.
- [124] E. Brézin, J. Le Guillou, J. C. Zinn-Justin, Field theoretical approach to critical phenomena, in: C. Domb, M. S. Green (Eds.), Phase transitions and critical phenomena, vol. 6, Academic Press, London (UK), 1976.
- [125] F. J. Wegner, The Critical State, General Aspects, in: C. Domb, M. S. Green (Eds.), Phase transitions and critical phenomena, vol. 6, Academic Press, London (UK), 1976.
- [126] M. E. Fisher, G. W. Milton, Classifying first-order phase transitions, Phsica A 138 (1986) 22. doi:10.1016/0378-4371(86) 90172-X.
- [127] M. E. Fisher, Renormalization group theory: Its basis and formulation in statistical physics, Rev. Mod. Phys. 70 (1998) 653. doi:10.1103/RevModPhys.70.653.
- [128] L. P. Kadanoff, Spin-spin correlations in the two-dimensional Ising model, Nuovo Cimento B 44 (1966) 276. doi: 10.1007/BF02710808.
- [129] M. E. Fisher, Critical phenomena, in: M. S. Green (Ed.), Proceedings of the International School of Physics "Enrico Fermi", Varenna, Italy, July 27–August 8, 1970. Course 51, Academic Press, New York, 1971.
- [130] A. Aharony, Dependence of universal critical behavior on symmetry and range of interaction, in: C. Domb, M. S. Green (Eds.), Phase transitions and critical phenomena, vol. 6, Academic Press, London (UK), 1976.
- [131] M. Creutz, Quarks, gluons and lattices, Cambridge University Press, Cambridge (UK), 1983.
- [132] D. B. Abraham, Surface structures and phase transitions Exact results, in: C. Domb, J. L. Lebowitz (Eds.), Phase

- transitions and critical phenomena, Vol. 10, Academic Press, New York, 1986.
- [133] G. G. Cabrera, R. Jullien, Universality of finite-size scaling: Role of the boundary conditions, Phys. Rev. Lett. 57 (1986) 393. doi:10.1103/PhysRevLett.57.393.
- [134] J. Cardy (Ed.), Finite-size scaling, North Holland, Amsterdam (Netherlands), 1988.
- [135] V. E. Privman, Finite size scaling and numerical simulation of statistical system, World Scientific, Singapore (Singapore), 1990.
- [136] V. Privman, P. C. Hohenberg, A. Aharony, Universal critical-point amplitude relations, in: C. Domb, J. L. Lebowitz (Eds.), Phase transitions and critical phenomena, Vol. 14, Academic Press, London, 1991.
- [137] J. Cardy, Scaling and renormalization in statistical physics, Cambridge University Press, Cambridge, 1996. doi:10.1017/ CB09781316036440.
- [138] M. Campostrini, A. Pelissetto, E. Vicari, Finite-size scaling at quantum transitions, Phys. Rev. B 89 (2014) 094516.
 arXiv:1401.0788, doi:10.1103/PhysRevB.89.094516.
- [139] M. P. A. Fisher, P. B. Weichman, G. Grinstein, D. S. Fisher, Boson localization and the superfluid-insulator transition, Phys. Rev. B 40 (1989) 546. doi:10.1103/PhysRevB.40.546.
- [140] B. Schmittmann, R. K. P. Zia, Statistical mechanics of driven diffusive systems, in: C. Domb, J. L. Lebowitz (Eds.), Phase transitions and critical phenomena, Vol. 17, Academic Press, London, 1995.
- [141] L. D. Landau, On the theory of phase transitions. I., Phys. Z. Sowjetunion 11 (1937) 26.
- [142] L. D. Landau, On the theory of phase transitions. II., Phys. Z. Sowjetunion 11 (1937) 545.
- [143] R. Savit, Duality in Field Theory and Statistical Systems, Rev. Mod. Phys. 52 (1980) 453. doi:10.1103/RevModPhys. 52.453.
- [144] L. P. Kadanoff, Scaling laws for Ising models near T_c, Physics Physique Fizika 2 (1966) 263. doi:10.1103/ PhysicsPhysiqueFizika.2.263.
- [145] K. G. Wilson, Renormalization group and critical phenomena. I. Renormalization group and the Kadanoff scaling picture, Phys. Rev. B 4 (1971) 3174. doi:10.1103/PhysRevB.4.3174.
- [146] K. G. Wilson, Renormalization group and critical phenomena. II. Phase-space cell analysis of critical behavior, Phys. Rev. B 4 (1971) 3184. doi:10.1103/PhysRevB.4.3184.
- [147] E. Brézin, J. C. Le Guillou, J. Zinn-Justin, Discussion of critical phenomena for general n-vector models, Phys. Rev. B 10 (1974) 892. doi:10.1103/PhysRevB.10.892.
- [148] E. Vicari, J. Zinn-Justin, Fixed point stability and decay of correlations, New J. Phys. 8 (2006) 321. arXiv:cond-mat/0611353, doi:10.1088/1367-2630/8/12/321.
- [149] E. Vicari, Critical phenomena and renormalization-group flow of multi-parameter Φ⁴ field theories, PoS Lattice 2007 (2008) 023. arXiv:0709.1014, doi:10.22323/1.042.0023.
- [150] J. M. Carmona, A. Pelissetto, E. Vicari, The N component Ginzburg-Landau Hamiltonian with cubic anisotropy: A Six loop study, Phys. Rev. B 61 (2000) 15136. arXiv:cond-mat/9912115, doi:10.1103/PhysRevB.61.15136.
- [151] A. B. Harris, Effect of random defects on the critical behaviour of Ising models, J. Phys. C 7 (9) (1974) 1671. doi: 10.1088/0022-3719/7/9/009.
- [152] A. Pelissetto, E. Vicari, Randomly dilute spin models: A six-loop field-theoretic study, Phys. Rev. B 62 (2000) 6393. arXiv:cond-mat/0002402, doi:10.1103/PhysRevB.62.6393.
- [153] A. Aharony, Critical behavior of amorphous magnets, Phys. Rev. B 12 (1975) 1038. doi:10.1103/PhysRevB.12.1038.
- [154] P. Calabrese, A. Pelissetto, E. Vicari, Spin models with random anisotropy and reflection symmetry, Phys. Rev. E 70 (2004) 036104. arXiv:cond-mat/0311576, doi:10.1103/PhysRevE.70.036104.
- [155] H. Kawamura, Universality of phase transitions of frustrated antiferromagnets, J. Phys.: Condens. Matter 10 (1998) 4707. arXiv:cond-mat/9805134, doi:10.1088/0953-8984/10/22/004.
- [156] A. Pelissetto, P. Rossi, E. Vicari, Critical behavior of frustrated spin models with noncollinear order, Phys. Rev. B 63 (2001) 140414(R). arXiv:cond-mat/0007389, doi:10.1103/PhysRevB.63.140414.
- [157] A. Pelissetto, P. Rossi, E. Vicari, Large-N critical behavior of O(n)×O(m) spin models, Nucl. Phys. B 607 (2001) 605. arXiv:hep-th/0104024, doi:10.1016/S0550-3213(01)00223-1.
- [158] P. Calabrese, P. Parruccini, A. I. Sokolov, Chiral phase transitions: Focus driven critical behavior in systems with planar and vector ordering, Phys. Rev. B 66 (2002) 180403(R). arXiv:cond-mat/0205046, doi:10.1103/PhysRevB.66.180403.
- [159] B. Delamotte, D. Mouhanna, M. Tissier, Nonperturbative renormalization-group approach to frustrated magnets, Phys. Rev. B 69 (2004) 134413. arXiv:cond-mat/0309101, doi:10.1103/PhysRevB.69.134413.
- [160] P. Calabrese, P. Parruccini, A. Pelissetto, E. Vicari, Critical behavior of O(2)⊗O(N)-symmetric models, Phys. Rev. B 70 (2004) 174439. arXiv:cond-mat/0405667, doi:10.1103/PhysRevB.70.174439.
- [161] Y. Zhang, E. Demler, S. Sachdev, Competing orders in a magnetic field: Spin and charge order in the cuprate superconductors, Phys. Rev. B 66 (2002) 094501. arXiv:cond-mat/0112343, doi:10.1103/PhysRevB.66.094501.
- [162] S. Sachdev, Colloquium: Order and quantum phase transitions in the cuprate superconductors, Rev. Mod. Phys. 75 (2003) 913. arXiv:cond-mat/0211005, doi:10.1103/RevModPhys.75.913.
- [163] M. De Prato, A. Pelissetto, E. Vicari, Normal-to-planar superfluid transition in ³He, Phys. Rev B 70 (2004) 214519. arXiv:cond-mat/0312362, doi:10.1103/PhysRevB.70.214519.
- [164] M. De Prato, A. Pelissetto, E. Vicari, Spin-density-wave order in cuprates, Phys. Rev. B 74 (2006) 144507. arXiv: cond-mat/0601404, doi:10.1103/PhysRevB.74.144507.
- [165] A. Pelissetto, S. Sachdev, E. Vicari, Nodal quasiparticles and the onset of spin-density-wave order in cuprate superconductors, Phys. Rev. Lett. 101 (2008) 027005. arXiv:0802.0199, doi:10.1103/PhysRevLett.101.027005.
- [166] E.-A. Kim, M. J. Lawler, P. Oreto, S. Sachdev, E. Fradkin, S. A. Kivelson, Theory of the nodal nematic quantum phase transition in superconductors, Phys. Rev. B 77 (2008) 184514. arXiv:0705.4099, doi:10.1103/PhysRevB.77.184514.

- [167] A. Pelissetto, A. Tripodo, E. Vicari, Landau-Ginzburg-Wilson approach to critical phenomena in the presence of gauge symmetries, Phys. Rev. D 96 (2017) 034505. arXiv:1706.04365, doi:10.1103/PhysRevD.96.034505.
- [168] A. Pelissetto, A. Tripodo, E. Vicari, Criticality of O(N) symmetric models in the presence of discrete gauge symmetries, Phys. Rev. E 97 (2018) 012123. arXiv:1711.04567, doi:10.1103/PhysRevE.97.012123.
- [169] C. Bonati, A. Pelissetto, E. Vicari, Three-dimensional lattice multiflavor scalar chromodynamics: interplay between global and gauge symmetries, Phys. Rev. D 101 (2020) 034505. arXiv:2001.01132, doi:10.1103/PhysRevD.101.034505.
- [170] A. Butti, A. Pelissetto, E. Vicari, On the nature of the finite temperature transition in QCD, JHEP 08 (2003) 029. arXiv:hep-ph/0307036, doi:10.1088/1126-6708/2003/08/029.
- [171] A. Pelissetto, E. Vicari, Relevance of the axial anomaly at the finite-temperature chiral transition in QCD, Phys. Rev. D 88 (2013) 105018. arXiv:1309.5446, doi:10.1103/PhysRevD.88.105018.
- [172] M. E. Fisher, D. R. Nelson, Spin Flop, Supersolids, and Bicritical and Tetracritical Points, Phys. Rev. Lett. 32 (1974) 1350. doi:10.1103/PhysRevLett.32.1350.
- [173] D. R. Nelson, J. M. Kosterlitz, M. E. Fisher, Renormalization-Group Analysis of Bicritical and Tetracritical Points, Phys. Rev. Lett. 33 (1974) 813. doi:10.1103/PhysRevLett.33.813.
- [174] J. M. Kosterlitz, D. R. Nelson, M. E. Fisher, Bicritical and tetracritical points in anisotropic antiferromagnetic systems, Phys. Rev. B 13 (1976) 412. doi:10.1103/PhysRevB.13.412.
- [175] P. Calabrese, A. Pelissetto, E. Vicari, Multicritical phenomena in $O(n_1) \oplus O(n_2)$ -symmetric theories, Phys. Rev. B 67 (2003) 054505. arXiv:cond-mat/0209580, doi:10.1103/PhysRevB.67.054505.
- [176] C. Bonati, A. Pelissetto, E. Vicari, Multicritical point of the three-dimensional Z₂ gauge Higgs model, Phys. Rev. B 105 (2022) 165138. arXiv:2112.01824, doi:10.1103/PhysRevB.105.165138.
- [177] A. Pelissetto, E. Vicari, Interacting N-vector order parameters with O(N) symmetry, Condensed Matter Phys. 8 (2005) 87. arXiv:hep-th/0409214, doi:10.5488/CMP.8.1.87.
- [178] M. Hasenbusch, A. Pelissetto, E. Vicari, Instability of the O(5) multicritical behavior in the SO(5) theory of high-T(c) superconductors, Phys. Rev. B 72 (2005) 014532. arXiv:cond-mat/0502327, doi:10.1103/PhysRevB.72.014532.
- [179] A. Kudlis, A. Aharony, O. Entin-Wohlman, Effective exponents near bicritical points, Eur. Phys. J. Spec. Top. 232 (2023) 3471. arXiv:2304.08265, doi:10.1140/epjs/s11734-023-00971-w.
- [180] A. Aharony, 50 years of correlations with Michael Fisher and the renormalization group, in: A. Aharony, O. Entin-Wohlman, D. Huse, L. Radzihovsky (Eds.), 50 years of the renormalization group, dedicated to the memory of Michael. E. Fisher, World Scientific, Singapore (Singapore), 2024. arXiv:2305.13940.
- [181] M. Z. Hasan, C. L. Kane, Colloquium: Topological insulators, Rev. Mod. Phys. 82 (2010) 3045. arXiv:1002.3895, doi:10.1103/RevModPhys.82.3045.
- [182] X.-L. Qi, S.-C. Zhang, Topological insulators and superconductors, Rev. Mod. Phys. 83 (2011) 1057. arXiv:1008.2026, doi:10.1103/RevModPhys.83.1057.
- [183] C. Xu, Unconventional quantum critical points, Int. J. Mod. Phys. B 26 (2012) 1230007. arXiv:1202.6065, doi:10. 1142/S0217979212300071.
- [184] T. Gulden, M. Janas, Y. Wang, A. Kamenev, Universal finite-size scaling around topological quantum phase transitions, Phys. Rev. Lett. 116 (2016) 026402. arXiv:1508.03646, doi:10.1103/PhysRevLett.116.026402.
- [185] K. Gregor, D. A. Huse, R. Moessner, S. L. Sondhi, Diagnosing Deconfinement and Topological Order, New J. Phys. 13 (2011) 025009. arXiv:1011.4187, doi:10.1088/1367-2630/13/2/025009.
- [186] S. Dusuel, M. Kamfor, R. Orus, K. P. Schmidt, J. Vidal, Robustness of a perturbed topological phase, Phys. Rev. Lett. 106 (2011) 107203. arXiv:1012.1740, doi:10.1103/PhysRevLett.106.107203.
- [187] B. Huckestein, Scaling theory of the integer quantum Hall effect, Rev. Mod. Phys. 67 (1995) 357. arXiv:cond-mat/9501106, doi:10.1103/RevModPhys.67.357.
- [188] T. H. Hansson, M. Hermanns, S. H. Simon, S. F. Viefers, Quantum Hall physics: Hierarchies and conformal field theory techniques, Rev. Mod. Phys. 89 (2017) 025005. arXiv:1601.01697, doi:10.1103/RevModPhys.89.025005.
- [189] A. J. M. Giesbers, U. Zeitler, L. A. Ponomarenko, R. Yang, K. S. Novoselov, A. K. Geim, J. C. Maan, Scaling of the quantum Hall plateau-plateau transition in graphene, Phys. Rev. B 80 (2009) 241411(R). arXiv:0908.0461, doi: 10.1103/PhysRevB.80.241411.
- [190] H. Obuse, I. A. Gruzberg, F. Evers, Finite-size effects and irrelevant corrections to scaling near the integer quantum Hall transition, Phys. Rev. Lett. 109 (2012) 206804. arXiv:1205.2763, doi:10.1103/PhysRevLett.109.206804.
- [191] T. Senthil, A. Vishwanath, L. Balents, S. Sachdev, M. P. A. Fisher, Deconfined quantum critical points, Science 303 (2004) 1490. arXiv:cond-mat/0311326, doi:10.1126/science.1091806.
- [192] A. B. Kuklov, M. Matsumoto, N. V. Prokof'ev, B. V. Svistunov, M. Troyer, Deconfined Criticality: Generic First-Order Transition in the SU(2) Symmetry Case, Phys. Rev. Lett. 101 (2008) 050405. doi:10.1103/PhysRevLett.101.050405.
- [193] A. Banerjee, K. Damle, F. Alet, Impurity spin texture at a deconfined quantum critical point, Phys. Rev. B 82 (2010) 155139. arXiv:1002.1375, doi:10.1103/PhysRevB.82.155139.
- [194] L. Bartosch, Corrections to scaling in the critical theory of deconfined criticality, Phys. Rev. B 88 (2013) 195140. arXiv:1307.3276, doi:10.1103/PhysRevB.88.195140.
- [195] R. Ma, C. Wang, Theory of deconfined pseudocriticality, Phys. Rev. B 102 (2020) 020407. arXiv:1912.12315, doi: 10.1103/PhysRevB.102.020407.
- [196] P. Serna, A. Nahum, Emergence and spontaneous breaking of approximate O(4) symmetry at a weakly first-order deconfined phase transition, Phys. Rev. B 99 (2019) 195110. arXiv:1805.03759, doi:10.1103/PhysRevB.99.195110.
- [197] A. W. Sandvik, B. Zhao, Consistent scaling exponents at the deconfined quantum-critical point, Chin. Phys. Lett. 37 (2020) 057502. arXiv:2003.14305, doi:10.1088/0256-307X/37/5/057502.
- [198] S. M. Chester, N. Su, Bootstrapping Deconfined Quantum Tricriticality (2023). arXiv:2310.08343.

- [199] B. Zhao, J. Takahashi, A. W. Sandvik, Multicritical deconfined quantum-criticality and Lifshitz point of a helical valence-bond phase, Phys. Rev. Lett. 125 (25) (2020) 257204. arXiv:2005.10184, doi:10.1103/PhysRevLett.125.257204.
- [200] D.-C. Lu, C. Xu, Y.-Z. You, Self-duality protected multicriticality in deconfined quantum phase transitions, Phys. Rev. B 104 (20) (2021) 205142. arXiv:2104.05147, doi:10.1103/PhysRevB.104.205142.
- [201] Y. Cui, L. Liu, H. Lin, K. H. Wu, W. Hong, X. Liu, C. Li, Z. Hu, N. Xi, S. Li, R. Yu, A. W. Sandvik, W. Yu, Proximate deconfined quantum critical point in SrCu₂(BO₃)₂, Science 380 (6650) (2023) 1179. arXiv:2204.08133, doi:10.1126/science.adc9487.
- [202] M. Song, J. Zhao, L. Janssen, M. M. Scherer, Z. Y. Meng, Deconfined quantum criticality lost (2023). arXiv:2307.02547.
- [203] J. D'Emidio, A. W. Sandvik, Entanglement entropy and deconfined criticality: emergent SO(5) symmetry and proper lattice bipartition (2024). arXiv:2401.14396.
- [204] S. Elitzur, Impossibility of Spontaneously Breaking Local Symmetries, Phys. Rev. D 12 (1975) 3978. doi:10.1103/ PhysRevD.12.3978.
- [205] G. F. De Angelis, D. de Falco, F. Guerra, A Note on the Abelian Higgs-Kibble Model on a Lattice: Absence of Spontaneous Magnetization, Phys. Rev. D 17 (1978) 1624. doi:10.1103/PhysRevD.17.1624.
- [206] E. Rabinovici, S. Samuel, The CP^{n-1} Model: A Strong Coupling Lattice Approach, Phys. Lett. B 101 (1981) 323. doi:10.1016/0370-2693(81)90054-X.
- [207] P. Di Vecchia, A. Holtkamp, R. Musto, F. Nicodemi, R. Pettorino, Lattice CP^{N-1} Models and Their Large N Behavior, Nucl. Phys. B 190 (1981) 719. doi:10.1016/0550-3213(81)90047-X.
- [208] B. Berg, M. Lüscher, Definition and Statistical Distributions of a Topological Number in the Lattice O(3) Sigma Model, Nucl. Phys. B 190 (1981) 412. doi:10.1016/0550-3213(81)90568-X.
- [209] F. Delfino, A. Pelissetto, E. Vicari, Three-dimensional antiferromagnetic CP^{N-1} models, Phys. Rev. E 91 (2015) 052109. arXiv:1502.07599, doi:10.1103/PhysRevE.91.052109.
- [210] A. Pelissetto, E. Vicari, Large-N behavior of three-dimensional lattice CP^{N-1} models, J. Stat. Mech. 2003 (2020) 033209. arXiv:1912.04597, doi:10.1088/1742-5468/ab7747.
- [211] K. Kataoka, S. Hattori, I. Ichinose, Effective field theory for Sp(N) antiferromagnets and its phase structure, Phys. Rev. B 83 (2011) 174449. arXiv:1003.5412, doi:10.1103/PhysRevB.83.174449.
- [212] A. Nahum, J. T. Chalker, P. Serna, M. Ortuño, A. M. Somoza, 3D Loop Models and the CPⁿ⁻¹ Sigma Model, Phys. Rev. Lett. 107 (2011) 110601. arXiv:1104.4096, doi:10.1103/PhysRevLett.107.110601.
- [213] A. Nahum, J. T. Chalker, P. Serna, M. Ortuño, A. M. Somoza, Phase transitions in three-dimensional loop models and the CP^{n-1} sigma model, Phys. Rev. B 88 (2013) 134411. arXiv:1308.0144, doi:10.1103/PhysRevB.88.134411.
- [214] G. Bracci-Testasecca, A. Pelissetto, Multicomponent gauge-Higgs models with discrete Abelian gauge groups, J. Stat. Mech. 2304 (2023) 043101. arXiv:2211.01662, doi:10.1088/1742-5468/acc72f.
- [215] G. Murthy, S. Sachdev, Action of Hedgehog Instantons in the Disordered Phase of the (2+1)-dimensional CP^{N-1} Model, Nucl. Phys. B 344 (1990) 557. doi:10.1016/0550-3213(90)90670-9.
- [216] P. G. de Gennes, J. Prost, The Physics of Liquid Crystals, Oxford University Press, Oxford, 1993.
- [217] S. Caracciolo, R. G. Edwards, A. Pelissetto, A. D. Sokal, New universality classes for two-dimensional sigma models, Phys. Rev. Lett. 71 (1993) 3906. arXiv:hep-lat/9307022, doi:10.1103/PhysRevLett.71.3906.
- [218] A. Pelissetto, A. D. Sokal, S. Caracciolo, Analytic results for mixed O(N)-RP^{N-1} sigma models in two-dimensions, Nucl. Phys. B (Proc. Suppl.) 34 (1994) 683. doi:10.1016/0920-5632(94)90482-0.
 [219] M. Hasenbusch, O(N) and RP^{N-1} models in two-dimensions, Phys. Rev. D 53 (1996) 3445. arXiv:hep-lat/9507008,
- [219] M. Hasenbusch, O(N) and RP^{N-1} models in two-dimensions, Phys. Rev. D 53 (1996) 3445. arXiv:hep-lat/9507008 doi:10.1103/PhysRevD.53.3445.
- [220] F. Niedermayer, P. Weisz, D.-S. Shin, On the question of universality in RP^{n-1} and 0(n) lattice sigma models, Phys. Rev. D 53 (1996) 5918. arXiv:hep-lat/9507005, doi:10.1103/PhysRevD.53.5918.
- [221] S. M. Catterall, M. Hasenbusch, R. R. Horgan, R. L. Renken, The nature of the continuum limit in the 2-D RP² gauge model, Phys. Rev. D 58 (1998) 074510. arXiv:hep-lat/9801032, doi:10.1103/PhysRevD.58.074510.
- [222] G. Delfino, Y. Diouane, N. Lamsen, Absence of nematic quasi-long-range order in two-dimensional liquid crystals with three director components, J. Phys. A 54 (3) (2021) 03LT01. arXiv:2005.06307, doi:10.1088/1751-8121/abd2fc.
- [223] C. Bonati, A. Franchi, A. Pelissetto, E. Vicari, Asymptotic low-temperature behavior of two-dimensional RP^{N-1} models, Phys. Rev. D 102 (2020) 034513. arXiv:2006.13061, doi:10.1103/PhysRevD.102.034513.
- [224] L. A. Fernandez, V. Martín-Mayor, D. Sciretti, A. Tarancon, J. L. Velasco, Numerical study of the enlarged O(5) symmetry of the 3-D antiferromagnetic RP² spin model, Phys. Lett. B 628 (2005) 281. arXiv:cond-mat/0507491, doi:10.1016/j.physletb.2005.09.049.
- [225] F. Wilczek, QCD in extreme conditions, in: 9th CRM Summer School: Theoretical Physics at the End of the 20th Century, 1999, p. 567. arXiv:hep-ph/0003183.
- [226] F. Karsch, Lattice QCD at high temperature and density, Lect. Notes Phys. 583 (2002) 209. arXiv:hep-lat/0106019, doi:10.1007/3-540-45792-5_6.
- [227] S. Sharma, Recent Progress on the QCD Phase Diagram, PoS LATTICE2018 (2019) 009. arXiv:1901.07190, doi: 10.22323/1.334.0009.
- [228] C. Bonati, M. D'Elia, H. Panagopoulos, E. Vicari, Change of θ Dependence in 4D SU(N) Gauge Theories Across the Deconfinement Transition, Phys. Rev. Lett. 110 (25) (2013) 252003. arXiv:1301.7640, doi:10.1103/PhysRevLett.110. 252003.
- [229] C. Bonati, M. D'Elia, M. Mariti, G. Martinelli, M. Mesiti, F. Negro, F. Sanfilippo, G. Villadoro, Axion phenomenology and θ -dependence from $N_f=2+1$ lattice QCD, JHEP 03 (2016) 155. arXiv:1512.06746, doi:10.1007/JHEP03(2016)155.
- [230] R. A. Vig, T. G. Kovacs, Ideal topological gas in the high temperature phase of SU(3) gauge theory, Phys. Rev. D 103 (11) (2021) 114510. arXiv:2101.01498, doi:10.1103/PhysRevD.103.114510.

- [231] P. Calabrese, P. Parruccini, Five loop epsilon expansion for $U(n) \otimes U(m)$ models: Finite temperature phase transition in light QCD, JHEP 05 (2004) 018. arXiv:hep-ph/0403140, doi:10.1088/1126-6708/2004/05/018.
- [232] S. Navas, et al., Review of particle physics, Phys. Rev. D 110 (3) (2024) 030001. doi:10.1103/PhysRevD.110.030001.
- [233] C. Bonati, A. Pelissetto, E. Vicari, Three-dimensional Z₂-gauge N-vector models, Phys. Rev. B 109 (2024) 235121. arXiv:2404.07050.
- [234] C. Bonati, A. Pelissetto, E. Vicari, Uncovering gauge-dependent critical order-parameter correlations by a stochastic gauge fixing at O(N)* and Ising* continuous transitions, Phys. Rev. B 110 (2024) 125109. arXiv:2405.13485, doi: 10.1103/PhysRevB.110.125109.
- [235] J. B. Kogut, An introduction to lattice gauge theory and spin systems, Rev. Mod. Phys. 51 (1979) 659. doi:10.1103/ RevModPhys.51.659.
- [236] D. Belitz, T. R. Kirkpatrick, T. Vojta, Local versus nonlocal order-parameter field theories for quantum phase transitions, Phys. Rev. B 65 (2002) 165112. arXiv:cond-mat/0109547, doi:10.1103/PhysRevB.65.165112.
- [237] Z. Bi, E. Lake, T. Senthil, Landau ordering phase transitions beyond the Landau paradigm, Phys. Rev. Res. 2 (2020) 023031. arXiv:1910.12856, doi:10.1103/PhysRevResearch.2.023031.
- [238] J. McGreevy, Generalized Symmetries in Condensed Matter, Ann. Rev. Condensed Matter Phys. 14 (2023) 57. arXiv: 2204.03045, doi:10.1146/annurev-conmatphys-040721-021029.
- [239] W.-T. Xu, T. Rakovszky, M. Knap, F. Pollmann, Entanglement Properties of Gauge Theories from Higher-Form Symmetries (2023). arXiv:2311.16235.
- [240] D. Gaiotto, A. Kapustin, N. Seiberg, B. Willett, Generalized Global Symmetries, JHEP 02 (2015) 172. arXiv:1412.5148, doi:10.1007/JHEP02(2015)172.
- [241] Z. Nussinov, G. Ortiz, A symmetry principle for topological quantum order, Annals Phys. 324 (2009) 977. arXiv: cond-mat/0702377, doi:10.1016/j.aop.2008.11.002.
- [242] C. D. Batista, Z. Nussinov, Generalized Elitzur's theorem and dimensional reduction, Phys. Rev. B 72 (2005) 045137. arXiv:cond-mat/0410599, doi:10.1103/PhysRevB.72.045137.
- [243] R. Balian, J. M. Drouffe, C. Itzykson, Gauge Fields on a Lattice. I. General Outlook, Phys. Rev. D 10 (1974) 3376. doi:10.1103/PhysRevD.10.3376.
- [244] R. Ben-Av, D. Kandel, E. Katznelson, P. G. Lauwers, S. Solomon, Critical Acceleration of Lattice Gauge Simulations, J. Statist. Phys. 58 (1990) 125. doi:10.1007/BF01020288.
- [245] M. Caselle, R. Fiore, F. Gliozzi, M. Hasenbusch, P. Provero, String effects in the Wilson loop: A High precision numerical test, Nucl. Phys. B 486 (1997) 245. arXiv:hep-lat/9609041, doi:10.1016/S0550-3213(96)00672-4.
- [246] F. Gliozzi, M. Panero, P. Provero, Large center vortices and confinement in 3-D Z₂ gauge theory, Phys. Rev. D 66 (2002) 017501. arXiv:hep-lat/0204030, doi:10.1103/PhysRevD.66.017501.
- [247] O. Borisenko, V. Chelnokov, G. Cortese, M. Gravina, A. Papa, I. Surzhikov, Critical behavior of 3D Z(N) lattice gauge theories at zero temperature, Nucl. Phys. B 879 (2014) 80. arXiv:1310.5997, doi:10.1016/j.nuclphysb.2013.12.003.
- [248] N. Xu, C. Castelnovo, R. G. Melko, C. Chamon, A. W. Sandvik, Dynamic scaling of topological ordering in classical systems, Phys. Rev. B 97 (2018) 024432. arXiv:1711.03557, doi:10.1103/PhysRevB.97.024432.
- [249] R. Agrawal, L. F. Cugliandolo, L. Faoro, L. B. Ioffe, M. Picco, The geometric phase transition of the three-dimensional Z₂ lattice gauge model (2024). arXiv:2409.15123.
- [250] C. M. Fortuin, P. W. Kasteleyn, On the Random cluster model. 1. Introduction and relation to other models, Physica 57 (1972) 536. doi:10.1016/0031-8914(72)90045-6.
- [251] F. Gliozzi, Confining vacua and Q-state Potts models with Q < 1, PoS LATTICE2007 (2007) 304. arXiv:0708.4332, doi:10.22323/1.042.0304.
- [252] F. Gliozzi, S. Lottini, M. Panero, A. Rago, Random percolation as a gauge theory, Nucl. Phys. B 719 (2005) 255. arXiv:cond-mat/0502339, doi:10.1016/j.nuclphysb.2005.04.021.
- [253] C. Bonati, A. Pelissetto, E. Vicari, Scalar gauge-Higgs models with discrete Abelian symmetry groups, Phys. Rev. E 105 (2022) 054132. arXiv:2204.02907, doi:10.1103/PhysRevE.105.054132.
- [254] M. Hasenbusch, E. Vicari, Anisotropic perturbations in three-dimensional O(N)-symmetric vector models, Phys. Rev. B 84 (2011) 125136. arXiv:1108.0491, doi:10.1103/PhysRevB.84.125136.
- [255] M. Hasenbusch, Cubic fixed point in three dimensions: Monte Carlo simulations of the φ4 model on the simple cubic lattice, Phys. Rev. B 107 (2023) 024409. arXiv:2211.16170, doi:10.1103/PhysRevB.107.024409.
- [256] F. Kos, D. Poland, D. Simmons-Duffin, A. Vichi, Precision Islands in the Ising and O(N) Models, JHEP 08 (2016) 036. arXiv:1603.04436. doi:10.1007/JHEP08(2016)036.
- [257] M. Suzuki, Solution of Potts Model for Phase Transition, Prog. Theor. Phys. 37 (1967) 770. doi:10.1143/PTP.37.770.
- [258] J. Hove, A. Sudbø, Criticality versus q in the (2+1)-dimensional Z_q clock model, Phys. Rev. E 68 (2003) 046107. arXiv:cond-mat/0301499, doi:10.1103/PhysRevE.68.046107.
- [259] C. P. Korthals Altes, Duality for Z(N) Gauge Theories, Nucl. Phys. B 142 (1978) 315. doi:10.1016/0550-3213(78) 90207-9.
- [260] A. M. Polyakov, Quark Confinement and Topology of Gauge Groups, Nucl. Phys. B 120 (1977) 429. doi:10.1016/ 0550-3213(77)90086-4.
- [261] G. Bhanot, M. Creutz, The Phase Diagram of Z(n) and u(1) Gauge Theories in Three-dimensions, Phys. Rev. D 21 (1980) 2892. doi:10.1103/PhysRevD.21.2892.
- [262] K. Osterwalder, E. Seiler, Gauge Field Theories on the Lattice, Annals Phys. 110 (1978) 440. doi:10.1016/0003-4916(78) 90039-8.
- [263] H. D. Scammell, K. Patekar, M. S. Scheurer, S. Sachdev, Phases of SU(2) gauge theory with multiple adjoint Higgs fields in 2+1 dimensions, Phys. Rev. B 101 (2020) 205124. arXiv:1912.06108, doi:10.1103/PhysRevB.101.205124.

- [264] H. Shao, W. Guo, A. W. Sandvik, Quantum criticality with two length scales, Science 352 (6282) (2016) 213. arXiv: 1603.02171, doi:10.1126/science.aad5007.
- [265] G. Bhanot, B. A. Freedman, Finite Size Scaling for the 3-D Abelian Higgs Model, Nucl. Phys. B 190 (1981) 357. doi:10.1016/0550-3213(81)90566-6.
- [266] D. J. E. Callaway, L. J. Carson, The Abelian Higgs Model: A Monte Carlo Study, Phys. Rev. D 25 (1982) 531. doi: 10.1103/PhysRevD.25.531.
- [267] S. Wenzel, E. Bittner, W. Janke, A. M. J. Schakel, A. Schiller, Kertesz line in the three-dimensional compact U(1) lattice Higgs model, Phys. Rev. Lett. 95 (2005) 051601. arXiv:cond-mat/0503599, doi:10.1103/PhysRevLett.95.051601.
- [268] O. I. Motrunich, A. Vishwanath, Comparative study of Higgs transition in one-component and two-component lattice superconductor models (2008). arXiv:0805.1494.
- [269] D. Charrier, F. Alet, P. Pujol, Gauge Theory Picture of an Ordering Transition in a Dimer Model, Phys. Rev. Lett. 101 (2008) 167205. arXiv:0806.0559, doi:10.1103/PhysRevLett.101.167205.
- [270] J. Lou, A. W. Sandvik, N. Kawashima, Antiferromagnetic to valence-bond-solid transitions in two-dimensional SU(N) Heisenberg models with multispin interactions, Phys. Rev. B 80 (2009) 180414. arXiv:0908.0740, doi:10.1103/PhysRevB. 80.180414.
- [271] D. Charrier, F. Alet, Phase diagram of an extended classical dimer model, Phys. Rev. B 82 (2010) 014429. arXiv: 1005.2522, doi:10.1103/PhysRevB.82.014429.
- [272] E. V. Herland, T. A. Bojesen, E. Babaev, A. Sudbø, Phase structure and phase transitions in a three-dimensional SU(2) superconductor, Phys. Rev. B 87 (2013) 134503. arXiv:1301.3142, doi:10.1103/PhysRevB.87.134503.
- [273] A. Nahum, P. Serna, J. T. Chalker, M. Ortuño, A. M. Somoza, Emergent SO(5) Symmetry at the Néel to Valence-Bond-Solid Transition, Phys. Rev. Lett. 115 (2015) 267203. arXiv:1508.06668, doi:10.1103/PhysRevLett.115.267203.
- [274] Y.-C. He, J. Rong, N. Su, A roadmap for bootstrapping critical gauge theories: decoupling operators of conformal field theories in d>2 dimensions, SciPost Phys. 11 (2021) 111. arXiv:2101.07262, doi:10.21468/SciPostPhys.11.6.111.
- [275] C. Bonati, A. Pelissetto, E. Vicari, Breaking of Gauge Symmetry in Lattice Gauge Theories, Phys. Rev. Lett. 127 (2021) 091601. arXiv:2104.09892, doi:10.1103/PhysRevLett.127.091601.
- [276] C. Bonati, A. Pelissetto, E. Vicari, Lattice gauge theories in the presence of a linear gauge-symmetry breaking, Phys. Rev. E 104 (2021) 014140. arXiv:2106.02503, doi:10.1103/PhysRevE.104.014140.
- [277] J. Glimm, A. Jaffe, Quantum Physics. A Functional Integral Point of View, Springer, 1987.
- [278] S. Hikami, Nonlinear Sigma Model of Grassmann Manifold and Nonabelian Gauge Field With Scalar Coupling, Prog. Theor. Phys. 64 (1980) 1425. doi:10.1143/PTP.64.1425.
- [279] Y. T. Millev, D. I. Uzunov, Weakly first-order transition in unconventional superconductors, Phys. Lett. A 145 (1990) 287. doi:10.1016/0375-9601(90)90367-W.
- [280] B. E. Lautrup, On High Order Estimates in QED, Phys. Lett. B 69 (1977) 109. doi:10.1016/0370-2693(77)90145-9.
- [281] G. Parisi, Singularities of the Borel Transform in Renormalizable Theories, Phys. Lett. B 76 (1978) 65. doi:10.1016/0370-2693(78)90101-6.
- [282] G. Parisi, The Borel Transform and the Renormalization Group, Phys. Rept. 49 (1979) 215. doi:10.1016/0370-1573(79) 90111-X.
- [283] G. Parisi, On Infrared Divergences, Nucl. Phys. B 150 (1979) 163. doi:10.1016/0550-3213(79)90298-0.
- [284] F. David, On the Ambiguity of Composite Operators, IR Renormalons and the Status of the Operator Product Expansion, Nucl. Phys. B 234 (1984) 237. doi:10.1016/0550-3213(84)90235-9.
- [285] S. Hikami, Renormalization Group Functions of CP^{N-1} Nonlinear Sigma Model and N Component Scalar QED Model, Prog. Theor. Phys. 62 (1979) 226. doi:10.1143/PTP.62.226.
- [286] J. March-Russell, On the possibility of second order phase transitions in spontaneously broken gauge theories, Phys. Lett. B 296 (1992) 364. arXiv:hep-ph/9208215, doi:10.1016/0370-2693(92)91333-5.
- [287] C. Bonati, A. Pelissetto, E. Vicari, Gauge fixing and gauge correlations in noncompact Abelian gauge models, Phys. Rev. D 108 (2023) 014517. arXiv:2304.14366, doi:10.1103/PhysRevD.108.014517.
- [288] C. Bonati, A. Pelissetto, E. Vicari, Abelian Higgs gauge theories with multicomponent scalar fields and multiparameter scalar potentials, Phys. Rev. B 108 (2023) 245154. arXiv:2310.08504, doi:10.1103/PhysRevB.108.245154.
- [289] M. Creutz, Gauge Fixing, the Transfer Matrix, and Confinement on a Lattice, Phys. Rev. D 15 (1977) 1128. doi: 10.1103/PhysRevD.15.1128.
- [290] A. S. Kronfeld, U. J. Wiese, SU(N) gauge theories with C periodic boundary conditions. 2. Small volume dynamics, Nucl. Phys. B 401 (1993) 190. arXiv:hep-lat/9210008, doi:10.1016/0550-3213(93)90302-6.
- [291] B. Lucini, A. Patella, A. Ramos, N. Tantalo, Charged hadrons in local finite-volume QED+QCD with C* boundary conditions, JHEP 02 (2016) 076. arXiv:1509.01636, doi:10.1007/JHEP02(2016)076.
- [292] P. A. M. Dirac, Gauge invariant formulation of quantum electrodynamics, Can. J. Phys. 33 (1955) 650. doi:10.1139/p55-081.
- [293] M. Hasenbusch, Monte Carlo study of an improved clock model in three dimensions, Phys. Rev. B 100 (2019) 224517. arXiv:1910.05916, doi:10.1103/PhysRevB.100.224517.
- [294] M. Campostrini, M. Hasenbusch, A. Pelissetto, E. Vicari, The Critical exponents of the superfluid transition in He-4, Phys. Rev. B 74 (2006) 144506. arXiv:cond-mat/0605083, doi:10.1103/PhysRevB.74.144506.
- [295] Y. Deng, H. W. J. Blöte, M. P. Nightingale, Surface and bulk transitions in three-dimensional O(n) models, Phys. Rev. E 72 (2005) 016128. arXiv:cond-mat/0504173, doi:10.1103/PhysRevE.72.016128.
- [296] M. E. Fisher, M. N. Barber, D. Jasnow, Helicity Modulus, Superfluidity, and Scaling in Isotropic Systems, Phys. Rev. A 8 (1973) 1111. doi:10.1103/PhysRevA.8.1111.
- [297] H. Kleinert, Gauge Fields in Condensed Matter, World Scientific, Singapore (Singapore), 1989.

- [298] H. Kleinert, F. S. Nogueira, Charged fixed point in the Ginzburg-Landau superconductor and the role of the Ginzburg parameter κ, Nucl. Phys. B 651 (2003) 361. arXiv:cond-mat/0104573, doi:{10.1016/S0550-3213(02)01075-1}.
- [299] M. Hasenbusch, Three-dimensional O(N)-invariant ϕ^4 models at criticality for $N \ge 4$, Phys. Rev. B 105 (2022) 054428. arXiv:2112.03783, doi:10.1103/PhysRevB.105.054428.
- [300] M. Campostrini, A. Pelissetto, P. Rossi, E. Vicari, Four point renormalized coupling constant in O(N) models, Nucl. Phys. B 459 (1996) 207. arXiv:hep-lat/9506002, doi:10.1016/0550-3213(95)00569-2.
- [301] C. Bonati, A. Pelissetto, E. Vicari, Strong-coupling critical behavior in three-dimensional lattice Abelian gauge models with charged N-component scalar fields and SO(N) symmetry, Phys. Rev. E 109 (2024) 064142. arXiv:2403.12758, doi:10.1103/PhysRevE.109.064142.
- [302] C.-N. Yang, Charge quantization, compactness of the gauge group, and flux quantization, Phys. Rev. D 1 (1970) 2360. doi:10.1103/PhysRevD.1.2360.
- [303] M.-h. Lau, C. Dasgupta, Numerical investigation of the role of topological defects in the three-dimensional Heisenberg transition, Phys. Rev. B 39 (1989) 7212. doi:10.1103/PhysRevB.39.7212.
- [304] M. Kamal, G. Murthy, New O(3) transition in three dimensions, Phys. Rev. Lett. 71 (1993) 1911. doi:10.1103/ PhysRevLett.71.1911.
- [305] T. A. DeGrand, D. Toussaint, Topological Excitations and Monte Carlo Simulation of Abelian Gauge Theory, Phys. Rev. D 22 (1980) 2478. doi:10.1103/PhysRevD.22.2478.
- [306] A. H. Guth, Existence Proof of a Nonconfining Phase in Four-Dimensional U(1) Lattice Gauge Theory, Phys. Rev. D 21 (1980) 2291. doi:10.1103/PhysRevD.21.2291.
- [307] R. A. Jalabert, S. Sachdev, Spontaneous alignment of frustrated bonds in an anisotropic, three-dimensional Ising model, Phys. Rev. B 44 (1991) 686. doi:10.1103/PhysRevB.44.686.
- [308] S. Sachdev, M. Vojta, Translational symmetry breaking in two-dimensional antiferromagnets and superconductors, J. Phys. Soc. Japan Supp. B 69 (2000) 1. arXiv:cond-mat/9910231.
 URL https://www.jps.or.jp/books/jpsjs/698/jpsj.69sb.001.pdf
- [309] T. Senthil, O. Motrunich, Microscopic models for fractionalized phases in strongly correlated systems, Phys. Rev. B 66 (2002) 205104. doi:10.1103/PhysRevB.66.205104.
- [310] O. I. Motrunich, T. Senthil, Exotic Order in Simple Models of Bosonic Systems, Phys. Rev. Lett. 89 (2002) 277004. arXiv:cond-mat/0205170, doi:10.1103/PhysRevLett.89.277004.
- [311] T. Senthil, M. P. A. Fisher, Z₂ gauge theory of electron fractionalization in strongly correlated systems, Phys. Rev. B 62 (2000) 7850. arXiv:cond-mat/9910224, doi:10.1103/PhysRevB.62.7850.
- [312] S. Sachdev, N. Read, Large N expansion for frustrated and doped quantum antiferromagnets, Int. J. of Mod. Phys. B 5 (1991) 219. arXiv:cond-mat/0402109, doi:10.1142/S0217979291000158.
- [313] P. E. Lammert, D. S. Rokhsar, J. Toner, Topology and nematic ordering, Phys. Rev. Lett. 70 (1993) 1650. doi: 10.1103/PhysRevLett.70.1650.
- [314] A. V. Chubukov, T. Senthil, S. Sachdev, Universal magnetic properties of frustrated quantum antiferromagnets in two dimensions, Phys. Rev. Lett. 72 (1994) 2089. arXiv:cond-mat/9311045, doi:10.1103/PhysRevLett.72.2089.
- [315] P. E. Lammert, D. S. Rokhsar, J. Toner, Topology and nematic ordering. I. A gauge theory, Phys. Rev. E 52 (1995) 1778. doi:10.1103/PhysRevE.52.1778.
- [316] J. Toner, P. E. Lammert, D. S. Rokhsar, Topology and nematic ordering. II. Observable critical behavior, Phys. Rev. E 52 (1995) 1801. doi:10.1103/PhysRevE.52.1801.
- [317] S. Sachdev, K. Park, Ground states of quantum antiferromagnets in two dimensions, Ann. of Phys. (NY) 298 (2002) 58. arXiv:cond-mat/0108214, doi:10.1006/aphy.2002.6232.
- [318] R. D. Sedgewick, D. J. Scalapino, R. L. Sugar, Fractionalized phase in an XY Z₂ gauge model, Phys. Rev. B 65 (2002) 54508. arXiv:cond-mat/0012028, doi:10.1103/PhysRevB.65.054508.
- [319] K. Park, S. Sachdev, Bond and Néel order and fractionalization in ground states of easy-plane antiferromagnets in two dimensions, Phys. Rev. B 65 (2002) 220405. arXiv:0112003, doi:10.1103/PhysRevB.65.220405.
- [320] K. Liu, J. Nissinen, Z. Nussinov, R.-J. Slager, K. Wu, J. Zaanen, Classification of nematic order in 2+1 dimensions: Dislocation melting and $O(2)/Z_N$ lattice gauge theory, Phys. Rev. B 91 (2015) 075103. arXiv:1405.2963, doi:10.1103/PhysRevB.91.075103.
- [321] K. Liu, J. Nissinen, R.-J. Slager, K. Wu, J. Zaanen, Generalized liquid crystals: Giant fluctuations and the vestigial chiral order of i, o, and t matter, Phys. Rev. X 6 (2016) 041025. arXiv:1512.07822, doi:10.1103/PhysRevX.6.041025.
- [322] A. J. Beekman, J. Nissinen, K. Wu, K. Liu, R.-J. Slager, Z. Nussinov, V. Cvetkovic, J. Zaanen, Dual gauge field theory of quantum liquid crystals in two dimensions, Phys. Rep. 683 (2017) 1. arXiv:1603.04254, doi:10.1016/j.physrep.2017. 03.004.
- [323] A. M. Ferrenberg, J. Xu, D. P. Landau, Pushing the limits of Monte Carlo simulations for the three-dimensional Ising model, Phys. Rev. E 97 (2018) 043301. arXiv:1806.03558, doi:10.1103/PhysRevE.97.043301.
- [324] M. Schuler, S. Whitsitt, L.-P. Henry, S. Sachdev, A. M. Lauchli, Universal Signatures of Quantum Critical Points from Finite-Size Torus Spectra: A Window into the Operator Content of Higher-Dimensional Conformal Field Theories, Phys. Rev. Lett. 117 (2016) 210401. arXiv:1603.030042, doi:10.1103/PhysRevLett.117.210401.
- [325] S. V. Isakov, R. G. Melko, M. B. Hastings, Universal Signatures of Fractionalized Quantum Critical Points, Science 335 (2012) 193. arXiv:1108.2055, doi:10.1126/science.1212207.
- [326] H. G. Ballesteros, L. A. Fernandez, V. Martín-Mayor, A. Muñoz-Sudupe, Finite size effects on measures of critical exponents in d = 3 O(N) models, Phys. Lett. B 387 (1996) 125. arXiv:cond-mat/9606203, doi:10.1016/0370-2693(96) 00984-7
- [327] P. Butera, M. Comi, N vector spin models on the sc and the bcc lattices: A Study of the critical behavior of the

- susceptibility and of the correlation length by high temperature series extended to order β^{21} , Phys. Rev. B 56 (1997) 8212. arXiv:hep-lat/9703018, doi:10.1103/PhysRevB.56.8212.
- [328] S. M. Chester, W. Landry, J. Liu, D. Poland, D. Simmons-Duffin, N. Su, A. Vichi, Carving out OPE space and precise O(2) model critical exponents, JHEP 06 (2020) 142. arXiv:1912.03324, doi:10.1007/JHEP06(2020)142.
- [329] P. Calabrese, A. Pelissetto, E. Vicari, Critical structure factors of bilinear fields in O(N) vector models, Phys. Rev. E 65 (2002) 046115. arXiv:cond-mat/0111160, doi:10.1103/PhysRevE.65.046115.
- [330] C. T. H. Davies, G. G. Batrouni, G. R. Katz, A. S. Kronfeld, G. P. Lepage, K. G. Wilson, P. Rossi, B. Svetitsky, Fourier Acceleration in Lattice Gauge Theories. 1. Landau Gauge Fixing, Phys. Rev. D 37 (1988) 1581. doi:10.1103/PhysRevD. 37.1581.
- [331] V. N. Gribov, Quantization of Nonabelian Gauge Theories, Nucl. Phys. B 139 (1978) 1. doi:10.1016/0550-3213(78) 90175-X.
- [332] I. M. Singer, Some Remarks on the Gribov Ambiguity, Commun. Math. Phys. 60 (1978) 7. doi:10.1007/BF01609471.
- [333] G. Grinstein, A. Luther, Application of the renormalization group to phase transitions in disordered systems, Phys. Rev. B 13 (1976) 1329–1343. doi:10.1103/PhysRevB.13.1329.
- $[334] \ \ S.\ F.\ Edwards,\ P.\ W.\ Anderson,\ Theory\ of\ spin\ glasses,\ J.\ Phys.\ F\ 5\ (5)\ (1975)\ 965.\ doi:10.1088/0305-4608/5/5/017.$
- [335] H. Nishimori, Internal energy, specific heat and correlation function of the bond-random Ising model, Prog. Theor. Phys. 66 (1981) 1169.
- [336] P. Le Doussal, A. B. Harris, Location of the Ising Spin-Glass Multicritical Point on Nishimori's Line, Phys. Rev. Lett. 61 (1988) 625. doi:10.1103/PhysRevLett.61.625.
- [337] M. Palassini, S. Caracciolo, Universal finite size scaling functions in the 3-D Ising spin glass, Phys. Rev. Lett. 82 (1999) 5128. arXiv:cond-mat/9904246, doi:10.1103/PhysRevLett.82.5128.
- [338] H. G. Ballesteros, A. Cruz, L. A. Fernández, V. Martín-Mayor, J. Pech, J. J. Ruiz-Lorenzo, A. Tarancón, P. Téllez, C. L. Ullod, C. Ungil, Critical behavior of the three-dimensional Ising spin glass, Phys. Rev. B 62 (2000) 14237. arXiv: cond-mat/0006211, doi:10.1103/PhysRevB.62.14237.
- [339] H. Nishimori, Statistical Physics of Spin Glasses and Information Processing: An Introduction, Oxford University Press, Oxford (UK), 2001.
- [340] H. G. Katzgraber, M. Korner, A. P. Young, Universality in three-dimensional Ising spin glasses: A Monte Carlo study, Phys. Rev. B 73 (2006) 224432. arXiv:cond-mat/0602212, doi:10.1103/PhysRevB.73.224432.
- [341] M. Hasenbusch, F. Parisen Toldin, A. Pelissetto, E. Vicari, Critical behavior of the three-dimensional ±J Ising model at the paramagnetic-ferromagnetic transition line, Phys. Rev. B 76 (2007) 094402. arXiv:0704.0427, doi:10.1103/ PhysRevB.76.094402.
- [342] M. Hasenbusch, F. Parisen Toldin, A. Pelissetto, E. Vicari, Magnetic-glassy multicritical behavior of the three-dimensional $\pm J$ Ising model, Phys. Rev. B 76 (2007) 184202. arXiv:0707.2866, doi:10.1103/PhysRevB.76.184202.
- [343] M. Hasenbusch, A. Pelissetto, E. Vicari, Critical behavior of three-dimensional Ising spin glass models, Phys. Rev. B 78 (2008) 214205. arXiv:0809.3329, doi:10.1103/PhysRevB.78.214205.
- [344] M. Hasenbusch, A. Pelissetto, E. Vicari, The critical behavior of 3D Ising spin glass models: universality and scaling corrections, Journal of Statistical Mechanics: Theory and Experiment 2008 (02) (2008) L02001. arXiv:0710.1980, doi:10.1088/1742-5468/2008/02/L02001.
- [345] G. Ceccarelli, A. Pelissetto, E. Vicari, Ferromagnetic-glassy transitions in three-dimensional Ising spin glasses, Phys. Rev. B 84 (2011) 134202. arXiv:1107.3005, doi:10.1103/PhysRevB.84.134202.
- [346] M. Baity-Jesi, R. A. Baños, A. Cruz, L. A. Fernandez, J. M. Gil-Narvion, A. Gordillo-Guerrero, D. Iñiguez, A. Maiorano, F. Mantovani, E. Marinari, V. Martín-Mayor, J. Monforte-Garcia, A. A. M. noz Sudupe, D. Navarro, G. Parisi, S. Perez-Gaviro, M. Pivanti, F. Ricci-Tersenghi, J. J. Ruiz-Lorenzo, S. F. Schifano, B. Seoane, A. Tarancon, R. Tripiccione, D. Yllanes, Critical parameters of the three-dimensional Ising spin glass, Phys. Rev. B 88 (2013) 224416. arXiv:1310.2910, doi:10.1103/PhysRevB.88.224416.
- [347] M. Lulli, G. Parisi, A. Pelissetto, Out-of-equilibrium finite-size method for critical behavior analyses, Phys. Rev. E 93 (2016) 032126. arXiv:1509.07814, doi:10.1103/PhysRevE.93.032126.
- [348] A. G. Cavaliere, A. Pelissetto, Disordered Ising model with correlated frustration, Journal of Physics A: Mathematical and Theoretical 52 (2019) 174002. arXiv:1904.12725, doi:10.1088/1751-8121/ab10f9.
- [349] R. Balian, J. M. Drouffe, C. Itzykson, Gauge Fields on a Lattice. II. Gauge Invariant Ising Model, Phys. Rev. D 11 (1975) 2098. doi:10.1103/PhysRevD.11.2098.
- [350] Z. Nussinov, A Derivation of the Fradkin-Shenker result from duality: Links to spin systems in external magnetic fields and percolation crossovers, Phys. Rev. D 72 (2005) 054509. arXiv:cond-mat/0411163, doi:10.1103/PhysRevD.72.054509.
- [351] A. M. Somoza, P. Serna, A. Nahum, Self-Dual Criticality in Three-Dimensional \mathbb{Z}_2 Gauge Theory with Matter, Phys. Rev. X 11 (2021) 041008. arXiv:2012.15845, doi:10.1103/PhysRevX.11.041008.
- [352] G. A. Jongeward, J. D. Stack, C. Jayaprakash, Monte carlo calculations on Z₂ gauge-higgs theories, Phys. Rev. D 21 (1980) 3360. doi:10.1103/PhysRevD.21.3360.
- [353] I. S. Tupitsyn, A. Kitaev, N. V. Prokof'ev, P. C. E. Stamp, Topological multicritical point in the phase diagram of the toric code model and three-dimensional lattice gauge Higgs model, Phys. Rev. B 82 (2010) 085114. arXiv:0804.3175, doi:10.1103/PhysRevB.82.085114.
- [354] L. Genovese, F. Gliozzi, A. Rago, C. Torrero, The Phase diagram of the three-dimensional Z₂ gauge Higgs system at zero and finite temperature, Nucl. Phys. B (Proc. Suppl.) 119 (2003) 894. arXiv:hep-lat/0209027, doi:10.1016/ S0920-5632(03)01713-4.
- [355] L. Oppenheim, M. Koch-Janusz, S. Gazit, Z. Ringel, Machine Learning the Operator Content of the Critical Self-Dual Ising-Higgs Gauge Model (2023). arXiv:2311.17994.

- [356] W.-T. Xu, F. Pollmann, M. Knap, Critical behavior of the Fredenhagen-Marcu order parameter at topological phase transitions (2024). arXiv:2402.00127.
- [357] C. Bonati, A. Pelissetto, E. Vicari, Comment on "Machine Learning the Operator Content of the Critical Self-Dual Ising-Higgs Gauge Model", arXiv:2311.17994v1 (2024). arXiv:2401.10563.
- [358] W. Caudy, J. Greensite, On the ambiguity of spontaneously broken gauge symmetry, Phys. Rev. D 78 (2008) 025018. arXiv:0712.0999, doi:10.1103/PhysRevD.78.025018.
- [359] N. Read, S. Sachdev, Large-N expansion for frustrated quantum antiferromagnets, Phys. Rev. Lett. 66 (1991) 1773. doi:10.1103/PhysRevLett.66.1773.
- [360] X. G. Wen, Mean-field theory of spin-liquid states with finite energy gap and topological orders, Phys. Rev. B 44 (1991) 2664. doi:10.1103/PhysRevB.44.2664.
- [361] F. A. Bais, P. van Driel, M. de Wild Propitius, Quantum symmetries in discrete gauge theories, Phys. Lett. B 280 (1992) 63. arXiv:hep-th/9203046, doi:10.1016/0370-2693(92)90773-W.
- [362] J. M. Maldacena, G. W. Moore, N. Seiberg, D-brane charges in five-brane backgrounds, JHEP 10 (2001) 005. arXiv: hep-th/0108152, doi:10.1088/1126-6708/2001/10/005.
- [363] A. Kitaev, Fault-tolerant quantum computation by anyons, Ann. Phys. 303 (2003) 2. arXiv:quant-ph/9707021, doi: 10.1016/S0003-4916(02)00018-0.
- [364] M. Freedman, C. Nayak, K. Shtengel, K. Walker, Z. Wang, A Class of P,T-Invariant Topological Phases of Interacting Electrons, Ann. Phys. 310 (2004) 428. arXiv:cond-mat/0307511, doi:10.1016/j.aop.2004.01.006.
- [365] T. H. Hansson, V. Oganesyan, S. L. Sondhi, Superconductors are topologically ordered, Annals Phys. 313 (2) (2004) 497. arXiv:cond-mat/0404327, doi:10.1016/j.aop.2004.05.006.
- [366] M. Grady, Exploring the 3D Ising gauge-Higgs model in exact Coulomb gauge and with a gauge-invariant substitute for Landau gauge (2021). arXiv:2109.04560.
- [367] C. Bonati, A. Pelissetto, E. Vicari, Confinement-Higgs transitions of the three-dimensional Z₂ gauge Higgs model within a stochastic gauge fixing, in preparation (2024).
- [368] O. Borisenko, M. Faber, G. Zinovev, On the deconfinement phase transition in hot gauge theories with dynamical matter fields (1998). arXiv:hep-lat/9804009.
- [369] K. Fredenhagen, M. Marcu, A Confinement Criterion for QCD With Dynamical Quarks, Phys. Rev. Lett. 56 (1986) 223. doi:10.1103/PhysRevLett.56.223.
- [370] B. Allés, O. Borisenko, A. Papa, Confinement-Higgs and deconfinement-Higgs transitions in three-dimensional Z(2) LGT (2024). arXiv:2410.02045.
- [371] J. Preskill, L. M. Krauss, Local Discrete Symmetry and Quantum Mechanical Hair, Nucl. Phys. B 341 (1990) 50. doi:10.1016/0550-3213(90)90262-C.
- [372] D. A. Huse, S. Leibler, Are sponge phases of membranes experimental gauge-Higgs systems?, Phys. Rev. Lett. 66 (1991) 437. doi:10.1103/PhysRevLett.66.437.
- [373] P. Serna, A. M. Somoza, A. Nahum, Worldsheet patching, 1-form symmetries, and "Landau-star" phase transitions (2024), arXiv:2403.04025.
- [374] R. Verresen, U. Borla, A. Vishwanath, S. Moroz, R. Thorngren, Higgs Condensates are Symmetry-Protected Topological Phases: I. Discrete Symmetries (2022). arXiv:2211.01376.
- [375] R. Thorngren, T. Rakovszky, R. Verresen, A. Vishwanath, Higgs Condensates are Symmetry-Protected Topological Phases: II. U(1) Gauge Theory and Superconductors (2023). arXiv:2303.08136.
- [376] A. M. Turing, Finite Approximations to Lie Groups, Ann. of Math. 39 (1938) 105. doi:10.2307/1968716.
- [377] C. Bonati, N. Francini, Noncompact lattice Higgs model with Abelian discrete gauge groups: Phase diagram and gauge symmetry enlargement, Phys. Rev. B 107 (2023) 035106. arXiv:2211.03590, doi:10.1103/PhysRevB.107.035106.
- [378] G. Georgi, Weak interactions and modern particle theory, The Benjamin/Cummings Publishing Company, Menlo Park (CA), 1984.
- [379] S. Gazit, F. F. Assaad, S. Sachdev, V. Vishwanath, C. Wang, Confinement transition of Z₂ gauge theories coupled to massless fermions: emergent QCD₃ and SO(5) symmetry, Proc. Natl. Acad. Sci. 115 (2018) E6987. arXiv:1804.01095, doi:10.1073/pnas.1806338115.
- [380] H. Shackleton, A. Thomson, S. Sachdev, Deconfined criticality and a gapless Z2 spin liquid in the square-lattice antifer-romagnet, Phys. Rev. B 104 (4) (2021) 045110. arXiv:2104.09537, doi:10.1103/PhysRevB.104.045110.
- [381] H. Georgi, S. L. Glashow, Unified weak and electromagnetic interactions without neutral currents, Phys. Rev. Lett. 28 (1972) 1494. doi:10.1103/PhysRevLett.28.1494.
- [382] S. Dimopoulos, S. Raby, L. Susskind, Light Composite Fermions, Nucl. Phys. B 173 (1980) 208. doi:10.1016/ 0550-3213(80)90215-1.
- [383] P. S. Bhupal Dev, A. Pilaftsis, Maximally Symmetric Two Higgs Doublet Model with Natural Standard Model Alignment, JHEP 12 (2014) 024, [Erratum: JHEP 11, 147 (2015)]. arXiv:1408.3405, doi:10.1007/JHEP12(2014)024.
- [384] C. Bonati, A. Pelissetto, E. Vicari, Three-dimensional phase transitions in multiflavor lattice scalar SO(N_c) gauge theories, Phys. Rev. E 101 (2020) 062105. arXiv:2003.08160, doi:10.1103/PhysRevE.101.062105.
- [385] S. Nadkarni, The SU(2) Adjoint Higgs Model in Three-dimensions, Nucl. Phys. B 334 (1990) 559. doi:10.1016/ 0550-3213(90)90491-U.
- [386] K. Kajantie, K. Rummukainen, M. E. Shaposhnikov, A Lattice Monte Carlo study of the hot electroweak phase transition, Nucl. Phys. B 407 (1993) 356. arXiv:hep-ph/9305345, doi:10.1016/0550-3213(93)90062-T.
- [387] P. B. Arnold, L. G. Yaffe, The epsilon expansion and the electroweak phase transition, Phys. Rev. D 49 (1994) 3003, [Erratum: Phys. Rev. D 55, 1114 (1997)]. arXiv:hep-ph/9312221, doi:10.1103/PhysRevD.49.3003.
- [388] W. Buchmuller, O. Philipsen, Phase structure and phase transition of the SU(2) Higgs model in three-dimensions, Nucl.

- Phys. B 443 (1995) 47. arXiv:hep-ph/9411334, doi:10.1016/0550-3213(95)00124-B.
- [389] M. Laine, Exact relation of lattice and continuum parameters in three-dimensional SU(2) + Higgs theories, Nucl. Phys. B 451 (1995) 484. arXiv:hep-lat/9504001, doi:10.1016/0550-3213(95)00356-W.
- [390] K. Kajantie, M. Laine, K. Rummukainen, M. E. Shaposhnikov, Is there a hot electroweak phase transition at $m_H \gtrsim m_W$?, Phys. Rev. Lett. 77 (1996) 2887. arXiv:hep-ph/9605288, doi:10.1103/PhysRevLett.77.2887.
- [391] A. Hart, O. Philipsen, J. D. Stack, M. Teper, On the phase diagram of the SU(2) adjoint Higgs model in (2+1)-dimensions, Phys. Lett. B 396 (1997) 217. arXiv:hep-lat/9612021, doi:10.1016/S0370-2693(97)00104-4.
- [392] K. Kajantie, M. Laine, K. Rummukainen, M. E. Shaposhnikov, 3-D SU(N) + adjoint Higgs theory and finite temperature QCD, Nucl. Phys. B 503 (1997) 357. arXiv:hep-ph/9704416, doi:10.1016/S0550-3213(97)00425-2.
- [393] A. Hart, O. Philipsen, The Spectrum of the three-dimensional adjoint Higgs model and hot SU(2) gauge theory, Nucl. Phys. B 572 (2000) 243. arXiv:hep-lat/9908041, doi:10.1016/S0550-3213(99)00742-7.
- [394] O. Gould, S. Güyer, K. Rummukainen, First-order electroweak phase transitions: A nonperturbative update, Phys. Rev. D 106 (2022) 114507. arXiv:2205.07238, doi:10.1103/PhysRevD.106.114507.
- [395] G. 't Hooft, Magnetic Monopoles in Unified Gauge Theories, Nucl. Phys. B 79 (1974) 276. doi:10.1016/0550-3213(74) 90486-6.
- [396] A. M. Polyakov, Particle Spectrum in Quantum Field Theory, JETP Lett. 20 (1974) 194.
- [397] H. Meyer-Ortmanns, Phase transitions in quantum chromodynamics, Rev. Mod. Phys. 68 (1996) 473. arXiv:hep-lat/9608098, doi:10.1103/RevModPhys.68.473.
- [398] C. Proust, L. Taillefer, The Remarkable Underlying Ground States of Cuprate Superconductors, Annual Review of Condensed Matter Physics 10 (2019) 409. arXiv:1807.05074, doi:https://doi.org/10.1146/ annurev-conmatphys-031218-013210.
- [399] K. Fujita, C. K. Kim, I. Lee, J. Lee, M. H. Hamidian, I. A. Firmo, S. Mukhopadhyay, H. Eisaki, S. Uchida, M. J. Lawler, E.-A. Kim, J. C. Davis, Simultaneous Transitions in Cuprate Momentum-Space Topology and Electronic Symmetry Breaking, Science 344 (2014) 612. arXiv:1403.7788, doi:10.1126/science.124878.
- [400] Y. He, Y. Yin, M. Zech, A. Soumyanarayanan, M. M. Yee, T. Williams, M. C. Boyer, K. Chatterjee, W. D. Wise, I. Zeljkovic, T. Kondo, T. Takeuchi, H. Ikuta, P. Mistark, R. S. Markiewicz, A. Bansil, S. Sachdev, E. W. Hudson, J. E. Hoffman, Simultaneous Transitions in Cuprate Momentum-Space Topology and Electronic Symmetry Breaking, Science 344 (2014) 608. arXiv:1305.2778, doi:10.1126/science.1248221.
- [401] L. D. Faddeev, V. N. Popov, Feynman Diagrams for the Yang-Mills Field, Phys. Lett. B 25 (1967) 29. doi:10.1016/0370-2693(67)90067-6.
- [402] C. Bonati, A. Pelissetto, I. Soler Calero, E. Vicari, Charged critical behavior and nonperturbative continuum limit of three-dimensional lattice $SU(N_c)$ gauge Higgs models (2024). arXiv:2409.03595.
- [403] A. Aharony, Comment on "Bicritical and Tetracritical Phenomena and Scaling Properties of the SO(5) Theory", Phys. Rev. Lett. 88 (2002) 059703. arXiv:cond-mat/0107585, doi:10.1103/PhysRevLett.88.059703.
- [404] A. Pelissetto, E. Vicari, Interacting N-vector order parameters with O(N) symmetry, Condensed Matter Phys. 8 (2005) 87. arXiv:hep-th/0409214, doi:10.5488/CMP.8.1.87.
- [405] A. Tanaka, X. Hu, Many-Body Spin Berry Phases Emerging from the π-Flux State: Competition between Antiferromagnetism and the Valence-Bond-Solid State, Phys. Rev. Lett. 95 (2005). doi:10.1103/PhysRevLett.95.036402.
- [406] T. Senthil, M. P. A. Fisher, Competing orders, non-linear sigma models, and topological terms in quantum magnets, Phys. Rev. B 74 (2006) 064405. arXiv:cond-mat/0510459, doi:10.1103/PhysRevB.74.064405.
- [407] J. Takahashi, A. W. Sandvik, Valence-bond solids, vestigial order, and emergent SO(5) symmetry in a two-dimensional quantum magnet, Phys. Rev. Res. 2 (3) (2020) 033459. arXiv:2001.10045, doi:10.1103/PhysRevResearch.2.033459.
- [408] Z. Zhou, L. Hu, W. Zhu, Y.-C. He, SO(5) Deconfined Phase Transition under the Fuzzy-Sphere Microscope: Approximate Conformal Symmetry, Pseudo-Criticality, and Operator Spectrum, Phys. Rev. X 14 (2) (2024) 021044. arXiv:2306.16435, doi:10.1103/PhysRevX.14.021044.
- [409] Z. Deng, L. Liu, W. Guo, H.-q. Lin, Diagnosing SO(5) Symmetry and First-Order Transition in the $J-Q_3$ Model via Entanglement Entropy (2024). arXiv:2401.12838.
- [410] S.-C. Zhang, A Unified Theory Based on SO(5) Symmetry of Superconductivity and Antiferromagnetism, Science 275 (5303) (1997) 1089. arXiv:cond-mat/9610140, doi:10.1126/science.275.5303.1089.
- [411] S.-C. Zhang, J.-P. Hu, E. Arrigoni, W. Hanke, A. Auerbach, Projected SO(5) models, Phys. Rev. B 60 (1999) 13070. arXiv:cond-mat/9904142, doi:10.1103/PhysRevB.60.13070.
- [412] E. Arrigoni, W. Hanke, Renormalized SO(5) Symmetry in Ladders with Next-Nearest-Neighbor Hopping, Phys. Rev. Lett. 82 (1999) 2115. arXiv:cond-mat/9712143, doi:10.1103/PhysRevLett.82.2115.
- [413] E. Arrigoni, W. Hanke, Critical properties of projected SO(5) models at finite temperatures, Phys. Rev. B 62 (2000) 11770. arXiv:cond-mat/0005385, doi:10.1103/PhysRevB.62.11770.
- [414] E. Demler, W. Hanke, S.-C. Zhang, SO(5) theory of antiferromagnetism and superconductivity, Rev. Mod. Phys. 76 (2004) 909. arXiv:cond-mat/0405038, doi:10.1103/RevModPhys.76.909.
- [415] A. C. Davis, A. Hart, T. W. B. Kibble, A. Rajantie, The Monopole mass in the three-dimensional Georgi-Glashow model, Phys. Rev. D 65 (2002) 125008. arXiv:hep-lat/0110154, doi:10.1103/PhysRevD.65.125008.
- [416] L. Niemi, K. Rummukainen, R. Seppa, D. J. Weir, Infrared physics of the 3D SU(2) adjoint Higgs model at the crossover transition, JHEP 02 (2023) 212. arXiv:2206.14487, doi:10.1007/JHEP02(2023)212.
- [417] G. Catumba, A. Hiraguchi, W.-S. Hou, K. Jansen, Y.-J. Kao, C. J. D. Lin, A. Ramos, M. Sarkar, Lattice study of SU(2) gauge theory coupled to four adjoint Higgs fields (2024). arXiv:2407.15422.
- [418] A. M. Polyakov, Compact Gauge Fields and the Infrared Catastrophe, Phys. Lett. B 59 (1975) 82. doi:10.1016/0370-2693(75)90162-8.

- [419] C. Bonati, A. Franchi, A. Pelissetto, E. Vicari, Two-dimensional lattice SU(N_c) gauge theories with multiflavor adjoint scalar fields, JHEP 05 (2021) 018. arXiv:2103.12708, doi:10.1007/JHEP05(2021)018.
- [420] N. D. Mermin, H. Wagner, Absence of ferromagnetism or antiferromagnetism in one-dimensional or two-dimensional isotropic Heisenberg models, Phys. Rev. Lett. 17 (1966) 1133. doi:10.1103/PhysRevLett.17.1133.
- [421] N. D. Mermin, Absence of ordering in certain classical systems, J. Math. Phys. 8 (1967) 1061. doi:https://doi.org/ 10.1063/1.1705316.
- [422] E. Brézin, S. Hikami, J. Zinn-Justin, Generalized Nonlinear Σ Models With Gauge Invariance, Nucl. Phys. B 165 (1980) 528. doi:10.1016/0550-3213(80)90047-4.
- [423] J. M. Kosterlitz, D. J. Thouless, Ordering, metastability and phase transitions in two-dimensional systems, J. Phys. C 6 (1973) 1181. doi:10.1088/0022-3719/6/7/010.
- [424] V. L. Berezinskii, Destruction of long range order in one-dimensional and two-dimensional systems having a continuous symmetry group. I. Classical systems, Sov. Phys. JETP 32 (1971) 493.
- [425] J. M. Kosterlitz, The Critical properties of the two-dimensional x y model, J. Phys. C 7 (1974) 1046.
- [426] C. Bonati, A. Pelissetto, E. Vicari, Two-dimensional multicomponent Abelian-Higgs lattice models, Phys. Rev. D 101 (2020) 034511, arXiv:1912.01315, doi:10.1103/PhysRevD.101.034511.
- [427] C. Bonati, A. Pelissetto, E. Vicari, Universal low-temperature behavior of two-dimensional lattice scalar chromodynamics, Phys. Rev. D 101 (2020) 054503, arXiv:2001.07386, doi:10.1103/PhysRevD.101.054503.
- [428] C. Bonati, A. Franchi, A. Pelissetto, E. Vicari, Asymptotic low-temperature critical behavior of two-dimensional multi-flavor lattice SO(Nc) gauge theories, Phys. Rev. D 102 (2020) 034512. arXiv:2006.16046, doi:10.1103/PhysRevD.102.034512.
- [429] C. Bonati, A. Franchi, A. Pelissetto, E. Vicari, Berezinskii-Kosterlitz-Thouless transitions in two-dimensional lattice SO(N_c) gauge theories with two scalar flavors, Phys. Rev. D 103 (2021) 014510. arXiv:2010.09412, doi:10.1103/ PhysRevD.103.014510.
- [430] C. Bonati, A. Franchi, Color-flavor reflection in the continuum limit of two-dimensional lattice gauge theories with scalar fields, Phys. Rev. E 105 (2022) 054117. arXiv:2203.06979, doi:10.1103/PhysRevE.105.054117.
- [431] A. M. Polyakov, Interaction of Goldstone Particles in Two-Dimensions. Applications to Ferromagnets and Massive Yang-Mills Fields, Phys. Lett. B 59 (1975) 79. doi:10.1016/0370-2693(75)90161-6.
- [432] E. Brézin, J. Zinn-Justin, Spontaneous Breakdown of Continuous Symmetries Near Two-Dimensions, Phys. Rev. B 14 (1976) 3110. doi:10.1103/PhysRevB.14.3110.
- [433] E. Brézin, J. Zinn-Justin, J. C. Le Guillou, Renormalization of the Nonlinear Sigma Model in (Two + Epsilon) Dimension, Phys. Rev. D 14 (1976) 2615. doi:10.1103/PhysRevD.14.2615.
- [434] W. A. Bardeen, B. W. Lee, R. E. Shrock, Phase Transition in the Nonlinear σ Model in $2 + \epsilon$ Dimensional Continuum, Phys. Rev. D 14 (1976) 985. doi:10.1103/PhysRevD.14.985.
- [435] A. D'Adda, M. Lüscher, P. Di Vecchia, A 1/n Expandable Series of Nonlinear Sigma Models with Instantons, Nucl. Phys. B 146 (1978) 63. doi:10.1016/0550-3213(78)90432-7.
- [436] E. Witten, Instantons, the Quark Model, and the 1/n Expansion, Nucl. Phys. B 149 (1979) 285. doi:10.1016/ 0550-3213(79)90243-8.
- [437] W. Bernreuther, F. J. Wegner, Four Loop Order Beta Function for Two-dimensional Nonlinear σ Models, Phys. Rev. Lett. 57 (1986) 1383. doi:10.1103/PhysRevLett.57.1383.
- [438] M. Falcioni, A. Treves, The Nonlinear σ Model: 3 Loops Renormalization and Lattice Scaling, Nucl. Phys. B 265 (1986) 671. doi:10.1016/0550-3213(86)90335-4.
- [439] S. Chakravarty, B. I. Halperin, D. R. Nelson, Two-dimensional quantum Heisenberg antiferromagnet at low temperatures, Phys. Rev. B 39 (1989) 2344. doi:10.1103/PhysRevB.39.2344.
- [440] M. Campostrini, P. Rossi, CPⁿ⁻¹ models in the 1/N expansion, Phys. Rev. D 45 (1992) 618, [Erratum: Phys. Rev. D 46, 2741 (1992)]. doi:10.1103/PhysRevD.45.618.
- [441] M. Campostrini, P. Rossi, E. Vicari, Monte Carlo simulation of CP^{N-1} models, Phys. Rev. D 46 (1992) 2647. doi: 10.1103/PhysRevD.46.2647.
- [442] M. Campostrini, P. Rossi, The 1/N expansion of two-dimensional spin models, Riv. Nuovo Cim. 16 (6) (1993) 1. doi: 10.1007/BF02730034.
- [443] S. Caracciolo, A. Pelissetto, Lattice perturbation theory for O(N) symmetric sigma models with general nearest neighbor action, Nucl. Phys. B 420 (1994) 141. arXiv:hep-lat/9401015, doi:10.1016/0550-3213(94)90378-6.
- [444] S. Caracciolo, A. Pelissetto, Four loop perturbative expansion for the lattice n vector model, Nucl. Phys. B 455 (1995) 619. arXiv:hep-lat/9510015, doi:10.1016/0550-3213(95)00438-X.
- [445] B. Allés, S. Caracciolo, A. Pelissetto, M. Pepe, Four-loop contributions to long distance quantities in the two-dimensional nonlinear sigma model on a square lattice: Revised numerical estimates, Nucl. Phys. B 562 (1999) 581. arXiv:hep-lat/ 9906014, doi:10.1016/S0550-3213(99)00481-2.
- [446] A. M. Polyakov, Gauge Fields and Strings, Harwood Academic Publ., London (UK), 1987.
- [447] A. D'Adda, P. Di Vecchia, M. Lüscher, Confinement and Chiral Symmetry Breaking in CPⁿ⁻¹ Models with Quarks, Nucl. Phys. B 152 (1979) 125. doi:10.1016/0550-3213(79)90083-X.
- [448] M. Campostrini, P. Rossi, E. Vicari, Topological susceptibility and string tension in the lattice CP^{N-1} models, Phys. Rev. D 46 (1992) 4643. arXiv:hep-lat/9207032, doi:10.1103/PhysRevD.46.4643.
- [449] E. Vicari, H. Panagopoulos, Theta dependence of SU(N) gauge theories in the presence of a topological term, Phys. Rept. 470 (2009) 93. arXiv:0803.1593, doi:10.1016/j.physrep.2008.10.001.
- [450] J. V. José, L. P. Kadanoff, S. Kirkpatrick, D. R. Nelson, Renormalization, vortices, and symmetry-breaking perturbations in the two-dimensional planar model, Phys. Rev. B 16 (1977) 1217, [Erratum: Phys. Rev. B 17, 1477 (1978)]. doi:

- 10.1103/PhysRevB.16.1217.
- [451] M. Hasenbusch, M. Marcu, K. Pinn, High precision renormalization group study of the roughening transition, Physica A 208 (1994) 124. arXiv:hep-lat/9404016, doi:10.1016/0378-4371(94)90536-3.
- [452] M. Hasenbusch, K. Pinn, Computing the roughening transition of Ising and solid-on-solid models by BCSOS model matching, J. Phys. A 30 (1997) 63. arXiv:cond-mat/9605019, doi:10.1088/0305-4470/30/1/006.
- [453] J. Balog, Kosterlitz-Thouless theory and lattice artifacts, J. Phys. A 34 (2001) 5237. arXiv:hep-lat/0011078, doi: 10.1088/0305-4470/34/25/306.
- [454] M. Hasenbusch, The Two dimensional XY model at the transition temperature: A High precision Monte Carlo study, J. Phys. A 38 (2005) 5869. arXiv:cond-mat/0502556, doi:10.1088/0305-4470/38/26/003.
- [455] A. Pelissetto, E. Vicari, Renormalization-group flow and asymptotic behaviors at the Berezinskii-Kosterlitz-Thouless transitions, Phys. Rev. E 87 (2013) 032105. arXiv:1212.2322, doi:10.1103/PhysRevE.87.032105.
- [456] R. Moessner, S. L. Sondhi, E. Fradkin, Short-ranged resonating valence bond physics, quantum dimer models and Ising gauge theories, Phys. Rev. B 65 (2002) 024504. arXiv:cond-mat/0103396, doi:10.1103/PhysRevB.65.024504.
- [457] R. Samajdar, D. G. Joshi, Y. Teng, S. Sachdev, Emergent Z₂ Gauge Theories and Topological Excitations in Rydberg Atom Arrays, Phys. Rev. Lett. 130 (2023) 043601. arXiv:2204.00632, doi:10.1103/PhysRevLett.130.043601.
- [458] E. Zohar, J. I. Cirac, B. Reznik, Quantum Simulations of Lattice Gauge Theories using Ultracold Atoms in Optical Lattices, Rept. Prog. Phys. 79 (2016) 014401. arXiv:1503.02312, doi:10.1088/0034-4885/79/1/014401.
- [459] M. C. Bañuls, R. Blatt, J. Catani, A. Celi, J. I. Cirac, M. Dalmonte, L. Fallani, K. Jansen, M. Lewenstein, S. Montangero, C. A. Muschik, B. Reznik, E. Rico, L. Tagliacozzo, K. Van Acoleyen, F. Verstraete, U.-J. Wiese, M. Wingate, J. Zakrzewski, P. Zoller, Simulating Lattice Gauge Theories within Quantum Technologies, Eur. Phys. J. D 74 (8) (2020) 165. arXiv:1911.00003, doi:10.1140/epjd/e2020-100571-8.
- [460] M. C. Bañuls, K. Cichy, Review on Novel Methods for Lattice Gauge Theories, Rept. Prog. Phys. 83 (2020) 024401. arXiv:1910.00257, doi:10.1088/1361-6633/ab6311.
- [461] E. A. Martinez, C. A. Muschik, P. Schindler, D. Nigg, A. Erhard, M. Heyl, P. Hauke, M. Dalmonte, T. Monz, P. Zoller, R. Blatt, Real-time dynamics of lattice gauge theories with a few-qubit quantum computer, Nature 534 (2016) 516. arXiv:1605.04570, doi:10.1038/nature18318.
- [462] H. Bernien, S. Schwartz, A. Keesling, H. Levine, A. Omran, H. Pichler, S. Choi, A. S. Zibrov, M. Endres, M. Greiner, V.Vuletić, M. D. Lukin, Probing many-body dynamics on a 51-atom quantum simulator, Nature 551 (2017) 579. doi: 10.1038/nature24622.
- [463] N. Klco, E. F. Dumitrescu, A. J. McCaskey, T. D. Morris, R. C. Pooser, M. Sanz, E. Solano, P. Lougovski, M. J. Savage, Quantum-classical computation of Schwinger model dynamics using quantum computers, Phys. Rev. A 98 (3) (2018) 032331. arXiv:1803.03326, doi:10.1103/PhysRevA.98.032331.
- [464] C. Schweizer, F. Grusdt, M. Berngruber, L. Barbiero, E. Demler, N. Goldman, I. Bloch, M. Aidelsburger, Floquet approach to Z_2 lattice gauge theories with ultracold atoms in optical lattices, Nature Phys. 15 (2019) 1168. arXiv: 1901.07103, doi:10.1038/s41567-019-0649-7.
- [465] F. Görg, K. Sandholzer, J. Minguzzi, R. Desbuquois, M. Messer, T. Esslinger, Realization of density-dependent Peierls phases to engineer quantized gauge fields coupled to ultracold matter, Nature Phys. 15 (11) (2019) 1161. arXiv:1812. 05895, doi:10.1038/s41567-019-0615-4.
- [466] A. Mil, T. V. Zache, A. Hegde, A. Xia, R. P. Bhatt, M. K. Oberthaler, P. Hauke, J. Berges, F. Jendrzejewski, A scalable realization of local U(1) gauge invariance in cold atomic mixtures, Science 367 (6482) (2020) 1128. arXiv:1909.07641, doi:10.1126/science.aaz5312.
- [467] C. Bonati, A. Pelissetto, E. Vicari, Breaking the gauge symmetry in lattice gauge-invariant models., PoS LATTICE2021 (2022) 101. arXiv:2110.07941, doi:10.22323/1.396.0101.
- [468] P. C. Hohenberg, B. I. Halperin, Theory of dynamic critical phenomena, Rev. Mod. Phys. 49 (1977) 435. doi:10.1103/ RevModPhys.49.435.
- [469] R. Folk, G. Moser, Critical dynamics: a field-theoretical approach, J. Phys. A 39 (2006) R207. doi:10.1088/0305-4470/39/24/R01.
- [470] D. Zwanziger, Covariant Quantization of Gauge Fields Without Gribov Ambiguity, Nucl. Phys. B 192 (1981) 259. doi:10.1016/0550-3213(81)90202-9.
- [471] E. Floratos, J. Iliopoulos, Equivalence of Stochastic and Canonical Quantization in Perturbation Theory, Nucl. Phys. B 214 (1983) 392. doi:10.1016/0550-3213(83)90240-7.
- [472] H. Nakazato, M. Namiki, I. Ohba, K. Okano, Equivalence of Stochastic Quantization Method to Conventional Field Theories Through Supertransformation Invariance, Prog. Theor. Phys. 70 (1983) 298. doi:10.1143/PTP.70.298.
- [473] J. Zinn-Justin, Renormalization and Stochastic Quantization, Nucl. Phys. B 275 (1986) 135. doi:10.1016/0550-3213(86) 90592-4.
- [474] J. Zinn-Justin, D. Zwanziger, Ward Identities for the Stochastic Quantization of Gauge Fields, Nucl. Phys. B 295 (1988) 297. doi:10.1016/0550-3213(88)90358-6.
- [475] F. Liu, M. Mondello, N. Goldenfeld, Kinetics of the superconducting transition, Phys. Rev. Lett. 66 (1991) 3071. doi: 10.1103/PhysRevLett.66.3071.
- [476] K. Rajagopal, F. Wilczek, Static and dynamic critical phenomena at a second order QCD phase transition, Nucl. Phys. B 399 (1993) 395. arXiv:hep-ph/9210253, doi:10.1016/0550-3213(93)90502-G.
- [477] H. Weber, H. J. Jensen, Monte Carlo Calculation of the Linear Resistance of a Three Dimensional Lattice superconductor Model in the London Limit, Phys. Rev. Lett. 78 (1997) 2620. arXiv:cond-mat/9609040, doi:10.1103/PhysRevLett.78. 2620
- [478] J. Lidmar, M. Wallin, C. Wengel, S. M. Girvin, A. P. Young, Dynamical universality classes of the superconducting phase

- transition, Phys. Rev. B 58 (1998) 2827. arXiv:cond-mat/9711236, doi:10.1103/PhysRevB.58.2827.
- [479] V. Aji, N. Goldenfeld, Critical Dynamics of a Vortex-Loop Model for the Superconducting Transition, Phys. Rev. Lett. 87 (2001) 197003. arXiv:cond-mat/0105622, doi:10.1103/PhysRevLett.87.197003.
- [480] G. J. Stephens, L. M. A. Bettencourt, W. H. Zurek, Critical dynamics of gauge systems: Spontaneous vortex formation in 2-D superconductors, Phys. Rev. Lett. 88 (2002) 137004. arXiv:cond-mat/0108127, doi:10.1103/PhysRevLett.88. 137004.
- [481] C. Lannert, S. Vishveshwara, M. P. A. Fisher, Critical Dynamics of Superconductors in the Charged Regime, Phys. Rev. Lett. 92 (2004) 097004. doi:10.1103/PhysRevLett.92.097004.
- [482] M. Dudka, R. Folk, G. Moser, Gauge dependence of the critical dynamics at the superconducting phase transition, Cond. Matter Phys. 10 (2007) 189. arXiv:cond-mat/0612643, doi:10.5488/CMP.10.2.189.
- [483] S. Benvenuti, H. Khachatryan, Easy-plane QED₃'s in the large N_f limit, JHEP 05 (2019) 214. arXiv:1902.05767, doi:10.1007/JHEP05(2019)214.
- [484] Z. Bi, T. Senthil, Adventure in Topological Phase Transitions in 3+1-D: Non-Abelian Deconfined Quantum Criticalities and a Possible Duality, Phys. Rev. X 9 (2) (2019) 021034. arXiv:1808.07465, doi:10.1103/PhysRevX.9.021034.
- [485] T. Appelquist, D. Nash, L. C. R. Wijewardhana, Critical Behavior in (2+1)-Dimensional QED, Phys. Rev. Lett. 60 (1988) 2575. doi:10.1103/PhysRevLett.60.2575.
- [486] E. Dagotto, A. Kocic, J. B. Kogut, Chiral Symmetry Breaking in Three-dimensional QED With N_f Flavors, Nucl. Phys. B 334 (1990) 279. doi:10.1016/0550-3213(90)90665-Z.
- [487] M. Salmhofer, E. Seiler, Proof of chiral symmetry breaking in strongly coupled lattice gauge theory, Commun. Math. Phys. 139 (1991) 395, [Erratum: Commun.Math.Phys. 146, 637 (1992)]. doi:10.1007/BF02352501.
- [488] J. A. Gracey, Gauge independent critical exponents for QED coupled to a four fermi interaction with and without a Chern-Simons term, Annals Phys. 224 (1993) 275. arXiv:hep-th/9301113, doi:10.1006/aphy.1993.1047.
- [489] J. A. Gracey, Analysis of Abelian gauge theory with four Fermi interaction at O(1/N²) in arbitrary dimensions, J. Phys. A 26 (1993) 1431, [Erratum: J. Phys. A 51, 479501 (2018)]. arXiv:hep-th/9301117, doi:10.1088/0305-4470/26/6/024.
- [490] J. A. Gracey, Computation of critical exponent eta at $O(1/N_f^2)$ in quantum electrodynamics in arbitrary dimensions, Nucl. Phys. B 414 (1994) 614. arXiv:hep-th/9312055, doi:10.1016/0550-3213(94)90257-7.
- [491] M. Vojta, Y. Zhang, S. Sachdev, Quantum Phase Transitions in d-Wave Superconductors, Phys. Rev. Lett. 85 (2000) 4940. arXiv:cond-mat/0007170, doi:10.1103/PhysRevLett.85.4940.
- [492] S. J. Hands, J. B. Kogut, L. Scorzato, C. G. Strouthos, Non-compact three-dimensional with $N_f=1$ and $N_f=4$, Phys. Rev. B 70 (2004) 104501. arXiv:hep-lat/0404013, doi:10.1103/PhysRevB.70.104501.
- [493] M. Hermele, T. Senthil, M. P. A. Fisher, Algebraic spin liquid as the mother of many competing orders, Phys. Rev. B 72 (2005) 104404, [Erratum: Phys. Rev. B 76, 149906 (2007)]. arXiv:cond-mat/0502215, doi:10.1103/PhysRevB.72.104404.
- [494] C. Strouthos, J. B. Kogut, The Phases of Non-Compact QED(3), PoS LATTICE2007 (2007) 278. arXiv:0804.0300, doi:10.22323/1.042.0278.
- [495] F. S. Nogueira, H. Kleinert, Compact quantum electrodynamics in 2+1 dimensions and spinon deconfinement: A Renormalization group analysis, Phys. Rev. B 77 (2008) 045107. arXiv:0705.3541, doi:10.1103/PhysRevB.77.045107.
- [496] A. H. Castro Neto, F. Guinea, N. M. R. Peres, K. S. Novoselov, A. K. Geim, The electronic properties of graphene, Rev. Mod. Phys. 81 (2009) 109. arXiv:0709.1163, doi:10.1103/RevModPhys.81.109.
- [497] W. Armour, J. B. Kogut, C. Strouthos, Chiral symmetry breaking and monopole dynamics in non-compact QED3 coupled to a four-fermi interaction, Phys. Rev. D 82 (2010) 014503. arXiv:1004.3053, doi:10.1103/PhysRevD.82.014503.
- [498] W. Armour, S. Hands, J. B. Kogut, B. Lucini, C. Strouthos, P. Vranas, Magnetic monopole plasma phase in (2+1)d compact quantum electrodynamics with fermionic matter, Phys. Rev. D 84 (2011) 014502. arXiv:1105.3120, doi: 10.1103/PhysRevD.84.014502.
- [499] J. Braun, H. Gies, L. Janssen, D. Roscher, Phase structure of many-flavor QED₃, Phys. Rev. D 90 (3) (2014) 036002. arXiv:1404.1362, doi:10.1103/PhysRevD.90.036002.
- [500] L. Janssen, Y.-C. He, Critical behavior of the QED₃-Gross-Neveu model: Duality and deconfined criticality, Phys. Rev. B 96 (20) (2017) 205113. arXiv:1708.02256, doi:10.1103/PhysRevB.96.205113.
- [501] T. Alanne, S. Blasi, Abelian gauge-Yukawa β -functions at large N_f , Phys. Rev. D 98 (11) (2018) 116004. arXiv: 1808.03252, doi:10.1103/PhysRevD.98.116004.
- [502] R. Boyack, A. Rayyan, J. Maciejko, Deconfined criticality in the QED3 Gross-Neveu-Yukawa model: The 1/N expansion revisited, Phys. Rev. B 99 (19) (2019) 195135. arXiv:1812.02720, doi:10.1103/PhysRevB.99.195135.
- [503] W. Wang, D.-C. Lu, X. Y. Xu, Y.-Z. You, Z. Y. Meng, Dynamics of Compact Quantum Electrodynamics at Large Fermion Flavor, Phys. Rev. B 100 (8) (2019) 085123. arXiv:1906.06929, doi:10.1103/PhysRevB.100.085123.
- [504] N. Zerf, R. Boyack, P. Marquard, J. A. Gracey, J. Maciejko, Critical properties of the Néel-algebraic-spin-liquid transition, Phys. Rev. B 100 (23) (2019) 235130. arXiv:1905.03719, doi:10.1103/PhysRevB.100.235130.
- [505] X. Y. Xu, Y. Qi, L. Zhang, F. F. Assaad, C. Xu, Z. Y. Meng, Monte Carlo Study of Lattice Compact Quantum Electrodynamics with Fermionic Matter: The Parent State of Quantum Phases, Phys. Rev. X 9 (2019) 021022. arXiv: 1807.07574, doi:10.1103/PhysRevX.9.021022.
- [506] L. Janssen, W. Wang, M. M. Scherer, Z. Y. Meng, X. Y. Xu, Confinement transition in the QED₃-Gross-Neveu-XY universality class, Phys. Rev. B 101 (2020) 235118. arXiv:2003.01722, doi:10.1103/PhysRevB.101.235118.
- [507] N. Zerf, R. Boyack, P. Marquard, J. A. Gracey, J. Maciejko, Critical properties of the valence-bond-solid transition in lattice quantum electrodynamics, Phys. Rev. D 101 (9) (2020) 094505. arXiv:2003.09226, doi:10.1103/PhysRevD.101.
- [508] Z. Li, D. Poland, Searching for gauge theories with the conformal bootstrap, JHEP 03 (2021) 172. arXiv:2005.01721, doi:10.1007/JHEP03(2021)172.

- [509] C. Borgs, R. Kotecký, A rigorous theory of finite-size scaling at first-order phase transitions, J. Stat. Phys. 61 (1990) 79. doi:10.1007/BF01013955.
- [510] M. Campostrini, J. Nespolo, A. Pelissetto, E. Vicari, Finite-Size Scaling at First-Order Quantum Transitions, Phys. Rev. Lett. 113 (2014) 070402. arXiv:1405.6823, doi:10.1103/PhysRevLett.113.070402.
- [511] M. E. Fisher, M. N. Barber, Scaling Theory for Finite-Size Effects in the Critical Region, Phys. Rev. Lett. 28 (1972) 1516. doi:10.1103/PhysRevLett.28.1516.
- [512] M. N. Barber, Finite-size scaling, in: C. Domb, J. L. Lebowitz (Eds.), Phase transitions and critical phenomena, vol. 8, Academic Press, London (UK), 1983.
- [513] H. W. Diehl, Field-theoretic approach to critical behaviour at surfaces, in: C. Domb, J. L. Lebowitz (Eds.), Phase transitions and critical phenomena, Vol. 10, Academic Press, London, 1986.
- [514] J. Salas, A. D. Sokal, Universal amplitude ratios in the critical two-dimensional Ising model on a torus, J. Stat. Phys. 98 (2000) 551. arXiv:cond-mat/9904038, doi:10.1023/A:1018611122166.
- [515] V. L. Berezinskii, Destruction of long-range order in one-dimensional and two-dimensional systems possessing a continuous symmetry group. II. Quantum systems, Sov. Phys. JETP 34 (1972) 610.
- [516] D. J. Amit, Y. Y. Goldschmidt, S. Grinstein, Renormalisation group analysis of the phase transition in the 2D Coulomb gas, Sine-Gordon theory and XY-model, J. Phys. A: Math. Gen. 13 (1980) 585. doi:10.1088/0305-4470/13/2/024.
- [517] M. Caselle, M. Hasenbusch, A. Pelissetto, E. Vicari, Irrelevant operators in the two-dimensional Ising model, J. Phys. A: Math. Gen. 35 (2002) 4861. doi:10.1088/0305-4470/35/23/305.
- [518] H. W. Diehl, D. Grüneberg, M. Hasenbusch, A. Hucht, S. B. Rutkevich, F. M. Schmidt, Exact thermodynamic Casimir forces for an interacting three-dimensional model system in film geometry with free surfaces, Eur. Phys. Lett. 100 (2012) 10004. arXiv:1205.6613, doi:10.1209/0295-5075/100/10004.
- [519] A. Pelissetto, E. Vicari, Four-point renormalized coupling constant and Callan-Symanzik β-function in O(N) models, Nucl. Phys. B 519 (1998) 626. arXiv:cond-mat/9711078, doi:10.1016/S0550-3213(98)00164-3.
- [520] A. Pelissetto, E. Vicari, Low-temperature effective potential of the Ising model, Nucl. Phys. B 540 (1999) 639. arXiv: cond-mat/9805317, doi:10.1016/S0550-3213(98)00779-2.
- [521] F. M. Gasparini, M. O. Kimball, K. P. Mooney, M. Diaz-Avila, Finite-size scaling of ⁴He at the superfluid transition, Rev. Mod. Phys. 80 (2008) 1009. doi:10.1103/RevModPhys.80.1009.
- [522] E. A. Cornell, C. E. Wieman, Nobel lecture: Bose-Einstein condensation in a dilute gas, the first 70 years and some recent experiments, Rev. Mod. Phys. 74 (2002) 875. doi:10.1103/RevModPhys.74.875.
- [523] W. Ketterle, Nobel lecture: When atoms behave as waves: Bose-Einstein condensation and the atom laser, Rev. Mod. Phys 74 (2002) 1131. doi:10.1103/RevModPhys.74.1131.
- [524] T. Donner, S. Ritter, T. Bourdel, A. Öttl, M. Köhl, T. Esslinger, Critical behavior of a trapped interacting Bose gas, Science 315 (2007) 1556. arXiv:0704.1439, doi:10.1126/science.1138807.
- [525] I. Bloch, J. Dalibard, W. Zwerger, Many-body physics with ultracold gases, Rev. Mod. Phys. 80 (2008) 885. arXiv: 0704.3011, doi:10.1103/RevModPhys.80.885.
- [526] M. Campostrini, M. Vicari, Critical behavior and scaling in trapped systems, Phys. Rev. Lett. 102 (2009) 240601, [Erratum: Phys. Rev. Lett. 103, 269901 (2009)]. arXiv:0903.5153, doi:10.1103/PhysRevLett.102.240601.
- [527] M. Campostrini, M. Vicari, Trap-size scaling in confined-particle systems at quantum transitions, Phys. Rev. A 81 (2010) 023606. arXiv:0906.2640. doi:10.1103/PhysRevA.81.023606.
- [528] H. Panagopoulos, E. Vicari, Out-of-equilibrium scaling of the energy density along the critical relaxational flow after a quench of the temperature, Phys. Rev. E 109 (6) (2024) 064107. arXiv:2403.11866, doi:10.1103/PhysRevE.109.064107.
- [529] D. Rossini, E. Vicari, Interplay between short-range and critical long-range fluctuations in the out-of-equilibrium behavior of the particle density at quantum transitions, Phys. Rev. B 110 (2024) 035126. arXiv:2405.04364, doi:10.1103/ PhysRevB.110.035126.
- [530] K. Binder, Critical behavior at surfaces, in: C. Domb, J. L. Lebowitz (Eds.), Phase transitions and critical phenomena, Vol. 8, Academic Press, London, 1983.
- [531] P. Calabrese, M. Caselle, A. Celi, A. Pelissetto, E. Vicari, Nonanalyticity of the Callan-Symanzik Beta function of two-dimensional O(N) models, J. Phys. A 33 (2000) 8155. arXiv:hep-th/0005254, doi:10.1088/0305-4470/33/46/301.
- [532] A. J. Bray, Theory of phase-ordering kinetics, Adv. Phys. 43 (1994) 357. arXiv:cond-mat/9501089, doi:10.1080/00018739400101505.
- [533] B. Nienhuis, M. Nauenberg, First Order Phase Transitions in Renormalization Group Theory, Phys. Rev. Lett. 35 (1975) 477. doi:10.1103/PhysRevLett.35.477.
- [534] M. E. Fisher, A. N. Berker, Scaling for first-order phase transitions in thermodynamic and finite systems, Phys. Rev. B 26 (1982) 2507. doi:10.1103/PhysRevB.26.2507.
- [535] V. Privman, M. E. Fisher, Finite-size effects at first-order transitions, J. Stat. Phys. 33 (1983) 385. doi:10.1007/BF01009803.
- [536] H. W. J. Blöte, M. P. Nightingale, Critical behaviour of the two-dimensional Potts model with a continuous number of states; A finite size scaling analysis, Physica A 112 (1982) 405. doi:10.1016/0378-4371(82)90187-X.
- [537] M. E. Fisher, V. Privman, First-order transitions breaking O(n) symmetry: Finite-size scaling, Phys. Rev. B 32 (1985) 447. doi:10.1103/PhysRevB.32.447.
- [538] M. S. S. Challa, D. P. Landau, K. Binder, Finite-size effects at temperature-driven first-order transitions, Phys. Rev. B 34 (1986) 1841. doi:10.1103/PhysRevB.34.1841.
- [539] J. Lee, J. M. Kosterlitz, Finite-size scaling and Monte Carlo simulations of first-order phase transitions, Phys. Rev. B 43 (1991) 3265. doi:10.1103/PhysRevB.43.3265.
- [540] K. Vollmayr, J. D. Reger, M. Scheucher, K. Binder, Finite size effects at thermally-driven first order phase transitions:

- A phenomenological theory of the order parameter distribution, Z. Phys. B 91 (1993) 113. doi:10.1007/BF01316713.
- [541] S. Cabasino, et al., The APE with a small jump, Nucl. Phys. B (Proc. Suppl.) 17 (1990) 218. doi:10.1016/0920-5632(90) 90241-L.
- [542] M. Fukugita, H. Mino, M. Okawa, A. Ukawa, Resolving the Order of Phase Transitions in Monte Carlo Simulations, J. Phys. A 23 (1990) L561.
- [543] J. F. McCarthy, Determination of the order of phase transitions in numerical simulations, Phys. Rev. B 41 (1990) 9530. doi:10.1103/PhysRevB.41.9530.
- [544] A. Billoire, First order phase transitions of spin systems, Nucl. Phys. B (Proc. Suppl.) 42 (1995) 21. arXiv:hep-lat/9501003, doi:10.1016/0920-5632(95)00183-A.
- [545] F. Y. Wu, The Potts model, Rev. Mod. Phys. 54 (1982) 235. doi:10.1103/RevModPhys.54.235.
- [546] R. J. Baxter, Exactly Solver Model in Statistical Mechanics, Dover Publications, Inc., Mineola (New York), 2007.
- [547] R. Guida, J. Zinn-Justin, Critical exponents of the N vector model, J. Phys. A 31 (1998) 8103. arXiv:cond-mat/9803240, doi:10.1088/0305-4470/31/40/006.
- [548] M. V. Kompaniets, E. Panzer, Minimally subtracted six loop renormalization of O(n)-symmetric ϕ^4 theory and critical exponents, Phys. Rev. D 96 (2017) 036016. arXiv:1705.06483, doi:10.1103/PhysRevD.96.036016.
- [549] G. De Polsi, I. Balog, M. Tissier, N. Wschebor, Precision calculation of critical exponents in the O(N) universality classes with the nonperturbative renormalization group, Phys. Rev. E 101 (2020) 042113. arXiv:2001.07525, doi: 10.1103/PhysRevE.101.042113.
- [550] M. Campostrini, A. Pelissetto, P. Rossi, E. Vicari, 25th order high temperature expansion results for three-dimensional Ising like systems on the simple cubic lattice, Phys. Rev. E 65 (2002) 066127. arXiv:cond-mat/0201180, doi:10.1103/ PhysRevE.65.066127.
- [551] Y. Deng, H. W. J. Blöte, Simultaneous analysis of several models in the three-dimensional Ising universality class, Phys. Rev. E 68 (2003) 036125, doi:10.1103/PhysRevE.68.036125.
- [552] M. Hasenbusch, Finite size scaling study of lattice models in the three-dimensional Ising universality class, Phys. Rev. B 82 (2010) 174433. arXiv:1004.4486, doi:10.1103/PhysRevB.82.174433.
- [553] S. A. Antonenko, A. I. Sokolov, Critical exponents for a three-dimensional O(n)-symmetric model with n > 3, Phys. Rev. E 51 (1995) 1894. arXiv:hep-th/9803264, doi:10.1103/PhysRevE.51.1894.
- [554] J. C. Le Guillou, J. Zinn-Justin, Critical exponents for the n-vector model in three dimensions from field theory, Phys. Rev. Lett. 39 (1977) 95. doi:10.1103/PhysRevLett.39.95.
- [555] J. C. Le Guillou, J. Zinn-Justin, Critical exponents from field theory, Phys. Rev. B 21 (1980) 3976. doi:10.1103/ PhysRevB.21.3976.
- [556] G. A. Baker, B. G. Nickel, M. S. Green, D. I. Meiron, Ising-model critical indices in three dimensions from the Callan-Symanzik equation, Phys. Rev. Lett. 36 (1976) 1351. doi:10.1103/PhysRevLett.36.1351.
- [557] G. Parisi, Field-theoretic approach to second-order phase transitions in two- and three-dimensional systems, J. Stat. Phys. 23 (1980) 49. doi:10.1007/BF01014429.
- [558] K. G. Chetyrkin, S. G. Gorishny, S. A. Larin, F. V. Tkachov, Five-loop renormalization group calculations in the $g\phi^4$ theory, Phys. Lett. B 132 (1983) 351. doi:10.1016/0370-2693(83)90324-6.
- [559] K. G. Wilson, M. E. Fisher, Critical exponents in 3.99 dimensions, Phys. Rev. Lett. 28 (1972) 240. doi:10.1103/ PhysRevLett.28.240.
- [560] G. 't Hooft, M. Veltman, Regularization and renormalization of gauge fields, Nucl. Phys. B 44 (1972) 189. doi:10.1016/0550-3213(72)90279-9.
- [561] D. Poland, S. Rychkov, A. Vichi, The conformal bootstrap: Theory, numerical techniques, and applications, Rev. Mod. Phys. 91 (2019) 015002. arXiv:1805.04405, doi:10.1103/RevModPhys.91.015002.
- [562] M. Hasenbusch, Monte Carlo studies of the three-dimensional Ising model in equilibrium, Int. J. Mod. Phys. C 12 (2001) 911. doi:10.1142/S0129183101002383.
- [563] M. Hasenbusch, A Monte Carlo study of leading order scaling corrections of φ^4 theory on a three-dimensional lattice, J. Phys. A: Math. Gen. 32 (1999) 4851. arXiv:hep-lat/9902026, doi:10.1088/0305-4470/32/26/304.
- [564] E. Burovski, J. Machta, N. Prokof'ev, B. Svistunov, High-precision measurement of the thermal exponent for the three-dimensional XY universality class, Phys. Rev. B 74 (2006) 132502. arXiv:cond-mat/0507352, doi:10.1103/PhysRevB. 74.132502.
- [565] J. A. Lipa, J. A. Nissen, D. A. Stricker, D. R. Swanson, T. C. P. Chui, Specific heat of liquid helium in zero gravity very near the lambda point, Phys. Rev. B 68 (2003) 174518. arXiv:cond-mat/0310163, doi:10.1103/PhysRevB.68.174518.
- [566] J. A. Lipa, D. R. Swanson, J. A. Nissen, Z. K. Geng, P. R. Williamson, D. A. Stricker, T. C. P. Chui, U. E. Israelsson, M. Larson, Specific heat of helium confined to a 57-μm planar geometry near the lambda point, Phys. Rev. Lett. 84 (2000) 4894. doi:10.1103/PhysRevLett.84.4894.
- [567] J. A. Lipa, D. R. Swanson, J. A. Nissen, T. C. P. Chui, U. E. Israelsson, Heat capacity and thermal relaxation of bulk helium very near the lambda point, Phys. Rev. Lett. 76 (1996) 944. doi:10.1103/PhysRevLett.76.944.
- [568] S. M. Chester, W. Landry, J. Liu, D. Poland, D. Simmons-Duffin, N. Su, A. Vichi, Bootstrapping Heisenberg magnets and their cubic instability, Phys. Rev. D 104 (2021) 105013. arXiv:2011.14647, doi:10.1103/PhysRevD.104.105013.
- [569] M. Campostrini, M. Hasenbusch, P. Pelissetto, P. Rossi, E. Vicari, Critical exponents and equation of state of the three-dimensional Heisenberg universality class, Phys. Rev. B 65 (2002) 144520. arXiv:cond-mat/0110336, doi:10.1103/PhysRevB.65.144520.
- [570] M. Hasenbusch, Monte Carlo study of a generalized icosahedral model on the simple cubic lattice, Phys. Rev. B 102 (2020) 024406. arXiv:2005.04448, doi:10.1103/PhysRevB.102.024406.